GENETIC AND MOLECULAR CHARACTERIZATION OF HOST RESISTANCE AND SUSCEPTIBILITY TO *PYRENOPHORA TERES* F. *TERES* IN *HORDEUM VULGARE*

A Dissertation
Submitted to the Graduate Faculty
of the
North Dakota State University
of Agriculture and Applied Science

By

Jonathan Kertz Richards

In Partial Fulfillment of the Requirements
for the Degree of
DOCTOR OF PHILOSPOHY

Major Department:
Plant Pathology

November 2016

Fargo, North Dakota

North Dakota State University
Graduate School

Title

GENETIC AND MOLECULAR CHARACTERIZATION OF HOST RESISTANCE AND SUSCEPTIBILITY TO *PYRENOPHORA TERES* F. *TERES* IN *HORDEUM VULGARE*

By

Jonathan Kertz Richards

The Supervisory Committee certifies that this ***disquisition*** complies with North Dakota State University's regulations and meets the accepted standards for the degree of

DOCTOR OF PHILOSOPHY

SUPERVISORY COMMITTEE:

Dr. Robert Brueggeman
Chair

Dr. Timothy Friesen

Dr. Luis del Rio

Dr. Phil McClean

Approved:

November 10, 2016
Date

Dr. Jack Rasmussen
Department Chair

ABSTRACT

Pyrenophora teres f. *teres*, a necrotrophic fungal pathogen and causal agent of net form net blotch (NFNB), is an economically important pathogen of barley (*Hordeum vulgare)* and has potential to cause significant yield losses in barley production regions of the world. Host resistance is the most desirable means of disease management, yet the genetic nature of this pathosystem is exceedingly complex. With the goal of identifying novel sources of resistance to NFNB, a diverse population of barley accessions was utilized to conduct a genome wide association study which identified a total of 78 significant markers associated with disease reaction to three North American *P. teres* f. *teres* isolates, corresponding to 16 genomic loci. Five novel loci were detected and will be of importance for barley breeders for the improvement of elite barley lines. Dominant susceptibility harbored by barley cultivars Rika and Kombar to *P. teres* f. *teres* isolates 6A and 15A, respectively, were previously identified to exist in repulsion and mapped at low-resolution. Using 2976 recombinant gametes derived from a cross of Rika x Kombar and markers developed through mining of syntenous genes in *Brachypodium distachyon*, we mapped the *Spt1* locus to ~0.24 cM near the centromere of chromosome 6H. Within the delimited *Spt1* region, a receptor-like protein was identified as the primary candidate *Spt1* gene designated *Spt1.cg*. Allele analysis of diverse barley lines exhibited a strong correlation with the presence of a Rika, Kombar, or Morex allele of *Spt1.cg* and susceptibility to *P. teres* f. *teres* isolates 6A, 15A, or Tra-A5/Tra-D10, respectively. Alleles of *Spt1.cg* appear highly diverged, stemming from selection pressures in wild barley populations and may be targeted by several unique necrotrophic effectors. The barley cultivar Morex *rpr2* mutant, previously characterized to have lost *Rpg1*-mediated resistance to *Puccinia graminis* f. sp. *tritici*, also has compromised resistance to *P. teres* f. *teres*. Exome capture revealed a 12 base-pair

deletion in a gene containing fibronectin and plant homeodomain domains with homology to Arabidopsis VIN3-like proteins. This gene may function in the perception of pathogen effector proteins, that disrupt cell wall integrity, eliciting early damage associated molecular pattern immunity responses.

ACKNOWLEDGEMENTS

I would first like to acknowledge and thank my advisor, Dr. Robert Brueggeman, for giving me a chance, as an undergraduate student with no real laboratory experience, to learn and mature as a young scientist. I was given every opportunity to expand my knowledge, take control of my research, and think outside the box. His guidance, expertise, and perseverance allowed me to develop a true passion for scientific research.

I would also like to recognize Dr. Timothy Friesen for all of his support and advice throughout my years as a Ph.D student. His expertise with the barley-*Pyrenophora teres* f. *teres* pathosystem has been an amazing help throughout the last six years. I would also like to thank members of my Ph.D committee, Drs. Luis del Rio and Phil McClean, for their help and encouragement.

I would like to acknowledge all technicians, as well as present and former students of the Brueggeman lab. Many thanks to Patrick Gross, who assisted me with all greenhouse activities and provided me with all materials needed for my experiments. I would also like to thank Danielle Holmes for all of her assistance with my inoculations and advice for fungal culturing and inoculum preparation. Additionally, I would also like to thank all students and the entire Plant Pathology department at North Dakota State University, as my time as a graduate student was an outstanding experience due to the great people I was surrounded with.

I would especially like to acknowledge my wonderful girlfriend, Claudia Munoz, who has been unbelievably supportive and motivating.

Finally, I would like to extend my deepest gratitude to my parents, Barbara and Bradley Richards, my brother Robert Richards, and the rest of my family, for always being there for me throughout this long journey.

TABLE OF CONTENTS

ABSTRACT iii

ACKNOWLEDGEMENTS v

LIST OF TABLES xi

LIST OF FIGURES xii

CHAPTER 1. LITERATURE REVIEW 1

Barley 1

Domestication of Barley 2

Synteny and the Barley Genome 5

Net Blotch of Barley 9

Taxonomy and Life Cycle of *Pyrenophora teres* f. *teres* 11

Genetic and Phenotypic Diversity of *Pyrenophora teres* f. *teres* 12

Toxins Produced by *Pyrenophora teres* f. *teres* 20

Host Resistance and Susceptibility to Net Form Net Blotch of Barley 23

Molecular Mechanisms of Host Resistance 26

Association Mapping 32

Literature Cited 34

CHAPTER 2. ASSOCIATION MAPPING UTILIZING DIVERSE BARLEY LINES REVEALS NET FORM NET BLOTCH SEEDLING RESISTANCE/SUSCEPTIBILITY LOCI 45

Abstract 45

Introduction 46

Materials and Methods 49

Biological Materials 49

Phenotyping 50

Genotyping 50

Imputation, Allele Similarity, and Linkage Disequilibrium 51
Population Structure 51
Marker Trait Association Models 52
QTL Identification 53
Results 53
Phenotypic Analysis 53
Marker Properties 61
Linkage Disequilibrium, PCA, and Structure 61
Association Mapping 64
Isolate 15A 64
Isolate 6A 67
Isolate LDN 67
Discussion 71
Literature Cited 77
CHAPTER 3. FINE MAPPING OF THE BARLEY CHROMOSOME 6H NET FORM NET BLOTCH SUSCEPTIBILITY LOCUS 82
Abstract 82
Introduction 83
Materials and Methods 87
Biological Materials 87
Genotyping and Recombinant Gamete Identification 88
STS/SNP Marker Development 89
PCR-GBS Library Preparation and Ion Torrent Sequencing 91
SNP Calling 93
Phenotyping 93
High-Resolution Map Construction 94

Barley iSelect 9K Chip 94
BAC Library Screening and Physical Map Construction 94
BAC Library Sequencing and Assembly 95
Results 96
Initial Genotyping and Phenotyping of Critical Recombinants 96
Phenotyping of the ICR Lines 96
Marker Development and High-Resolution Map Construction 98
PCR-GBS Sequencing and SNP Calling 100
BAC Library Screening and Physical Map Construction 100
Discussion 105
Acknowledgements 109
Literature Cited 109
CHAPTER 4. IDENTIFACTION OF *SPT1*: A MULTI-ALLELIC RECEPTOR-LIKE PROTEIN CONFERRING ISOLATE SPECIFIC NET FORM NET BLOTCH SUSCEPTIBILITY IN BARLEY 114
Abstract 114
Introduction 115
Materials and Methods 120
DNA Extraction 120
Candidate Gene Identification 121
Genome Walking and Candidate Gene Sequence Analysis 122
Phenotyping of Steptoe x Morex DH Population 125
Linkage Mapping and QTL Analysis 126
Allele and Association Analysis 126
Phylogenetic Analysis 128
BSMV-VIGS 128

RNA Extraction, cDNA Synthesis, and qPCR 131
Results 132
Candidate Gene Identification 132
Genome Walking and Candidate Gene Sequence Comparison 133
Phenotyping 137
Linkage Mapping and QTL Analysis 138
Allele and Association Analysis 140
Phylogenetic Analysis 144
BSMV-VIGS 144
Discussion 146
Literature Cited 152
CHAPTER 5. EXOME CAPTURE IDENTIFIES *RPR2* ACTING AS A KEY COMPONENT OF BASAL RESISTANCE IN *HORDEUM VULGARE* 157
Abstract 157
Introduction 158
Materials and Methods 163
Biological Materials and Phenotyping 163
DNA Extraction 163
Exome Capture and Sequencing 164
Bioinformatics 167
Mutation Validation 168
Candidate Gene and Putative Effector Analysis 168
Results 169
Phenotyping 169
Sequencing and Bioinformatics 170
Candidate Gene Analysis 171

Discussion 174

Literature Cited 179

CONCLUSION 185

LIST OF TABLES

Table Page

2.1. Haplotypes of 52 barley accessions highly resistant to *P. teres* f. *teres* isolates 15A, 6A, and LDN 55

2.2. Mean Squared Difference (MSD) Values for Nine Association Models 64

2.3. Significant markers associated with disease reaction to *P. teres* f. *teres* isolate 15A 65

2.4. Significant markers associated with disease reaction to *P. teres* f. *teres* isolate 6A. 68

2.5. Significant markers associated with disease reaction to *P. teres* f. *teres* isolate LDN 69

3.1. Sequences of primers designed from barley ESTs identified via synteny analysis 90

3.2. Average disease scores for Rika, Kombar, and resistant/susceptible ICRs with *Ptt* isolates 98

3.3. Bacterial artificial chromosome (BAC) clones identified from all markers on high-resolution map and corresponding sequence contigs and fingerprinted contigs 104

4.1. Candidate *Spt1* Genes Identified from *Brachypodium distachyon* Synteny 133

4.2. Allele analysis of barley lines with candidate *Spt1* allele specific markers 141

4.3. Phenotypic analysis of BSMV-VIGS plants inoculated with *P. teres* f. *teres* 15A x 6A progeny isolates harboring virulence QTL VK1 and VK2 146

4.4. Relative expression levels candidate *Spt1* of BSMV-VIGS plants 146

LIST OF FIGURES

Figure Page

2.1. A three dimensional representation of the principal components analysis conducted using 957 barley lines genotyped with the barley Illumina 9K iSelect chip. PC1 is illustrated on the x-axis, PC2 is listed on the z-axis, and PC3 is represented on the y-axis. The distinct clustering of the barley genotypes into two groups is representative of 2-row and 6-row barley populations 62

2.2. Results of a STRUCTURE analysis conducted using 957 diverse barley lines. Hypothetical subpopulation levels are listed on the x-axis and Delta K values are listed on the y-axis. The largest Delta K value corresponds to a hypothetical sub-population of two, representing 2-row and 6-row barley classes 63

2.3. Graphical representation of a STRUCTURE analysis using 957 barley genotypes. Using genetic positions of the iSelect consensus map (Muñoz-Amatriaín et al. 2014), a single marker was selected from each locus and used in the analysis, resulting in a total of 1744 SNP markers. The results indicate that the barley lines used in this study are divided into two subpopulations. Subpopulation membership is listed on the y-axis ranging from 0.00-1.00. Red indicates membership to subpopulation one and green to subpopulation two. Individuals with membership to a single subpopulation of less than 0.80 were considered admixture 63

2.4. Association mapping analyses of disease reaction to *P. teres* f. *teres* isolates 15A (California), LDN (North Dakota), and 6A (California). Barley chromosomes are listed on the x-axis. A –log10(p) scale of significance is represented on the y-axis with the red horizontal line representing the significance threshold of –log10(p) = 3. The colored pixels represent individual SNP markers used in the association analyses. Both previously identified and newly designated QTL are listed at the top of the figure. Boxes are drawn around the distinct significant loci detected..... 70

3.1. Genetic and partial physical map of the *Spt1* locus in synteny with *Brachypodium distachyon* 102

4.1. Gene model of candidate *Spt1*. (Top) Genomic DNA region. (Middle) Predicted mRNA structure. (Bottom) Protein domain structure, including a predicted N-terminal transmembrane domain (TM) and C-terminal LRR. 134

4.2. Predicted amino acid alignment of candidate *Spt1* alleles from Rika (*Spt.R*), Kombar (*Spt.K*), and Morex (*Spt.R*) 135

4.3. High-resolution map of the *Spt1* locus (light grey shaded area). Individual recombinant lines, including parents Rika and Kombar, are listed at the top of the figure. Below each individual name are the corresponding phenotypes to *P. teres* f. *teres* isolates 6A and 15A: Resistant (R), Moderately Susceptible (MS), and Susceptible (S). Red corresponds to Rika genotype, blue corresponds to Kombar genotype. "X" designates recombination events. Genetic distances are listed as map units to the right of the thick black line. Genetic markers are listed to the left of the thick black line. The "*" designates the marker corresponding to the primary candidate gene 136

4.4. (A) Phenotypic reaction of Steptoe (left) and Morex (right) inoculated with *P. teres* f. *teres* isolate Tra-A5. (B) Phenotypic reaction of Steptoe (left) and Morex (right) inoculated with *P. teres* f. *teres* isolate Tra-D10 137

4.5. Distribution of Disease Reaction Scores of the SM DH individuals to *P. teres* f. *teres* isolates Tra-A5 (left) and Tra-D10 (right). Disease score is illustrated on the x-axis and frequency is seen on the y-axis 138

4.6. QTL analysis of resistance/susceptibility towards *P. teres* f. *teres* isolates Tra-A5 (red) and Tra-D10 (green) in the SM DH population. Markers are illustrated on the x-axis and LOD values on the y-axis. The dashed line represents the LOD threshold of 4.71 as determined by 1000 permutations 139

4.7. High-resolution association analysis. Physical positions (Mb) are illustrated on the x-axis. Marker significance reported as $-\log_{10}(p)$ is shown on the y-axis. Blue corresponds to isolate 15A, red corresponds to isolate 6A. Green arrows indicate orientation of genes within the region. "*" indicates the position of candidate *Spt1* 143

4.8. Phylogenetic analysis using 56 SNPs within the 3'-LRR of candidate *Spt1* 145

4.9. Proposed model illustrating function of *Spt1*. The conserved extracellular C-terminal LRR region of the recognizes a PAMP and signals into the cytoplasm to trigger PTI via association with a RLK (right). Alternatively, the receptor may be under purifying selection to recognize an avirulence protein secreted from a biotrophic pathogen, triggering ETI. *P. teres* f. *teres* evolved NEs to target the diverged extracellular portion of the N-terminal region, intentionally triggering NETs (left). The negative outcome of this interaction places a diversifying selection on the region of the protein, leading to high levels of diversity 152

5.1. Preliminary phenotypic reaction of Morex wild-type and Morex *rpr2* mutant inoculated with *P. teres* f. *teres* isolates 0-1, 15A, and 6A 169

5.2. Coverage level of exome capture target regions which were anchored to the draft genome sequence of barley cultivar Morex. Level of coverage in reads per base pair is shown on the x-axis and amount of sequence covered at specified level is shown on the y-axis. Coverage of the Morex wild-type sample is illustrated by the red line and the Morex *rpr2* $BC_1F_{2:4}$ pooled sample is shown by the blue line. 171

5.3. Sequencing alignment of reads mapping to MLOC_66063.2 of the Morex *rpr2* $BC_1F_{2:4}$ sample (top frame) and Morex wild-type sample (bottom frame) 172

5.4. Genotyping of Morex wild-type (1), Morex *rpr2* mutant (2), Morex/Morex *rpr2* $BC_1F_{2:4}$ individuals (3-14), and a non-template control (15) with a primer pair specific to the 12 base pair deletion within MLOC_66063.2.....172

5.5. Gene model illustrating the genomic DNA sequence (top), mRNA structure (middle), and protein structure including a predicted nuclear localization signal (NLS), plant homeodomain finger (PHD), and fibronectin III (FNIII) domain. (bottom) 173

5.6. Proposed model of the function of RPR2. (a) Spores of *P. teres* f. *teres* and *P. graminis* f. sp. *tritici* land on the plant cell surface and produce spore coat effector proteins RGD-binding protein and VPS9. (b) RGD-binding protein interacts with HvNDR1, either alone or along with VPS9. The pathogen may have evolved this interaction to disrupt the plasma membrane-ECM interface, allowing for the development of an adherence pad. NDR1 signals interior to the cell via RIN4 to phosphorylate RPG1 in response to pathogen adherence. (c) In the wild-type plant (left) RPR2 intercepts the complex of RGD-binding protein/VPS9, preventing manipulation of RPG1 and ensuring continuance of the defense response. Alternatively, RPR2 may localize to the nucleus, triggering components required for the defense response. In the mutant plant (right), the mutation in RPR2 may lose the ability to bind the spore coat effectors. Alternatively, the mutation may compromise the ability to localize to the nucleus or transmit signals via phosphorylation.....179

CHAPTER 1. LITERATURE REVIEW

Barley

Barley (*Hordeum vulgare*), a member of the tribe Triticeae Dumortier, is an important crop used primarily for the malting industry, but also has been utilized for human consumption and livestock feed (von Bothmer and Jacobsen 1985). Barley varieties are divided into two growth habits, spring and winter. As its name implies, spring barley is sown in the spring, but in regions such as the southwestern United States, may be planted in the fall. Additionally, spring barley generally does not respond to vernalization and does not have a rosette-growth stage (USDA 1979). Barley can also be classified based upon its spike morphology. At each node of the rachis, three spikelets are attached. In two-rowed barley, the central spikelet is fertile and the lateral spikelets are sterile, whereas in six-rowed barley, all three spikelets at each node are fertile (USDA 1979).

Barley production began in the American settlements likely from early settlers bringing seeds from their home country to the newly formed colonies. Varieties from England, such as Chevalier and Thorpe, as well as Dutch and Spanish varieties began to be sown along the east coast of the American colonies. Soon after, barley production became an important facet of the agriculture industry in New York. In the middle of the 19th century, barley began moving westward and expanded into the Midwest, Pacific Northwest, and California. By the end of the 19th century, barley production in the Red River Valley and the Pacific Northwest ousted New York as the nation's leading barley producing region (USDA 1979).

Global barley production in 2015 was projected at 148.63 million metric tons and is projected to reach approximately 145.24 million metric tons in 2016 (USDA-FAS, 2016). North Dakota is consistently one of the top barley producing states in the United States, along with

Montana and Idaho. In 2015, North Dakota led the United States in barley production by harvesting 1,050,000 acres averaging a yield of 64.0 bushels per acre (USDA-NASS).

Domestication of Barley

Archaeological evidence indicates that cultivated barley was originally domesticated in the Fertile Crescent approximately 10,000 years ago from the wild progenitor *Hordeum vulgare* ssp. *spontaneum C*. Koch. (Bothmer and Jacobsen 1985; Badr et al. 2000; Pourkheirandish and Komatsuda 2007). The Fertile Crescent region is generally defined as spanning Israel, Jordan, Syria, and western Iran. Additionally, several other crops including peas, emmer and einkorn wheat, and lentils are believed to have been domesticated within this same region (Zohary 1973; Bothmer and Jacobsen 1985). Several of the most important traits selected for during barley domestication include a six-rowed spike, non-brittle rachis, and reduced dormancy and vernalization requirements (Pourkheirandish and Komatsuda 2007).

Although strong archaeological evidence points to the Fertile Crescent as the origin of barley domestication, several other locales have been thought to be potential secondary sites of domestication, including the Himalayas, Morocco, and Ethiopia. However, Badr et al. (2000) genotyped a collection of 317 wild barley accessions and 57 barley cultivars with amplified fragment length polymorphism (AFLP) markers to further clarify the origin of barley. Results indicate a monophyletic origin stemming from the region of Israel and Jordan and the authors suggested that the proposed alternative domestication sites are regions of barley diversification (Badr et al. 2000).

In contrast to the results of Badr et al. (2000), analysis of haplotypes of geographically distinct samples indicated the potential of a second barley domestication event east of the Fertile Crescent (Morrell and Clegg 2007). The results revealed haplotypes of wild barley that were

present in cultivated varieties from eastern Asia and were not found in wild barley accessions from the Fertile Crescent. Additionally, allele similarity analysis of landraces from eastern and western Asia indicated a clear differentiation between geographic locations. Evidence for a polyphyletic domestication of barley increased following a study by Dai et al. (2012). A total of 75 wild barley accessions from the Near East (Israel, Jordan, Iran, and Turkey), 95 accessions from Tibet, and 68 globally diverse cultivated barley lines (Tibet, Algeria, China, France, Denmark, Australia, Canada, United States, Japan, United Kingdom, and Germany) were genotyped using diversity array technology (DArT) markers followed by validation of results with single nucleotide polymorphism (SNP) markers derived from four genes to conduct cluster analyses. Population structure analysis divided the barley accessions into four subpopulations: wild barley from the Near East, wild barley from Tibet, cultivated barley, as well as a subpopulation comprised of various Tibetan wild barley accessions and six-rowed cultivated barley of Chinese origin. These results indicate a significant differentiation between the two wild barley populations, possibly due to the adaptation of Tibetan wild barley to high altitudes and cold temperatures (Dai et al. 2012). Also, a lower level of genetic diversity was observed in wild barley accessions from Tibet and may be attributed to a later migration of wild barley to this region, followed by a second domestication (Dai et al. 2012). Another phylogenetic study using sequence of two nuclear genes of wild barley lines from the Fertile Crescent, Central Asia, Tibet, and cultivated Chinese barley lines support the domestication of barley in Tibet and that Chinese cultivars are derived from the wild barley populations of the Tibetan Plateau (Ren et al. 2013).

In addition to Tibet being considered a potential second center of barley domestication, Morocco has also been identified as a possible origin. Restriction fragment length polymorphism (RFLP) analysis of wild barley lines derived from nine locations (Morocco, Crete, Cyprus,

Afghanistan, Iraq, Iran, Israel, Turkey and Libya) revealed a distinct cluster of Moroccan wild barley lines from accessions derived from the Fertile Crescent (Molina-Cano et al. 1999). These results agree with a previous study of wild barley populations from these regions using morphological and biochemical markers (Molina-Cano et al. 1987) and support Morocco as an alternative center of domestication. Further investigation of Moroccan wild barley contrasts with previous results. Phylogenetic analysis conducted with 13 wild barley populations (Cyprus, Greece, Morocco, Iran, Israel, Libya, Tadjikistan, Turkmenistan, and Uzbekistan), 29 geographically diverse cultivated barley lines (Afghanistan, Albania, Colombia, Egypt, Ethiopia, Germany, France, Iran, Iraq, Japan, Jordan, Libya, Morocco, Nepal, Portugal, Slovakia, Spain, Sudan, Tibet, Tunisia, and Turkey), as well as *Hordeum bulbosum*, *Hordeum vulgare* subsp. *agriocrithon*, and *Hordeum marinum* Huds. subsp. *marinum* as outgroups indicated a monophyletic origin of barley in the Fertile Crescent. These conflicting results may be due to the previous research not including outgroups or cultivated lines in their analyses and that Moroccan wild barley appears to have been introgressed with cultivated lines (Blattner and Badani Mendez 2001).

One of the most important domestication traits in barley is the non-brittle rachis. A brittle rachis allows for the ease of seed dispersal, resulting in a fitness advantage for the plant. However, spikes on barley plants possessing a non-brittle rachis allowed for ancient farmers to harvest much more effectively (Pourkeirandish and Komatsuda 2007). Two tightly linked dominant genes, *Btr1* and *Btr2*, confer the phenotype of a brittle rachis. A recessive allele containing a putative mutation of either gene induces the non-brittle phenotype. Via a map-based cloning strategy, Pourkheirandish et al. (2015) identified *Btr1* and *Btr2* only separated by approximately 100 kb on chromosome 3H with both genes containing frameshift mutations.

Although no functional domains were identified and the biological mechanisms of these genes are unknown, evolutionary analysis indicate that selection for each of these mutants occurred at two separate sites of domestication for this trait. It is postulated that the *btr1* mutation arose in southern Levant and the *btr2* mutation occurred in northern Levant (Pourkheirandish et al. 2015). This conflicts with the conclusions of Badr et al. (2000), in which the authors speculated that the mutations conferring a non-brittle rachis occurred at a single location.

The Fertile Crescent remains as the accepted primary center of barley domestication. However, several phylogenetic studies have indicated potential secondary sites of domestication in the Himalayas, Morocco, and Ethiopia, while other research posits that these regions are sites of barley diversification. The monophyletic versus polyphyletic nature of barley evolution is still under constant debate and a definitive answer is not clear, but as sequencing technology continues to evolve and sample sizes grow, the clarification of barley domestication may emerge.

Synteny and the Barley Genome

Barley is considered to be a model organism within the Triticeae tribe. It is a true diploid with seven chromosomes (2n=14), however, it has a large haploid genome size of approximately 5.1 gigabases (Gb) (IBGSC 2012). The focus being placed on elucidating the molecular mechanisms underlying important aspects of plant physiology, including disease resistance, development and agronomic traits, requires gene identification which is greatly aided by a quality reference genome sequence (Mayer et al. 2011). The prospect of a barley reference genome sequence was daunting, given its large size with a high proportion of repetitive elements (IBGSC 2012)

Often times, the genome of the organism being studied is not easily amenable to genomic studies due to a large size often confounded by repetitive elements (Vision 2005). One method to

extrapolate gene content information is through the comparison of an organism with an annotated genome sequence to closely related species based on the concept of synteny, where collinearity of gene order on homoeologous chromosomes is often observed (McCouch 2001; Vision 2005). Although crops such as sorghum (*Sorghum bicolor*), maize (*Zea mays*), rice (*Oryza sativa*), and wheat (*Triticum aestivum*) phylogenetically diverged from a progenitor approximately 55-70 million years ago (Kellogg 2001), genic regions remained generally conserved regarding their gene content and order. However, the genome sizes of these species differ greatly, but can be attributed to the variable presence and accumulation of repetitive elements/sequences (Bennetzen and Freeling 1997; Kellogg 2001). The conserved nature of genes as well as their function can be illustrated by the barley *Mla1* gene conferring resistance to powdery mildew (Zhou et al. 2001). Jordan et al. (2011) identified an ortholog of the barley *Mla1* gene in the diploid wheat *Triticum monococcum* which was ~78% homologous at the amino acid level to the barley MLA1 protein. It was determined that the homolog in *T. monococcum* also conferred resistance to the powdery mildew pathogen, indicating the conserved functional nature of this gene between two diverged species. Concerning barley, the organism *Brachypodium distachyon* has been extensively used to expedite map-based cloning projects via marker development and gene identification (IBI 2010; Mur et al. 2011) Youssef et al. (2014) utilized the syntenic relationship between barley and *Brachypodium distachyon* to identify SNPs and develop cleaved amplified polymorphic sequence (CAPS) markers. The newly developed markers were then used to map the recessive *lab* gene, which causes the development of zero to three fertile spikelets at each internode. Zang et al. (2015) fine mapped the *Un8* true loose smut resistance gene and exploited the *B. distachyon* genome to identify orthologous genes between the flanking markers of the genetic map. In order to make the synteny information more

accessible, Mayer et al. (2011) developed "genome-zippers". By incorporating techniques such as next-generation sequencing, chromosome sorting, and array hybridization along with synteny data from *B. distachyon*, rice, and sorghum, 21,766 barley genes were putatively placed in a linear order.

Although the use of *B. distachyon* has its utility, to definitively establish barley as a model system, a reference sequence needed to be synthesized. An important step towards the establishment of a contiguous genome sequence was the development of a bacterial artificial chromosome (BAC) library. Barley cultivar Morex was used to construct a BAC library using the restriction enzyme *Hin*dIII and resulted in a BAC library containing 313,344 clones with an estimated genome coverage of 6.3x (Yu et al. 2000). The development of this library allowed researchers to physically map their genetic regions via chromosome walking as well as laid the framework for the development of a reference genome. Using the same BAC library, Muñoz-Amatriaín et al. (2015) sequenced 15,622 BAC clones that were determined to harbor genes. This resulted in the generation of approximately 1.7 Gb of sequence, which is predicted to include approximately two thirds of all annotated high confidence and low confidence genes in barley cultivar Morex (IBGSC 2012; Muñoz-Amatriaín et al. 2015). As expected, gene dense regions were generally localized near the telomere, however, several gene rich regions were also observed in regions with suppressed recombination including some gene rich regions near centromeres (Muñoz-Amatriaín et al. 2015).

Through an international collaborative effort, a draft barley genome was developed. Six independent BAC libraries containing 571,000 BAC clones were fingerprinted and assembled into a total of 9265 contigs, creating a physical representation of the genome. The total length of the assembled contigs was approximately 4.98 Gb, nearly the estimated size of the entire barley

genome. Additionally, shotgun sequencing from selected BAC clones and BAC end sequence (BES) resulted in the assembly of approximately 1.14 Gb of sequence and enriched the previously constructed physical map. In addition to the development of a sequence enhanced barley physical map, insights into the repetitiveness of the genome were found. It was seen that approximately 84% of the entire barley genome is composed of repetitive elements (IBGSC 2012). In order to improve the draft genome assembly, a population sequencing (POPSEQ) method was employed (Mascher et al. 2013). A recombinant inbred line (RIL) population was developed from a cross between barley cultivars Morex and Barke and survey sequence was subsequently generated. Following read mapping to the previously developed Morex whole genome shotgun (WGS) sequences, SNPs were detected and mapped within the population, and WGS contigs were assigned a genetic position (Mascher et al. 2013). The utilization of POPSEQ greatly enhanced the ordering of the WGS contigs through the power of genetics by anchoring 927 Mb of sequence to genetic positions, compared to the 410 Mb that was previously anchored (Mascher et al. 2013). Additionally, this method may be applicable to other organisms that do not have any genomic sources readily available.

In addition to the development of a draft barley genome, advanced genomic tools are being developed to aid researchers in gene identification. Exome capture is a technique which sequences the gene coding regions of the genome and differs from RNA-seq in that no bias from mRNA expression levels is introduced. This method has previously been used in human studies to investigate genes involved in Mendelian disorders (Bamshad et al. 2011). Recently, Mascher et al. (2013) developed an exome capture array for barley through the incorporation of RNA-seq reads, full length cDNA sequence, and predicted genes, resulting in a capture space of approximately 61.6 Mb. This newly developed tool along with genetic analyses was utilized to

identify the *mnd* mutation in barley, which demonstrate a faster rate of leaf emergence, in an expedited fashion (Mascher et al. 2014).

With the advent of the draft genome sequence of barley as well as the development of methods such as POPSEQ and exome capture, barley has truly moved into the genomics age and has established itself as a true monocot model system, for which it has recently been given the model system designation by the National Science Foundation. Ongoing efforts are being placed on the clone by clone sequencing of the minimum tiling path (MTP) of BACs across the barley genome to create a contiguous physical sequence. The results of these developments will no doubt expedite the process of gene identification and enhance our knowledge of the molecular mechanisms occurring in the various physiological processes of barley.

Net Blotch of Barley

Pyrenophora teres Drechsler (anamorph *Drechslera teres* [Sacc.] Shoem.) is a necrotrophic fungal pathogen which is the causal agent of the foliar disease net blotch of barley. This economically important disease is present in most barley production regions of the world and generally causes yield losses of 10%-40%, but may induce complete yield loss under conducive conditions (Mathre 1997; Murray and Brennan 2010). Although foliar infection of barley by *P. teres* has a larger impact on yield loss, the pathogen also has the ability to infect other above ground plant structures, such as kernels, leaf sheaths, and stems (Liu et al. 2011). Symptoms of kernel infection are similar to that of various plant pathogenic fungi and appear as a dark, diffuse pattern (Shipton et al. 1973). As malting quality is of the upmost importance in elite barley, it is of major concern that this pathogen can also negatively affect these characteristics by reducing the plumpness, size, and bulk density of the kernels (Grewal et al. 2008). Two forms of this pathogen exist, *P. teres* f. *teres* and *P. teres* f. *maculata*, and cause

distinctly different symptoms. These two forms cannot be differentiated based on morphological characteristics, however, molecular analyses have greatly aided the correct identification of a specific form. Molecular markers such as simple sequence repeat (SSR) (Keiper et al. 2008), AFLP (Leisova et al. 2005), randomly amplified polymorphic DNA (RAPD) (Williams et al. 2001), and SNP markers specific to the mating type genes (Lu et al. 2010) have been developed which facilitate a precise diagnosis.

P. teres f. *teres* is the causal agent of net form net blotch which is characterized by the longitudinal and transverse necrotic striations produced on the foliar tissue of barley, forming its namesake net pattern, first described by Atanasoff and Johnson (1920). Additionally, chlorosis may appear surrounding the net type lesion (Shipton 1973). Symptoms begin to develop within 24 hours of direct penetration of leaf tissue as pin-point lesions. As the disease progresses, lesions are seen growing near the leaf vein, eventually forming the typical netting symptom (Liu et al. 2011).

A spot-type symptom was observed on barley leaves infected with *P. teres* and Smedegard-Petersen (1971) suggested the intraspecific classification of a new form, *P. teres* f. *maculata*. Typical symptoms of spot form net blotch include the presence of dark brown fusiform or elliptical regions of necrosis. Initially, the symptoms begin as pinpoint lesions and can increase to a size of approximately 3 x 6 mm, which may be surrounded by chlorosis in a susceptible reaction (McLean et al. 2009).

Laboratory experiments determined that *P teres* f. *teres* and *P. teres* f. *maculata* have the ability to hybridize and produce fertile progeny (Smedegard-Petersen 1971). Additionally, Campbell et al. (1999) demonstrated recombination in the progeny from a cross between *P. teres* f. *teres* and *P. teres* f. *maculata* using AFLP and RAPD markers and following inoculation on

barley, an intermediate symptom of circular spot symptoms with jagged edges were observed. It has often been postulated that mating of *P. teres* f. *teres* and *P. teres* f. *maculata* does not commonly occur in nature (Rau et al. 2003; Rau et al. 2005). However, Campbell et al. (2002) determined that an isolate collected from a field in South Africa represented a hybrid between the two forms on the basis of phylogenetic analysis and the presence of both net and spot form alleles from the use of RAPD markers. A similar result was seen in two isolates collected from fields in Eastern Europe as evidenced by an intermediate cluster in a principal components analysis and AFLP haplotype (Leisova et al. 2005).

The management of net blotch can be accomplished by several methods but likely should be combined in an integrated pest management strategy. As net blotch is a stubble-borne disease, cultural practices such as crop rotation can help reduce the accumulation of primary inoculum (Liu et al. 2011). Additionally, seed treatments with the chemicals triadimenol or maneb were seen to result in yield increases of 12.6% and 12.4%, respectively (Martin 1985). However, the deployment of effective genetic resistance is often considered to be the most environmentally friendly and desirable means of control (Shipton; Mathre 1997).

Taxonomy and Life Cycle of *Pyrenophora teres* f. *teres.*

Pyrenophora teres is taxonomically classified into the Kingdom Fungi, the Phylum Ascomycota, the Class of Dothideomycetes, the Order Pleosporales, the Family Pleosporaceae, the Genus *Pyrenophora,* and the Species *teres*. Originally, *Pyrenophora teres* was placed into the genus *Helminthosporium,* however, its status was later changed due to cylindrical nature of its conidia, association with *Pyrenophora* species, and the germination of all conidial cells. (Shoemaker 1959; Alcorn 1988). Using mating type gene sequence, phylogenetic analysis reaffirmed *P. teres* classification into the Pleosporales order (Rau et al. 2005).

P. teres f. *teres* overwinters on barley residue as sexual fruiting bodies known as pseudothecia. In laboratory conditions, pseudothecia may form in as little as two months. However, it has been observed that under field conditions, fertile pseudothecia may require up to six months to develop and may be dependent on the moisture content of the barley stubble (Shipton et al. 1973). Additionally, temperatures of approximately 10-15 °C are optimal for pseudothecia formation (Shipton et al. 1973). At the beginning of the following growing season, ascospores are actively released from the pseudothecia, become wind-borne, and act as the primary inoculum. Alternatively, mycelium from infected seed may become the primary inoculum, although may not be an important factor in disease development (Shipton et al. 1973; Jordan 1981). Following primary infection, the production of conidia is initiated and acts as secondary inoculum. Multiple generations of conidia occur throughout the growing season, which can be disseminated via rain splash or wind and unlike ascospores, are not forcibly discharged (Shipton et al. 1973; Mathre 1997). To complete the cycle, senescent tissue is then colonized by the pathogen whereby pseudothecia may be formed to produce primary inoculum for the following growing season.

Genetic and Phenotypic Diversity of *Pyrenophora teres* f. *teres*

Understanding the dynamics of a plant pathogen population allows researchers to effectively deploy host resistance genes. As many plant pathogens are highly adaptable, great care must be taken in regards to the type and manner in which host resistance is utilized. Organisms with high levels of mutation that reproduce both sexually and asexually, and exist in large populations with possible gene flow are considered to have evolutionary potential (McDonald and Linde 2002). These pathogens in particular are of concern to the plant pathology community, as they are more likely to adapt and overcome the selection pressures exerted on

them, such as the application of fungicides or deployment of genetic resistance. Thus, knowledge of the genetic structure of a pathogen population will be of great use to combat the ever-evolving pathogen (McDonald and Linde 2002).

The emergence of molecular techniques allowed for the thorough investigation of population genetics and several groups have utilized them to specifically characterize global collections of *P. teres* f. *teres*. Peever and Milgroom (1994) studied the genetic variation of five *P. teres* f. *teres* populations derived from Germany, New York (U.S.A.), North Dakota (U.S.A.), and two from Alberta (Canada) by developing RAPD markers. By analyzing allelic diversities between and within populations, it was determined that 46% of the genetic diversity stemmed from differences among populations. The two least differentiated populations were both from Alberta and only exhibited 5% genetic differentiation, likely due to their close proximity of only 20 km. Additionally, 23 multilocus genotypes were identified among individuals, with the New York and German populations possessing five and nine unique multilocus genotypes, respectively. A possible explanation for the relatively high level of genetic differentiation could be restricted migration of the pathogen, thereby limiting gene flow. Additionally, it was determined that the majority of marker pairs were randomly associated for all populations except New York, indicating gametic equilibrium and suggesting that sexual reproduction is occurring in these regions (Peever and Milgroom 1994). In regards to diversity levels within fields and gametic disequilibrium, similar results were observed in *P. teres* f. *teres* populations derived from two barley fields in Sweden from varieties Golf and Svani (Jonsson et al. 2000). Using three primer sets producing 19 reproducible RAPD bands, 64 isolates from each field were genotyped and a high level of diversity was observed as each isolate represented a unique multilocus genotype. Low levels of gametic disequilibrium were detected, indicating a

prevalence of sexual recombination within each population. Additionally, only 5.3% of the variation was due to genetic differentiation between fields. This agrees with the results of the comparison of two fields in Alberta, Canada by Peever and Milgroom (1994), where similar to the fields sampled in Sweden, were only separated by 20 km and had 5% of variation attributed to differentiation between sites (Jonsson et al. 2000). Rau et al. (2003) collected 150 isolates from five regions in Sardinia, Italy, identifying both net form and spot form isolates proportioned at 45% and 55%, respectively, of the total isolates based on symptomatology. Molecular and subsequent cluster analysis using AFLP markers split isolates into two distinct groups corresponding to net and spot form isolates. Although several net form isolates clustered with spot form isolates, further phenotypic analysis verified the molecular classification, indicating the robustness of the AFLP analysis for diagnostic purposes. Incorrect placement of isolates into net or spot form groups based on the symptoms exhibited on the host may have occurred due to misdiagnosis or isolation of the alternative form due to the occurrence of both forms on the same sampled tissue. Differentiation between net form populations was similar to that observed by Peever and Milgroom (1994), with 43% of the variation being attributed to differences among the populations. Of the 68 individuals in the net form cluster, 46 haplotypes were detected and low levels of linkage disequilibrium indicated that in congruence with previous studies, *P. teres* f. *teres* undergoes sexual reproduction under field conditions. However, based on an Index of Association test, it appeared that both sexual and asexual reproduction occurred in different spot form populations, possibly due to environmental differences (Rau et al. 2003). Illustrating the diversity within *P. teres* f. *teres* populations, Serenius et al. (2005) utilized 175 AFLP markers to identify 70 distinct multilocus genotypes from 72 isolates collected in Finland. Additionally, isolates were genotyped with markers specific to the mating type genes (Rau et al. 2005) and

were determined to occur in approximately equal proportions. The mating type data along with AFLP genotype diversity suggest random mating occurring in the fields of Finland. This research also supports previous results of significant differentiation between populations, suggesting genetic isolation and limited gene flow (Serenius et al. 2005). Unlike previous studies, Leisova et al. (2005) found that genetic differentiation occurred between *P. teres* f. *teres* populations in the Czech and Slovak Republics when comparing the years in which they were sampled and not based on geographic location. Additionally, based on AFLP haplotypes, genetic variability decreased in *P. teres* f. *teres* populations from 2002-2003. Variability in the year 2002 was deemed similar to the level of diversity observed from 1996-2001. The authors speculate that this may be due to wide-spread flooding occurring at the end of the 2002 growing season in Europe or by a decrease in sexual reproduction (Leisova et al. 2005). Population structure was further studied on a global scale using two *P. teres* f. *teres* collections (Serenius et al. 2007). One collection (MTT) consisted of 167 isolates sampled from Finland, Russia, Sweden, United States, United Kingdom, Denmark, Canada, Australia, and the Czech Republic. Another collection (SARDI) used in this study contains 139 isolates strictly from Australia. *P. teres* f. *teres* was the most prevalent form observed in the MTT collection, whereas *P. teres* f. *maculata* comprised the majority of isolates in the Australian SARDI collection. Similar to the findings of Leisova et al. (2005), significant genetic differentiation occurred between sampling years in the Finnish population. The Russian population was observed to be the most diverse, as evidenced by each isolate harboring a unique AFLP genotype and the relative amount of polymorphic markers identified. It is postulated that the high levels of diversity seen in the Russian *P. teres* f. *teres* population may be due to its proximity to the center of origin of barley in the Fertile Crescent, where pathogen populations generally exhibit higher levels of variation (Serenius et al.

2007). Although previous research has indicated the prevalence of sexual reproduction occurring in the natural environment, its occurrence has also been seen to be variable depending on location. The hypothesis of random mating was rejected in the Finnish *P. teres* f. *teres* population and may be explained by the cold climate of this region and cultural methods, such as the lack of no-till practices, thereby reducing the amount of barley stubble near the soil surface (Serenius et al. 2007). Local population structure has been analyzed using two *P. teres* f. *teres* populations derived from Fargo, ND and Langdon, ND consisting of 75 isolates (Liu et al. 2012). Genotyping of this collection with 13 SSR markers revealed 40 distinct haplotypes, indicating high levels of genetic variation. However, in three site-years (Fargo 2005, Langdon 2005, and Fargo 2007), nearly clonal populations were observed, possibly due to a strict mode of asexual reproduction. A small but significant genetic differentiation was seen between the Fargo and Langdon populations with 11% of the variation being attributed to location. As observed by Leisova et al. (2005) and Serenius et al. (2007), a large amount of variation was attributed to the sampling year, possibly due to the pathogen rapidly adapting to local selection pressures. Additionally, sexual reproduction appears to be occurring in ND, as very low proportion of pairwise marker comparisons exhibited significant gametic disequilibrium and both mating type genes were present in pathogen populations in equal proportions (Liu et al. 2012).

In order to properly deploy effective resistance towards NFNB in elite barley lines, extensive knowledge of the local pathotypes of the pathogen population must be attained. As *P. teres* is a prevalent and economically important disease in Canada, investigation into the virulence structure of pathogen populations was warranted. A survey in the prairie provinces of Canada in 1974 identified three biotypes of *P. teres* (N-type, VN-type, and S-type) by utilizing a differential set comprised of four barley lines: Betzes, Fergus, Bonanza, and CI5791. Two of the

biotypes corresponded to NFNB caused by *P. teres* f. *teres* and one biotype exhibiting circular necrotic symptoms corresponded to the recently classified *P. teres* f. *maculata* (Tekauz and Buchannon 1977; Smedegaard-Petersen 1971). Additionally, resistance to the net form isolates did not correlate with resistance to the spot form isolates, indicating that host resistance to these two forms is under separate control (Tekauz and Buchannon 1977). An additional survey was conducted of Western Canada in 1976 to determine the distribution and incidence of the three previously identified *P. teres* biotypes (Tekauz 1978). A total of 114 fields were sampled and net blotch was identified in every two-rowed field (44 fields) and 61% of six-rowed fields (70 fields). The N-type and VN-type were most predominant with incidences of 58% and 39%, respectively. Incidence of the spot form biotype (S-type) only comprised 3% of the isolates collected. Additionally, the distribution of each biotype varied by province. N-type was predominant in Alberta, but rare in Manitoba. The VN-type was the most common biotype in Manitoba, but not in Alberta. Both biotypes were found equally as common in the province of Saskatchewan (Tekauz 1978). Although these surveys gave an initial impression of the diversity and distribution of *P. teres* in Canada, a more extensive study was needed to investigate the pathotype diversity of this pathogen. A survey conducted in 1985 sampled 219 barley fields across Western Canada from southeastern Manitoba to British Columbia (Tekauz 1990). A total 219 isolates were collected and virulence was analyzed using a differential set consisting of 12 barley lines. Following characterization, it was determined that net form isolates comprised 82% of the isolates collected and could be differentiated into 45 pathotypes based on the phenotypes of the differential lines. These results indicated high levels of diversity present in the pathogen population in Western Canada and were shown to be considerably greater than previous studies, possibly indicating ongoing sexual recombination. However, it is also likely due to the alteration

and increase of the differential lines used (Tek`auz 1990). A more recent survey of Western Canada was conducted from 2009-2012 and identified 39 *P. teres* f. *teres* isolates (Akhavan et al. 2016). The isolates were inoculated onto a set of barley differentials consisting of nine lines and the results indicated the presence of 16 distinct pathotypes. Additionally, a total of seven novel pathotypes were identified and three previously reported pathotypes were not observed, indicating a potential shift in virulence patterns within the pathogen population (Akhavan et al. 2016).

In addition to the research on the diversity of pathogen virulence in Canada, several studies have characterized and identified pathotypes from pathogen populations collected in the United States. Steffenson and Webster (1992) collected 91 *P. teres* f. *teres* isolates in California from 1984-1986 and utilized 22 barley genotypes as a differential set. Results indicate the presence of 13 pathotypes with varying predominance from 28.6% of the total isolates collected for pathotype 3-10-15-19-21 to less than 7% for the least common pathotypes. The amount of variation may be expected, as the sexual stage of the pathogen has been identified in California barley fields (Steffenson and Webster 1992). Another phenotypic diversity study using a small but diverse set of isolates identified 15 pathotypes through the evaluation of 25 differential barley lines (Wu et al. 2003). The isolates were collected from North Dakota (U.S.A.), California (U.S.A.), Minnesota (U.S.A.), Montana (U.S.A.), Saskatchewan (Canada), Manitoba (Canada), Norway, Australia, New Zealand, Israel, Morocco, Australia, and the United Kingdom. Although the amount of pathotypes identified is relatively high compared to the amount isolates used, this likely is attributed to the geographic diversity of the collection. Additionally, eight lines from the differential set were resistant to all *P. teres* f. *teres* isolates tested, indicating that they may be a useful source of resistance for breeding programs (Wu et al. 2003). More recently, a survey was

conducted in North Dakota to determine the virulence profile of the local *P. teres* f. *teres* population (Liu et al. 2012). From 2004 to 2007, a total of 75 isolates were collected from Fargo, ND and Langdon, ND. Evaluation of a differential set consisting of 22 barley lines resulted in the identification of 49 pathotypes in the ND population, indicating a high level of phenotypic diversity. Comparison of specific lines used in the differential set to the previous studies of Steffenson and Webster (1992) and Wu et al. (2003) revealed marked differences in virulence patterns. Previously, the barley line Prato was susceptible to the majority of *P. teres* f. *teres* isolates collected from California, whereas barley genotypes originating from China were resistant. The opposite was true with the ND population, with a large proportion of the ND isolates being avirulent on Prato but highly virulent on lines of Chinese descent (Steffenson and Webster 1992; Wu et al. 2003; Liu et al. 2012). Additionally, three barley lines from the differential set (CI5791, Heartland, and Algerian) exhibited high levels of resistance to all isolates collected from ND and may be of use to local barley breeders to incorporate into their programs.

Extensive research has been conducted to determine genetic variability of *P. teres* f. *teres* populations, as well as the diversity of virulence patterns. It appears that this pathogen has the propensity to adapt to its local selection pressures rapidly and has a high evolutionary potential due to its ability to reproduce both sexually and asexually. The results of population genetics research of this pathogen correlate with findings of phenotypic diversity studies, as both find high variability at the genetic and virulence level. For the optimal management of this disease, these aspects of pathogen populations need to be continually monitored in barley producing regions, as quick genetic diversification may lead to the breakdown of the deployed NFNB resistance.

Toxins Produced by *Pyrenophora teres f. teres*

Host-selective toxins (HSTs) are molecules such as small proteins or low molecular weight metabolites produced by a pathogen that function in pathogenicity and when targeting a specific host possessing a corresponding sensitivity gene, facilitate a compatible reaction (Wolpert et al. 2002). The infiltration of HSTs into a sensitive host results in a typical programmed cell death (PCD) response including the production of reactive oxygen species (ROS), DNA laddering, fragmentation of the nucleus, loss of mitochondrial function, and electrolyte leakage (Wolpert et al. 2002; van Doorn and Woltering 2005; Liu et al. 2015). Additionally, transcriptional reprogramming of genes involved in cell death pathways associated with the defense response occurs, as evidenced in the *Pyrenophora tritici-repentis*-wheat system (Adhikari et al. 2009; Pandelova et al. 2009).

It has been documented that *P. teres* f. *teres* has the ability to produce HSTs, or necrotrophic effectors, both proteinaceous and non-proteinaceous. Smedegard-Peterson (1977) isolated and purified two toxins from *P. teres* f. *teres* culture filtrates designated toxin A and toxin B. It was observed that both toxins are stable in acidic and alkaline conditions, as well as heat stable. Phytotoxicity assays determined that toxin A was more potent than toxin B. Both toxins induced similar symptoms of chlorosis formation within three days and necrosis within five days, however, approximately five to six times the concentration of toxin B was needed to cause the same degree of symptoms (Smedegard-Peterson 1977). In addition to toxin A and toxin B, a third molecule, toxin C, was identified (Bach et al. 1979). The structure of toxin A was determined to be N-(2-amino-2-carboxyethyl) aspartic acid, which had previously never been characterized from nature. Toxin B, an anhydroaspergillomarasmine A compound, may be an artifact of toxin isolation, or a byproduct of toxin C production, an aspergillomarasmine A

compound. Additionally, it was observed that one of the amino groups in toxin B did not have basic properties due to acylation and therefore was believed to have low toxic effects, in agreement with previous studies (Smedegard-Peterson 1977; Bach et al. 1979). It was later determined that anhydroaspergillomarasmine A (toxin B) is derived from aspergillomarasmine A (toxin C) at low pH and that due to low levels of anhydroaspergillomarasmine A in *P. teres* cultures, toxin C is the molecule with a major effect on virulence (Friis et al. 1991). Following the identification of toxins produced by *P. teres* f. *teres*, Weiergang et al. (2002) investigated the correlation between the elicitation of chlorosis and necrosis by the toxin and susceptibility to the pathogen. Following treatment with toxin A, chlorosis appeared between 48-72 hours post-treatment and necrosis began to appear after 120 hours. Symptoms elicited by toxin C were different, with necrosis being the predominant symptom observed, appearing after 48 hours. A high correlation between toxin induced symptom development and susceptibility to the fungus, with only a few exceptions. Barley cultivar Alexis was highly susceptible to *P. teres*, however, following treatment with toxin A and C, only medium and weak symptoms were observed, respectively. Additionally, susceptible barley line Jenny exhibited high levels of chlorosis following treatment of toxin A, but weak symptoms from toxin C. Although the correlation is not perfect, this study demonstrates the use of toxins for a rapid screening of barley germplasm for NFNB resistance (Weiergang et al. 2002).

Further studies have been conducted to identify additional virulence components from *P. teres* f. *teres*. In addition to the isolation of low molecular weight HST compounds, proteinaceous metabolites were also identified from cell-free filtrates of *P. teres* f. *teres* and *P. teres* f. *maculata* (Sarpeleh et al. 2007). It was determined that depending on concentration, protease treatment severely inhibited or abolished any phytotoxic properties of these proteins,

which range in size from 10-100 kD. Additionally, the isolated proteins induced a necrotic response, whereas the low molecular weight molecules elicited a general chlorosis. The necrosis induced by the proteinaceous metabolites were host specific, as evidenced by the appearance of necrotic symptoms on the susceptible line Sloop, minimal symptoms on resistant line CI9214, and no symptom development on non-hosts wheat, triticale, rye, and faba bean. The chlorosis caused by the low molecular weight non-proteinaceous compounds appeared to be non-selective, appearing on resistant and susceptible barley lines as well as other species tested (Sarpeleh et al. 2007). Further characterization of these proteins determined that they possess properties such as relative heat stability and light dependency, similar to toxins isolated from related fungal species, such as *Ptr* ToxA from *Pyrenophora tritici-repentis* (Ballance et al. 1989; Manning et al. 2005; Sarpeleh et al. 2008). Another study identified a proteinaceous effector of approximate size 6.5-12.3 kD, designated PttNE1, in the intracellular wash fluids (IWFs) of susceptible barley cultivar Hector inoculated with *P. teres* f. *teres* isolate 0-1. Following infiltration of the IWFs, necrosis was observed on susceptible variety Hector, however, no symptoms were elicited in resistant line NDB112. Sensitivity to the IWFs was mapped in a Hector x NDB112 recombinant inbred line (RIL) population and was localized to the commonly mapped centromeric region of chromosome 6H (Liu et al. 2015).

Ongoing efforts are being placed on the identification of necrotrophic effectors via the power of pathogen genetics. Two *P. teres* f. *teres* isolates, 15A and 6A, are virulent on barley cultivars Kombar and Rika, respectively. A bi-parental population was developed derived from a cross of isolates 15A and 6A and utilized to conduct a quantitative trait loci (QTL) analysis to identify loci associated with pathogen virulence (Shjerve et al. 2014). Two virulence QTL were identified from each isolate, designated VK1, VK2, VR1, and VR2. Progeny isolates with single

Mendelized virulence loci were used to phenotype a Rika x Kombar double haploid population and susceptibility to each progeny isolate mapped to the previously mapped region near the centromere of chromosome 6H (reviewed below). These results indicate that *P. teres* f. *teres* isolates 15A and 6A both produce two unique necrotrophic effectors that are recognized by a single or multiple genes within the same genomic region (Shjerve et al. 2014).

It is apparent that the production of low molecular weight compounds and proteins by *P. teres* f. *teres* play an active role in virulence and symptom development. Additionally, the host specific nature of proteinaceous effectors indicates the requirement of a corresponding host sensitivity gene, whereas the toxins inducing chlorosis appear to be general elicitors. The research conducted on the mechanisms of virulence that *P. teres* f. *teres* utilizes illustrates the diverse nature of its repertoire and further investigation of the necrotrophic effectors it produces will grant insight into the complex molecular nature of how this disease occurs.

Host Resistance and Susceptibility to Net Form Net Blotch of Barley

Although the first documented research of genetic inheritance of host resistance to NFNB found that it operated as a single dominant R-gene (Geschele 1928), genetic resistance to *P. teres* f. *teres* has been observed to be remarkably complex, as dominant, incomplete, and recessive resistances have been identified (Friesen et al. 2006, Mode and Schaller 1958; Abu Qamar et al. 2008). Douiyssi et al. (1996) investigated the genetic inheritance of NFNB resistance under greenhouse conditions using Moroccan *P. teres* f. *teres* isolates and barley cultivar Heartland as the resistant parent. Heartland was crossed to susceptible cultivars Rabat 071, Arig 8, and ACSAD 176 and $F_{2:3}$ families were examined to determine the manner of inheritance. It was determined that Heartland possessed both monogenic dominant and recessive resistances. Also, the Heartland x Arig 8 population did not fit monogenic segregation ratios, indicating a more

complex mode of resistance or susceptibility (Douiyssi et al. 1996). Utilizing crosses of resistant barley lines Ming, Canadian Lake Shore, CI 4922, Harbin, and Manchurian to susceptible lines Atlas and Atlas 46, Mode and Schaller (1958) determined that resistance may be incompletely dominant, as evidenced by the individual plant scores within segregating $F_{2:3}$ families. As NFNB is an economically important disease, breeding for durable resistance is a priority. However, the quantitative nature of resistance complicates breeding schemes, whereas dominant resistance needs to be incorporated into elite lines but recessive resistance, or dominant susceptibility, needs to be removed (Liu et al. 2011). At least 18 studies have been conducted using bi-parental populations to identify QTL associated with resistance or susceptibility to NFNB. QTL have been identified on all barley chromosomes at both seedling and adult stages and it appears that in some cases, the same source of resistance may be effective at both the adult plant and seedling stages, such as a locus detected on chromosome 6H (Grewal et al. 2008). The major seedling NFNB resistance QTL, the chromosome on which they reside, and the population in which they were identified to date are summarized as follows: three unnamed QTL (4H and two on 6H), Steptoe/Morex, (Steffenson et al. 1996); *Pt,,a* (3HL), Igri/Franka (Graner et al. 1996); three unnamed QTL (3H and two on 6H), Areno/Hor9088 (Richter et al. 1998); *QRpts2S* (2HS), *QRpts3L* (3HL), Alexis/Sloop (Raman et al. 2003); *QRpts2L* (2HL), *QRpts3La* (3HL), Arapiles/Franklin (Raman et al. 2003); *QRpts3lb* (3HL), *QRpts4* (4H), Sloop/Halcyon (Raman et al. 2003); *QRpts6L* (6HL), Sloop-sib/Alexis (Raman et al. 2003); three unnamed QTL (2H, 3H, and 6H), Tallon/Kaputar (Cakir et al. 2003); unnamed QTL (6H), VB9524/ND11231 (Cakir et al. 2003); two unnamed QTL (2HS and 6HS), Chevron/Stander (Ma et al. 2004); two unnamed QTL (2H and 6H), VB9524/ND11231 (Emebiri et al. 2005); *Rpt-1H-5-6* (1H), *Rpt-3H-4* (3H), *Rpt-4H-5-7* (4H), OUH602/Harrington (Yun et al. 2005); *Rpt5* (6H), Rolfi/CI9819 (Manninen et

al. 2000,2006); unnamed QTL (6H), Q21861/SM89010 (Friesen et al. 2006); *QRpt6* (6H), *QRptts2* (2H), *QRptts4* (4H), CDC Dolly/TR251 (Grewal et al. 2008); *rpt.r*/*rpt.k* (6H), Rika/Kombar (Abu Qamar et al. 2008); two unnamed QTL (6H-bin2 and 6H-bin6), M120/Sep2-72 (St. Pierre et al. 2010); *QRpt6* (6H), *QRptts1.1* (1H), *QRptts1.2* (1H), CDC Bold/TR251 (Grewal et al. 2012); *Iso_QLB* (7HS), *QTL*$_{UHs}$-3H (3H), *QTL*$_{UHs}$-7H (7HS), *QTL*$_{UHs}$-3H-1 (3HS), *QTL*$_{UHs}$-3H-2 (3HS), Uschi/HHOR3073 (Konig et al. 2014); *QTL*$_{PHs}$*-3H* (3H), *QTL*$_{PHs}$*-4H* (4HL), *QTL*$_{PHs}$*-5H* (5HS), (P x V)/HHOR9484 (Konig et al. 2014); nine unnamed QTL (1HL, 2HS, 3HS, 3H centromere, 3HL, three QTL on 5HS, and two on 6H), Hector/NDB112 (Liu et al. 2015).

The centromeric region of chromosome 6H has been observed to be a very important locus for NFNB resistance or susceptibility. Numerous QTL analyses have been conducted utilizing a diverse host populations and equally diverse pathogen isolates with many of the associations mapping to the centromere of chromosome 6H (Steffenson et al. 1996; Graner et al. 1996; Richter et al. 1998; Raman et al. 2003; Cakir et al. 2003; Ma et al. 2004; Emebiri et al. 2005; Yun et al. 2005; Manninen et al. 2000; Manninen et al. 2006; Friesen et al. 2006; Grewal et al. 2008; Abu Qamar et al. 2008; St. Pierre et al. 2010; Liu et al. 2015). It is postulated that since so many studies have resulted in the identification of dominant resistance and susceptibility at the same centromeric 6H locus, a cluster of genes may be harbored within this region, governing reaction to NFNB. This would also indicate that there must be a strongly diverse repertoire of necrotrophic effectors or avirulence gene products present in the pathogen populations that may be recognized directly or indirectly by these host sensitivity or resistance genes.

Efforts have also been placed on mapping NFNB resistance/susceptibility at a higher resolution. Abu Qamar (2008) utilized a double haploid (DH) population derived from a cross of barley cultivars Rika and Kombar to map recessive resistance genes *rpt.r* and *rpt.k*, hereafter referred to as dominant susceptibility, to two NFNB isolates, 6A and 15A. It was seen that Rika was susceptible to isolate 6A but Kombar was resistant. The opposite was true with isolate 15A, where Rika was resistant and Kombar was susceptible. F_2 segregation analysis resulted in a 3:1 (S:R), confirming the nature of the susceptibility as dominant. The population was genotyped with SSR markers and later saturated with additional SSR, sequence tagged site (STS), CAPS, and RFLP markers. The dominant susceptibility to both isolates mapped to the centromeric region of chromosome 6H to approximately 5.9 cM and was tightly linked in repulsion (Abu Qamar 2008). The region was further delimited by Liu et al. (2010). Marker development was initiated via the mining of barley expressed sequence tags (ESTs) to identify sequences containing SSRs. Additionally, STS markers were designed from EST sequence which did not contain sufficient repeats (Liu et al. 2010). The addition of newly developed markers onto the genetic map further delimited the dominant susceptibility locus to approximately 3.3 cM (Liu et al. 2010). These mapping efforts greatly advance the progress towards positional cloning of the *P. teres* f. *teres* isolate 6A and 15A dominant susceptibility factors. The eventual cloning and characterization of this gene(s) will grant the scientific community a greater understanding of the intricate molecular mechanisms at work within this pathosystem and enhance the ability of a breeder to effectively develop NFNB resistant barley cultivars.

Molecular Mechanisms of Host Resistance

Recent research on the plant immune system has illustrated its complexity at the genetic and molecular level. However, pioneering research by H.H. Flor (1956) began this investigation

with the establishment of his seminal gene-for-gene theory. By studying the genetics of both flax (*Linum usitatissimum*) and phytopathogen flax rust (*Melamspora lini*), a novel genetic relationship was observed. Flor determined that the presence of a dominant host resistance gene and a dominant pathogen avirulence gene conditioned an incompatible reaction, or resistance (Flor 1956). The lack of either the resistance or avirulence gene resulted in the loss of pathogen recognition by the plant and a compatible reaction. Later research determined that the resistance reaction occurs due to a programmed cell death response initiated by the host upon recognition of the biotrophic pathogen, essentially eliminating the pathogen's nutrient source and effectively preventing further infection and colonization (Dangl and Jones 2001). However, in regards to necrotrophic pathogens, which feed from senescing tissue, a similar model holds true but differs mainly in the outcome of the interaction. In the inverse gene-for-gene model, a dominant host susceptibility gene recognizes a necrotrophic effector secreted from the pathogen, resulting in a compatible reaction (Friesen et al. 2007). Lack of recognition due to the absence of the host susceptibility gene or pathogen effector fails to trigger programmed cell death, thus withholding a food source from the necrotroph. Additionally, as the gene-for-gene interaction with flax and flax rust is a qualitative reaction, inverse gene-for-gene interactions appear to operate in a quantitative fashion (Friesen et al. 2008).

To defend against the multitude of pathogens that attempt to infect and colonize plants, a two-tiered immune system evolved. The two layers consist of a basal response, which recognizes conserved motifs from various classes of pathogens, and a race-specific recognition response, which perceives molecules produced by specific pathotypes of a pathogen species. An ongoing battle is occurring between the host and pathogen and is often illustrated on an evolutionary scale as the 'zig zag' model (Jones and Dangl 2006).

Pathogen associated molecular patterns (PAMPs), also known as microbe associated molecular patterns (MAMPs), are molecules necessary for the maintenance of high levels of pathogen fitness, the loss of which results in an evolutionary disadvantage (Zipfel 2008). Recognition of PAMPs is mediated by a PAMP recognition receptor (PRR) (Boller and He 2009). PRRs are often membrane anchored leucine-rich repeat receptor like kinases (LRR-RLK) and upon perception, initiate an intracellular signaling cascade to trigger a rapid, localized cell death known as the PAMP triggered immunity (PTI) response. Cellular responses such as signaling via mitogen activated protein kinases (MAPKs), production of reactive oxygen species, as well as calcium ion influxes and transcription of pathogenesis related (PR) proteins occur following induction of PTI (Jones and Dangl 2006; Zipfel 2008; Zipfel 2009; Dodds and Rathjen 2010; Thomma et al. 2011; Bigeard et al. 2015). Additionally, receptor like proteins (RLPs) that contain a LRR and transmembrane domain but lack a kinase domain may work in conjunction with a LRR-RLK via the formation of a heterodimer to trigger the PTI pathway (Zipfel et al. 2009; Dodds and Rathjen 2010). Alternatively, two LRR-RLKs may form a homodimer to begin the same response (Zipfel 2008). A hallmark example of a PAMP is from bacterial flagella. Flagella allow plant pathogenic bacteria to be motile and aid in the infiltration and colonization of host tissue. The loss of functional flagella can cause a severe inhibition or abolition of pathogenicity (Tans-Kersten et al. 2001). The N-terminus of bacterial flagella is highly conserved and it was determined that a 22 amino acid peptide (flg22) from the bacterial flagellin protein acts as a PAMP. Direct recognition of flg22 by host LRR-RLK FLS2 initiates PTI, offering basal resistance to many bacterial pathogens (Gomez-Gomez and Boller 2002; Chinchilla et al. 2006). PTI mediated by the recognition of PAMPs by host PRRs represents

phase one of the zig zag model and is the plant's first line of defense against a plethora of potential pathogens.

As the host's innate immune system successfully blocked pathogen infection through the recognition of vital PAMPs, pathogens developed virulence mechanisms to suppress and evade PTI (Jones and Dangl 2006; Boller and He 2009; Dodds and Rathjen 2010). The bacterial pathogen *Pseudomonas syringae* produces the effector AvrPtoB, which was found to target the kinase domain of the aforementioned host protein FLS2 for degradation via a C-terminal E3 ligase (Gohre et al. 2008). Also, it was determined that AvrPtoB and additional *P. syringae* effector AvrPto physically disrupt the formation of the FLS2/BAK1 complex, effectively inhibiting PTI at the receptor complex level (Shan et al. 2008). AvrPto also has the ability to interact with the kinase domain of FLS2, inhibiting its signaling function (Xiang et al. 2008). Manipulation or removal of FLS2 from the plasma membrane, as well as the interference of the ability of BAK1 to complex with FLS2, enhances the virulence of the pathogen by eliminating the potential of detection and allows subsequent infection.

As plant pathogens evolved to evade PTI, plants also responded to the new pressure of pathogen virulence factors through the development of cytoplasmic receptors. Many of these cytoplasmic proteins are comprised of two main domains, a nucleotide binding site (NBS) and a leicine rich repeat (LRR), and function to recognize pathogen effectors (Hammond-Kosack and Jones 1997; Ellis et al. 2000; Dangl and Jones 2001; Jones and Dangl 2006; Dodds and Rathjen 2010). An example of direct recognition of a pathogen protein by a host resistance gene is in the flax-flax rust pathosystem. Resistance alleles at the flax rust resistance L locus directly recognize diverse pathogen avirulence proteins in an allele specific manner. This recognition event triggers an elevated hypersensitive response and sequesters the biotrophic pathogen, preventing

colonization (Dodds et al. 2006). In the context of a biotroph, this response is known as effector triggered immunity (ETI). However, necrotrophs have evolved to intentionally initiate this cell death response and essentially generate a source of nutrients via host cell death. Similar to recognition of a biotroph, this may occur directly or indirectly. This phenomenon, termed necrotrophic effector triggered susceptibility (NETS), has been well documented in several pathosystems, such as the indirect perception of ToxA by Tsn1 in the *Pyrenophora tritici-repentis*-wheat system (Faris et al. 2010).

The evolutionary arms race does not stop following the development of host resistance proteins capable of recognizing pathogen virulence factors. Biotrophic pathogens will continually diversify their repertoire to evade detection, while the host will diversify its recognition mechanisms to maintain recognition specificity. However, in the case of inverse-gene-for-gene model, the host is under the selective pressure to avoid the specific interactions that result in the inappropriate elicitation of cell death by a necrotroph (Jones and Dangl 2006). The 'zig-zag' model illustrates this evolutionary relationship in a clear manner, however, the actual mechanisms of recognition are not as simple as direct interaction as in the aforementioned flax-flax rust system. Several models have been proposed and modified in recent years to explain on a biological level how host and pathogen proteins functioned in the initiation of the plant defense response. One such model is the guard hypothesis, which posits that two proteins, the resistance gene and the guardee, are required for proper plant defense. In this model, the resistance gene would recognize a pathogen induced manipulation of the guardee and trigger the defense pathways, thus indirectly detecting the pathogen effector (Dangl and Jones 2001; Jones and Dangl 2006). This model relies on the assumption that the guardee has a significant biological function within the plant defense response and alteration of it by the pathogen would

therefore enhance virulence (Dangl and Jones 2001). The decoy model was proposed to explain the opposing selective forces that may act on a guardee. In the absence of the resistance gene, diversifying selection would be placed on the guardee to evade manipulation by the pathogen and maintain host fitness. However, in the presence of the resistance gene, purifying selection would act on the guardee to improve its ability to recognize the pathogen effector (van der Hoorn and Kamoun 2008). The decoy model hypothesizes that plants may develop effector target mimics, which can be altered by pathogen effectors but do not biologically function in the host and therefore, manipulation by the pathogen would not have a detrimental effect on the host (van der Hoorn and Kamoun 2009). More recently, evidence has mounted for an improved model known as the integrated decoy model (Cesari et al. 2014). It was observed that in several systems, two proteins with NBS and LRR domains were required to initiate the defense response, however, one of the NBS-LRRs contained an unusual domain. It was proposed that these two proteins form a complex and the additional domain fused to a NBS-LRR acts as an effector target, eliciting a signaling response by the secondary NBS-LRR following pathogen detection (Cesari et al. 2014). An example in barley is the pair of genes *Rpg5* and *HvRga1,* which are required for resistance to the wheat stem rust pathogen *Puccinia graminis* f. sp. *tritici*. *HvRga1* is a typical NBS-LRR while *Rpg5* is comprised of a NBS, LRR, and serine-threonine protein kinase (STPK) domain (Wang et al. 2013). It is hypothesized that the protein products of these genes dimerize and the STPK domain of RPG5 is targeted by an effector, possibly due to a current biochemical function or due to homology to an ancestral effector target, followed by a signaling cascade initiated by HvRGA1 which results in resistance (Cesari et al. 2104; Wu et al. 2015).

Association Mapping

The identification of genes underlying a trait of interest has historically been accomplished through the development of bi-parental mapping populations stemming from a cross of two lines exhibiting a differential phenotype. This method works well in the detection of less common alleles, however, the level of diversity and genetic recombination is limited and the development of suitable mapping populations takes a considerable amount of time (Zhu et al. 2008; Rafalski 2010). Linkage disequilibrium (LD) is the nonrandom correlation between specific alleles at separate loci (Flint-Garcia et al. 2003). Association mapping exploits this phenomenon and offers an alternative to traditional mapping methods. In lieu of utilizing bi-parental populations, genome wide association studies (GWAS) utilize natural populations composed of diverse germplasm, thereby taking advantage of evolutionary recombination (Zhu et al. 2008). This alternative method offers several advantages compared to the use of bi-parental populations, such as the potential to detect marker trait associations (MTAs) at high-resolution depending on LD and marker density, ability to detect a greater number of positively associated loci, and being able to obtain results quicker due to the use of natural populations (Flint-Garcia et al. 2003; Yu et al. 2006; Zhu et al. 2008). In order to conduct a successful and biologically meaningful association study, the selection of the correct model for analysis is highly important. False positive associations are a concern when conducting a GWAS, and models that correct for population structure via principle components analysis or using Bayesian clustering methods, as well as accounting for familial relatedness, help to reduce this error rate (Pritchard et al. 2000; Yu et al. 2006; Zhao et al. 2007). Using these principles, additional models have been proposed that use a variation of relationship matrices by altering clustering or compression parameters to increase statistical power and decrease time of analysis (Zhang et al. 2010; Li et al. 2014).

In recent years, next generation sequencing has given researchers the ability to discover vast amounts of SNPs within their species of interest in a short period of time, with cost of discovery decreasing annually, such as the Infinium iSelect SNP assay for barley (Knief 2014; Muñoz-Amatriaìn et al. 2014). The identification of informative markers can be used for many applications, such as association mapping which has been employed to successfully identify genomic loci associated with disease resistance in economically important crop species, such as barley. Using 3072 SNP and 558 DArT markers, Roy et al. (2010) genotyped 318 wild barley accessions to generate genotypic information for association mapping of spot blotch resistance caused by the fungal pathogen *Cochliobolus sativus*. Association mapping conducted using the newly generated genotypic data and phenotypic data from inoculations of barley accessions with pathotype 1 representative isolate ND85F resulted in the identification 12 loci associated with resistance, of which, five had been previously identified (Roy et al. 2010). Another GWAS investigated potential sources of resistance to Fusarium head blight in barley breeding lines. Association mapping using 1536 SNPs and 768 advanced breeding lines from the Upper Midwest identified eight loci associated with deoxynivalenol (DON) accumulation and four loci for disease severity (Massman et al. 2011). Utilizing 360 elite Australian barley breeding lines, Ziems et al. (2014) employed an association mapping strategy and identified 15 MTAs for leaf rust (*Puccinia hordeii)* resistance, including five previously reported resistance genes (*rph1, Rpg3/19, Rph8/14/15, Rph20,* and *Rph21*) and four previously identified regions, as well as four novel loci. Although a GWAS has not been conducted for NFNB resistance, Tamang et al. (2015) conducted association mapping using the barley core collection consisting of 2062 previously genotyped barley lines (Muñoz-Amatriaìn et al. 2014) and four diverse *P. teres* f. *maculata* isolates collected from ND (U.S.A.), New Zealand, Australia, and Denmark. This

study detected 138 markers significantly associated with seedling resistance or susceptibility corresponding to loci on all seven barley chromosomes, including 21 previously unidentified QTL (Tamang et al. 2015).

As evidenced in barley, association mapping is a powerful tool that allows for the detection of novel genomic loci associated with a disease trait of interest. Depending on the marker density and the extent of LD, detection of significant associations at high resolution is possible. Additionally, GWAS allows for the rapid detection of markers significantly associated with disease resistance and therefore gives breeders immediate tools for marker assisted selection (MAS) and subsequent improvement of barley varieties.

Literature Cited

Abu Qamar, M., Liu, Z. H., Faris, J. D., Chao, S., Edwards, M. C., Lai, Z., Franckowiak, J. D., and Friesen, T. L. 2008. A region of barley chromosome 6H harbors multiple major genes associated with net type net blotch resistance. Theor. Appl. Genet. 117:1261

Adhikari, T. B., Bai, J., Meinhardt, S. W., Gurung, S., Myrfield, M., Patel, J., Ali, S., Gudmestad, N. C., and Rasmussen, J. B. 2009. *Tsn1*-Mediated Host Responses to ToxA from *Pyrenophora tritici-repentis.* Mol. Plant Microbe In. 22:1056-1068

Akhavan, A., Turkington, T. K., Askarian, H., Tekauz, A., Xi, K., Tucker, J. R., Kutcher, H. R., and Strelkov, S. E. 2016. Can. J. Plant Pathol. 38:183-196

Alcorn, J. L. 1988. The taxonomy of '*Helminthosporium*' species. Ann. Rev. Phytopathol. 26:37-56

Atanasoff, D., and Johnson, A. G. 1920. Treatment of cereal seeds by dry heat. J. Agric. Res. 18:379-390

Bach, E., Christensen, S., Dalgaard, L., Larsen, P. O., and Olsen, C. E. 1979. Structures, properties, and relationship to the aspergillomarasmines of toxins produced by *Pyrenophora teres*. Physiol. Plant Pathol. 14:41-46

Badr, A., Muller, K., Schafer-Pregl, R., El Rabey, H., Effgen, S., Ibrahim, H. H., Pozzi, C., Rohde, W., and Salamini, F. 2000. On the Origin and Domestication History of Barley (*Hordeum vulgare*). Mol. Biol. Evol. 17:499-510

Ballance, G. M., Lamari, L., and Bernier, C. C. 1989. Purification and characterization of a host-selective necrosis toxin from *Pyrenophora tritici-repentis*. Physiol. Mol. Plant Pathol. 35:203-213

Bamshad, M. J., Ng, S. B., Bigham, A. W., Tabor, H. K., Emond, M. J., Nickerson, D. A., and Shendure, J. 2011. Exome sequencing as a tool for Mendelian disease gene discovery. Nat. Rev. Genet. 12:745-755

Bennetzen, J. L. and Freeling, M. 1997. The Unified Grass Genome: Synergy in Synteny. Genome Res. 7:301-306

Bigeard, J., Colcombet, J., and Hirt, H. 2015. Signaling Mechanisms in Pattern-Triggered Immunity (PTI). Mol. Plant. 8:521-539

Blattner, F. R., and Mendez, A. G. B. 2001. RAPD data do not support a second center of barley domestication in Morocco. Genet. Res. Crop Evol. 48:13-19

Boller, T., and He, S. Y. 2009. Innate Immunity in Plants: An Arms Race Between Pattern Recognition Receptors in Plants and Effectors in Microbial Pathogens. Science. 324:742-744

Cakir, M., Gupta, S., Platz, G. J., Ablett, G. A., Loughman, R., Emebiri, L. C., Poulsen, D., Li, C. D., Lance, R. C. M., Galwey, N. W., Jones, M. G. K., and Appels, R. 2003. Mapping and validation of the genes for resistance to *Pyrenophora teres* f. *teres* in barley (*Hordeum vulgare* L.). Aust. J. Agric. Res. 54:1369-1377

Campbell, G. F., Crous, P. W., and Lucas, J. A. 1999. *Pyrenophora teres* f. *maculata*, the cause of Pyrenophora leaf spot of barley in South Africa. Mycol. Res. 103:257-267

Campbell, G. F., Lucas, J. A., and Crous, P. W. 2002. Evidence of recombination between net- and spot-type populations of *Pyrenophora teres* as determined by RAPD analysis. Mycol. Res. 106:602-608

Cesari, S., Bernoux, M., Moncuquet, P., Kroj, T., and Dodds, P. N. 2014. A novel conserved mechanism for plant NLR protein pairs: the "integrated decoy" hypothesis. Front. Plant Sci. 5:606

Chinchilla, D., Bauer, Z., Regenass, M., Boller, T., and Felix, G. 2006. The *Arabidopsis* Receptor Kinase FLS2 Binds flg22 and Determines the Specificity of Flagellin Perception. Plant Cell. 18:465-476

Dai, F., Nevo, E., Wu, D., Comadran, J., Zhou, M., Qiu, L., Chen, Z., Beiles, A., Chen, G., and Zhang, G. 2012. Tibet is one of the centers of domestication of cultivated barley. Proc. Natl. Acad. Sci. 109:16969-16973

Dangl, J. L., and Jones, J. D. G. 2001. Plant pathogens and integrated defence responses to infection. Nature 411:826-833

Dodds, P. N., and Rathjen, J. P. 2010. Plant immunity: towards an integrated view of plant-pathogen interactions. Nature Genet. 11:539-548

Dodds, P. N., Lawrence, G. J., Catanzariti, A., The, T., Wang, C. A., Ayliffe, M. A., Kobe, B., and Ellis, J. G. 2006. Direct protein interaction underlies gene-for-gene specificity and coevolution of the flax resistance genes and flax rust avirulence genes. Proc. Natl. Acad. Sci. 103:8888-8893

Douiyssi, A., Rasmusson, D. C., and Wilcoxson, R. D. 1996. Inheritance of Resistance to Net Blotch in Barley in Morocco. Plant Disease. 80:1269-1272

Ellis, J., Dodds, P., and Pryor, T. 2000. Structure, function and evolution of plant disease resistance genes. Curr. Opin. Plant Biol. 3:278-284

Ellwood, S. R., Liu, Z., Syme, R. A., Lai, Z., Hane, J. K., Keiper, F., Moffat, C. S., Oliver, R. P., and Friesen, T. L. 2010. A first genome assembly of the barley fungal pathogen *Pyrenophora teres* f. *teres*. Genome Biol. 11:R109

Emebiri, L. C., Platz, G., and Moody, D. B. 2005. Disease resistance genes in a doubled haploid population of two-rowed barley segregating for malting quality attributes. Aust. J. Agric. Res. 56:49-56

Faris, J. D., Zhang, Z., Lu, H., Lu, S., Reddy, L., Cloutier, S., Fellers, J. P., Meinhardt, S. W., Rasmussen, J. B., Xu, S. S., Oliver, R. P., Simons, K. J., and Friesen, T. L. 2010. A unique wheat disease resistance-like gene governs effector-triggered susceptibility to necrotrophic pathogens. Proc. Natl. Acad. Sci. 107:13544-13549

Flint-Garcia, S. A., Thornsberry, J. M., and Buckler, E. S. 2003. Structure of Linkage Disequilibrium in Plants. Annu. Rev. Plant Biol. 54:357-374

Flor, H. H. 1956. The Complementary Genic Systems in Flax and Flax Rust. Adv. Genet. 8:29-54

Friesen, T. L., Faris, J. D., Lai, Z., and Steffenson, B. J. 2006. Identification and chromosomal location of major genes for resistance to *Pyrenophora teres* in a doubled-haploid barley population. Genome. 49:855-859

Friesen, T. L., Faris, J. D., Solomon, P. S., and Oliver, R. P. 2008. Host-specific toxins: effectors of necrotrophic pathogenicity. Cell. Microbiol. 10:1421-1428

Friesen, T. L., Meinhardt, S. W., and Faris, J. D. 2007. The *Stagonospora nodorum*-wheat pathosystem involves multiple proteinaceous host-selective toxins and corresponding host sensitivity genes that interact in an inverse gene-for-gene manner. Plant J. 51:681-692

Friis, P., Olsen, C. E., and Moller, B. L. 1991. Toxin Production in *Pyrenophora teres*, the Ascomycete Causing the Net-spot Blotch Disease of Barley (*Hordeum vulgare* L.). J. Biol. Chem. 20:13329-13335

Geschele, E. E. 1928. The response of barley to parasitic fungi *Helminthosporium teres* Sacc. Bull. Appl. Bot. Genet. Plant Breed. 19:371-384

Gohre, V., Spallek, T., Haweker, H., Mersmann, S., Mentzel, T., Boller, T., de Torres, M., Mansfield, J. W., Robatzek, S. 2008. Plant Pattern-Recognition Receptor FLS2 Is Directed for Degradation by the Bacterial Ubiquitin Ligase AvrPtoB. Curr. Biol. 18:1824-1832

Gomez-Gomez, L., and Boller, T. 2002. Flagellin perception: a paradigm for innate immunity. Trends Plant Sci. 7:251-256

Graner, A., Foroughi-wehr, B., and Tekauz, A. 1996. RFLP mapping of a gene in barley conferring resistance to net blotch (*Pyrenophora teres*). Euphytica. 91:229-234

Grewal, T. S., Rossnagel, B. G., and Scoles, G. J. 2012. Mapping quantitative trait loci associated with spot blotch and net blotch resistance in a doubled-haploid barley population. Mol. Breeding 30:267-279

Hammond-Koksack, K. E., and Jones, J. D. G. 1997. Plant Disease Resistance Genes. Ann. Rev. Plant Physiol. Plant Mol. Biol. 48:575-607

International Barley Genome Sequencing Consortium. 2012. A physical, genetic and functional sequence assembly of the barley genome. Nature. 491:711-716

International Brachypodium Initiative. 2010. Genome sequencing and analysis of the model grass *Brachypodium distachyon*. Nature. 463:763–768.

Jones, J. D. G., and Dangl, J. L. 2006. The plant immune system. Nature 444:323-329

Jonsson, R., Sall, T., and Bryngelsson, T. 2000. Genetic diversity for random amplified polymorphic DNA (RAPD) markers in two Swedish populations of *Pyrenophora teres*. Can. J. Plant Pathol. 22:258-264

Jordan, T., Seeholzer, S., Schwizer, S., Toller, A., Somssich, I. E., and Keller, B. 2011. The wheat *Mla* homologue *TmMla1* exhibits an evolutionarily conserved function against powdery mildew in both wheat and barley. Plant J. 65:610-621

Jordan, V. W. L. 1981. Aetiology of barley net blotch caused by *Pyrenophora teres* and some effects on yield. Plant Pathol. 30:77-87

Keiper, F. J., Grcic, M., Capio, E., and Wallwork, H. 2008. Diagnostic microsatellite markers for the barley net blotch pathogens, *Pyrenophora teres* f. *maculata* and *Pyrenophora teres* f. *teres*. Australas. Plant Pathol. 37:428-430

Kellogg, E. A. 2001. Evolutionary history of the grasses. Plant Physiol. 125:1198-205

Knief, C. 2014. Analysis of plant microbe interactions in the era of next generation sequencing technologies. Front. Plant Sci. 5:1-23

Konig, J., Perovic, D., Kopahnke, D., and Ordon, F. 2014. Mapping seedling resistance to net form of net blotch (*Pyrenophora teres* f. *teres*) in barley using detached leaf assay. Plant Breeding. 133:356-365

Leisova, L., Kucera, L., Minarikova, V., and Ovesna, J. 2005. AFLP-based PCR markers that differentiate spot and net forms of *Pyrenophora teres*. Plant Pathol. 54:66-73

Leisova, L., Minarikova, V., Kucera, L., and Ovesna, J. 2005. Genetic Diversity of *Pyrenophora teres* Isolates as Detected by AFLP Analysis. J. Phytopathol. 153:569-578

Li, M., Liu, X., Bradbury, P., Yu, J., Zhang, Y., Todhunter, R. J., Buckler, E. S., and Zhang, Z. 2014. Enrichment of statistical power for genome-wide association studies. BMC Biol. 12:73

Liu, Z. H., Zhong, S., Stasko, A. K., Edwards, M. C., and Friesen, T. L. 2012. Virulence Profile and Genetic Structure of a North Dakota Population of *Pyrenophora teres* f. *teres*, the Causal Agent of Net Form Net Blotch of Barley. Phytopathol. 102:539-546

Liu, Z., Ellwood, S. R., Oliver, R. P., and Friesen, T. L. 2011. *Pyrenophora teres*: profile of an increasingly damaging barley pathogen. Mol. Plant Pathol. 12:1-19

Liu, Z., Faris, J. D., Edwards, M. C., and Friesen, T. L. 2010. Development of Expressed Sequence Tag (EST)-based Markers for Genomic Analysis of a Barley 6H Region Harboring Multiple Net Form Net Blotch Resistance Genes. Plant Genome. 3:41-52

Liu, Z., Holmes, D. J., Faris, J. D., Chao, S., Brueggeman, R. S., Edwards, M. C., and Friesen, T. L. 2015. Necrotrophic effector-triggered susceptibility (NETS) underlies the barley-*Pyrenophora teres* f. *teres* interaction specific to chromosome 6H. Mol. Plant Pathol. 16:188-200

Lu, S., Platz, G. J., Edwards, M. C., and Friesen, T. L. 2010. Mating Type Locus-Specific Polyerase Chain Reaction Markers for Different *Pyrenophora teres* f. *teres* and *P. teres* f. *maculate*, the Causal Agents of Barley Net Blotch. Phytopathol. 100:1298-1306

Ma, Z., Lapitan, N. L. V., and Steffenson, B. 2004. QTL mapping of net blotch resistance genes in a doubled-haploid population of six-rowed barley. Euphytica. 137:291-296

Manninen, O. M., Jalli, M., Kalendar, R., Schulman, A., Afanasenko, O., and Robinson, J. 2006. Mapping of major spot-type and net-type net-blotch resistance genes in the Ethiopian barley line CI 9819. Genome. 49:1564-1571

Manninen, O., Kalendar, R., Robinson, J., and Schulman, A. H. 2000. Application of *BARE*-1 retrotransposon markers to the mapping of a major resistance gene for net blotch in barley. Mol. Gen. Genet. 264:325-334

Martin, R. A. 1985. Disease progression and yield loss in barley associated with net blotch, as influenced by fungicide seed treatment. Can. J. Plant Pathol. 7:83-90

Mascher, M., Muehlbauer, G. J., Rokshar, D. S., Chapman, J., Schmutz, J., Barry, K., Muñoz-Amatriaìn, M., Close, T. J., Wise, R. P., Schulman, A. H., Himmelbach, A., Mayer, K. F. X.,

Scholz, U., Poland, J. A., Stein, N., and Waugh, R. 2013. Anchoring and ordering NGS contig assemblies by population sequencing (POPSEQ). Plant J. 76:718-727

Mascher, M., Richmond, T. A., Gerhardt, D. J., Himmelbach, A., Clissold, L., Sampath, D., Ayling, S., Steuernagel, B., Pfeifer, Mm., D'Ascenzo, M., Akhunov, E. D., Hedley, P. E., Gonzalez, A. M., Morrell, P. L., Kilian, B., Blattner, F. R., Scholz, U., Mayer, K. F. X., Flavell, A. J., Muehlbauer, G. J., Waugh, R., Jeddeloh, J. A., and Stein, N. 2013. Barley whole exome capture: a tool for genomic research in the genus *Hordeum* and beyond. Plant J. 76:494-505

Mascher, Mm., Jost, M., Kuon, J., Himmelbach, A., Abfalg, Z., Beier, S., Scholz, U., Graner, A., and Stein, N. 2014. Mapping-by-sequencing accelerates forward genetics in barley. Genome Biol. 15:R78

Massman, J., Cooper, B., Horsley, R., Neate, S., Dill-Macky, R., Chao, S., Dong, Y., Schwarz, P., Muehlbauer, G. J., and Smith, K. P. 2011. Genome-wide association mapping of Fusarium head blight resistance in contemporary barley breeding germplasm. Mol. Breeding. 27:439-454

Mathre, D. E. 1997. Compendium of Barley Diseases. The American Phytopathological Society. St. Paul

Mayer, K. F. X., Martis, M., Hedley, P. E., Simkova, H., Liu, H., Morris, J. A., Steuernagel, B., Taudien, S., Roessner, S., Gundlach, H., Kubalakova, M., Suchankova, P., Murat, F., Felder, M., Nussbaumer, T., Graner, A., Salse, J., Endo, T., Sakai, H., Tanaka, T., Itoh, T., Sato, K., Platzer, M., Matsumota, T., Scholz, U., Dolezel, J., Waugh, R., and Stein, N. 2011. Unlocking the Barley Genome by Chromosomal and Comparative Genomics. Plant Cell. 23:1249-1263

McCouch, S. R. 2001. Genomics and Synteny. Plant Physiol. 125:152-155

McDonald, B. A., and Linde, C. 2002. Pathogen Population Genetics, Evolutionary Potential, and Durable Resistance. Ann. Rev. Phytopathol. 40:349-379

McLean, M. S., Howlett, B. J., and Hollaway, G. J. 2009. Epidemiology and control of spot form of net blotch (*Pyrenophora teres* f. *maculata*) of barley: a review. Crop Pasture Sci. 60:303-315

Mode, C. J., and Schaller, C. W. 1958. Two Additional Factors for Host Resistance to Net Blotch in Barley. Agron. J. 50:15-18

Molina-Cano, J. L., Fra-Mon, P., Salcedo, G., Aragoncillo, C., Roca de Togores, F., and Garcia-Omedo, F. 1987. Morocco as a possible domestication center for barley: biochemical and agromorphological evidence. Theor. Appl. Genet. 73:531-536

Molina-Cano, J. L., Moralejo, M., Egartua, E., and Romagosa, I. 1999. Further evidence supporting Morocco as a centre of origin of barley. Theor. Appl. Genet. 98:913-918

Morrell, P. L., and Clegg, M. T. 2007. Genetic evidence for a second domestication of barley (*Hordeum vulgare*) east of the Fertile Crescent. Proc. Natl. Acad. Sci. 104:3289-3294

Muñoz-Amatriaìn, M., Cuesta-Marcos, A., Endelman, J. B., Comadran, J., Bonman, J. M., Bockelman, H. E., Chao, S., Russell, J., Waugh, R., Hayes, P. M., and Muehlbauer, G. J. 2014. The USDA Barley Core Collection: Genetic Diversity, Population Structure, and Potential for Genome-Wide Association Studies. PLoS One 9:e94688

Muñoz-Amatriaìn, M., Lonardi, S., Luo, M., Madishetty, K., Svensson, J. T., Moscou, M. J., Wanamaker, S., Jiang, T., Kleinhofs, A., Muehlbauer, G. J., Wise, R. P., Stein, N., Ma, Y., Rodriguez, E., Kudrna, D., Bhat, P. R., Chao, S., Condamine, P., Heinen, S., Resnik, J., Wing, R., Witt, H. N., Alpert, M., Beccuti, M., Bozdag, S., Cordero, F., Mirebrahim, H., Ounit, R., Wu, Y., You, F., Zheng, J., Simkova, H., Dolezel, J., Grimwood, J., Schmutz, J., Duma, D., Altschmied, L., Blake, T., Bregitzer, P., Cooper, L., Dilbirligi, M., Falk, A., Feiz, L., Graner, A., Gustafson, P., Hayes, P. M., Lemaux, P., Mammadov, J., and Close, T. J. 2015. Sequencing of 15,6222 gene-bearing BACs clarifies the gene-dense regions of the barley genome. Plant J. 84:216-227

Mur, L. A., Allainguillaume, J., Catalán, P., Hasterok, R., Jenkins, G., Lesniewska, K., Thomas, I., and Vogel, J. 2011. Exploiting the Brachypodium Tool Box in cereal and grass research. New Phytol. 191:334-347

Murray, G. M. and Brennan, J. P. 2010. Estimating disease losses to the Australian barley industry. Austral. Plant Pathol. 39:85-96

Pandelova, I., Betts, M. F., Manning, V. A., Wilhelm, L. J., Mockler, T. C., and Ciufetti, L. M. 2009. Analysis of Transcriptome Changes Induced by Ptr ToxA in Wheat Provides Insights into the Mechanisms of Plant Susceptibility. Mol. Plant 2:1067-1083

Peever, T. L. and Milgroom, M. G. 1994. Genetic structure of *Pyrenophora teres* populations determined with random amplified polymorphic DNA markers. Can. J. Bot. 72:915-923

Pourkheirandish, M., and Komatsuda, T. 2007. The Importance of Barley Genetics and Domestication in a Global Perspective. Ann. Bot. 5:999-1008

Pourkheirandish, M., Hensel, G., Kilian, B., Senthil,N., Chen, G., Sameri, M., Azhaguvel, P., Sakuma, S., Dhanagond, S., Sharma, R., Mascher, M., Himmelbach, A., Gottwald, S., Nair, S. K., Tagiri, A., Yukuhiro, F., Nagamura, Y., Kanamori, H., Matusumoto, T., Wilcox, G., Middleton, C. P., Wicker, T., Walther, A., and Waugh, R. 2015. Evolution of the Grain Dispersal System in Barley. Cell 162:527-539

Pritchard, J. K., Stephens, M., and Donnelly, P. 2000. Inference of Population Structure Using Multilocus Genotype Data. Genetics. 155:945-959

Rafalski, J. A. 2010. Association genetics in crop improvement. Curr. Opin. Plant Biol. 13:174-180

Raman, H., Platz, G. J., Chalmers, K. J., Raman, R., Read, B. J., Barr, A. R., and Moody, D. B. 2003. Mapping of genomic regions associated with net form of net blotch resistance in barley. Aust. J. Agric. Res. 54:1359-1367

Rau, D., Brown, A. H. D., Brubaker, C. L., Attene, G., Balmas, V., Saba, E., and Papa, R. 2003. Population genetic structure of *Pyrenophora teres* Drechs. the causal agent of net blotch in Sardinian landraces of barley (*Hordeum vulgare* L.). Theor. Appl. Genet. 106:947-959

Rau, D., Maier, F. J., Papa, R., Brown, A. H. D., Balmas, V., Saba, E., Schaefer, W., and Attene, G. 2005. Isolation and characterization of the mating-type locus of the barley pathogen *Pyrenophora teres* and frequencies of mating-type idiomorphs within and among fungal populations collected from barley landraces. Genome. 48:855-869

Ren, X., Nevo, E., and Sun, G. 2013. Tibet as a Potential Domestication Center of Cultivated Barley of China. PLoS ONE 8:e62700

Richter, K., Schondelmaier, J., and Jung, C. 1998. Mapping of quantitative trait loci affecting *Drechslera teres* resistance in barley with molecular markers. Theor. Appl. Genet. 97:1225-1234

Roy, J. K., Smith, K. P., Muehlbauer, G. J., Chao, S., Close, T. J., and Steffenson, B. J. 2010. Association mapping of spot blotch resistance in wild barley. Mol. Breeding 26:243-256

Sarpeleh, A., Wallwork, H., Catcheside, D. E. A., Tate, M. E., and Able, A. J. 2007. Proteinaceous Metabolites from *Pyrenophora teres* Contribute to Symptom Development of Barley Net Blotch. Phytopathol. 97:907-915

Sarpeleh, A., Wallwork, H., Tate, M. E., Catcheside, D. E. A., and Able, A. J. 2008. Initial characterization of phytotoxic proteins isolated from *Pyrenophora teres*. Physiol. Mol. Plant Pathol. 72:73-79

Serenius, M., Manninen, O., Wallwork, H., and Williams, K. 2007. Genetic differentiation in *Pyrenophora teres* populations measured with AFLP markers. Mycol. Res. 111:213-223

Serenius, M., Mironenko, N., and Manninen, O. 2005. Genetic variation, occurrence of mating types and different forms of *Pyrenophora teres* causing net blotch of barley in Finland. Mycol. Res. 109:809-817

Shan, L., He, P., Li, J., Heese, A., Peck, S. C., Nurnberger, T., Martin, G., and Sheen, J. 2008. Bacterial Effectors Target the Common Signaling Partner BAK1 to Disrupt Multiple MAMP Receptor-Signaling Complexes and Impede Plant Immunity. Cell Host Microbe 4:17-27

Shipton, W. A., Khan, T. N., and Boyd, W. J. R. 1973. Net blotch of barley, Rev. Plant Pathol. 52:269-290

Shjerve, R. A., Faris, J. D., Brueggeman, R. S., Yan, C., Zhu, Y., Koladia, V., and Friesen, T. L. 2014. Evaluation of a *Pyrenophora teres* f. *teres* mapping population reveals multiple independent interactions with a region of barley chromosome 6H. Fungal Genet. Biol. 70:104-112

Shoemaker, R. A. 1959. Nomenclature of *Drechslera* and *Bipolaris*, grass parasites segregated from '*Helminthosporium*'. Can. J. Bot. 37:879-887

Smedegard-Peterson, V. 1977. Isolation of two toxins produced by *Pyrenophora teres* and their significance in disease development of net-spot blotch of barley. Physiol. Plant Pathol. 10:203-211

St. Pierre, S., Gustus, C., Steffenson, B., Dill-Macky, R., and Smith, K. P. 2010. Mapping Net Form Net Blotch and Septoria Speckled Leaf Blotch Resistance Loci in Barley. Phytopathol. 100:80-84

Steffenson, B. J. and Webster, R. K. 1992. Pathotype Diversity of *Pyrenophora teres* f. *teres* on Barley. Phytopathol. 82:170-177

Steffenson, B. J., Hayes, P. M., and Kleinhofs, A. 1996. Genetics of seedling and adult plant resistance to net blotch (*Pyrenophora teres* f. *teres*) and spot blotch (*Cochliobolus sativus*) in barley. Theor. Appl. Genet. 92:552-558

Tamang, P., Neupane, A., Mamidi, S., Friesen, T. L., and Brueggeman, R. 2015. Association Mapping of Seedling Resistance to Spot Form Net Blotch in a Worldwide Collection of Barley. Phytopathol. 105:500-508

Tans-Kersten, J., Huang, H., and Allen, C. 2001. *Ralstonia solanacearum* Needs Motility for Invasive Virulence on Tomato. J. Bacteriol. 183:3597-3605

Tekauz, A. 1978. Incidence and severity of net blotch of barley and distribution of *Pyrenophora teres* biotypes in the Canadian prairies in 1976. Can. Plant Dis. Surv. 58:9-11

Tekauz, A. 1990. Characterization and distribution of pathogenic variation in *Pyrenophora teres* f. *teres* and *P. teres* f. *maculata* from western Canada. Can. J. Plant Pathol. 12:141-148

Tekauz, A., and Buchannon, K. W. 1977. Distribution of and Sources of Resistance to Biotypes of *Pyrenophora teres* in Western Canada. Can. J. Plant Sci. 57:389-395

Tekauz, A., and Mills, J. T. 1974. New Types of Virulence in *Pyrenophora teres* in Canada. Can. J. Plant Sci. 54:731-734

Thomma, B. P. H. J., Nurnberger, T., and Joosten, M. H. A. J. 2011. Of PAMPs and Effectors: The Blurred PTI-ETI Dichotomy. Plant Cell 23:4-15

USDA Agricultural Research Service. 1979. Introduction of barley into the New World. By Wiebe, G. A. In: Barley: Origin, Botany, Culture, Winder Hardiness, Genetics, Utilization, Pests.
USDA Foreign Agricultural Service. 2015. World Agricultural Production. Available at: http://www.fas.usda.gov/. Accessed: 9/5/2016

van der Hoorn, R. A. L., and Kamoun, S. 2008. From Guard to Decoy: A New Model for Perception of Plant Pathogen Effectors. Plant Cell. 20:2009-2017

Van Doorn, W. G. and Woltering, E. J. 2005. Many ways to exit? Cell death categories in plants. Trends Plant Sci. 10:117-122

Vision, T. J. 2005. Gene order in plants: a slow but sure shuffle. New Phytol. 168:51-60

von Bothmer, R., and Jacobsen, N. 1985. Origin, taxonomy, and related species. Barley. 19-56

Wang, X., Richards, J., Gross, T., Druka, A., Kleinhofs, A., Steffenson, B., Acevedo, M., and Brueggeman, R. 2013. The *rpg4*-Mediated Resistance to Wheat Stem Rust (*Puccinia graminis*) in Barley (*Hordeum vulgare*) Requires *Rpg5*, a Second NBS-LRR Gene, and an Actin Depolymerization Factor. Mol. Plant Microbe In. 26:407-418

Weiergang, I., Lyngs Jorgensen, H. J., Moller, I. M., Friis, P., and Smedegaard-Petersen, V. 2002. Correlation between sensitivity of barley to *Pyrenophora teres* toxins and susceptibility to the fungus. Physiol. Mol. Plant Pathol. 60:121-129

Williams, K. J., Smyl, C., Lichon, A., Wong, K. Y., and Wallwork, H. 2001. Development and use of an assay based on the polymerase chain reaction that differentiates the pathogens causing spot form and net form of net blotch of barley. Australas. Plant Path. 30:37-44

Wolpert, T. J., Dunkle, L. D., and Ciuffetti, L. M. 2002. Host-Selectie Toxins and Avirulence Determinants: What's in a Name? Annu. Rev. Phytopathol. 40:251-285

Wu, C., Krasileva, K. V., Banfield, M. J., Terauchi, R., and Kamoun, S. 2015. The "sensor domains" of plant NLR proteins: more than decoys? Front. Plant Sci. 6:134

Wu, H. L., Steffenson, B. J., Li, Y., Oleson, A. E., and Zhong, S. 2003. Genetic variation for virulence and RFLP markers in *Pyrenophora teres*. Can. J. Plant Pathol. 25:82-90

Xiang, T., Zong, N., Zou, Y., Wu, Y., Zhang, J., Xing, W., Li, Y., Tang, X., Zhu, L., Chai, J., and Zhou, J. 2008. *Pseudomonas syringae* Effector AvrPto Blocks Innate Immunity by Targeting Receptor Kinases. Curr. Biol. 18:74-80

Youssef, H. M., Koppolu, R., Rutten, T., Korzun, V., Schweizer, P., and Schurbusch, T. 2014. Genetic mapping of the *labile* (*lab*) gene: a recessive locus causing irregular spikelet fertility in *labile*-barley (*Hordeum vulgare* convar. *labile*). Theor. Appl. Genet. 127:1123-1131

Yu, J., Pressoir, G., Briggs, W. H., Bi, I. V., Yamasaki, M., Dolebley, J. F., McMullen, M. D., Gaut, B. S., Nielsen, D. M., Holland, J. B., Kresovich, S., and Buckler, E. S. 2006. A unified mixed-model method for association mapping that accounts for multiple levels of relatedness. Nature Genet. 38:203-208

Yu, Y., Tomkins, J. P., Waugh, R., Frisch, D. A., Kudrna, D., Kleinhofs, A., Brueggeman, R. S., Muehlbauer, G. J., Wise, R. P., and Wing, R. A. 2000. Theor. Appl. Genet. 101:1093-1099

Yun, S. J., Gyenis, L., Hayes, P. M., Matus, I., Smith, K. P., Steffenson, B. J., and Muehlbauer, G. J. 2005. Quantitative Trait Loci for Multiple Disease Resistance in Wild Barley. Crop Sci. 45:2563-2572

Zang, W., Eckstein, P. E., Colin, M., Voth, D., Himmelbach, A., Beier, S., Stein, N., Scoles, G. J., and Beattie, A. D. 2015. Fine mapping and identification of a candidate gene for the barley *Un8* true loose smut resistance gene. Theor. Appl. Genet. 128:1343-1357

Zhang, Z., Ersoz, E., Lai, C., Todhunter, R. J., Tiwari, H. K., Gore, M. A., Bradbury, P. J., Yu, J., Arnett, D. K., Ordovoas, J. M., and Buckler, E. S. 2010. Mixed linear model approach adapted for genome-wide association studies. Nature Genet. 42:355-360

Zhao, K., Aranzana, M. J., Kim, S., Lister, C., Shindo, C., Tang, C., Toomajian, C., Zheng, J., Dean, C., Marjoram, P., and Nordborg, M. 2007. An *Arabidopsis* Example of Association Mapping in Structured Samples. PLoS Genet. 3:e4

Zhou, F., Kurth, J., Wei, F., Elliot, C., Vale, G., Yahiaoui, N., Keller, B., Somerville, S., Wise, R., and Schulze-Lefert, P. 2001. Cell-Autonomous Expression of Barley *Mla1* Confers Race-Specific Resistance to the Powdery Milder Fungus via a *Rar1*-Independent Signaling Pathway. Plant Cell. 13:337-350

Zhu, C., Gore, M., Buckler, E. S., and Yu, J. 2008. Status and Prospects of Association Mapping in Plants. Plant Genome. 1:5-20

Ziems. L. A., Hickey, L. T., Hunt, C. H., Mace, E. S., Platz, G. J., Frankowiak, J. D., and Jordan, D. R. 2014. Association mapping of resistance to *Puccinia hordei* in Australian barley breeding germplasm. Theor. Appl. Genet. 127:1199-1212

Zipfel, C. 2008. Pattern-recognition receptors in plant innate immunity. Curr. Opin. Immunol. 20:10-16

Zipfel, C. 2009. Early molecular events in PAMP-triggered immunity. Curr. Opin. Plant Biol. 12:414-420

Zohary, D. and Hopf, M. 1973. Domestication of Pulses in the Old World. Science. 182:887-894

CHAPTER 2. ASSOCIATION MAPPING UTILIZING DIVERSE BARLEY LINES REVEALS NET FORM NET BLOTCH SEEDLING RESISTANCE/SUSCEPTIBILITY LOCI

Abstract

Pyrenophora teres f. *teres* is a necrotrophic fungal pathogen and the causal agent of the economically important foliar disease net form net blotch (NFNB) of barley. The deployment of effective and durable resistance against *P. teres* f. *teres* has been hindered by the complexity of quantitative resistance and susceptibility. Several bi-parental mapping populations have been used to identify QTL associated with NFNB disease on all seven barley chromosomes. Here we report the first genome-wide association study (GWAS) to detect marker trait associations for resistance or susceptibility to *P. teres* f. *teres*. Geographically diverse barley genotypes from a world barley core collection (957) were genotyped with the Illumina barley iSelect chip and phenotyped with three *P. teres* f. *teres* isolates collected in two geographical regions of the USA (15A, 6A and LDNH04Ptt19). The best of nine regression models tested were identified for each isolate and used for association analysis resulting in the identification of 78 significant marker trait associations (MTA; -log10p-value >3.0). The MTA identified corresponded to 16 unique genomic loci as determined by analysis of local linkage disequilibrium between markers that didn't meet a correlation threshold of R^2 = >0.1, indicating that the markers represented distinct loci. Five loci identified represent novel QTL and were designated *QRptts-3HL*, *QRptts-4HS*, *QRptts-5HL.1*, *QRptts-5HL.2*, and *QRptts-7HL.1*. Additionally, 55 of the barley lines examined exhibited a high level of resistance to all three isolates and the SNP markers identified will provide useful genetic resources for barley breeding programs.

Introduction

Net blotch is a damaging foliar disease of barley (*Hordeum vulgare*) and infects the crop in most major production regions across the world. Caused by the necrotrophic fungal pathogen *Pyrenophora teres*, net blotch impacts the supply of quality barley for the malting industry due to its impact on yield and malting quality (Murray and Brennan 2010). Two forms of the pathogen exist, including *Pyrenophora teres* f. *teres* and *Pyrenophora teres* f. *maculata*, causal agents of net form net blotch (NFNB) and spot form net blotch (SFNB), respectively. The two forms are morphologically identical but can be differentiated by the unique symptoms they elicit on the host (Smedegard-Peterson 1971; McLean et al. 2009). Additionally, phylogenetic analysis using mating type (MAT) gene sequence from net form and spot form isolates revealed a distinct genetic isolation (Rau et al. 2007). Several management strategies are recommended to combat this disease, including the destruction of crop residue and crop rotation to reduce the presence of primary inoculum, as well as fungicide applications. However, the deployment of genetic resistance is considered the most desirable means of disease management (Mathre 1997).

Sexual populations of *P. teres* f. *teres* occur worldwide and contribute to a highly variable and diverse pathogen population (Peever et al. 1994; Jonsson et al. 2000; Rau et al. 2005). A recent diversity survey utilized 75 isolates collected from North Dakota, assayed on 22 differential lines, identifying 49 different pathotypes. Additionally, molecular analysis using simple-sequence repeat (SSR) markers showed 40 unique genotypes and the MAT genes were present in statistically equal proportions, indicative of a diverse sexual population in part due to the occurrence of random mating (Liu et al. 2012). Tekauz (1990) had previously sampled 182 *P. teres* f. *teres* isolates in another North America population study to investigate the diversity in western Canada. Inoculation of the 182 isolates onto 12 barley differentials revealed 45 distinct

pathotypes. More recently, Akhavan et al. (2016) analyzed the virulence of 39 *P. teres* f. *teres* isolates collected from western Canada using nine differential lines and identified 16 unique pathotypes. Additionally, an apparent shift in virulence in *P. teres* f. *teres* populations in this region has occurred as evidenced by the appearance of seven novel pathotypes and the absence of three pathotype groups identified by Tekauz (1990). However, because of the low number of isolates utilized in this study its probable that these pathotypes could still be present in the population (Akhavan et al. 2016). These population studies of North American *P. teres* f. *teres* populations show the diversity available and how dynamic the populations can be, given the ability to recombine to form new combinations of virulence genes coupled with the selection pressure exerted by popular local barley varieties. This pathogen has the high propensity to rapidly adapt its virulence repertoire to overcome resistances present in popular barley cultivars being grown locally (Liu et al. 2012). The variable nature of the pathogen indicates that a thorough understanding of the virulence present in the population and multiple sources of resistance or lack of susceptibility need to be deployed to efficiently control this disease.

Traditional linkage mapping methods utilizing recombinant inbred lines (RILs) or doubled haploid (DH) populations have been widely used to identify quantitative trait loci (QTL) providing resistance or susceptibility to *P. teres* f. *teres* at seedling and adult plant stages. Seedling resistance QTL have been identified on all seven barley chromosomes (reviewed by Liu et al. 2011), including the detection of a common major QTL on or near the centromere of barley chromosome 6H. (Steffenson et al. 1996, Graner et al. 1996, Richter et al. 1998, Raman et al. 2003, Cakir et al. 2003, Ma et al. 2004, Emebiri et al. 2005, Yun et al. 2005, Manninen et al. 2000, Manninen et al. 2006, Friesen et al. 2006, Grewal et al. 2008, Abu Qamar et al. 2008, St. Pierre et al. 2010) Additionally, this pathosystem appears remarkably complex, as resistance has

been observed to be dominant, incomplete, and recessive suggesting different mechanisms of host-parasite interaction leading to compatibility (susceptibility) or incompatibility (resistance).

The use of bi-parental mapping populations for the identification of QTL requires the time consuming task of developing mapping populations and only captures the diversity stemming from the two founding parents, but does have the benefit of detecting rare alleles with functional polymorphisms between the two parents (Zhu et al. 2008; Rafalski 2010). Association mapping (AM), or linkage disequilibrium (LD) mapping, provides an alternative to traditional linkage mapping through the use of diverse panels of host genotypes to identify marker-trait associations (MTAs). The use of diverse germplasm collections instead of bi-parental populations allows for the exploitation of ancestral recombination events occurring over the plants evolutionary history (Zhu et al 2008). Association mapping has several advantages including the ability to detect QTL at a higher resolution, less time required to conduct the genetic analyses, and the potential to identify a greater number of loci associated with the phenotype (Yu et al. 2006; Zhu et al 2008). Successful association mapping requires the selection of a correct statistical model that suitably controls the detection of false positive associations. Several methods have been described to control this type I error rate, such as the inclusion of population structure (Zhao et al. 2007) and familial relatedness (Yu et al. 2006). Additionally, methods such as the compressed mixed linear model (CMLM) (Zhang et al. 2010) and the enriched compressed mixed linear model (ECMLM) utilize a clustering of individuals to create a compressed kinship matrix (Li et al. 2014). These methods promise an increase in statistical power as well as a decrease in computation time.

Association mapping has emerged as a powerful tool to identify loci controlling quantitative traits in various economically important crop species. Using a nested association

mapping (NAM) population, loci associated with complex traits including leaf architecture and southern leaf blight resistance have been identified throughout the maize genome (Tian et al. 2011; Kump et al. 2011). Additionally, Huang et al. (2010) used 517 rice land races with highly saturated genotypic data of ~3.6 million single nucleotide polymorphisms (SNPs) to successfully identify genomic regions associated with 14 different genetically complex agronomic traits. The use of genome wide association studies (GWAS) has also been applied to barley, with significant loci being identified for association with resistance to Fusarium head blight, stem rust, spot blotch, and leaf rust (Massman et al. 2011; Zhou et al. 2014; Zhou et al. 2013; Ziems et al. 2014). Additionally, a diverse panel of barley accessions was evaluated for disease reaction to *P. teres* f. *maculata* (Neupane et al. 2015) and the GWAS identified 21 novel loci associated with resistance or susceptibility to *P. teres* f. *maculata*, as well as six previously identified QTL (Tamang et al. 2015).

This study utilized a GWAS approach to identify loci associated with disease resistance or susceptibility to North American isolates of the barley pathogen *P. teres* f. *teres*. The utilization of the world barley core collection allowed for the identification of MTA and the underlying SNP markers that can be utilized by barley breeders to incorporate resistances or eliminate susceptibility from elite barley germplasm providing more tools and knowledge to begin effectively combating this economically important yet shifty and dynamic pathogen.

Materials and Methods

Biological Materials

A total of 1050 accessions from the globally diverse barley core collection including cultivars, breeding lines, landraces, and genetic stocks were acquired from the National Small Grain Collection, Aberdeen, Idaho (Muñoz-Amatriaín et al. 2014). Three North American *P.*

teres f. *teres* isolates (15A, 6A and LDNH04Ptt19) were used to phenotype the barley core collection accessions. *P. teres* f. *teres* isolate 15A was collected in Fresno County, California (Wu et al. 2003), isolate 6A was collected from Fresno County, California (Steffenson and Webster 1992), and isolate LDNH04Ptt19 (hereafter referred to as LDN) was collected in North Dakota.

Phenotyping

Barley accessions were arranged into blocks consisting of 60 lines per block. Three seeds per accession were planted in cones, placed in a rack bordered with the barley cultivar Robust, and grown under greenhouse conditions until the 2-3 leaf stage, approximately 14 days. Inoculations were performed as described in Friesen et al. (2006). Disease reactions were evaluated 7 days post-inoculation using a 1-10 rating scale (Tekauz 1985). A total of three replicates were completed for each isolate per block. The average disease score of the three replicates were used in the association analyses.

Genotyping

A total of 2,417 barley lines, consisting of landraces, breeding lines, and cultivars from the National Small Grains Collection were genotyped utilizing the 9k Illumina Infinium iSELECT assay (Muñoz-Amatriaín et al. 2014). Genotypic data for 998 accessions, which were phenotyped with the aforementioned *Ptt* isolates, with less than 30% missing data were downloaded from The Triticeae Toolbox (T3) barley database (https://triticeaetoolbox.org/barley/). Additionally, genetic positions of the SNP markers on the iSelect consensus map were used for this analysis (Muñoz-Amatriaín et al. 2014). Sequences of significant SNP markers were used in BLAST searches of the barley genome to identify genetic

positions based on population sequencing (POPSEQ) from which the relative marker position could be estimated (IBSC 2012; Mascher et al. 2013).

Imputation, Allele Similarity, and Linkage Disequilibrium

Heterozygote genotypes were recoded as missing data and missing genotypic data were imputed in fastPhase 1.3 (Scheet and Stephens 2006) with default settings. An allele similarity matrix was calculated in JMP Genomics v6.1 (SAS Institute Inc.) using the imputed genotypic data to eliminate any redundant barley genotypes. Linkage disequilibrium was calculated as squared allele frequency correlations (R^2) between all intrachromosomal marker pairs in JMP Genomics v6.1.

Population Structure

The software STRUCTURE v.2.3.4 (Pritchard et al. 2000) was used to determine the population structure of the selected core collection lines and assign membership to subpopulations. Using genetic positions derived from the barley iSelect consensus map (Muñoz-Amatriaín et al. 2014), a single marker was selected from each locus, resulting in 1744 markers to be used in STRUCTURE analysis. Initially, an admixture model was used with a burn-in of 10,000, followed by 25,000 Monte Carlo Markov Chain (MCMC) replications for k=1 to k=10 with five iterations. The Δk method (Evanno et al 2005) was used in STRUCTURE HARVESTER (Earl et al 2012) to identify the ideal level of subpopulations. Following the identification of the optimum k value, individuals were placed into subpopulations by running a new STRUCTURE analysis with a burn-in of 100,000 and 100,000 MCMC iterations at the optimum k value. An individual was considered to be a member of a subpopulation if its membership probability was greater than 0.80. STRUCTURE output was then used as a covariate (Q) in several association models. Principal components analysis (PCA) was conducted

in the R package Genome Association and Prediction Integrated Tool (GAPIT) (Lipka et al 2012; Tang et al. 2016) and TASSEL 5.0 (Bradbury et al. 2007) with default settings. Principal components explaining at least 25% were used as a covariate in association analyses (PC_{25}). A kinship matrix (K) was constructed using the Loiselle algorithm (Loiselle et al. 1995) in GAPIT by setting the 'group.from' and 'group.to' parameters equal to the population size and the 'group.by' parameter equal to one. Additionally, using the enriched compressed mixed linear model (ECMLM) proposed by Li et al. (2014), an optimal compressed kinship matrix (K_{comp}) was calculated in GAPIT using the Loiselle algorithm and the parameters of 'group.from = 300', 'group.to = 957', and 'group.by = 50'. Kinship clustering methods tested were average, ward, and complete. Kinship group summary methods used were mean and maximum.

Marker Trait Association Models

Nine models were tested for the identification of MTAs and conducted in TASSEL 5.0 and GAPIT (Bradbury et al. 2007; Lipka et al. 2012; Tang et al. 2016). A naïve model utilizing only genotypic and phenotypic data and not accounting for population structure or relatedness was conducted using the general linear model (GLM) procedure in TASSEL 5.0. Correcting for population structure, an additional model using population structure (Q) as a fixed effect was also analyzed using the GLM procedure in TASSEL 5.0. Additionally, in a similar manner, another model accounting for population structure using the first three principal components (PC_{25}) was analyzed. A fourth model, accounting for relatedness, utilized the kinship matrix (K) as a random effect in a mixed linear model (MLM) using GAPIT. Another model accounting for relatedness used the compressed kinship matrix (K_{comp}) as a random effect in a MLM. Finally, four additional models accounting for population structure and kinship (Q+K, PCA_{25}+K, Q+K_{comp}, and PC_{25}+K_{comp}) were analyzed as a MLM with Q and PC_{25} as a fixed effects and kinship as a

random effect in GAPIT. The mean squared deviation (MSD) was calculated for each model (Mamidi et al., 2011) and the model with the lowest MSD value was selected for further analysis. Markers-trait associations with a p-value < 0.001 were declared significant. Additionally, p-values from the optimal model for each trait were adjusted using a false discovery rate (FDR) multiple testing correction procedure in GAPIT and markers with a p-value < 0.1 were considered highly significant. Manhattan plots were generated in the R package 'qqman' (Turner 2014).

QTL Identification

The genetic positions of the significant markers detected were determined via BLAST searches of the barley genome (http://webblast.ipk-gatersleben.de/barley/viroblast.php) to anchor them to a POPSEQ position (Mascher et al. 2013). Loci were initially declared distinct if separated by more than 5 cM. As LD can be variable throughout the genome, to ensure loci were indeed distinct, local LD was examined between the most significant markers at each intrachromosomal locus. If R^2 values between significant marker pairs were less than 0.10, the loci were considered distinct.

Results

Phenotypic Analysis

A total of 1050 barley accessions from the barley core collection (Muñoz-Amatriaín et al. 2014) were evaluated for disease reaction to three North American *P. teres* f. *teres* isolates (15A, 6A, and LDN). Average disease reaction scores for isolate 15A ranged from highly resistant 1 to highly susceptible 9.67 with an overall mean of 4.40. Similarly, average disease reaction scores for isolate 6A ranged from 1 to 9.33 with an overall mean of 4.10. Average disease reaction scores for isolate LDN ranged from 1 to 9.67 with an overall mean of 5.40. A total of 55 barley

accessions were highly resistant to all three isolates with an average disease reaction score of less than or equal to 2.5 for each isolate. Examination of the alleles of the highly resistant lines for 19 significant markers revealed 16 markers with a predominant allele being present in over 75% of the highly resistant lines (Table 2.1).

Table 2.1. Haplotypes of 52 barley accessions highly resistant to *P. teres* f. *teres* isolates 15A, 6A, and LDN.

Marker[1]	Chr[2]	cM[3]	Alleles[4]	PI67381	PI531896	PI226639	PI606305	PI168328	CIho14260	PI344936	PI151795	PI620640
12_30690	2H	120.04	(T/C)	C	C	C	C	C	T	C	T	C
12_10579	2H	125.35	(T/G)	G	G	G	G	G	T	T	G	T
SCRI_RS_119379	3H	2.41	(A/G)	G	A	A	A	G	G	G	G	G
11_20356	3H	46.03	(A/G)	A	G	G	G	G	A	G	G	G
SCRI_RS_235849	3H	83.99	(A/G)	G	G	A	G	A	G	G	G	G
SCRI_RS_188420	3H	N/A	(A/C)	C	C	C	A	C	C	C	C	A
SCRI_RS_154517	4H	1.13	(A/G)	G	G	G	G	G	G	G	G	A
SCRI_RS_181886	4H	52.69	(A/C)	C	A	C	C	A	C	C	A	C
SCRI_RS_152347	5H	69.31	(A/G)	G	G	G	G	G	G	G	G	G
11_21314	5H	87.71	(A/C)	A	A	A	A	A	A	A	A	A
11_10013	6H	49.22	(T/C)	T	T	T	T	T	T	T	T	T
12_10199	6H	49.79	(A/G)	G	G	G	G	G	A	G	G	G
11_20835	6H	54.82	(A/G)	G	A	G	G	G	G	A	G	G
SCRI_RS_7104	6H	54.89	(T/C)	C	C	C	C	C	C	C	C	C
SCRI_RS_176650	6H	55.03	(T/C)	C	C	C	C	C	C	C	C	C
SCRI_RS_106581	6H	59.92	(A/G)	G	G	G	G	G	A	G	G	G
SCRI_RS_139937	6H	65.86	(A/C)	A	C	A	C	A	A	C	C	C
12_31055	7H	70.54	(T/G)	G	G	T	T	G	G	G	T	G
SCRI_RS_183593	7H	131.02	(T/G)	T	T	T	G	T	T	G	G	G

[1]Most significant marker from each QTL identified associated with NFNB resistance or susceptibility to *P. teres* f. *teres* isolates 15A, 6A, and LDN.
[2]Chromosome assignment derived from POPSEQ (Mascher et al. 2013)
[3]POPSEQ derived genetic position (Mascher et al. 2013)
[4]Specific alleles of each significant SNP marker

Table 2.1. Haplotypes of 52 barley accessions highly resistant to *P. teres* f. *teres* isolates 15A, 6A, and LDN (continued).

Marker	Chr	cM	Alleles	CIho11792	PI28624	PI26179	PI182681	PI264208	PI611599	CIho14286	CIho7491	CIho7492
12_30690	2H	120.04	(T/C)	C	C	C	C	C	C	C	C	C
12_10579	2H	125.35	(T/G)	G	G	G	G	G	T	G	G	G
SCRI_RS_119379	3H	2.41	(A/G)	A	G	A	G	A	G	A	A	G
11_20356	3H	46.03	(A/G)	G	A	G	G	G	G	G	G	G
SCRI_RS_235849	3H	83.99	(A/G)	G	G	A	A	G	G	G	G	G
SCRI_RS_188420	3H	N/A	(A/C)	A	C	C	C	C	C	C	C	C
SCRI_RS_154517	4H	1.13	(A/G)	G	G	G	G	G	A	G	G	G
SCRI_RS_181886	4H	52.69	(A/C)	C	C	A	C	A	C	A	A	A
SCRI_RS_152347	5H	69.31	(A/G)	G	G	A	G	A	G	A	A	A
11_21314	5H	87.71	(A/C)	A	A	A	A	A	A	A	A	A
11_10013	6H	49.22	(T/C)	T	T	T	T	T	T	T	T	T
12_10199	6H	49.79	(A/G)	G	G	G	G	G	G	G	G	G
11_20835	6H	54.82	(A/G)	G	G	G	G	A	G	G	G	G
SCRI_RS_7104	6H	54.89	(T/C)	C	C	C	C	C	C	C	C	C
SCRI_RS_176650	6H	55.03	(T/C)	C	C	C	C	T	C	C	C	C
SCRI_RS_106581	6H	59.92	(A/G)	G	G	G	G	G	G	G	G	G
SCRI_RS_139937	6H	65.86	(A/C)	C	A	C	C	C	C	C	C	C
12_31055	7H	70.54	(T/G)	T	G	G	G	T	G	G	G	G
SCRI_RS_183593	7H	131.02	(T/G)	G	T	G	G	T	G	G	G	G

[1]Most significant marker from each QTL identified associated with NFNB resistance or susceptibility to *P. teres* f. *teres* isolates 15A, 6A, and LDN.
[2]Chromosome assignment derived from POPSEQ (Mascher et al. 2013)
[3]POPSEQ derived genetic position (Mascher et al. 2013)
[4]Specific alleles of each significant SNP marker

Table 2.1. Haplotypes of 52 barley accessions highly resistant to *P. teres* f. *teres* isolates 15A, 6A, and LDN (continued).

Marker	Chr	cM	Alleles	PI159126	CIho7504	PI564598	PI330398	PI356580	CIho14880	PI221307	PI386601	PI386993
12_30690	2H	120.04	(T/C)	C	C	C	C	C	C	C	C	C
12_10579	2H	125.35	(T/G)	G	G	G	G	G	G	G	G	G
SCRI_RS_119379	3H	2.41	(A/G)	G	A	A	G	A	A	G	A	A
11_20356	3H	46.03	(A/G)	G	G	G	G	G	G	G	G	G
SCRI_RS_235849	3H	83.99	(A/G)	G	A	A	G	G	G	G	A	A
SCRI_RS_188420	3H	N/A	(A/C)	C	C	C	C	A	C	C	A	A
SCRI_RS_154517	4H	1.13	(A/G)	G	G	G	A	G	G	A	G	G
SCRI_RS_181886	4H	52.69	(A/C)	A	A	C	A	C	C	A	C	C
SCRI_RS_152347	5H	69.31	(A/G)	A	A	A	G	G	G	G	G	G
11_21314	5H	87.71	(A/C)	A	A	A	A	A	A	A	A	A
11_10013	6H	49.22	(T/C)	T	T	T	C	T	T	T	T	T
12_10199	6H	49.79	(A/G)	G	G	G	G	G	G	G	G	G
11_20835	6H	54.82	(A/G)	G	G	G	G	G	G	G	G	G
SCRI_RS_7104	6H	54.89	(T/C)	C	C	C	C	C	C	C	C	C
SCRI_RS_176650	6H	55.03	(T/C)	C	C	C	C	C	C	C	C	C
SCRI_RS_106581	6H	59.92	(A/G)	G	G	G	G	G	G	G	G	G
SCRI_RS_139937	6H	65.86	(A/C)	C	C	C	A	C	C	C	C	C
12_31055	7H	70.54	(T/G)	G	G	G	G	T	T	G	T	T
SCRI_RS_183593	7H	131.02	(T/G)	G	G	G	G	G	G	G	G	G

[1]Most significant marker from each QTL identified associated with NFNB resistance or susceptibility to *P. teres* f. *teres* isolates 15A, 6A, and LDN.
[2]Chromosome assignment derived from POPSEQ (Mascher et al. 2013)
[3]POPSEQ derived genetic position (Mascher et al. 2013)
[4]Specific alleles of each significant SNP marker

Table 2.1. Haplotypes of 52 barley accessions highly resistant to *P. teres* f. *teres* isolates 15A, 6A, and LDN (continued).

Marker	Chr	cM	Alleles	PI564637	PI237581	PI295958	PI223446	PI190786	PI264209	PI605699	CIho5057	PI611472
12_30690	2H	120.04	(T/C)	C	C	C	C	C	C	C	C	C
12_10579	2H	125.35	(T/G)	G	T	G	G	T	G	T	G	G
SCRI_RS_119379	3H	2.41	(A/G)	G	G	G	G	G	G	A	G	A
11_20356	3H	46.03	(A/G)	G	G	G	A	G	G	G	A	G
SCRI_RS_235849	3H	83.99	(A/G)	G	A	G	G	G	G	G	G	G
SCRI_RS_188420	3H	N/A	(A/C)	C	A	C	C	C	C	C	C	C
SCRI_RS_154517	4H	1.13	(A/G)	G	G	G	G	A	G	G	G	A
SCRI_RS_181886	4H	52.69	(A/C)	A	A	C	C	C	A	C	C	A
SCRI_RS_152347	5H	69.31	(A/G)	G	G	G	A	G	G	G	G	G
11_21314	5H	87.71	(A/C)	A	A	A	A	A	A	A	A	A
11_10013	6H	49.22	(T/C)	T	T	T	T	T	T	T	T	C
12_10199	6H	49.79	(A/G)	G	G	A	A	G	A	G	G	G
11_20835	6H	54.82	(A/G)	G	G	G	G	G	G	G	G	G
SCRI_RS_7104	6H	54.89	(T/C)	C	C	C	C	C	C	C	C	C
SCRI_RS_176650	6H	55.03	(T/C)	C	C	C	C	C	C	C	C	C
SCRI_RS_106581	6H	59.92	(A/G)	G	G	G	A	G	G	G	G	G
SCRI_RS_139937	6H	65.86	(A/C)	C	C	A	A	C	C	C	A	C
12_31055	7H	70.54	(T/G)	G	T	T	T	G	G	T	G	T
SCRI_RS_183593	7H	131.02	(T/G)	G	G	T	T	G	G	G	T	G

[1]Most significant marker from each QTL identified associated with NFNB resistance or susceptibility to *P. teres* f. *teres* isolates 15A, 6A, and LDN.
[2]Chromosome assignment derived from POPSEQ (Mascher et al. 2013)
[3]POPSEQ derived genetic position (Mascher et al. 2013)
[4]Specific alleles of each significant SNP marker

Table 2.1. Haplotypes of 52 barley accessions highly resistant to *P. teres* f. *teres* isolates 15A, 6A, and LDN (continued).

Marker	Chr	cM	Alleles	PI643310	PI643314	PI643364	PI643244	PI319867	PI422232	PI447260	CIho11533	PI584971
12_30690	2H	120.04	(T/C)	C	C	C	C	C	C	C	C	C
12_10579	2H	125.35	(T/G)	G	G	G	G	G	G	G	G	G
SCRI_RS_119379	3H	2.41	(A/G)	A	A	A	A	A	A	G	G	G
11_20356	3H	46.03	(A/G)	G	G	G	G	G	G	G	G	A
SCRI_RS_235849	3H	83.99	(A/G)	G	G	G	G	A	G	G	G	G
SCRI_RS_188420	3H	N/A	(A/C)	C	C	C	C	A	A	C	C	C
SCRI_RS_154517	4H	1.13	(A/G)	A	A	A	A	G	G	A	G	G
SCRI_RS_181886	4H	52.69	(A/C)	A	A	A	A	C	C	A	A	C
SCRI_RS_152347	5H	69.31	(A/G)	G	G	G	G	G	G	A	G	G
11_21314	5H	87.71	(A/C)	A	A	A	A	A	A	A	A	A
11_10013	6H	49.22	(T/C)	C	C	T	C	T	T	T	T	T
12_10199	6H	49.79	(A/G)	G	G	G	G	G	G	G	G	G
11_20835	6H	54.82	(A/G)	G	G	G	G	G	G	G	G	G
SCRI_RS_7104	6H	54.89	(T/C)	C	C	C	C	C	C	C	C	C
SCRI_RS_176650	6H	55.03	(T/C)	C	C	C	C	C	C	C	C	C
SCRI_RS_106581	6H	59.92	(A/G)	G	G	A	G	G	G	G	G	G
SCRI_RS_139937	6H	65.86	(A/C)	C	C	C	C	C	C	C	C	A
12_31055	7H	70.54	(T/G)	G	T	G	T	T	T	T	G	G
SCRI_RS_183593	7H	131.02	(T/G)	G	G	G	G	G	G	G	G	T

[1]Most significant marker from each QTL identified associated with NFNB resistance or susceptibility to *P. teres* f. *teres* isolates 15A, 6A, and LDN.
[2]Chromosome assignment derived from POPSEQ (Mascher et al. 2013)
[3]POPSEQ derived genetic position (Mascher et al. 2013)
[4]Specific alleles of each significant SNP marker

Table 2.1. Haplotypes of 52 barley accessions highly resistant to *P. teres* f. *teres* isolates 15A, 6A, and LDN (continued).

Marker	Chr	cM	Alleles	CIho15364	PI608667	PI438585	PI573611	PI296192	PI636084	PI611534
12_30690	2H	120.04	(T/C)	C	C	C	C	C	C	C
12_10579	2H	125.35	(T/G)	G	G	G	T	G	G	G
SCRI_RS_119379	3H	2.41	(A/G)	A	A	G	A	G	G	G
11_20356	3H	46.03	(A/G)	G	G	A	G	A	A	G
SCRI_RS_235849	3H	83.99	(A/G)	G	G	A	A	G	G	G
SCRI_RS_188420	3H	N/A	(A/C)	C	C	C	C	C	A	C
SCRI_RS_154517	4H	1.13	(A/G)	G	G	G	G	G	G	G
SCRI_RS_181886	4H	52.69	(A/C)	A	A	A	C	C	C	A
SCRI_RS_152347	5H	69.31	(A/G)	G	G	G	A	G	G	G
11_21314	5H	87.71	(A/C)	A	A	A	C	A	A	A
11_10013	6H	49.22	(T/C)	T	T	T	C	T	T	C
12_10199	6H	49.79	(A/G)	G	G	G	G	A	A	G
11_20835	6H	54.82	(A/G)	G	G	G	G	G	G	G
SCRI_RS_7104	6H	54.89	(T/C)	C	C	C	C	C	C	C
SCRI_RS_176650	6H	55.03	(T/C)	C	C	C	T	C	C	C
SCRI_RS_106581	6H	59.92	(A/G)	G	G	G	G	A	G	G
SCRI_RS_139937	6H	65.86	(A/C)	C	C	A	C	A	C	C
12_31055	7H	70.54	(T/G)	T	T	G	G	G	G	T
SCRI_RS_183593	7H	131.02	(T/G)	T	G	G	G	G	T	G

[1]Most significant marker from each QTL identified associated with NFNB resistance or susceptibility to *P. teres* f. *teres* isolates 15A, 6A, and LDN.
[2]Chromosome assignment derived from POPSEQ (Mascher et al. 2013)
[3]POPSEQ derived genetic position (Mascher et al. 2013)
[4]Specific alleles of each significant SNP marker

Marker Properties

Among the 1050 barley lines that were phenotyped with *P. teres* f. *teres*, 998 accessions had genotypic data that met our quality thresholds. This resulted in a total of 6525 high-quality SNPs with a minimum minor allele frequency (MAF) ≥ 5% and missing data per individual marker ≤ 50% to be used in association analyses. Additionally, allele similarity analysis eliminated 41 lines from the association panel due to genotypic redundancy, resulting in a total of 957 barley accessions used in subsequent analyses.

Linkage Disequilibrium, PCA, and Structure

PCA identified three principal components that accounted for at least 25% of the cumulative variation, with the first three principal components accounting for approximately 14%, 7%, and 5%, respectively (Figure 2.1). Initial STRUCTURE analysis indicated an optimal k value of 2, with 234 and 552 individuals belonging to sub-population one and two, respectively (Figure 2.2). The remaining 171 lines had membership probabilities of less than 0.80 to either of the populations and are considered admixed individuals. Visualization of the results of PCA (Figure 2.1) and STRUCTURE analysis (Figure 2.3) reveal a similar pattern of barley lines being clustered into groups corresponding to 2-row or 6-row classes. Population one from the STRUCTURE analysis corresponded to 2-row barley lines and population two represented 6-row barley lines.

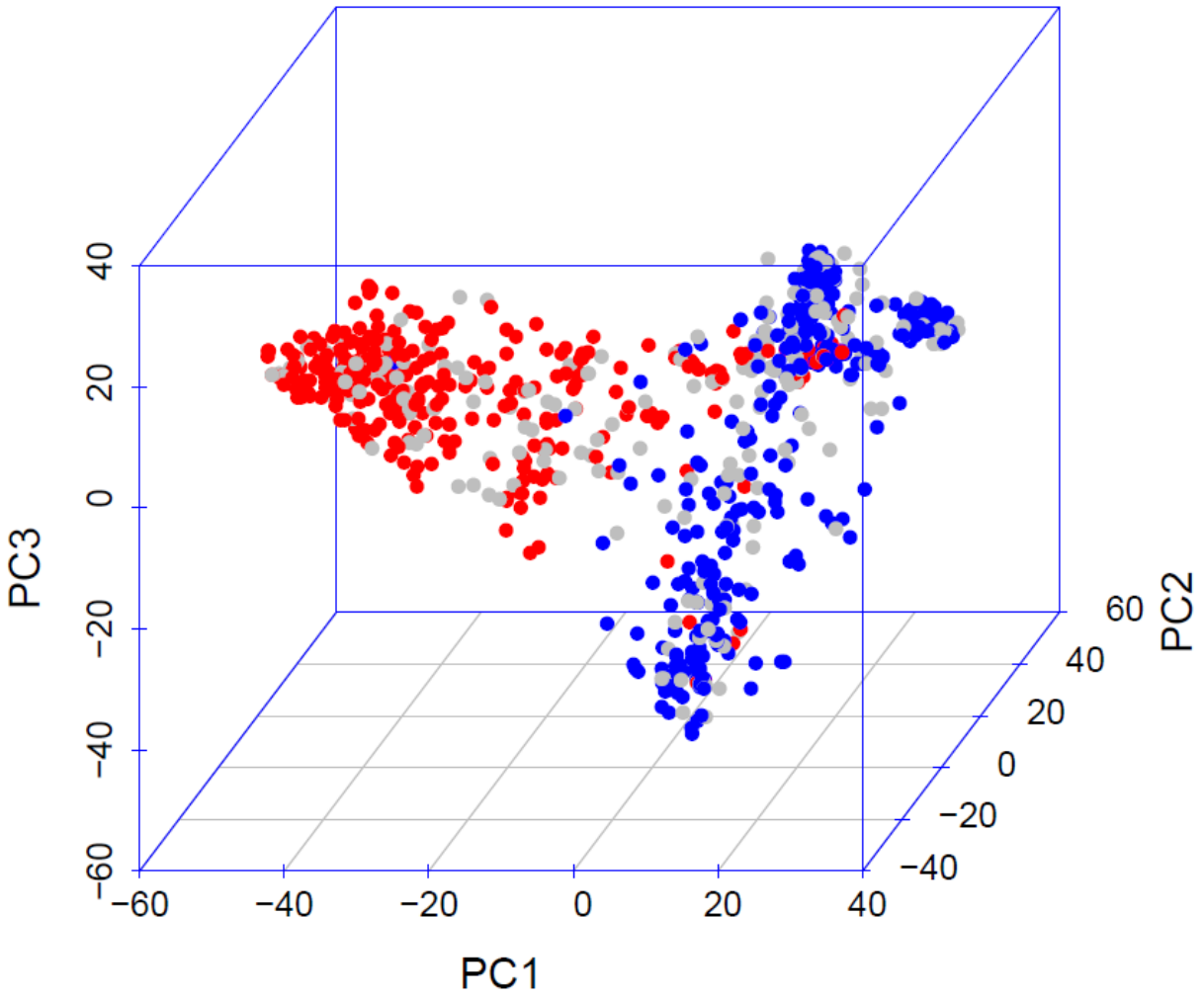

Fig. 2.1. A three dimensional representation of the principal components analysis conducted using 957 barley lines genotyped with the barley Illumina 9K iSelect chip. PC1 is illustrated on the x-axis, PC2 is listed on the z-axis, and PC3 is represented on the y-axis. Red dots correspond to 2-row individuals, blue dots correspond to 6-row individuals, and grey dots represent accessions with an unknown row-type. The distinct clustering of the barley genotypes into two groups is representative of 2-row and 6-row barley populations.

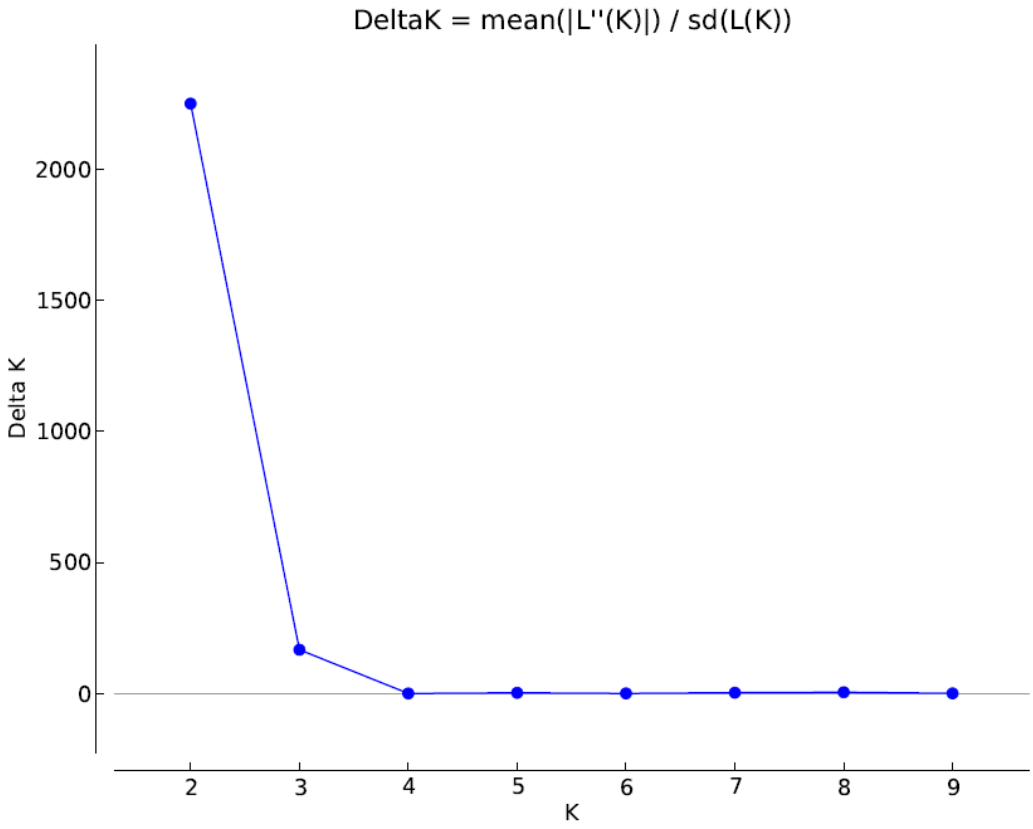

Fig. 2.2. Results of a STRUCTURE analysis conducted using 957 diverse barley lines. Hypothetical subpopulation levels are listed on the x-axis and Delta K values are listed on the y-axis. The largest Delta K value corresponds to a hypothetical sub-population of two, representing 2-row and 6-row barley classes.

Fig. 2.3. Graphical representation of a STRUCTURE analysis using 957 barley genotypes. Using genetic positions of the iSelect consensus map **(**Muñoz-Amatriaín et al. 2014), a single marker was selected from each locus and used in the analysis, resulting in a total of 1744 SNP markers. The results indicate that the barley lines used in this study are divided into two subpopulations. Subpopulation membership is listed on the y-axis ranging from 0.00-1.00. Red indicates membership to subpopulation one and green to subpopulation two. Individuals with membership to a single subpopulation of less than 0.80 were considered admixture.

Association Mapping

A total of nine models were used for association analyses and the optimal model was chosen by the calculation of the MSD. Very small differences were observed in the MSD values for models incorporating a kinship matrix, indicating that the inclusion of relatedness in association analyses appropriately corrected for the possibility of spurious associations. Results from models including kinship were very similar, but the model with the lowest MSD was chosen for further analysis (Table 2.2).

Table 2.2. Mean Squared Difference (MSD) Values for Nine Association Models

Isolate	Naïve[1]	PC_{25}[2]	Q[3]	PC_{25}+K[4]	Q+K[5]	PC_{25}+K_{comp}[6]	Q+K_{comp}[7]	K[8]	K_{comp}[9]
15A	0.15896	0.06081	0.07646	0.00008	0.00007	0.00008	0.00007	**0.00006**	0.00007
6A	0.23484	0.07791	0.06219	0.00012	0.00022	0.0001	**0.00008**	0.00013	0.00017
LDN	0.1549	0.04875	0.08141	**0.00001**	0.00002	0.00002	0.00002	0.00002	0.00001

[1]Association model not correcting for population structure or familial relatedness
[2]First three principal components accounting for ~25% cumulative variation
[3]Population structure
[4]First three principal components and kinship matrix
[5]Population struture and kinship matrix
[6]First three principal components and compressed kinship matrix
[7]Population structure and compressed kinship matrix
[8]Kinship matrix
[9]Compressed kinship matrix

Isolate 15A

The best model for association tests using average disease scores for isolate 15A only included an uncompressed kinship matrix (K) and had a MSD of 0.00006 (Table 2.2). A total of 41 markers with MAF ranging from 0.054-0.489 were significantly associated with average disease score at the threshold of $p < 0.001$ (Table 2.3). The –log10(p) of the significant markers ranged from 3.00-8.80 and explained between 0.73% to 2.51% of the phenotypic variation (R^2) per marker (Table 2.3). Significant markers were located on five barley chromosomes corresponding to eight unique loci. Two markers were located on 2H, two on 3H, one on 4H, 35

on 6H, and one on 7H (Table 2.3). The unique genomic regions identified include two on 2H (120.04 cM and 125.35 cM), two on 3H (47.1 cM and 150 cM), one on 4H (1.13 cM), two on 6H (48.94 cM to 49.79 cM, 53.6 cM to 55.52 cM), and one on 7H (131.02 cM) (Table 2.3). BLAST searches of the barley genome with marker SCRI_RS_188420 did not result in the anchoring to a POPSEQ genetic position, however, its iSelect consensus map position places it near the telomere of the long arm of chromosome 3H at ~150 cM. Additionally, three markers on chromosome 6H (11_20936, SCRI_RS_111556, and SCRI_RS_111820) were unable to be anchored to a POPSEQ position via BLAST searches of the barley genome, however, comparison of their respective consensus map positions and the POPSEQ positions of other markers at a similar consensus map locus allowed for the inclusion of them into corresponding unique loci. Marker 11_20936 was placed in the 6H 48.94 cM to 49.79 cM bin and markers SCRI_RS_111556 and SCRI_RS_111820 were placed into the 6H 53.6 cM to 55.52 cM bin.

Table 2.3. Significant markers associated with disease reaction to *P. teres* f. *teres* isolate 15A

Marker	Chr.[a]	Position[b]	P-value[c]	FDR[d]	R^{2}[e]	MAF[f]
12_30690	2H	120.04	3.21	0.114	0.008	0.176
12_10579	2H	125.35	5.67	0.003	0.015	0.110
12_30721	3H	47.1	3.24	0.112	0.008	0.054
SCRI_RS_188420	3H	N/A	3.59	0.060	0.009	0.068
SCRI_RS_154517	4H	1.13	3.08	0.140	0.008	0.306
SCRI_RS_213547	6H	48.94	4.09	0.024	0.011	0.237
SCRI_RS_162581	6H	49.08	5.03	0.009	0.013	0.231
SCRI_RS_196459	6H	49.08	4.84	0.009	0.013	0.393
SCRI_RS_120783	6H	49.08	4.30	0.019	0.011	0.488
SCRI_RS_151282	6H	49.15	5.57	0.003	0.015	0.229
SCRI_RS_119674	6H	49.22	5.92	0.002	0.016	0.344
SCRI_RS_196458	6H	49.22	4.80	0.009	0.013	0.487
SCRI_RS_142506	6H	49.22	3.79	0.042	0.010	0.372
11_10013	6H	49.22	6.19	0.002	0.017	0.213

Table 2.3. Significant markers associated with disease reaction to *P. teres* f. *teres* isolate 15A (continued).

Marker	Chr.[a]	Position[b]	P-value[c]	FDR[d]	R^{2e}	MAF[f]
12_30316	6H	49.22	4.15	0.022	0.011	0.481
SCRI_RS_168111	6H	49.5	5.96	0.002	0.016	0.344
12_30658	6H	49.79	4.73	0.010	0.013	0.367
11_10539	6H	49.79	4.30	0.019	0.011	0.460
12_31479	6H	53.6	3.95	0.031	0.010	0.104
SCRI_RS_162504	6H	53.9	3.94	0.031	0.010	0.175
SCRI_RS_153797	6H	54.32	3.16	0.121	0.008	0.177
SCRI_RS_144579	6H	54.82	3.49	0.071	0.009	0.173
SCRI_RS_162760	6H	54.87	4.88	0.009	0.013	0.168
SCRI_RS_188305	6H	54.89	4.33	0.019	0.011	0.121
SCRI_RS_144162	6H	55.03	4.85	0.009	0.013	0.174
SCRI_RS_148652	6H	55.03	3.29	0.105	0.008	0.172
SCRI_RS_207083	6H	55.03	3.23	0.112	0.008	0.171
SCRI_RS_224389	6H	55.03	4.16	0.022	0.011	0.404
12_30749	6H	55.03	3.38	0.088	0.008	0.169
SCRI_RS_176650	6H	55.03	8.80	0.000	0.025	0.217
SCRI_RS_188243	6H	55.03	4.38	0.019	0.011	0.085
12_31178	6H	55.03	3.00	0.158	0.007	0.197
SCRI_RS_136604	6H	55.03	4.37	0.019	0.011	0.119
SCRI_RS_195914	6H	55.03	3.55	0.064	0.009	0.144
12_31006	6H	55.21	3.68	0.053	0.009	0.160
SCRI_RS_118255	6H	55.38	3.64	0.056	0.009	0.171
SCRI_RS_239917	6H	55.52	3.01	0.158	0.007	0.326
11_20936	6H	N/A	3.20	0.114	0.008	0.462
SCRI_RS_111556	6H	N/A	4.23	0.020	0.011	0.174
SCRI_RS_111820	6H	N/A	4.23	0.020	0.011	0.174
SCRI_RS_183593	7H	131.02	3.12	0.129	0.008	0.280

[a] Chromosome
[b] Genetic position derived from anchoring via POPSEQ (Mascher et al. 2013)
[c] –log10(p) of each marker
[d] False discovery rate (FDR) adjusted p-values
[e] Estimate of phenotypic variation due to a marker effect
[f] Minor allele frequency

Isolate 6A

An association model incorporating both population structure (Q) and a compressed kinship matrix (K_{comp}) was found to be the optimal model with a MSD of 0.00008 (Table 2.2). A total of 24 significant markers were detected with –log10(p) values ranging from 3.00-8.70 and MAF ranging from 0.08-0.47. Phenotypic variation attributed to each marker (R^2) ranged from 0.55% to 1.85%. Significant markers were located on four barley chromosomes corresponding to seven unique loci. Two markers were located on chromosome 4H, two on 5H, 17 on 6H, and three on 7H (Table 2.4). The distinct genomic regions detected include one on 4H (52.69 cM), one on 5H (93.4cM), three on 6H (49.79 cM, 54.82 cM to 55.38 cM, and 59.92 cM), and two on 7H (70.54 cM and 131.02 cM). Additionally, a marker (SCRI_RS_158011) was unmapped in the iSelect consensus map and was assigned to chromosome 6H through BLAST searches of the barley genome, however, no specific genetic locus was obtained through this method. BLAST searches of an additional marker (11_21310) from chromosome 6H did not yield POPSEQ positions, however, due to its consensus map position in comparison to nearby markers, it was placed into the chromosome 6H 59.92 to 60.48 cM bin. Marker SCRI_RS_4717 was unmapped on the iSelect consensus map, however, BLAST searches of the barley genome anchored it to the short arm of chromosome 5H.

Isolate LDN

A model including the first three principal components explaining approximately 25% of the cumulative variation (PC_{25}) and an uncompressed kinship matrix (K) was selected as the best model for the isolate LDN with a MSD of 0.00001 (Table 2.2). A total of 23 significant markers were identified with seven markers located on chromosome 3H, one on 4H, one on 5H, 13 on 6H, and one on 7H. The –log10(p) of the significant markers ranged from 3.03 to 8.22 and had a

MAF ranging from 0.15 to 0.49. Phenotypic variation (R^2) of individual markers varied from 0.79% to 2.48% (Table 2.5). A total of nine distinct genomic loci were detected, including three on 3H (2.41 cM to 2.69 cM, 46.03 cM, and 83.99 cM), one on 4H (52.69 cM), one on 5H (69.31

Table 2.4. Significant markers associated with disease reaction to *P. teres* f. *teres* isolate 6A.

Marker	Chr.[a]	Position[b]	P-value[c]	FDR[d]	R^{2e}	MAF[f]
SCRI_RS_181886	4H	52.69	4.26	0.061	0.008	0.291
SCRI_RS_170494	4H	52.69	3.05	0.245	0.006	0.232
11_21314	5H	93.4	3.05	0.245	0.006	0.085
SCRI_RS_4717	5H	N/A	3.14	0.245	0.006	0.313
12_10199	6H	49.79	3.16	0.245	0.006	0.099
11_20835	6H	54.82	8.70	0.000	0.019	0.332
11_10227	6H	54.89	5.00	0.016	0.010	0.308
SCRI_RS_7104	6H	54.89	3.42	0.223	0.006	0.158
SCRI_RS_165041	6H	54.89	3.17	0.245	0.006	0.424
SCRI_RS_188305	6H	54.89	3.28	0.244	0.006	0.121
SCRI_RS_213566	6H	55.03	6.29	0.002	0.013	0.280
SCRI_RS_188243	6H	55.03	5.33	0.010	0.011	0.085
12_30857	6H	55.03	3.50	0.223	0.007	0.339
SCRI_RS_136604	6H	55.03	4.44	0.048	0.009	0.119
12_30254	6H	55.03	3.39	0.223	0.006	0.146
SCRI_RS_142541	6H	55.38	3.24	0.245	0.006	0.421
SCRI_RS_138529	6H	55.38	3.17	0.245	0.006	0.371
SCRI_RS_138001	6H	55.38	3.03	0.245	0.006	0.157
SCRI_RS_106581	6H	59.92	3.33	0.237	0.006	0.189
11_21310	6H	N/A	3.47	0.223	0.007	0.474
SCRI_RS_158011	6H	N/A	3.98	0.099	0.008	0.380
11_10700	7H	70.54	3.00	0.245	0.006	0.361
12_31055	7H	70.54	3.12	0.245	0.006	0.360
SCRI_RS_183593	7H	131.02	3.62	0.198	0.007	0.280

[a] Chromosome
[b] Genetic position derived from anchoring via POPSEQ (Mascher et al. 2013)
[c] –log10(p) of each marker
[d] False discovery rate (FDR) adjusted p-values
[e] Estimate of phenotypic variation due to a marker effect
[f] Minor allele frequency

cM), three on 6H (49.08 cM to 49.22 cM, 53.60 cM to 55.38 cM, 65.86 cM), and one on 7H (131.02 cM). Additionally, one marker (SCRI_RS_182648) was not anchored on the iSelect consensus map but was assigned to chromosome 6HL via BLAST searches of the barley genome.

Table 2.5. Significant markers associated with disease reaction to *P. teres* f. *teres* isolate LDN

Marker	Chr.[a]	Position[b]	P-value[c]	FDR[d]	R^{2}[e]	MAF[f]
SCRI_RS_119379	3H	2.41	7.88	0.000	0.024	0.492
SCRI_RS_180343	3H	2.69	6.35	0.001	0.019	0.298
12_31409	3H	2.69	4.67	0.023	0.013	0.330
SCRI_RS_172351	3H	2.69	4.44	0.030	0.012	0.207
11_20159	3H	2.69	4.21	0.044	0.012	0.216
11_20356	3H	46.03	4.47	0.030	0.013	0.150
SCRI_RS_235849	3H	83.99	3.40	0.153	0.009	0.443
SCRI_RS_181886	4H	52.69	3.77	0.101	0.010	0.292
SCRI_RS_152347	5H	69.31	3.06	0.259	0.008	0.339
SCRI_RS_152174	6H	49.08	3.14	0.238	0.008	0.320
SCRI_RS_211299	6H	49.08	3.10	0.245	0.008	0.456
SCRI_RS_140158	6H	49.22	3.68	0.106	0.010	0.365
11_21124	6H	53.60	3.03	0.267	0.008	0.148
SCRI_RS_7104	6H	54.89	8.22	0.000	0.025	0.156
12_31178	6H	55.03	7.70	0.000	0.023	0.196
SCRI_RS_13935	6H	55.03	3.86	0.089	0.011	0.241
SCRI_RS_138001	6H	55.38	7.62	0.000	0.023	0.156
SCRI_RS_138529	6H	55.38	3.52	0.124	0.009	0.373
SCRI_RS_137464	6H	55.38	3.31	0.179	0.009	0.480
11_10377	6H	55.38	3.28	0.180	0.009	0.179
SCRI_RS_139937	6H	65.86	3.71	0.106	0.010	0.363
SCRI_RS_182648	6H	N/A	3.64	0.106	0.010	0.242
SCRI_RS_183593	7H	131.02	3.60	0.111	0.010	0.283

[a] Chromosome
[b] Genetic position derived from anchoring via POPSEQ (Mascher et al. 2013)
[c] –log10(p) of each marker
[d] False discovery rate (FDR) adjusted p-values
[e] Estimate of phenotypic variation due to a marker effect
[f] Minor allele frequency

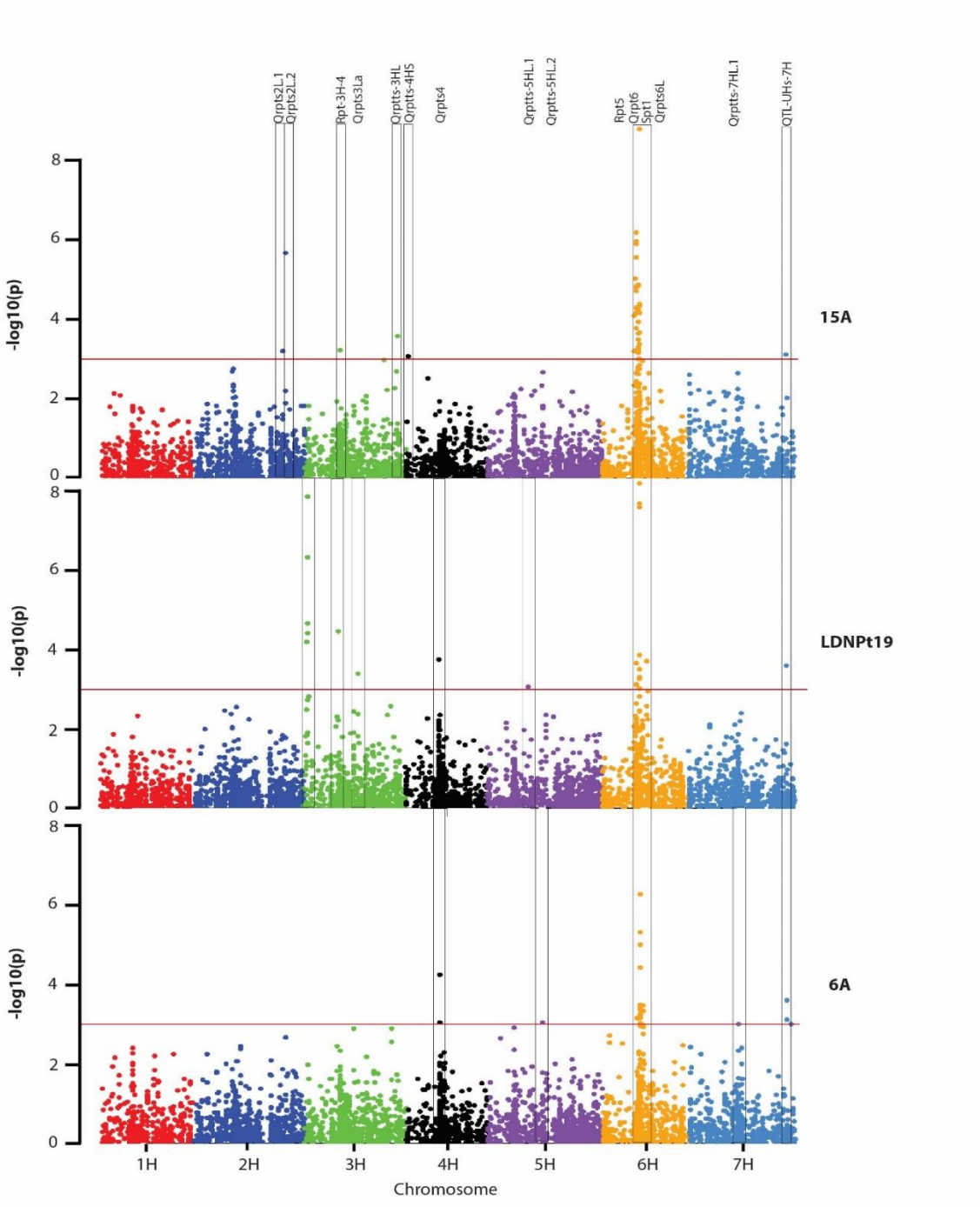

Fig. 2.4. Association mapping analyses of disease reaction to *P. teres* f. *teres* isolates 15A (California), LDN (North Dakota), and 6A (California). Barley chromosomes are listed on the x-axis. A –log10(p) scale of significance is represented on the y-axis with the red horizontal line representing the significance threshold of –log10(p) = 3. The colored pixels represent individual SNP markers used in the association analyses. Both previously identified and newly designated QTL are listed at the top of the figure. Boxes are drawn around the distinct significant loci detected.

Discussion

Net form net blotch of barley has the potential to cause severe economic impacts in all barley production regions of the world. Thus, the identification of barley resistance/susceptibility QTL that interact with the effectors present within the highly diverse pathogen populations is important to effectively deploy durable genetic resistance against this adaptable enemy. Regions of the barley genome associated with resistance or susceptibility to *P. teres* f. *teres* have previously been identified through traditional QTL analysis methods utilizing bi-parental populations (reviewed by Liu et al. 2011). Although this method provides a powerful genetic approach to characterize these complex interactions, it does have limitations that can be overcome using the GWAS approach. These limitations include the time required to develop bi-parental populations and the ability to select parents representing the greatest amount of functional polymorphism. The amount of functional polymorphism captured by each host population only represents a very small proportion available in the primary barley germplasm pool because of the high variability of effectors in pathogen populations and the diverse interacting host resistance or necrotrophic effector susceptibility targets. Here we utilize GWAS as an alternative to identify NFNB resistance/susceptibility QTL. Using a diverse panel of barley germplasm, GWAS identified 16 distinct loci associated with disease reaction to three North American *P. teres* f. *teres* isolates.

Although GWAS is a very powerful approach it also has its own limitations. A major concern when conducting GWAS is the detection of false associations, but the error can be reduced by accounting for population structure and kinship in the linear models. A total of nine models were tested in this study, utilizing population structure derived from Bayesian clustering in STRUCTURE (Q) (Pritchard et al. 2000) and the use of PCs accounting for at least 25% of

cumulative variation (PC_{25}), as well as accounting for familial relatedness using a kinship matrix produced using the Loiselle algorithm (K and K_{comp}) (Loiselle et al. 1995). Additionally, both uncompressed and compressed kinship matrices were used to evaluate any differences in the reduction of spurious associations or an increase in statistical power (Zhang et al. 2010; Li et al. 2014). Overall, the performance of models that included kinship (K or K_{comp}) were very similar, regardless of the inclusion of population structure. This indicated that using relatedness was sufficient for the control of false positive MTA and that using population structure alone was not stringent enough in the diversity panel used.

The lowest MSD value was used as the model selection criteria and selected a different model for each isolate (Table 2.2). GWAS using the best model for each isolate revealed 16 unique genomic regions represented by a total of 78 significant markers. Following FDR p-value adjustment, seven loci did not meet the adjusted p-value threshold of < 0.10. However, further examination reveals that the FDR adjustment may be too stringent for these analyses. One of the loci on chromosome 4H fell below the significance threshold after FDR adjustment for isolate LDN but remained significant for isolate 6A and this QTL region had been previously identified via bi-parental mapping (Steffenson et al. 1996; Grewal et al. 2008). Also, a locus on chromosome 7H, which was common to all three isolates and represented the previously identified locus QTL_{UHs}-7H in bi-parental population analyses (König et al. 2013) also did not meet the adjusted FDR p-value criteria. Additionally, a distinct locus near the commonly mapped chromosome 6H centromere (Steffenson et al. 1996) did not meet the adjusted p-value threshold for isolates 6A and LDN, but remained significant for isolate 15A. The data suggest that these are not false associations due to the fact that loci appeared significant at unadjusted p-values of < 0.001 between more than a single isolate and corresponded to QTL previously mapped in bi-

parental populations, thus, indicating that FDR adjustment may be too stringent at some loci resulting in the loss of true positive associations. Therefore, the unadjusted p-values were used as the determinant of significance for the association analyses.

Two markers on the long arm of chromosome 2H, 12_30690 and 12_10579, were found to be significantly associated with disease reaction to *P. teres* f. *teres* isolate 15A and are approximately 5.31 cM apart based on genetic anchoring via POPSEQ (Mascher et al. 2013). Analysis of local LD between these two markers revealed a very low level of correlation with an R^2 value of 0.004, indicating that these two markers may represent two distinct loci and that significance did not arise due to tight linkage. Previously, Raman et al. (2003) identified a QTL on the long arm of chromosome 2H designated *QRpts2L* which accounted for approximately 7% of the phenotypic variation in a bi-parental population. Due to the low resolution of the mapping in the Raman and colleagues study and the use of AFLP and RFLP markers, it was not possible to determine a POPSEQ position for the QTL they reported with any certainty. Thus, one or both of the MTA detected here may be linked to the resistance gene/genes underling the previously identified *QRpts2L* QTL, thus we have designated these loci, *QRpts2L.1* and *QRpts2L.2*.

A total of four distinct loci were detected on chromosome 3H with two corresponding to disease reaction to either *P. teres* f. *teres* isolate LDN or isolate 15A. A strongly associated locus comprised of five significant markers was identified at approximately 2.41 cM to 2.69 cM. A QTL was previously identified at this locus in a Hector × NDB112 RIL population explaining approximately 20% of the phenotypic variation (Liu et al. 2015). Additionally, the isolate used to detect this QTL in the Hector × NDB112 population was collected from the same region as LDN, indicating that they likely possess the same necrotrophic effector which interacts with a host gene at this locus. An additional locus was identified that was unique to isolate LDN at

approximately 83.99 cM on chromosome 3H. QTL had been previously detected on chromosome 3H at approximately 75 cM (*QRpts3La*) and 89 cM with R^2 values of 0.16 and 0.07, respectively (Raman et al. 2003; Liu et al. 2015). Since the locus detected in our association analysis falls within this region, it may be the same as those previously identified (Fig. 2.4). The analysis conducted using isolate 15A revealed a unique locus near the telomere of the long arm of chromosome 3H designated *QRptts-3HL* (Fig. 2.4). As the strongest associated marker (SCRI_RS_188420) at this locus was not anchored to a POPSEQ position, markers flanking this position (11_10935 and SCRI_RS_126369) from the iSelect consensus map were used in BLAST searches to estimate its position placing it in the approximate interval of 142.2 cM to 143.13 cM. The nearest QTL previously identified on the long arm of chromosome 3H are located at approximately 109 and 114 cM (Liu et al. 2015; Raman et al. 2003). This indicates that the significant association detected in this study represents a novel locus linked to disease reaction to isolate 15A and was given the designation *QRptts-3HL* (Fig. 2.4). A fourth locus was identified near the centromere on chromosome 3H in the interval from 46.03 cM to 47.01 cM and was common to both isolates LDN and 15A. A study had previously mapped a QTL designated *Rpt-3H-4*, to a similar locus (~46 cM) near the centromere of chromosome 3H with R^2 value of 0.12, indicating that this associated locus is likely the same QTL as *Rpt-3H-4* (Fig. 2.4: Yun et al. 2005).

A common locus was detected near the centromere of chromosome 4H at POPSEQ position 52.69 cM associated with disease reaction to isolates 6A and LDN. This centromeric locus had been previously identified in the bi-parental population of Steptoe × Morex (Steffenson et al. 1996) as evidenced by BLAST searches of the barley genome using the sequence of the nearby marker, ABG484, of the previously mapped QTL (LOD=11.1 and

R^2=0.31). Also, Grewal et al. (2008) identified the same QTL, designated *QRpts4* (Fig. 2.4), in a CDC Dolly × TR251 DH population with a LOD of 4.2 and an R^2 of 5%. Interestingly, it was also determined that this QTL was associated with resistance to spot form net blotch and represents a potential source of resistance to two closely related yet distinct pathogens (Tamang et al., 2015). An additional locus was identified near the telomere of the short arm of chromosome 4H associated with isolate 15A at POPSEQ position 1.13 cM designated *QRptts-4HS* (Fig. 4). No previously identified QTL have been reported near this locus, indicating that it is a novel QTL. Two distinct loci were detected on the long arm of chromosome 5H at POPSEQ positions 69.31 and 93.4 cM associated with disease reaction to isolates LDN and 6A designated *QRptts-5HL.1* and *QRptts-5HL.2* (Fig. 2.4), respectively. Previously, no QTL had been detected on the long arm of chromosome 5H, indicating that both of these loci are novel. Additionally, marker SCRI_RS_4717 was significantly associated to disease reaction to isolate 6A, and was localized to the short arm of chromosome 5H. Although no POPSEQ position could be derived, it is possible that this marker belongs to the locus described by Liu et al. (2015) at the ~45 cM position using the same isolate.

The centromeric region of barley chromosome 6H has long been associated with resistance or susceptibility to NFNB. Various studies have mapped both dominant resistances and dominant susceptibilities to the same region using a diverse array of barley genotypes and pathogen isolates (Steffenson et al. 1996, Graner et al. 1996, Richter et al. 1998, Raman et al. 2003, Cakir et al. 2003, Ma et al. 2004, Emebiri et al. 2005, Yun et al. 2005, Manninen et al. 2000, Manninen et al. 2006, Friesen et al. 2006, Grewal et al. 2008, Abu Qamar et al. 2008, St. Pierre et al. 2010). Unsurprisingly, 58 of the total 79 significant markers detected in this study were localized to the centromeric region of chromosome 6H within the interval of ~49-66 cM,

with four distinct loci. These loci were detected at the approximate positions of 49, 55, 60, and 66 cM. The ~60 cM locus was specific to isolate 6A while the ~65 cM locus was only associated with isolate LDN. Additionally, the ~66 cM locus was detected by Liu et al. (2015) using a Hector × NDB112 bi-parental population and Japanese isolate JPT9901. This indicates that the North Dakota isolate LDN used in this GWAS and JPT9901, although geographically diverse, may possess a common necrotrophic effector targeting a host gene at this locus. Both the ~49 cM and ~ 55 cM loci were significantly associated with disease reaction to all three isolates, however, 33 of the 58 significant MTAs at the centromeric 6H region belong to the ~55 cM locus. This indicates that underlying this region is likely a cluster of resistance or susceptibility genes. A recent high-resolution mapping study of the region at POPSEQ position corresponding to ~54 cM localized the dominant susceptibility gene *Spt1* to a small ~ 0.24 cM region (Richards et al., 2016). Yet, surprisingly it appeared that at least four different virulence genes (Shjerve et al., 2014) targeted a single susceptibility locus at this region suggesting that alleles of the same susceptibility gene are targeted by multiple distinct necrotrophic effectors or a tight cluster of susceptibility genes are present at this locus (Richards et al., 2016).

A common locus near the telomere of chromosome 7HL was detected in all three isolates at ~131 cM (Fig. 4). König et al. (2013) described a minor QTL, QTL_{UHs}-7H, on the short arm of chromosome 7H in the DH population of Uschi × HHOR3073, however, BLAST searches of the sequences of the markers reported in their linkage group on the short arm of 7H are not co-linear with the POPSEQ consensus positions. Additionally, marker GBM1464, which is tightly linked to the identified QTL, is positioned at ~130 cM, indicating that the previously detected QTL is likely the same as the MTA detected in this study, however positioned incorrectly on the previously published map. Additionally, a novel locus was detected at ~70 cM on the long arm

of chromosome 6H designated *QRptts-7HL.1* (Fig. 2.4) and is associated with disease reaction to isolate 6A.

This study reports on the first use of GWAS for the detection of markers significantly associated with disease reactions of barley to the necrotrophic fungal pathogen *P. teres* f. *teres*. A total of 78 MTAs were detected, corresponding to 16 unique genomic loci associated with resistance or susceptibility to three North American *P. teres* f. *teres* isolates, exemplifying the diversity of interactions occurring and complexity of this pathosystem. The loci identified could harbor either resistances or susceptibility targets because both dominant gene-for-gene and recessive inverse gene-for-gene types of resistances have been previously described in barley-*P. teres* f. *teres* genetic interactions. Haplotype analysis of the significant SNP markers at each QTL of the highly resistant barley lines revealed a predominance of shared genotypes providing a useful resource for marker assisted selection. The results provide foundational genetic information for the effective deployment of resistance or the elimination of host susceptibility factors from elite barley lines, providing a durable means of management for this economically important disease.

Literature Cited

Abu Qamar, M., Liu, Z. H., Faris, J. D., Chao, S., Edwards, M. C., Lai, Z., Frankowiak, J. D., and Friesen, T. L. 2008. A region of barley chromosome 6H harbors multiple major genes associated with the net type net blotch resistance. Theor Appl Genet 117:1261-1270

Akhavan, A., Turkington, T. K., Askarian, H., Tekauz, A., Xi, K., Tucker, J. R., Kutcher, H. R., and Strelkov, S. E. 2016. Virulence of *Pyrenophora teres* populations in western Canada. Can J Plant Pathol http://dxdoiorg/101080/0706066120161159617

Bradbury, P. J., Zhang, Z., Kroon, D. E., Casstevens, T. M., Ramdoss, Y., and Buckler, E. S. 2007. TASSEL: software for association mapping of complex traits in diverse samples. Bioinformatics 23:2633-2635

Cakir, M., Gupta, S., Platz, G. J., Ablett, G. A., Loughman, R., Embiri, L. C., Poulsen, D., Li, C., Lance, R. C. M., Galway, N. W., Jones, M. G. K., and Appels, R. 2003. Mapping and validation

of the genes for resistance to Pyrenophora teres f teres in barley (Hordeum vulgare L). Aust J Agric Res 54:1369-1377

Earl, D. A. and von Holdt, B. M. 2012. STRUCTURE HARVESTER: a website and program for visualizing STRUCTURE output and implementing the Evanno method. Conservation Genet Resour 4(2):359-361

Emebiri, L. C., Platz, G., and Moody, D. B. 2004. Disease resistance genes in a doubled haploid population of two-rowed barley segregating for malting quality attributes Aust J Agric Res 56(1):49-56

Evanno, G., Regnaut, S., and Goudet, J. 2005. Detecting the number of clusters of individuals using the software STRUCTURE: a simulation study. Mol Ecol 14(8):2611-2620

Friesen, T. L., Faris, J. D., Lai, Z., and Steffenson, B. J. 2006. Identification and chromosomal location of major genes for resistance to Pyrenophora teres in a barley doubled haploid population. Genome 409:855-859

Graner, A., Foroughi-Wehr, B., and Tekauz, A. 1996. RFLP mapping of a gene in barley conferring resistance to net blotch (*Pyrenophora teres*). Euphytica 91:229-234

Grewal, T. S., Rossnagel, B. G., Pozniak, C. J., and Scoles, G. J. 2008. Mapping quantitative trait loci associated with barley net blotch resistance. Theor Appl Genet 116:529-539

Ho, K. M., Tekauz, A., Choo, T. M., and Martin, R. A. 1996. Genetic studies on net blotch resistance in a barley cross. Can J Plant Sci 76(4):715-719

International Barley Genome Sequencing Consortium. 2012. A physical, genetic and functional sequence assembly of the barley genome. Nature 491(7426):711-716

Kump, K. L., Bradbury, P. J., Wisser, R., Buckler, E. S., Belcher, A. R., Oropeza-Rosas, M. A., Zwonitzer, J. C., Kresovich, S., McMullen, M. D., Ware, D., Balint-Kurti, P. J., Holland, and J. B. 2011. Genome-wide association study of quantitative resistance to southern leaf blight in the maize nested association mapping population. Nature Genetics 43:163-168

Li, M., Liu, X., Bradbury, P., Yu, J., Zhang, Y., Todhunter, R. J., Buckler, E. S., and Zhang, Z. 2014. Enrichment of statistical power for genome-wide association studies. BMC Biol 12:73

Lipka, A. E., Tian, F., Wang, Q., Peiffer, J., Li, M., Bradbury, P. J., Gore, M. A., Buckler, E. S., and Zhang, Z. 2012 GAPIT: genome association and prediction integrated tool. Bioinformatics 28(18):2397-2399

Liu, Z. H., Zhong, S., Stasko, A. K., Edwards, M. C., and Friesen, T. L. 2012. Virulence Profile and Genetic Structure of a North Dakota Population of *Pyrenophora teres* f *teres*, the Causal Agent of Net Form Net Blotch of Barley. Phytopathology 102(5):539-546

Loiselle, B. A., Sork, V. L., Nason, J., and Graham, C. 1995. Spatial genetic structure of a tropical understory shrub, Psychotria officinalis (Rubiaceae). Am J Bot 82:1420-1425

Mamidi, S., Chikara, S., Goos, J. R., Hyten, D. L., Annam, D., Mafi Moghaddam, S., Lee, R. K., Cregan, P. C., and McClean, P. E. 2011. Genome-Wide Association Analysis Identifies Candidate Genes Associated with Iron Deficiency Chlorosis in Soybean. Plant Genome 4:154-164

Ma, Z. A., Lalpitan, N. L. V., and Steffenson, B. 2004. QTL mapping of net blotch resistance genes in a doubled-haploid population of six-rowed barley. Euphytica 137:291-296

Manninen, O., Kalendar, R., Robinson, J., and Schulman, A. H. 2000. Application of BARE-1 retrotransposon markers to the mapping of a major resistance gene for net blotch in barley. Mol Genet Genomics 264:325-334

Manninen, O. M., Jalli, M., Kalendar, R., Schulman, A., Afanasenko, O., and Robinson, J. 2006. Mapping of major spot-type and net-type net-blotch resistance genes in the Ethiopian barley line CI 9819. Genome 49:1564-1571

Mascher, M., Muehlbauer, G. J., Rokhsar, D. S., Chapman, J., Schmutz, J., Barry, K., Muñoz-Amatriaín, M., Close, T. J., Wise, R. P., Schulman, A. H., Himmelbach, A., Mayer, K. F., Scholz, U., Poland, J. A., Stein, N., and Waugh, R. 2013. Anchoring and ordering NGS contig assemblies by population sequencing (POPSEQ). Plant J 76(4):718-727

Massman, J., Cooper, B., Horsley, R., Neate, S., Dill-Macky, R., Chao, S., Dong, Y., Schwarz, P., Muehlbauer, G. J., and Smith, K. P. 2011. Genome-wide association mapping of Fusarium head blight resistance in contemporary barley breeding germplasm. Mol Breeding 27:439-454

Mathre, D. E. 1997. Compendium of Barley Diseases, 2nd edn. St Paul, MN

Muñoz-Amatriaín, M., Cuesta-Marcos, A., Endelman, J. B., Comadran, J., Bonman, J. M., Bockelman, H. E., Chao, S., Russell, J., Waugh, R., Hayes, P. M., and Muehlbauer, G. J. 2014. The USDA Barley Core Collection: Genetic Diversity, Population Structure, and Potential for Genome-Wide Association Studies. PLoS One 94:e94688

McLean, M. S., Howlett, B. J., and Hollaway, G. J. 2009. Epidemiology and control of spot form of net blotch (Pyrenophora teres f maculata) of barley: a review. Crop Pasture Sci 60:303-315

Neupane, A., Tamang, P., Brueggeman, R. S., and Friesen, T. L. 2015. Evaluation of a Barley Core Collection for Spot Form Net Blotch Reaction Reveals Distinct Genotype-Specific Pathogen Virulence and Host Susceptibility. Phytopathology 105(4):509-517

Peever, T. L. and Milgroom, M. G. 1994. Genetic structure of *Pyrenophora teres* populations determined with random amplified polymorphic DNA markers. Can J Bot 72:915-923

Pritchard, J. K., Stephens, M., and Donnelly, P. 2000. Inference of Population Structure Using Multilocus Genotype Data Genetics. 155(2):945-959

Rafalski, J. A. 2010. Association genetics in crop improvement. Curr Opin Plant Biol 13:174-180

Raman, H., Platz, G. J., Chalmers, K. J., Raman, R., Read, B. J., Barr, A. R., and Moody, D. B. 2003. Mapping of genetic regions associated with net form of net blotch resistance in barley. Aust J Agric Res 54:1359-1367

Rau, D., Maier, F. J., Papa, R., Brown, A. H. D., Balmas, V., Saba, E., Schaefer, W., and Attene, G. 2005. Isolation and characterization of the mating-type locus of the barley pathogen *Pyrenophora teres* and frequencies of mating-type idomorphs within and among fungal populations collected from barley landraces. Genome 48(5):855-869

Rau, D., Attene, G., Brown, A. H. D., Nanni, L., Maier, F. J., Balmas, V., Saba, E., Schafer, W., and Papa, R. 2007. Phylogeny and evolution of mating-type genes from *Pyrenophora teres*, the causal agent of barley "net blotch" disease. Curr Genet 51:377-392

Richards, J., Chao, S., Friesen, T., and Brueggeman, R. 2016. Fine Mapping of the Barley Chromosome 6H Net Form Net Blotch Susceptibility Locus. G3 G3-116

Scheet, P. and Stephens, M. 2006. A fast and flexible statistical model for large-scale population genotype data: applications to inferring missing genotypes and haplotypic phase. Am J Hum Genet 78(4):629-644

Serenius, M., Manninen, O., Wallwork, H., and Williams, K. 2007. Genetic differentiation in *Pyrenophora teres* populations measured with AFLP markers. Mycol Res 111(2):213-223

Shjerve, R. A., Faris, J. D., Brueggeman, R. S., Yan, C., Zhu, Y., Koladia, V., and Friesen, T. L. 2014. Evaluation of a *Pyrenophora teres* f. *teres* mapping population reveals multiple independent interactions with a region of barley chromosome 6H. Fungal Genet Biol 70:104-112

Smedegård-Petersen, V. 1971. *Pyrenophora teres* f *maculata* f nov and *Pyrenophora teres* f. *teres* on barley in Denmark. Kgl Vet Landbohojsk Arsskr 124–144

St Pierre, S., Gustus, C., Steffenson, B., Dill-Macky, R., and Smith, K. P. 2010. Mapping net form net blotch and Septoria speckled leaf blotch resistance loci in barley. Phytopathol 100(1):80-84

Steffenson, B. J. and Webster, R. K. 1992. Quantitative resistance to *Pyrenophora teres* f. *teres* in barley. Phytopathol 82(4):407-411

Steffenson, B. J., Hayes, H. M., and Kleinhofs, A. 1996. Genetics of seedling and adult plant resistance to net blotch (*Pyrenophora teres* f. *teres*) and spot blotch (*Cochliobolus sativus*) in barley. Theor Appl Genet 92:552-558

Tamang, P., Neupane, A., Mamidi, S., Friesen, T., and Brueggeman, R. 2015. Association Mapping of Seedling Resistance to Spot Form Net Blotch in a Worldwide Collection of Barley Phytopathology. 105(4):500-508

Tekauz, A. 1985. A Numerical Scale to Classify Reactions of Barley to *Pyrenophora teres.* Can J Plant Pathol 7(2):181-183

Tekauz, A. 1990. Characterization and distribution of pathogenic variation in *Pyrenophora teres* f. *teres* and *P teres* f. *maculata* from western Canada. Can J Plant Pathol 12(2):141-148

Tian, F., Bradbury, P. J., Brown, P. J., Hung, H., Sun, Q., Flint-Garcia, S., Rocheford, T. R., McMullen, M. D., Holland, J. B., and Buckler, E. S. 2011. Genome-wide association study of leaf architecture in the maize nested association mapping population. Nature Genetics 43:159-162

Wu, H. L., Steffenson, B. J., Zhong, S., Li, Y., and Oleson, A. E. 2003. Genetic variation for virulence and RFLP markers in *Pyrenophora teres.* Can J Plant Path 25(1):82-90

Tang, Y., Liu, X., Wang, J., Li, M., Wang, Q., Tian, F., Su, Z., Pan, Y., Lipka, A. E., Buckler E, S., and Zhang, Z. 2016. GAPIT Version 2: An Enhanced Integrated Tool for Genomic Association and Prediction Plant Genome. 9(2):103835/plantgenome2015110120

Yu, J., Pressoir, G., Briggs, W. H., Bi, I. V., Yamasaki, M., Doebley, J. F., McMullen, M. D., Gaut, B. S., Nielsen, D. M., Holland, J. B., Kresovich, S., and Buckler, E. S. 2006. A unified mixed-model method for association mapping that accounts for multiple levels of relatedness. Nature Genetics 38:203-208

Yun, S. J., Gyenis, L., Hayes, P. M., Matus, I., Smith, K. P., Steffenson, B. J., and Muehlbauer, G. J. 2005. Quantitative Trait Loci for Multiple Disease Resistance in Wild Barley. Crop Sci 45(6):2563-2572

Zhang, Z., Ersoz, E., Lai, C., Todhunter, R. J., Tiwari, H. K., Gore, M. A., Bradbury, P. J., Yu, J., Arnett, D. K., Ordovas, J. M., and Buckler, E. S. 2010. Mixed linear model approach adapted for genome-wide association studies. Nature Genetics 42:355-360

Zhao, K., Aranzana, M. J., Kim, S., Lister, C., Shindo, C., Tang, C., Toomajian, C., Zheng, H., Dean, C., Marjoram, P., and Nordborg, M. 2007. An Arabidopsis Example of Association Mapping in Structured Samples. PLOS Genet http://dxdoiorg/101371/journalpgen0030004

Zhou, H. and Steffenson, B. 2013. Genome-wide association mapping reveals genetic architecture of durable spot blotch resistance in US barley breeding germplasm. Mol Breeding 32:139-154

Zhou, H., Steffenson, B. J., Muehlbauer, G., Wanyera, R., Njau, P., and Ndeda, S. 2014. Association mapping of stem rust race TTKSK resistance in US barley breeding germplasm. Theor Appl Genet 127(6):1293-1304

Zhu, C., Gore, M., Buckler, E. S., and Yu, J. 2008. Status and Prospects of Association Mapping in Plants. Plant Genome 1(1):5-20

Zierms LA, Hickey LT, Hunt CH, Mace ES, Platz GJ, Franckowiak JD, Jordan DR (2014) Association mapping of resistance to *Puccinia hordei* in Australian barley breeding germplasm. Theor Appl Genet 127:1199-1212

CHAPTER 3. FINE MAPPING OF THE BARLEY CHROMOSOME 6H NET FORM NET BLOTCH SUSCEPTIBILITY LOCUS[1]

Abstract

Net form net blotch caused by the necrotrophic fungal pathogen *Pyrenophora teres* f. *teres* is a destructive foliar disease of barley with the potential to cause significant yield loss in major production regions throughout the world. The complexity of the host-parasite genetic interactions in this pathosystem hinders the deployment of effective resistance in barley cultivars, warranting a deeper understanding of the interactions. Here we report on the high-resolution mapping of the dominant susceptibility locus near the centromere of chromosome 6H in the barley cultivars Rika and Kombar that are putatively targeted by necrotrophic effectors from *P. teres* f. *teres* isolates 6A and 15A, respectively. Utilization of progeny isolates derived from a cross of *P. teres* f. *teres* isolates 6A × 15A harboring single major virulence loci (*VK1*, *VK2* and *VR2*) allowed for the Mendelization of single inverse gene-for-gene interactions in a high-resolution population consisting of 2976 Rika × Kombar recombinant gametes. *Brachypodium distachyon* synteny was exploited to develop and saturate the susceptibility region with markers, delimiting it to ~0.24 cM and a partial physical map was constructed. This genetic and physical characterization further resolved the dominant susceptibility locus, designated *Spt1* (susceptibility to *P. teres* f. *teres*). The high-resolution mapping and cosegregation of the *Spt1*.*R*

[1] The material in this chapter is reprinted under a Creative Commons Attribution License (https://creativecommons.org/licenses/by/4.0/) applied by the journal G3:Genes|Genomes|Genetics from the article Ricards, J., Chao, S., Friesen, T., and Bruggeman, R. 2016. Fine Mapping of the Barley Chromosome 6H Net Form Net Blotch Susceptibility Locus. G3. 6:1809-1818. Jonathan Richards conducted the experiments, analyzed the data, formulated conclusions, wrote and revised the manuscript following suggestions of the co-authors and reviewers.

and *Spt1.K* gene/s indicates tightly linked genes in repulsion or alleles possibly targeted by different necrotrophic effectors. Newly developed barley genomic resources greatly enhance the efficiency of positional cloning efforts in barley as demonstrated by the *Spt1* fine mapping and physical contig identification reported here.

Introduction

The necrotrophic fungus *Pyrenophora teres* is the causal agent of net blotch of barley (*Hordeum vulgare*) and exists in two forms, which although morphologically indistinguishable under the microscope, can be differentiated by the symptoms observed on susceptible barley genotypes (McLean *et al.* 2009; Smedegard-Peterson 1971). The disease net form net blotch (NFNB) caused by *P. teres* f. *teres* is manifested by necrotic lesions with transverse and longitudinal striations, forming a net-like pattern of necrosis often accompanied by chlorosis (Mathre 1997). The disease spot form net blotch (SFNB) caused by *P. teres* f. *maculata* produces elliptical necrotic lesions surrounded by chlorosis (McLean *et al.* 2009; Smedegard-Peterson, 1971). Both NFNB and SFNB are destructive foliar diseases, which can cause yield losses of 10-40% (Mathre 1997; Murray & Brennan, 2010) and reduction in barley end use quality. Although similar fungicide applications and cultural practices can be used to manage these diseases, the preferred method of management is through host resistance (Mathre 1997). However, even though these two pathogens are closely related and genetically very similar, their host-pathogen genetic interactions are distinct (reviewed in Liu *et al.* 2011), thus they must be treated as different diseases when deploying genetic resistances.

Using globally diverse barley cultivars and *P. teres* f. *teres* isolates, several genetic studies have positioned both dominant and recessive resistance to NFNB at the centromeric region of barley chromosome 6H, suggesting the presence of multiple diverse resistance or

susceptibility genes. It is hypothesized that these host genes interact with different *P. teres* f. *teres* effectors/avirulence proteins from diverse isolates resulting in the differential compatible or incompatible reactions observed in this pathosystem (Ho *et al.* 1996; Steffenson *et al.* 1996; Raman *et al.* 2003; Cakir *et al.* 2003; Ma *et al.* 2004; Manninen *et al.* 2006; Friesen *et al.* 2006a; Abu Qamar *et al.* 2008; St. Pierre *et al.* 2010). Abu Qamar *et al.* (2008) mapped two recessive resistance genes, which exist in repulsion, in a double haploid population derived from a cross between the barley lines Rika and Kombar. Rika is resistant to *P. teres* f. *teres* isolate 15A and susceptible to *P. teres* f. *teres* isolate 6A, while Kombar is resistant to *P. teres* f. *teres* isolate 6A and susceptible to *P. teres* f. *teres* isolate 15A. The susceptibility loci were mapped to an ~5.9 cM region near the centromere on barley chromosome 6H. The region was further delimited to an ~3.3 cM interval through the use of EST-based markers (Liu *et al.* 2010).

A comprehensive genetic analysis utilizing a bi-parental population of *P. teres* f. *teres* isolates 6A and 15A, which exhibit reciprocal virulence on Rika and Kombar, respectively, identified four virulence QTL in the pathogen. Two of the QTL, designated *VR1* and *VR2* for virulence on Rika 1 & 2, were identified for *P. teres* f. *teres* isolate 6A and two QTL, *VK1* and *VK2*, for virulence on Kombar 1 & 2, were identified for *P. teres* f. *teres* isolate 15A (Shjerve *et al.* 2014). It was postulated that host selective toxins or necrotrophic effectors underlie these virulence QTL as it was recently shown in this pathosystem that a proteinaceous effector from *P. teres* f. *teres* isolate 0-1, designated PttNE1, interacts with a single dominant susceptibility gene on chromosome 6H in barley cv. Hector, inducing necrotrophic effector triggered susceptibility (NETS) (Liu *et al.* 2015). Also, other closely related necrotrophic ascomycete fungi, such as *Pyrenophora tritici-repentis* and *Parastagonospora nodorum* produce necrotrophic effectors that alter the host's innate immunity responses resulting in enhanced disease (Tomas *et al.* 1990;

Strelkov *et al.* 1999; Liu *et al.* 2009; Liu *et al.* 2012; Gao *et al.* 2015). The proteinaceous necrotrophic effector ToxA produced by *P. tritici-repentis* (Ptr ToxA) and *P. nodorum* (SnToxA), interact with the dominant host sensitivity protein Tsn1 (Friesen *et al.* 2006b; Faris *et al.* 2010). Tsn1 has protein domains similar to typical resistance proteins that confer resistance to biotrophic pathogens through the induction of tightly regulated programmed cell death (PCD) pathways. These pathways are typically thought to have evolved to sequester biotrophic pathogens which require living host tissues to complete their lifecycle. The inappropriate elicitation of these innate resistance pathways through the use of necrotrophic effectors by the necrotrophic pathogens allow them to subvert and utilize the host immunity pathways to infect and complete their lifecycle in the host. Thus, they utilize necrotrophic effectors to target specific host susceptibility genes, that otherwise represent immune receptors, to elicit NETS. These interactions between the host and pathogen are similar to H.H. Flor's classical gene-for-gene paradigm (Flor 1956), yet are considered to be an inverse gene-for-gene relationship in which the specific interactions leading to PCD result in a compatible interaction (susceptibility) in a quantitative manner due to the nature of the pathogens lifestyle (Friesen *et al.* 2007). However, it also appears that classical gene-for-gene or dominant resistances also exist in this pathosystem as Friesen *et al.* (2006a) identified dominant resistance to three different NFNB isolates, which interestingly also mapped to the centromeric region of barley chromosome 6H.

Grass species, such as the globally important crops barley, wheat (*Triticum aestivum*), maize (*Zea mays*), rice (*Oryza sativa*), and sorghum (*Sorghum bicolor*), diverged from a common ancestor ~55-70 million years ago (Kellogg 2001). Throughout their evolutionary history, it has been shown that the relative gene content and order have been conserved between the grass species, with much of the change in genome size being due to an increase of repetitive

elements (Bennetzen & Freeling 1997; Kellogg 2001). Although synteny breaks attributed to chromosome insertions and translocations are observed, the overall gene order is well conserved (IBI 2010). The sequencing and annotation of the *Brachypodium distachyon* genome provided a useful tool for gene discovery in other grass species, especially crop species with large genomes as the result of expansion of repetitive DNA elements. These large repetitive genomes complicate genome sequence assembly such that there is adequate assembly of low copy gene spaces but many gaps at repeat regions, thus robust genome assemblies have not been achieved (Mur *et al.* 2011; IBGSC 2012). Syntenic conservation between the model grass genome sequence and barley and wheat expedites the development of markers in the large grass genomes allowing for the rapid saturation of regions for positional cloning (IBI 2010; Mur *et al.* 2011)

The draft assembly of the barley gene space was recently completed, however, a nearly complete genome assembly of the ~5.1 Gb genome, which consists of approximately 84% repetitive elements is a challenging task with the current bioinformatic software, but a draft physical map of the barley genome has been assembled via high-information content fingerprinting of bacterial artificial chromosome (BAC) clones and incorporation of whole-genome shotgun (WGS) sequence, BAC end sequence (BES), sequence from selected BAC clones, and integration of genetic mapping data (IBGSC 2012). Furthermore, additional anchoring of WGS contigs was accomplished through population sequencing (POPSEQ) and BAC clones have been assembled into minimum tiling paths across assembled contigs (Mascher *et al.* 2013; Ariyadasa *et al.* 2014) Additionally, 15,622 cv. Morex BACs were sequenced and subsequently integrated with consensus map and synteny analyses into the easily accessible software HarvEST (Muñoz-Amatriaín *et al.* 2015). The use of this resource allows for the

physical mapping of regions identified by genetic map-based cloning strategies, which facilitates the identification of candidate genes in a more efficient manner.

The dominant susceptibility genes *Spt1.R/Spt1.K* (formerly *rpt.k/rpt.r)* which are hypothesized to confer dominant susceptibility to *P. teres* f. *teres* isolates 6A and 15A appear to operate in a complex fashion. We hypothesize that alleles of *Spt1, Spt1.R* and *Spt1.K,* or several tightly linked genes, confer major effect dominant susceptibility to *P. teres* f. *teres* isolates 6A and 15A, respectively. Here we describe the high resolution mapping of a dominant susceptibility locus located in the centromeric region of barley chromosome 6H. Mapping was done utilizing markers developed via the exploitation of the syntenic relationship with *B. distachyon* chromosome 3. Additionally, the identification of barley physical contigs, enabled by the newly developed barley genomic resources, were used to construct a partial physical map of the region. The results of this research will soon facilitate the identification of the dominant susceptibility gene *Spt1* and allow for the subsequent functional analysis of its alleles that are hypothesized to function by NETS. This research will fill gaps in knowledge concerning these complex host-parasite genetic interactions and the underlying molecular mechanisms determining compatible interactions in this complex barley-NFNB pathosystem.

Materials and Methods

Biological Materials

The two *P. teres* f. *teres* isolates 6A and 15A and progeny identified as containing single virulence QTL for VK1, VK2, and VR2 (Shjerve *et al.* 2014) from the cross between isolates 6A and 15A were utilized for phenotyping. The *P. teres* f. *teres* isolate 6A was collected from Fresno County, California (Wu *et al.* 2003) and isolate 15A was collected from Solano County, California (Steffenson and Webster 1992).

The Scandinavian two-rowed barley variety Rika and US six-rowed barley variety Kombar were previously identified as having reciprocal reactions to *P. teres* f. *teres* isolates 6A and 15A. Rika is susceptible to *P. teres* f. *teres* isolate 6A and resistant to *P. teres* f. *teres* isolate 15A. Kombar exhibits an opposite reaction, being susceptible to *P. teres* f. *teres* isolate 15A and resistant to *P. teres* f. *teres* isolate 6A (Abu Qamar *et al.* 2008). Rika and Kombar were crossed and advanced to generate a population of 1488 F_2 individuals, representing 2976 gametes, that were subsequently genotyped to identify recombinant gametes within the *Spt1* region. Previously identified critical recombinant double haploid (DH) progeny identified from a population consisting of 118 individuals derived from a Rika and Kombar cross (Abu Qamar *et al.* 2008) were also genotyped to validate the DH recombinants within the NFNB *Spt1* region that was previously referred to as the *rpt.k* and *rpt.r* recessive resistance genes.

Genotyping and Recombinant Gamete Identification

Two previously identified flanking simple sequence repeat (SSR) markers, Bmag0173 on the distal side and Rbah21g15 on the proximal side (Liu *et al.* 2010), were used to genotype the 1488 Rika × Kombar F_2 individuals. The DNA isolation for the initial F_2 genotyping was performed at the US Department of Agriculture-Agricultural Research Service (USDA-ARS) cereal genotyping center, Fargo, ND, USA, using the high-throughput procedure described by Tsilo *et al.* (2009).

After the F_2 individuals with recombination within the *Spt1* region were identified from the initial round of genotyping with the SSR markers on the ABI sequencer, the recombinant seedlings were transplanted from conetainers into 6 inch pots, grown in the greenhouse, and allowed to self to produce $F_{2:3}$ seed. Fifteen $F_{2:3}$ plants from each family were grown in the greenhouse and genomic DNA isolated from approximately 2 cm long leaf tissue samples

collected in 1.5 mL Eppendorf tubes. The leaf tissue was homogenized in 400 µL of extraction buffer (200 mM Tris-HCl pH 7.5, 250 mM NaCl, 25 mM EDTA, 0.5% SDS) with a disposable tissue grinder followed by the addition of 200 µL of chloroform. Samples were vortexed for 10 s and centrifuged at 15,600 g for 10 min. The supernatant (~300 µL) was transferred to a new 1.5 mL tube and 300 µL of isopropanol was added. The samples were mixed by inversion and incubated at room temperature for 5 minutes followed by centrifugation at 15,600 g for 10 minutes. The pellets were rinsed with 70% ethanol, dried, and resuspended in 100 µL of ddH_2O. The fifteen $F_{2:3}$ individuals from each F_2 family identified with a critical recombination in the *Spt1* region were genotyped utilizing the co-dominant marker rpt-M4 to identify homozygous recombinant individuals which represent immortal critical recombinants (ICR). The ICR individuals were given a progeny designation and were utilized for all further phenotyping and genotyping.

STS/SNP Marker Development

Utilizing the syntenic relationship between barley chromosome 6H and *B. distachyon* chromosome 3, genetic markers were developed to saturate the *Spt1* region through the use of the annotated *B. distachyon* genome sequence (IBI 2010). Orthologous loci in *B. distachyon* corresponding to the distal flanking EST marker BE636841 and the proximal SSR marker Rbah21g15 were used to identify the ~1.02 Mb of syntenic *B. distachyon* genomic DNA sequence. Orthologous barley expressed sequence tags (ESTs) were identified, utilizing Blastn searches limiting to ESTs other_*Hordeum vulgare* that correspond to *B. distachyon* genes within the region. A set of these ESTs were selected at ~60 kb intervals using predicted function as the criteria for selection, as certain genes have a higher probability of containing polymorphisms compared to others. For example, NBS-LRR genes typically have more diversity than highly

conserved house-keeping genes. Oligonucleotide primers were designed from the barley EST sequences and used to produce amplicons from Rika and Kombar genomic DNA by PCR (Table 3.1).

Table 3.1. Sequences of primers designed from barley ESTs identified via synteny analysis

Marker	Class	Forward Primer	Reverse Primer
rpt-M4-1[1]	STS	AGGAAATGGTCTCTCCAAAGTCTC	ACATCTCATCATCTGGCCACCATAC
rpt-M4-2[1]	STS	TGAAGAGGAAGCGTGAACAAGATAG	TGACTACGAATGAATACCTCTTCAG
rpt-M5[b]	STS	AAAGAAGATCAGGCTTACCAGCATC	ATGCGACAACCAGGTAAGTAGAGTG
rpt-M8	SNP	GCTGGCCTCCAGCTTCGACGTGATG	AACGTAAGCTCATTCTACATAAGAC
rpt-M12.r[2]	STS	ATGGCCAACCAGCTTAAATATCCCA	TCACTCATGCAGAGTGGCGTACACCA
rpt-M12.k[3]	STS	GTGCCTACTTCTCTGTATATTCACG	GTCTCATTGCATGCGCTGTCACCTC
rpt-M13	STS	GCAGAACTCTACCAGCACTTCAGAG	CTTCCAGATGATTCAGGTTCATTAC
rpt-M20	SNP	CCATCAATACAGTGTTTATCACCAA	GCTCAAAATGTCCACAGTATTATCC
rpt-M32	SNP	ATGTATGGTAAATGTGGGGGTATC	GAGTAAATCAACCATTAGGCCATAG
rpt-M61	SNP	ACCTTTCGCCACCAACAACACAGAC	GTATGATGTCAAGCTGAACAATGCC
rpt-M62	Indel	GAATTAGCAGGAGACCAATGTAAGA	TTTCTTATTAGGTGATGCGTTTGTT
rpt-M14	SNP	AAGCACCACCCTGGACAGATAGAAG	ATGAGATCAGACCAAGTGAGTTCAC

[1]Co-dominant marker when multiplexed in a single PCR reaction
[2]Rika specific
[3]Kombar specific

Genomic DNA was extracted as previously described. The parameters for the PCR reactions were as follows: 94º C for 5 minutes, followed by 35 cycles of 94º C for 30 seconds, 62º C for 30 seconds, and 72º C for 60 seconds, followed by a final extension at 72º C for 7 minutes. The PCR reactions consisted of 1.25 units NEB Standard Taq polymerase, forward and reverse primers (1.2 µM), NEB Standard Taq buffer (1x), dNTPs (200 µM), in 25 µL reactions. PCR products were visualized on a 1% agarose gel containing GelRed (Biotium, CA) and subsequently purified using E.Z.N.A. Cycle Pure Kit (Omega Bio-Tek, Norcross, GA) following the manufacturers standard protocol. The amplicons were sequenced (McLab and Genscript) and single nucleotide polymorphisms (SNPs) were identified by alignment using Vector NTI

software (Invitrogen) and NCBI nucleotide sequence alignment tools. Sequence tagged site (STS) markers were developed from the SNPs by designing genotype specific primers with SNP specific nucleotides corresponding to the 3' terminal nucleotide of the primers (Table 3.1). If a robust STS marker was unable to be developed, the critical recombinants were amplified using the original primer pairs and the amplicons were Sanger sequenced (Genscript).

PCR-GBS Library Preparation and Ion Torrent Sequencing

A PCR genotyping-by-sequencing (PCR-GBS) panel was also constructed consisting of two previously designed SNP markers from the T3 database (https://triticeaetoolbox.org/barley/) and 11 primer pairs designed from the predicted coding, intron, or 3' UTR sequence from barley orthologs of *B. distachyon* genes within the region with the aim of SNP discovery. Additionally, four previously designed STS markers were included in the panel for re-genotyping and internal control. A 22 nucleotide CS1 adaptor (5'-ACACTGACGACATGGTTCTACA-3') (Fluidigm) was added to the 5' end of forward primers and a 22 nucleotide CS2 adaptor (5'-TACGGTAGCAGAGACTTGGTCT-3') (Fluidigm) was added to the 5' end of the reverse primers. Barcoded adaptor primers were designed containing the Ion Torrent A adaptor sequence, unique 12 nucleotide barcode, and the CS1 adaptor sequence (5'-CCATCTCATCCCTGCGTGTCTCCGACTCAG(NNNNNNNNCGAT)ACACTGACGACATGGTTCTACA-3'). A universal reverse primer was designed containing the Ion Torrent P1 adaptor sequence and the CS2 adaptor sequence (5'-CCACTACGCCTCCGCTTTCCTCTCTATGGGCAGTCGGTGATTACGGTAGCAGAGACTTGGTCT-3'). Primers were multiplexed by adding 5 µL of each forward and reverse primer (100 µM) into a sterile 1.5 mL Eppendorf tube and 820 µL of nuclease free H_2O for a final primer pool volume of 1 mL. PCR reactions consisted of 1.5 µL genomic DNA, 1 µL of primer

pool (100 nM each primer), and 2.5 µL Platinum Multiplex PCR Master Mix (Life Technologies). DNA concentrations were normalized to ~20 ng/µL and 1.5 µL of each sample was pipetted into individual wells on a 96 well plate. Replicates of Rika, Kombar, RK107, RK121, and RK122 were also included on the plate. The primary PCR reaction was conducted as follows: Initial denaturation at 94° C for 10 minutes, 10 cycles of 94° C for 20 seconds and 64° C decreasing each cycle by 0.8° C for 60 seconds, followed by 20 cycles of 94° C for 20 seconds, 57° C for 60 seconds, and 68° C for 30 seconds, ending with a final extension of 72° C for 3 minutes. The PCR plate was then briefly centrifuged and 15 µL of nuclease-free H_2O was added to each sample. The plate was then sealed, vortexed, briefly centrifuged, and 2 µL of each sample was aliquoted into a new 96 well plate. Additionally, 2 µL of each reaction was separated on a 1% agarose gel containing GelRed to ensure successful reactions. The barcoding PCR reaction consists of 0.235 µL of H_2O, 0.625 µL NEB Standard Taq Buffer (1.25 x), 0.1 µL dNTPs (500 µM), 1 µL universal reverse primer (1 µM), 1 µL unique barcode adaptor primer (0.4 µM), 0.04 µL of NEB Taq polymerase (0.2 units), and 2 µL template (diluted primary PCR reaction). PCR parameters are the same as the primary reaction. Following PCR, the plate was briefly centrifuged and each sample was diluted by adding 15 µL of H_2O. Samples were pooled by aliquoting 5 µL of each sample into a 1.5 mL Eppendorf tube and purified using the E.Z.N.A. Cycle Pure Kit. The pooled library was then amplified to prepare for sequencing. PCR reactions consisted of a 2 µL sequencing library, 13 µL H_2O, 2.5 µL NEB Standard Taq Buffer (1x), 3 µL ABC1 primer (0.6 µM), 3 µL P1 primer (0.6 µM), 0.5 µL dNTPs (200 µM), and 1 µL NEB Taq polymerase (5 units). PCR parameters were as follows: initial denaturation at 95° C for 5 minutes, followed by 8 cycles of 94° C for 30 seconds, 62° C for 30 seconds, and 72° C for 30 seconds, ending with a final extension at 72° C for 7 minutes. The amplified library was

quantified using the Qubit dsDNA High Sensitivity Kit and the Qubit Fluorometer (Life Technologies) and diluted to ~3 pg/µL. Sequencing was conducted on the Ion Torrent PGM utilizing the Ion PGM Template OT2 200 Kit, Ion PGM Sequencing 200 Kit v2, and an Ion 314 Chip (Life Technologies).

SNP Calling

Sequencing reads were trimmed by 22 nucleotides on the 5'and 3' ends to remove the PCR adaptors. Trimmed reads were aligned to a reference file consisting of previously identified amplicon sequences from the T3 database, orthologous barley EST sequence corresponding to select *B. distachyon* genes within the region, and sequence from previously designed STS markers using the BWA-MEM algorithm with default settings (Li and Durbin 2009) and the alignments were converted to BAM files using SAMtools (Li *et al.* 2009). SNPs were identified using the Genome Analysis Toolkit's Unified Genotyper tool (DePristo *et al.* 2011). Called SNPs were then filtered based on the parameters of a minimum genotype quality of 10 and a minimum read depth per site per individual of 3.

Phenotyping

The ICRs were phenotyped with *P. teres* f. *teres* isolates 6A, 15A, and the progeny isolates 15 × 6A #20, 15A × 6A #63, and 15A × 6A #72, with the Mendelized virulence QTL *VK1*, *VK2*, and *VR2*, respectively. Phenotyping was conducted as described by Friesen *et al.* (2006a). Briefly, inoculum was prepared by plating agarose plugs of the *P. teres* f. *teres* isolates on V8 PDA media (150 mL V8 Juice, 10 g Potato Dextrose Agar, 10 g agarose, 3 g $CaCO_3$, and 850 mL H_2O). Fungal cultures were incubated at room temperature in the dark for 5 days, placed under light at room temperature for 24 hours, and then returned to the dark at 15^{o} C for 24 hours. Conidia were harvested by flooding the plates with H_2O and scraping the culture with a sterile

inoculation loop. Inoculum was adjusted to a concentration of ~2000 spores/mL and one drop of Tween 20 was added per 50 mL of inoculum. Three seeds of each ICR line were planted in a single conetainer (Stuewe and Sons, Inc., Corvallis, OR.) and three conetainers were planted for each ICR, totaling nine seedlings per line. Seedlings were grown under greenhouse conditions until the second leaf was fully expanded, approximately 14 days. Inoculum was applied as described by Friesen *et al.* (2006a) and incubated at 21 °C and 100% relative humidity for 22-24 hours. Plants were then moved to a growth chamber at 21° C with a 12 hour photoperiod and were scored 7 days post inoculation using a 1-10 scale (Tekauz 1985). Nine plants per line were scored collectively as one experimental unit and inoculations were replicated three times.

High-Resolution Map Construction

A total of 14 ICRs harboring a recombination between flanking markers Bmag0173 and Rbah21g15 were identified and utilized in the construction of a high-resolution map. Genetic distances were calculated based on recombination frequency between markers and denoted as map units (M.U.).

Barley iSelect 9K Chip

The barley *9k* Illumina *Infinium* iSELECT assay was utilized to genotype the parents Rika and Kombar and eight of the ICR lines (RK122, 125, 130, 139, 151, 173, 183, and 188) with recombination in the *Spt1* region. The genotyping was performed as described by Munoz-Amatriaín *et al.* (2014).

BAC Library Screening and Physical Map Construction

Utilizing the current barley physical map (IBGSC 2012) containing anchored WGS and BAC sequences, as well as the Morex 6H minimum tiling path (MTP) BAC library (Mascher *et al.* 2013; Ariyadasa *et al.* 2014), genetic markers from the high-resolution map were anchored to

physical contigs. Sequences of the markers within the region were used in BLAST searches of the Morex WGS database to identify positive WGS contigs (http://webblast.ipk-gatersleben.de/barley/viroblast.php). When possible, positions of the WGS contigs on larger fingerprinted contigs (FPCs) were identified. Those markers that did not yield anchored WGS contigs were used to screen the Morex 6H MTP BAC library via PCR (INRA-CNRGV) to identify its position on a FPC. Additionally, a Morex BAC library (Yu *et al.* 2000) was screened with markers rpt-M8, rpt-M12, and rpt-M13 as described by Brueggeman *et al.* (2002). Positively identified BAC clones were plated on LB plates containing chloramphenicol (50 µg/mL) and incubated overnight at 37° C. Colonies were then inoculated into liquid LB containing chloramphenicol (50 µg/mL) and incubated for 16 hours at 37° C with shaking at 230 rpm. BAC DNA was isolated as described in Brueggeman *et al.* (2002). PCR was conducted on BAC DNA with the markers rpt-M8, rpt-M12, and rpt-M13 to identify corresponding BAC clones using the aforementioned PCR protocol. Additionally, the HarvEST database which houses BAC sequences from the Yu *et al.* (2000) library was BLAST searched with marker sequences to identify and confirm additional BAC clones (Muñoz-Amatriaín *et al.* 2015).

BAC Library Sequencing and Assembly

DNA from the selected BACs 783N21 and 650G13 (Yu *et al.* 2000) was isolated as previously described. BAC DNA was pooled and sequenced at the Washington State University Molecular Biology and Genomics Core using Ion Torrent PGM technology. Sequencing reads were de novo assembled using CLC Bio Genomics Workbench (Qiagen) requiring 95% sequence homology and minimum contig size of 1 kb for assembly.

Data and reagents are available upon request. File S1 contains genotypes of the ICRs from the newly developed markers. File S2 contains the raw phenotypic data for Rika, Kombar, and the ICRs from inoculations with the aforementioned *P. teres* f. *teres* isolates.

Results

Initial Genotyping and Phenotyping of Critical Recombinants

A total of 1488 F_2 individuals and 118 DH lines derived from a cross of Rika × Kombar were genotyped with the flanking SSR markers Bmag0173 and Rbah21g15. Thirteen F_2 individuals and one DH line were identified that contained recombination within the previously delimited *rpt.r/rpt.k* region, know referred to as the *Spt1* region. Subsequently, the $F_{2:3}$ families of these thirteen critical recombinants were genotyped with the co-dominant marker rpt-M4 and an immortal critical recombinant (ICR) individual was identified for each $F_{2:3}$ family.

Phenotyping of the ICR lines

Individuals from each ICR family and the lone DH individual were then phenotyped with *Pyrenophora teres* f. *teres* isolates 15A, 6A, 15×6A #20, 15A×6A #63, and 15A×6A #72. Lines that exhibited an average disease reaction of five or less were classified as resistant and lines that displayed average reactions greater than five were considered susceptible. Following inoculations with isolate 15A, Rika and Kombar exhibited average reactions of 1.67 and 7.5, respectively. A total of five ICRs were classified as resistant with individual averages ranging from 1 to 3.33 and an overall average of 1.77. The remaining nine ICRs exhibited individual average disease reactions ranging from 6.83 to 7.83 with an overall average of 7.59 and were classified as susceptible (Table 3.2). When inoculated with progeny isolate 15A×6A #20 (Shjerve *et al.* 2014) containing only the *VK1* virulence locus, Rika and Kombar exhibited average disease reactions of 1.83 and 6.83, respectively. Five ICRs were considered resistant and

nine classified as susceptible. The average disease reaction of the resistant lines ranged from 1.83 to 3.83 with an overall average of 2.73. For the susceptible group, individual averages ranged from 6.67 to 8.83 with an overall mean of 7.74 (Table 3.2). Phenotypic data from inoculations with a second progeny isolate, 15A×6A #63, harboring only the *VK2* virulence locus (Shjerve *et al.* 2014) showed the same pattern. Disease reaction averages for Rika and Kombar were 2.17 and 7.17, respectively. The previously classified resistant and susceptible ICRs grouped together again. The disease score averages of resistant individuals ranged from 1.5 to 2 with an overall mean of 1.77. Susceptible individuals exhibited average disease scores ranging from 5.33 to 7.17 and an overall average of 6.35 (Table 3.2).

Following inoculations of the ICRs with isolate 6A, Rika and Kombar displayed reaction types of 9.5 and 4.17, respectively. Average disease reaction types for six resistant lines ranged from 3.5 to 5 with an overall mean of 4.06. A total of eight individuals were considered susceptible and average reaction types ranged from 5.50 to 9.33 with an overall average of 7.65 (Table 3.2). After inoculation with progeny isolate 15A×6A #72 harboring only the *VR2* virulence locus (Shjerve *et al.* 2014), Rika and Kombar showed average reaction types of 7.83 and 1, respectively. A total of nine ICRs were considered resistant with average disease scores ranging from 1.00 to 1.50 and a total mean of 1.15. The susceptible class of ICRs consisted of five individuals with average disease ratings ranging from 7.17 to 8.67 and an overall average of 7.97 (Table 3.2). Several individuals (RK121, RK122, and RK173) exhibited intermediate reactions ranging from 5.50 to 6.17 when inoculated with isolate 6A and subsequently were classified as susceptible. However, due to the averages of these three individuals being near the mean score of Kombar and the 6A resistant individuals as well as these individuals being highly

resistant to isolate 15A×6A #72 (VR2), these apparent intermediate reactions may not accurately represent the classification of susceptible.

Table 3.2. Average disease scores for Rika, Kombar, and resistant/susceptible ICRs with *Ptt* isolates

	Average Reaction Type				
Genotype	15A	15A x 6A #20 (VK1)	15A x 6A #63 (VK2)	6A	15A x 6A #72 (VR2)
Rika	1.67 ± 0.58	1.83 ± 0.29	2.17 ± 0.29	9.5 ± 0.50	7.83 ± 1.04
Kombar	7.5 ± 0.50	6.83 ± 1.76	7.17 ± 1.44	4.17 ± 1.26	1 ± 0
Resistant ICRs	1.77 ± 0.92	2.73 ± 0.89	1.77 ± 0.25	4.06 ± 0.61	1.15 ± 0.18
Susceptible ICRs	7.59 ± 0.35	7.74 ± 0.83	6.35 ± 0.63	7.65 ± 1.62	7.97 ± 0.71

Marker Development and High-Resolution Map Construction

Utilizing synteny between barley and *B. distachyon*, orthologous *B. distachyon* genes Bradi3g48220.1 and Bradi3g49360.1 corresponding to the *Spt1* flanking markers BE636841 and Rbah21g15, respectively, were identified via BLAST searches. This approximately 1.02 Mb *B. distachyon* genomic region between the two orthologs harbors 149 annotated genes. *B. distachyon* genes containing syntenic barley orthologs at approximately 60 kb intervals were selected and used in BLAST searches to identify high confidence barley unigenes with EST support. Primers were designed from the 16 identified unigenes and used to produce gene specific amplicons from the barley cultivars Rika and Kombar. Sanger sequencing was performed on the amplicon and sequence alignments used to characterize allelic differences. Sequencing of the 16 selected unigenes yielded six robust amplicons containing at least one SNP between the parents. Allele specific primers with 3' terminal nucleotides specific to each parental SNP were designed and used as STS markers to genotype the ICRs to saturate the high-resolution map with markers at the *Spt1* locus. STS markers were unable to be developed from SNPs within two barley orthologs, designated as rpt-M8 and rpt-M14. The original primer pairs

were used to produce amplicons from each ICR and subsequently Sanger sequenced for genotyping. Markers rpt-M4, rpt-M5, and rpt-M8 cosegregated and mapped distal to the susceptibility locus, rpt-M12 and rpt-M13 cosegregated with *Spt1*, and rpt-M14 mapped proximal to the susceptibility locus. The newly developed markers delimited the *Spt1* locus to ~0.43 cM between the distal flanking marker rpt-M8 and the proximal flanking marker rpt-M14. The delimited region in barley corresponded to ~540 kb of *B. distachyon* sequence which contained 69 annotated genes. Using the aforementioned process of marker development via synteny, focus was then placed on the further saturation of the region. A total of 17 orthologous barley unigenes were identified from *B. distachyon* genes within this region and targeted for marker development, of which, allele sequencing further identified two orthologs containing SNPs. The newly identified markers, rpt-M20 and rpt-M61, were subsequently genotyped via PCR directed genotype-by-sequencing of target amplicons due to the inability to develop efficient STS markers. Additionally, a robust indel marker, rpt-M62, was developed from the same ortholog as rpt-M61. Data procured from the barley iSelect 9K chip also revealed a SNP marker, SCRI_RS_165041, which further delimits the region. Currently, the *Spt1* gene is delimited by markers rpt-M8 and SCRI_RS_165041 to an ~0.24 cM region. (Fig. 3.1). The ~0.24 cM region delimiting *Spt1* in barley corresponds to ~466 kb of *B. distachyon* sequence harboring 62 annotated genes and is predicted to contain 49 barley genes using anchoring data from the barley genome database and POPSEQ data, as well as BLAST searches of the barley genome using *B. distachyon* genes as the query. Attempts to utilize these genes to further saturate the genetic map identified 15 orthologous barley genes within the region. However, allele sequencing of introns, 3’ UTRs, and coding regions from Rika and Kombar of these select orthologs determined that these genes did not contain polymorphism in our population (Fig. 3.1)

PCR-GBS Sequencing and SNP Calling

Sequencing on the Ion Torrent PGM platform resulted in a total of 569,040 reads averaging 82 bp in length. However, due the presence of primer dimers, only 184,174 reads were amplicon specific which averaged to ~5581 reads per individual, which is sufficient to call SNPs for amount of markers in this panel. Amplicons within the library were represented to a varying degree due to the differences in PCR efficiency. The two SNP markers from the T3 database (11_21216 and 11_20651) were not polymorphic between Rika and Kombar. However, we were able to identify polymorphism between Rika and Kombar within the amplicon of a single selected ortholog of a *B. distachyon* gene within the region, designated rpt-M32. The SNP marker rpt-M32 mapped proximal to SCRI_RS_165041 and distal to rpt-M14 (Figure 1). Additionally, two of the four previously identified STS markers (rpt-M4 and rpt-M8) had enough representative sequence to call SNPs and confirmed previous genotyping.

BAC Library Screening and Physical Map Construction

Screening of a barley cultivar Morex BAC library with markers rpt-M8, rpt-M13, and rpt-M12 identified four BAC clones and were confirmed via PCR (Table 3.3). Marker rpt-M8 did not amplify from any of the identified BAC DNA templates. The markers rpt-M12 and rpt-M13 both amplified from 783N21, 302J12, and 082C13 BAC DNA template, indicating these BAC clones comprise a MTP in which both markers reside. Additionally, via BLAST searches on the HarvEST database (Muñoz-Amatriaín *et al.* 2015), the location of markers rpt-M13 and rpt-M12 on BAC clones 783N21 was confirmed, as well as identified an additional BAC, 650G13, corresponding to marker rpt-M12. All the markers used in genotyping the high-resolution mapping population were also BLAST searched utilizing the HarvEST server to identify the BACs from the Yu *et al.* (2000) library on which they reside, resulting in the

identification of corresponding BAC clones for each marker, except rpt-M8 and rpt-M14 (Table 3.3). Also, the marker sequences were BLAST searched using the IPK Barley BLAST server to identify corresponding sequenced BAC clones, cv. Morex WGS contigs, and if possible, position on larger FPCs. Markers rpt-M8, rpt-M20, rpt-M32, and rpt-M14 were also used to screen the cv. Morex MTP BAC library (INRA-CNRGV) to successfully identify corresponding BAC clones and a position on a FPC due to the inability to anchor them to an FPC via BLAST search methods (Table 3.3).

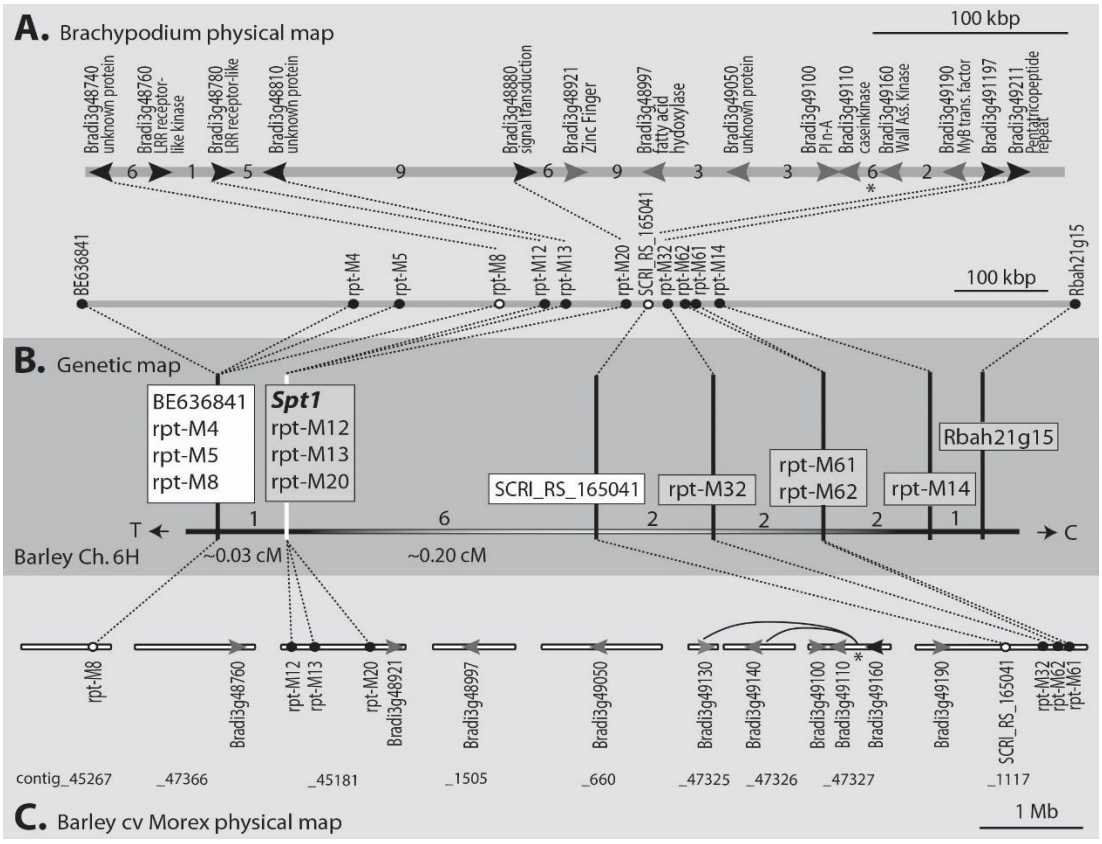

Fig. 3.1. Genetic and partial physical map of the *Spt1* locus in synteny with *Brachypodium distachyon*. Syntenous *B. distachyon* sequence, Rika × Kombar barley high-resolution map and barley cv Morex physical map at the *Spt1* locus. A) The grey horizontal bars represent the syntenous *B. distachyon* chromosome 3 sequence delimiting the *Spt1* gene region from barley. The lower bar shows the relative position of barley orthologous sequences used to develop markers from the annotated *B. distachyon* genes. Black dots represent marker positions and white dots represent the *Spt1* flanking markers. The upper bar is an expanded and more detailed representation of the delimited *Spt1* region with annotated *B. distachyon* genes shown with arrows and labeled above with putative gene functions. The black arrows represent genes from which barley orthologs were used to generate SNP markers and the grey arrows are genes that did not have polymorphisms in the Rika × Kombar population but were utilized to anchor physical contigs in panel C. The numbers between arrows are the number of additional *B. distachyon* genes present between each gene designated with an arrow. The 100 kb scale is shown above and below. B) Rika × Kombar chromosome 6H *Spt1* high-resolution map generated by screening 2976 recombinant F_2 gametes. The boxes contain co segregating markers with white boxes containing markers that delimit the *Spt1* locus. Numbers between the vertical lines connected to the marker boxes indicate the number of recombinants between the markers. T and C at the end of the horizontal line indicated direction of telomere and centromere, respectively. C) Barley cv Morex physical map showing the relative sizes of the supercontigs (white horizontal bars) with approximated positions of genetic markers generated from *B. distachyon* orthologous barley genes. The black circles indicate position of markers with the white circles indicating the *Spt1* region flanking markers. The position of the barley genes identified by *B. distachyon* orthologs that we were unable to develop markers from but could anchor to the barley

physical map are indicated by grey arrows. The proximal flanking SNP marker SCRI_RS_165041 identified from the barley *9k* Illumina *Infinium* iSELECT assay position is also designated with a white circle. The asterisk indicates two super contigs that were out of synteny between *B. distachyon* and barley. Barley contigs_47325 and _47326 were identified to contain barley orthologs of the annotated *B. distachyon* genes Bradi3g49130 and Bradi3g49140, which in the *B. distachyon* sequence are located between Bradi3g49110 and Bradi3g49160. The cv Morex supercontig designations (IBGSC, 2012) are provided below with the 1 Mb scale.

Table 3.3. Bacterial artificial chromosome (BAC) clones identified from all markers on high-resolution map and corresponding sequence contigs and fingerprinted contigs.

Marker[1]	Morex WGS Contig[2]	FPC Contig[3]	BAC Clone[4]	BAC Clone[5]
rpt-M4	morex_contig_38836	N/A	387C23, 442K9	N/A
rpt-M5	morex_contig_1564520	contig_4406	227HO5, 534F01, 729E01	N/A
rpt-M8	morex_contig_1573477	contig_45267	N/A	eA0312J23
rpt-M12	morex_contig_43862	contig_45181	783N21, 650G13, 82C13, 302J12	N/A
rpt-M13	morex_contig_64570	contig_45181	783N21, 82C13, 302J12	N/A
rpt-M20	morex_contig_37494	contig_45181	105J02, 606N13	hA0105J02, eA0192O20, mA0024H19
rpt-M32	morex_contig_102499	contig_1117	72B22, 154J12	mA0346B09, mA0406I23, hC0118K01
SCRI_RS_165041	morex_contig_1559439	contig_1117	575NO5	N/A
rpt-M61	morex_contig_45053	contig_1117	762H13, 344C02	mA0406I23
rpt-M62	morex_contig_45053	contig_1117	762H13, 344C02	mA0406I23
rpt-M14	morex_contig_52512	contig_6770	N/A	eA0049J16

[1] The rpt designation refers to the recessive resistance nomenclature previously used in the literature
[2] Whole genome sequencing contig from barley cultivar Morex identified via BLAST search (IPK)
[3] Fingerprint (FPC) contig identified via barley physical map browser or BAC MTP (IBGSC 2012; Ariyadasa *et al*. 2014)
[4] BAC clones identified from Morex BAC library (Yu et al 2000) by hybridization and BLAST (Muñoz-Amatriaín *et al.* 2015)
[5] BAC clones identified from Morex 6H MTP BAC library, screened by INRA or via BLAST search on IPK server (BAC prefix HVVMRXALL) (IBGSC 2012

Discussion

Previous studies on host resistance to NFNB in barley have been conducted utilizing diverse arrays of barley lines as well as fungal isolates from geographically distinct regions of the world. The results of these investigations were the identification of resistance/susceptibility loci distributed throughout the barley genome (Ho *et al.* 1996; Steffenson *et al.* 1996; Raman *et al.* 2003; Cakir *et al.* 2003; Ma *et al.* 2004; Manninen *et al.* 2006; Friesen *et al.* 2006a; Abu Qamar *et al.* 2008; St. Pierre *et al.* 2010). Although dominant susceptibility and/or resistance loci have been mapped to all seven barley chromosomes (reviewed by Liu *et al.* 2010), a common significant QTL near the centromere of chromosome 6H has repeatedly been associated with NFNB resistances and/or susceptibility. We have begun to characterize this important locus and it is likely that the QTL region contains several closely linked genes that interact with the putative necrotrophic effectors underlying the four major virulence QTL identified in a *P. teres* f. *teres* 6A × 15A pathogen population (Shjerve *et al.* 2014). However, allele analysis of the candidate genes identified in this research suggests that underlying this major susceptibility locus is a single gene, with divergent alleles that confer dominant susceptibility to the California *P. teres* f. *teres* isolates 15A and 6A (Richards, J. and Brueggeman, R., unpublished data).

The presence of multiple dominant susceptibility specificities (a.k.a. recessive resistance genes) at this locus (Abu Qamar *et al.* 2008; Liu *et al.* 2015) indicate that a repertoire of effector/virulence genes evolved in the pathogen to target a complex region of host biotrophic immunity receptors to elicit NETS. As seen in other fungal necrotrophic specialist pathosystems, the recessive resistance designation previously given to these host-pathogen genetic interactions are probably mediated by a functional dominant susceptibility gene product instead of a nonfunctional allele and should be more appropriately described as dominant

susceptibility within an inverse gene-for-gene model (Friesen *et al.* 2007). Similar to the classic gene-for-gene paradigm (Flor 1956), a dominant gene product produced by the host interacts with a dominant gene product from the pathogen, however, due to the necrotrophic lifestyle of this specialist pathogen, recognition by the host results in a PCD immunity response that is subverted by the necrotroph, resulting in a compatible reaction and disease. It has been observed that several necrotrophic plant pathogenic fungi, such as members of the genera *Pyrenophora* and *Parastagonospora,* produce effectors, which are recognized by a single host gene (Friesen *et al.* 2006b; Faris *et al.* 2010). Recognition of necrotrophic effectors and subsequent cellular signaling by the host may occur via 'resistance' genes encoding proteins with nucleotide binding site (NBS), leucine rich repeats (LRR), and/or serine-threonine protein kinase (STPK) domains (Lorang *et al.* 2007; Faris *et al.* 2010). Typical host resistance response mechanisms, such as the induction of programmed cell death, production of reactive oxygen species (ROS), and the up-regulation of PR genes, occur following host recognition of a necrotrophic effector (Lorang *et al.* 2007; Stergiopoulos *et al.* 2013; Liu *et al.* 2015). Although these responses provide effective defense against biotrophic pathogens, the necrotrophs that survive the hostile host induced environment produced as a barrier to colonization, also intentionally induce PCD immunity responses to obtain nutrients from the resulting dead host tissue. However, in contrast to biotrophic host resistance by these pathways that typically confer qualitative dominant resistances, these inverse gene-for-gene interactions appear to be quantitative in nature (Friesen *et al.* 2008).

Through high-resolution mapping of a Rika × Kombar F_2 population utilizing markers derived from orthologous *B. distachyon* genes within the previously delimited *rpt.k/rpt.r* region, we have delimited a putative dominant susceptibility locus, designated *Spt1*, to an ~0.24 cM

region near the centromere of barley chromosome 6H. This high-resolution mapping greatly refined the previously delimited ~3.3 cM region and facilitated the construction of a physical map using the new barley genome sequence. The use of the various newly available barley genomic resources, which are quickly being refined and updated, expedited the genetic to physical map construction and candidate *Spt1* gene identification. Although the physical map of the *Spt1* region is not completely contiguous, these tools have allowed for the positioning of physical sequences in correlation with our high-resolution map, as well as identification of flanking BAC clones to be used for further marker development and map saturation. Due to the identification of barley contigs containing the syntenic *B. distachyon* genes we expect that we have captured the majority of the *Spt1* physical region and show that it has been delimited to ~9.5 Mb of the barley genome which is predicted to contain 49 genes.

We hypothesize that the gene/s underlying the *Spt1* locus within the characterized region confers dominant susceptibility to NFNB isolates 6A and 15A through the recognition of necrotrophic effectors produced by the pathogen and the subsequent induction of PCD pathways in the host. It has recently been shown that *P. teres* f. *teres* produces necrotrophic effectors that induce the aforementioned host responses (Liu *et al.* 2015). Using intercellular wash fluids from barley leaf tissue inoculated with *P. teres* f. *teres* isolate 0-1, necrosis was induced on the susceptible cultivar Hector and sensitivity was subsequently mapped to the centromeric region of chromosome 6H. The segregation analysis indicated that a single locus at 6H likely contains a gene conferring sensitivity to an effector produced by *P. teres* f. *teres* isolate 0-1 (Liu *et al.* 2015). Additionally, four virulence loci, (*VR1*, *VR2*, *VK1*, and *VK2*), have been mapped in a *P. teres* f. *teres* mapping population derived from a cross of isolates 6A and 15A, identifying two major virulence QTL per isolate in different regions of the *P. teres* f. *teres* genome. Progeny

isolates containing single virulence loci were identified for *VK1*, *VK2* and *VR2*, essentially Mendelizing the major virulence QTL from 15A and one from 6A by isolating the specific necrotrophic effector-host interactions. These single QTL progeny isolates were inoculated onto the 6H critical recombinants to map the sensitivity genes, which we expect will encode immunity receptor-like proteins that govern susceptibility mediated by these unique effectors.

Susceptibility to the *VR2, VK1* and *VK2* single major virulence progeny isolates mapped to the same region on 6H and interestingly all mapped to the *Spt1* locus. This indicates that virulence conferred by isolate 15A may be governed by the recognition of two unique necrotrophic effectors by two tightly linked genes. Alternatively, a single gene at the *Spt1* locus may perceive both necrotrophic effectors produced by isolate 15A. The putative necrotrophic effector produced by a progeny isolate harboring *VR2*, conferring virulence to isolate 6A, may also interact directly or indirectly with a dominant susceptibility factor at the *Spt1* locus, which may or may not be alleles of a gene conferring susceptibility to isolate 15A. Alternatively, several effector targets within the ~0.24 cM *Spt1* genetic interval may exist in a 'susceptibility island', each recognizing a unique necrotrophic effector and eliciting PCD. We have delimited the genetic region to ~9.5 Mb of barley physical sequence, which based on POPSEQ anchoring of barley unigenes and BLAST searches of orthologous *B. distachyon* genes within the region against the barley genome sequence contains a predicted 39 high-confidence genes. Based on annotation of the functional domains, six of the genes encode predicted immunity receptor-like proteins. Thus, these genes are candidate *Spt1* genes and are being further analyzed via allele analysis and high resolution association mapping.

The barley-NFNB pathosystem proves to be genetically complex, consisting of dominant, recessive, and incomplete resistances, which are clustered at the 6H locus. This 6H complexity

complicates efforts to incorporate effective resistance into elite barley lines. The cloning of *Spt1*, as well as the effectors that interact directly or indirectly with them, will allow for greater knowledge and understanding of the molecular mechanisms underscoring this pathosystem as well as how necrotrophic specialist fungal pathogens have evolved to exploit the intricate immunity system of the host to induce beneficial PCD responses. The isolation of individual resistance/susceptibility genes implicated in this pathosystem will fill gaps in the understanding of the molecular basis of necrotrophic specialist-host interactions and allow researchers to effectively utilize identified sources of resistance. This work greatly advances the effort towards the positional cloning and functional analysis of the host gene/s involved in this complex pathosystem.

Acknowledgements

The authors would like to thank Danielle Holmes for technical assistance at the USDA-ARS, Cereal Crops Research Unit, Fargo ND. This project was supported by the National Research Initiative Competitive Grants CAP project 2011-68002-30029 from the USDA NIFA, NSF ND EPSCoR Track 1 grant 11A-1355466, and the National Science Foundation CAREER project Award Number 1253987.

Literature Cited

Abu Qamar, M., Liu, Z. H., Faris, J. D., Chao, S., Edwards, M. C., Lai, Z., Franckowiak, J. D., and Friesen, T. L. 2008. A region of barley chromosome 6H harbors multiple major genes associated with net type net blotch resistance. Theor. Appl. Genet. 117:1261

Ariyadasa, R., Mascher, M., Nussbaumer, T., Schulte, D., Frenkel, Z., Poursarebani, N., Zhou, R., Steurnagel, B., Gundlach, H., Taudien, S., Felder, M., Platzer, M., Himmelbach, A., Schmutzer, T., Hedley, P. E., Muehlbauer, G. J., Scholz, U., Korol, A., Mayer, K. F., Waugh, R., Langridge, P., Graner, A., and Stein, N. 2014. A sequence-ready physical map of barley anchored genetically by two million single-nucleotide polymorphisms. Plant Physiol. 164: 412-423.

Bennetzen, J. L. and Freeling, M. 1997. The Unified Grass Genome: Synergy in Synteny. Genome Res. 7: 301-306

Brueggeman, R., Rostoks, N., Kudrna, D., Kilian, A., Han, F., Chen, J., Druka, A., Steffenson, B., and Kleinhofs, A. 2002. The barley stem rust-resistance gene *Rpg1* is a novel disease-resistance gene with homology to receptor kinases. Proc. Natl. Acad. Sci. 99:9328-9333

Cakir, M., Gupta, S., Platz, G. J., Ablett, G. A., Loughman, R., Embiri, L. C., Poulsen, D., Li, C., Lance, R. C. M., Galway, N. W., Jones, M. G. K., and Appels, R. 2003. Mapping and validation of the genes for resistance to Pyrenophora teres f teres in barley (Hordeum vulgare L). Aust J Agric Res 54:1369-1377

DePristo, M. A., Banks, E., Poplin, R., Garimella, K. V., Maguire, J. R., Hartl, C., Phillippakis, A. A., del Angel, G., Rivas, M. A., Hanna, M., McKenna, A., Fennell, T. J., Kernytsky, A. M., Sivachenko, A. Y., Cibulskis, K., Gabriel, S. B., Altshuler, D., and Daly, M. J. 2011. A framework for variation discovery and genotyping using next-generation DNA sequencing data. Nature Genet. 43: 491-498.

Faris, J. D., Zhang, Z., Lu, H., Lu, S., Reddy, L., Cloutier, S., Fellers, J. P., Meinhardt, S. W., Rasmussen, J. B., Xu, S. S., Oliver, R. P., Simons, K. J., and Friesen, T. L. 2010. A unique wheat disease resistance-like gene governs effector-triggered susceptibility to necrotrophic pathogens. Proc. Natl. Acad. Sci. 107:13544-13549

Flor, H. H. 1956. The complementary genetic systems in flax and flax rust. Adv. Genet. 8: 29-54.

Friesen, T. L., Faris, J. D., Lai, Z., and Steffenson, B. J. 2006a. Identification and chromosomal location of major genes for resistance to Pyrenophora teres in a barley doubled haploid population. Genome. 409: 855-859.

Friesen, T. L., Stukenbrock, E. H., Liu, Z., Meinhardt, S., Ling, H., Faris, J. D., Rasmussen, J. B., Solomon, P. S., McDonald, B. A., and Oliver, R. P. 2006. Emergence of a new disease as a result of interspecific virulence gene transfer. Nature Genet. 38:953-956.

Friesen, T. L., Meinhardt, S. W., and Faris, J. D. 2007. The Stagonospora nodorum-wheat pathosystem involves multiple proteinaceous host-selective toxins and corresponding host sensitivity genes that interact in an inverse gene-for-gene manner. Plant J. 51: 681-692.

Friesen, T. L., Faris, J. D., Solomon, P. S., and Oliver, R. P. 2008. Host-specific toxins: effectors of necrotrophic pathogenicity. Cell. Microbiol. 10: 1421-1428.

Gao, Y., Faris, J. D., Liu, L., Kim, Y. M., Syme, R. A., Oliver, R. P., Xu, S. S., and Friesen, T. L. 2015. Identification and characterization of the SnTox6-Snn6 interaction in the Parastagonospora nodorum-wheat pathosystem. Mol. Plant Microbe In. 28: 615-325.

Ho, K. M., Tekauz, A., Choo, T. M., and Martin, R. A. 1996. Genetic studies on net blotch resistance in a barley cross. Can. J. Plant Sci. 76: 715-719

International Barley Genome Sequencing Consortium. 2012. A physical, genetic and functional sequence assembly of the barley genome. Nature. 491: 711-716.

International Brachypodium Initiative. 2010. Genome sequencing and analysis of the model grass *Brachypodium distachyon*. Nature. 463: 763–768.

Kellogg, E. A. 2001. Evolutionary history of the grasses. Plant Physiol. 125: 1198-205

Li, H. and Durbin, R. 2009. Fast and accurate short read alignment with Burrows-Wheeler Transform. Bioinformatics. 25: 1754-60

Li, H., Handsaker, B., Wysoker, A., Fennell, T., Ruan, J., Homer, N., Marth, G., Abecasis, G., and Durbin, R. 2009. The sequence alignment/map format and SAMtools. Bioinformatics. 25: 2078-2079.

Liu, Z., Ellwood, S. R., Oliver, R. P., and Friesen, T. L. 2011. Pyrenophora teres: profile of an increasingly damaging barley pathogen. Mol. Plant Pathol. 12: 1-19

Liu, Z., Faris, J. D., Edwards, M. C., and Friesen, T. L. 2010. Development of Expressed Sequence Tag (EST)-based Markers for Genomic Analysis of a Barley 6H Region Harboring Multiple Net Form Net Blotch Resistance Genes. Plant Genome. 3: 41-52

Liu, Z., Faris, J. D.,Oliver, R. P., Tan, K., Solomon, P. S., McDonald, M. C., McDonald, B. A., Nunez, A., Lu, S., Rasmussen, J. B., and Friesen, T. L. 2009. SnTox3 acts in effector triggered susceptibility to induce disease on wheat carrying the Snn3 gene. PLoS Pathog. 5: e1000581.

Liu, Z., Holmes, D. J., Faris, J. D., Chao, S., Brueggeman, R. S., Edwards, M. C., and Friesen, T. L. 2015. Necrotrophic effector-triggered susceptibility (NETS) underlies the barley-*Pyrenophora teres* f. *teres* interaction specific to chromosome 6H. Mol. Plant Pathol. 16:188-200

Liu, Z., Zhang, Z., Faris, J. D., Oliver, R. P., Syme, R., McDonald, M. C., McDonald, B. A., Solomon, P. S., Lu, S., Shelver, W. L., Xu, S., and Friesen, T. L. 2012. The cysteine rich necrotrophic effector SnTox1 produced by Stogonospora nodorum triggers susceptibility of wheat lines harboring Snn1. PLoS Pathog. 8: e1002467.

Lorang, J. M., Sweat, T. A., and Wolpert, T. J. 2007. Plant disease susceptibility conferred by a "resistance" gene. Proc. Natl. Acad. Sci. 104: 14861-14866.

Ma, Z. Q., Lalpitan, N. L. V., and Steffenson, B. 2004. QTL mapping of net blotch resistance genes in a doubled-haploid population of six-rowed barley. Euphytica. 137: 291-296.

Manninen, O., Kalendar, R., Robinson, J., and Schulman, A. H. 2006. Application of BARE-1 retrotransposon markers to the mapping of a major resistance gene for net blotch in barley. Mol. Genet. Genomics. 264: 325-334.

Mascher, M., Muehlbauer, G. J., Rokshar, D. S., Chapman, J., Schmutz, J., Barry, K., Muñoz-Amatriaìn, M., Close, T. J., Wise, R. P., Schulman, A. H., Himmelbach, A., Mayer, K. F. X., Scholz, U., Poland, J. A., Stein, N., and Waugh, R. 2013. Anchoring and ordering NGS contig assemblies by population sequencing (POPSEQ). Plant J. 76:718-727

Mathre, D. E. 1997. *Compendium of Barley Diseases*, 2nd Edition. American Phytopathological Society, St. Paul.

McLean, M. S., Howlett, B. J., and Hollaway, G. J. 2009. Epidemiology and control of spot form of net blotch (Pyrenophora teres f. maculata) of barley: a review. Crop Pasture Sci. 60: 303-315

Muñoz-Amatriaìn, M., Cuesta-Marcos, A., Endelman, J. B., Comadran, J., Bonman, J. M., Bockelman, H. E., Chao, S., Russell, J., Waugh, R., Hayes, P. M., and Muehlbauer, G. J. 2014. The USDA Barley Core Collection: Genetic Diversity, Population Structure, and Potential for Genome-Wide Association Studies. PLoS One 9:e94688

Muñoz-Amatriaìn, M., Lonardi, S., Luo, M., Madishetty, K., Svensson, J. T., Moscou, M. J., Wanamaker, S., Jiang, T., Kleinhofs, A., Muehlbauer, G. J., Wise, R. P., Stein, N., Ma, Y., Rodriguez, E., Kudrna, D., Bhat, P. R., Chao, S., Condamine, P., Heinen, S., Resnik, J., Wing, R., Witt, H. N., Alpert, M., Beccuti, M., Bozdag, S., Cordero, F., Mirebrahim, H., Ounit, R., Wu, Y., You, F., Zheng, J., Simkova, H., Dolezel, J., Grimwood, J., Schmutz, J., Duma, D., Altschmied, L., Blake, T., Bregitzer, P., Cooper, L., Dilbirligi, M., Falk, A., Feiz, L., Graner, A., Gustafson, P., Hayes, P. M., Lemaux, P., Mammadov, J., and Close, T. J. 2015. Sequencing of 15,622 gene-bearing BACs clarifies the gene-dense regions of the barley genome. Plant J. 84:216-227

Mur, L. A., Allainguillaume, J., Catalán, P., Hasterok, R., Jenkins, G., Lesniewska, K., Thomas, I., and Vogel, J. 2011. Exploiting the Brachypodium Tool Box in cereal and grass research. New Phytol. 191:334-347

Murray, G. M. and Brennan, J. P. 2010. Estimating disease losses to the Australian barley industry. Australas. Plant Pathol. 39: 85-96

Raman, H., Platz, G. J., Chalmers, K. J., Raman, R., Read, B. J., Barr, A. R., and Moody, D. B. 2003. Mapping of genetic regions associated with net form of net blotch resistance in barley. Aust J Agric Res 54:1359-1367

Shjerve, R. A., Faris, J. D., Brueggeman, R. S., Yan, C., Zhu, Y., Koladia, V., and Friesen, T. L. 2014. Evaluation of a *Pyrenophora teres* f. *teres* mapping population reveals multiple independent interactions with a region of barley chromosome 6H. Fungal Genet. Biol. 70:104-112

Smedegård-Petersen, V. 1971. *Pyrenophora teres* f. *maculata* f. nov. and *Pyrenophora teres* f. *teres* on barley in Denmark. Kgl. Vet. Landbohojsk. Arsskr. 124–144.

St. Pierre, S., Gustus, C., Steffenson, B., Dill-Macky, R., and Smith, K. P. 2010. Mapping net form net blotch and Septoria speckled leaf blotch resistance loci in barley. Phytopathol. 100: 80-84.

Steffenson, B. J., Hayes, H. M., and Kleinhofs, A. 1996. Genetics of seedling and adult plant resistance to net blotch (Pyrenophora teres f. teres) and spot blotch (Cochliobolus sativus) in barley. Theor. Appl. Genet. 92: 552-558.

Steffenson, B. J. and Webster, R. K. 1992. Quantitative resistance to Pyrenophora teres f. teres in barley. Phytopathol. 82: 407-411.

Stergiopoulos, I., Collemare, J., Mehrabi, R., and de Wit, P. J. 2013. Phytotoxic secondary metabolites and peptides produced by plant pathogenic Dothideomycete fungi. FEMS Microbiol Rev. 37: 67-93.

Strelkov, S. E., Lamari, L., and Ballance, G. M. 1999. Characterization of a host-specific protein toxin (PtrToxB) from Pyrenophora tritici-repentis. Mol. Plant Microbe In. 12: 726-732.

Tekauz, A. 1985. A numerical scale to classify reactions of barley to Pyrenophora teres. Can. J. Plant Pathol. 7: 181-183

Tomas, A., Feng, G. H., Reeck, G. R., Bockus, W. W., and Leach, J. E. 1990. Purification of a cultivar-specific toxin from Pyrenophora tritici-repentis, causal agent of tan spot of wheat. Mol. Plant Microbe In. 3: 221-224.

Tsilo, T. J., Chao, S., Jin, Y., and Anderson, J. A. 2009. Identification and validation of SSR markers linked to the stem rust resistance gene Sr6 on the short arm of chromosome 2D in wheat. Theor. Appl. Genet. 118: 515–524.

Wu, H. L., Steffenson, B. J., Zhong, S., Li, Y., and Oleson, A. E. 2003. Genetic variation for virulence and RFLP markers in Pyrenophora teres. Can. J. Plant Path. 25: 82-90.

Yu, Y., J. P. Tomkins, R. Waugh, D. A. Frisch, D. Kudrna *et al.*, 2000 A bacterial artificial Yu, Y., Tomkins, J. P., Waugh, R., Frisch, D. A., Kudrna, D., Kleinhofs, A., Brueggeman, R. S., Muehlbauer, G. J., Wise, R. P., and Wing, R. A. 2000. A bacterial artificial chromosome library for barley (Hordeum vulgare L.) and the identification of clones containing putative resistance genes. Theor. Appl. Genet. 101:1093-1099

CHAPTER 4. IDENTIFICATION OF *SPT1*: A MULTI-ALLELIC RECEPTOR-LIKE PROTEIN CONFERRING ISOLATE SPECIFIC NET FORM NET BLOTCH SUSCEPTIBILITY IN BARLEY

Abstract

Pyrenophora teres f. *teres*, a necrotrophic fungal pathogen, is the causal agent of net form net blotch of barley (*Hordeum vulgare*). NFNB occurs in most barley production regions of the world and has the potential to cause severe yield loss. Genetic resistance is regarded as the most desirable means of control, but the nature of host resistance is highly complex, warranting further investigation. Previously, the dominant NFNB susceptibility locus *Spt1* was fine mapped to ~0.24 cM near the centromere of barley chromosome 6H. Here report on the identification of a predicted receptor-like protein as a strong *Spt1* candidate (*Spt1.cg*). Examining the *Spt1* region at a high-resolution with results from a genome-wide association study effectively delimited the *Spt1* region to ~ 3.1 Mb, containing four genes with homology to plant immune receptors, with *Spt1.cg* being the only known polymorphic gene. Additionally, three alleles have been fully sequenced from barley cultivars Rika, Kombar, and Morex, revealing an extreme level of diversification. The LRR region of the predicted protein remains relatively conserved, while the N-terminus is nearly unrecognizable, except for several conserved motifs, from the other alleles. This diversification appears to have occurred in wild barley populations, as evidenced by the presence of at least 18 haplotypes within the relatively conserved LRR domain, in response to selection pressure from the pathogen. A strong correlation exists between the presence of a Rika, Kombar, or Morex allele and susceptibility to isolates 6A, 15A, and Tra-A5/Tra-D10, respectively, indicating *Spt1.cg* may be a multi-allelic necrotrophic effector target, conditioning susceptibility to specific isolates.

Introduction

Net form net blotch (NFNB) is a destructive foliar disease of barley (*Hordeum vulgare*) caused by the necrotrophic fungal pathogen *Pyrenophora teres* f. *teres*. The disease occurs in most barley production centers of the world, thriving under cool and wet conditions, and typically results in yield losses ranging from 10%-40% (Mathre 1997). Yield losses manifest themselves in reduced grain size, plumpness, carbohydrate content, and increased protein content, leading to rejection by the malting industry (Grewal et al. 2008; Kinzer 2015). Due to the ability of *P. teres* f. *teres* to overwinter on barley stubble as pseudothecia, cultural practices targeting the management of crop residue are used to combat this disease (Liu et al. 2011). Additionally, seed treatments with chemicals such as maneb or triadimenol have been observed to positively influence yield (Martin 1985). However, the deployment of durable genetic resistance has often been viewed as the most desirable means of disease management.

Plants possess a basal tier of immunity towards a broad range of pathogens known as pathogen associated molecular pattern (PAMP) triggered immunity (PTI). PAMPs are often beneficial and physiologically necessary molecules produced by a plant pathogen to maintain its ability to successfully proliferate (Zipfel et al. 2008). Thoroughly investigated examples of such molecules are flagellin from phytopathogenic bacteria or chitin from fungi, which aid in motility and cellular structure, respectively (Tans-Kersten et al. 2001; Gomez-Gomez and Boller 2002; Zipfel 2009). Recognition of PAMPs is generally mediated by membrane bound receptor-like kinases (RLKs) that contain an extracellular leucine rich repeat (LRR) domain that are typically involved in protein-protein interactions facilitating PAMP perception, a transmembrane domain, and an intracellular kinase domain responsible for signaling. PAMP recognition can also occur via the receptor-like proteins (RLPs), which have protein domain architecture similar to RLKs

yet are lacking the protein kinase (Jones and Dangl 2006; Zipfel 2008; Zipfel 2009; Dodds and Rathjen 2010; Thomma et al. 2011).

Groundbreaking research on the genetic basis of plant disease resistance was conducted by H.H. Flor in the flax rust-flax pathosystem. By studying the genetics of both host and pathogen populations, his seminal gene-for-gene hypothesis was developed (Flor 1956). Under the premise of this hypothesis, a dominant host resistance gene product recognizes a dominant pathogen avirulence gene product, resulting in an incompatible reaction. Many of the characterized dominant resistance genes operating in this manner contain nucleotide binding site (NBS) and leucine rich repeat (LRR) domains, and are localized to the cytoplasm (Jones and Dangl 2006). This recognition event may occur via direct interaction, as evidenced by dominant resistance gene *L6* alleles in flax directly perceiving unique Avr567 effectors produced by the flax rust pathogen *Melamspora lini* (Dodds et al. 2006). Recognition of the pathogen by the host initiates effector triggered immunity (ETI), resulting in a localized programmed cell death, which in the context of a biotrophic pathogen, equates to resistance. Additionally, receptor-like proteins (RLPs) have been implicated in the ETI pathway, as evidenced by the tomato gene *Cf-4* conferring dominant resistance to isolates of *Cladosporium fulvum* producing the effector Avr4. Cf-4, a membrane-bound receptor-like protein, recognizes Avr4 and is able to signal to the interior of the cell via direct association to the receptor-like kinase SOBIR1 (Liebrand et al. 2013).

The genetic nature of resistance or susceptibility to *P. teres* f. *teres* has been extensively researched and observed to be exceedingly complex. Both dominant and incomplete resistances have been identified (Koladia et al. 2016; Friesen et al. 2006; Mode and Schaller 1958). Additionally, recessive resistances, or more aptly termed dominant susceptibility, have also been

characterized in this pathosystem (Abu Qamar et al. 2008; Liu et al. 2015). Recent research has shed light on the molecular manner in which necrotrophic pathogens cause disease. Previously thought to mainly produce compounds such as cell-wall degrading enzymes to enable infection (Hematy et al. 2009), necrotrophs have now been observed to produce host-specific necrotrophic effectors (NEs) which are detrimentally perceived by the host's innate immune system triggering programmed cell death responses that typically confer resistance to biotrophic pathogens, but rather induce disease by the necrotrophic pathogen in an inverse gene-for-gene manner (Friesen et al. 2007). The NE ToxA, produced by necrotrophic fungal pathogens *Pyrenophora tritici-repentis* and *Parastagonospora nodorum*, indirectly interact with host dominant susceptibility factor Tsn1 in wheat, essentially tricking the host to initiate its defense responses (Friesen et al. 2006; Faris et al. 2010). *Tsn1* encodes a protein consisting of domains often associated with resistance, including NBS, LRR, and a serine-threonine protein kinase (STPK) domains. The intricate host-parasite genetic interactions, which can include both dominant resistances (gene-for-gene) and dominant susceptibilities (inverse gene-for-gene) that result in qualitative and quantitative compatible or incompatible interactions with necrotrophic pathogens, including *P. teres* f. *teres*, complicates breeding efforts, as both resistance genes and/or susceptibility quantitative trait loci (QTL) need to be incorporated or removed, respectively, from elite barley lines.

Genetic analysis of host resistance towards *P. teres* f. *teres* at both the seedling and adult plant stages have identified QTL localized throughout the barley genome on each chromosome (reviewed by Liu et al. 2011). However, the centromeric region of chromosome 6H has been commonly mapped in association with NFNB resistance or susceptibility using geographically diverse *P. tere* f. *teres* isolates and barley lines (Steffenson et al. 1996; Graner et al. 1996;

Richter et al. 1998; Raman et al. 2003; Cakir et al. 2003; Ma et al. 2004; Emebiri et al. 2005; Yun et al. 2005; Manninen et al. 2000; Manninen et al. 2006; Friesen et al. 2006; Grewal et al. 2008; Abu Qamar et al. 2008; St. Pierre et al. 2010; Liu et al. 2015; Koladia et al. 2016). Additionally, results of a genome wide association study (GWAS) of the disease reaction to three North American *P. teres* f. teres isolates illustrated the centromeric region of chromosome 6H as an integral hub of host resistance or susceptibility (Chapter 2). Abu Qamar et al. (2008) identified recessive resistance genes *rpt.r/rpt.k* in barley cultivars Rika and Kombar effective against *P. teres* f. *teres* isolates 6A and 15A, respectively, that exist in repulsion. The recessive resistance locus was mapped to the centromeric region of chromosome 6H to ~5.9 cM and the region was further refined via marker saturation to ~3.3 cM (Liu et al. 2010). Previously, using 2976 recombinant gametes and newly developed markers from orthologous *Brachypodium distachyon* genes, we conducted high-resolution mapping of this NFNB recessive resistance gene, now referred to as dominant susceptibility to *P. teres* 1 gene, *Spt1*, and subsequently localized it to an ~0.24 cM region (Richards et al. 2016; Chapter 2).

Here we report on five lines of strong circumstantial evidences that when taken together convincingly show that we have identified a very strong candidate *Spt1* gene. **First,** the candidate *Spt1* gene was predicted to encode a membrane-bound receptor like protein, which functionally fits our hypothesis that the susceptibility target protein would resemble an immunity-like receptor that could be targeted by apoplastic localized small secreted NEs. **Second**, three alleles of *Spt1* have been fully sequenced and characterized, revealing a high level of divergence at the amino acid level in the predicted apoplastic localized N-terminal region of the protein, the region we suspect is under diversifying selection due to interaction with diverse NEs from the pathogen population. Also, the genotype and phenotype analyses using diverse

barley lines shows a strong correlation with the presence of a Rika, Kombar, or Morex-like allele and susceptibility to *P .teres* f. *teres* isolates 6A, 15A, and Tra-A5/Tra-D10, respectively. This is more significant given that high resolution mapping of *Spt1* in a Rika x Kombar population shows co-segregation of *Spt1.r* and *Spt1.k* alleles and susceptibility to 6A and 15A, respectively. Also, mapping of the susceptibility to two Montana isolates of *P. teres* f. *teres*, Tra-A5 and Tra-D10, which are virulent on Morex, in a Steptoe x Morex double haploid population localized Morex susceptibility to the *Spt1.m* locus. **Third**, high-resolution association mapping delimited the *Spt1* region to ~3 Mb of the barley genome sequence which contains only four annotated candidate genes, one of which is the *Spt1* gene. **Fourth**, the chromosome 6H centromeric *Spt1* region shows very limited amounts of polymorphism in the genes within the delimited region yet the *Spt1* candidate gene is under very high levels of diversifying selection and the pathogen populations are also under a high level of diversifying selection with multiple distinct NE loci targeting in on the *Spt1* region. **Fifth**, phylogenetic analysis of wild barley accessions, landraces, and cultivated barley indicates that diversification of *Spt1* occurred in natural populations (at least 18 haplotypes) of *Hordeum vulgare* subsp. *spontaneum* in response to selection pressure presumably by the pathogen. Also, all the allelic diversity found to date in cultivated barley is present in the wild barley natural populations, suggesting that the *Spt1* allelic and NE diversity occurred during the molecular arms race between wild barley and *P. teres* f. *teres* in the center of diversity. It also suggests that we have only scratched the surface of the natural diversity of the *Spt1* gene, as well as the diversity of NE that target this susceptibility hub or weak link in the barley immunity system. Thus, although the direct evidence via complementation, mutagenesis or post-transcriptional silencing is still required to validate the RLP as *Spt1* we are confident that it is the gene.

Materials and Methods

DNA Extraction

Approximately 2 cm of leaf tissue was collected from the barley cultivars Rika, Kombar, Morex, and 31 lines from the barley core collection and NFNB differential set and homogenized with a disposable tissue grinder in 400 µL DNA extraction buffer (200 mM Tris-HCl pH 7.5, 250 mM NaCl, 25 mM EDTA, 0.5% SDS). A total of 200 µL of chloroform was added to each homogenized sample and subsequently vortexed for 10 seconds and centrifuged at 15,600 g for 10 min. Approximately 300 µL of supernatant was transferred to a 1.5 mL tube, followed by the addition of 300 µL isopropanol. Samples were mixed by inversion, incubated at room temperature for 5 minutes, and centrifuged at 15,600 g for 10 minutes. The precipitated DNA pellets were washed with ~ 1 mL of 70% ethanol, air dried for ~10 minutes, and resuspended in 100 µL of H_2O.

A subset of 79 diverse barley lines from the barley core collection were selected by differential reactions to the *P. teres* f. *teres* isolates 15A and 6A. This subset was selected on the basis of four phenotypic classes: resistant to both isolates, susceptible to both isolates, resistant to 15A but susceptible to 6A, and resistant to 6A but susceptible to 15A. Approximately 2 cm of seedling leaf tissue was collected from each genotype in a 96 well 2.2 mL deep-well plate and lyophilized overnight. Plates containing lyophilized tissue and silica beads were placed in a tissue grinder and homogenized on setting 20 for two minutes. The plates were centrifuged at 4000 rpm for one minutes to collect the samples. Extraction buffer (100 mM Tris base pH 8.0, 50 mM EDTA pH 8.0, 500 mM NaCl, and 1.25% SDS) was heated to 65 °C in a water bath and 500 µL was added to each sample. Plates were covered and incubated at 65 °C for 30 minutes, with ~ 5 seconds of vortexing every 10 minutes. Following incubation, the plates were placed in -20 °C

for 10 minutes. A total of 166 µL of protein precipitation solution (5M ammonium acetate) was added to each well, vortexed, and incubated for an additional 10 minutes at -20 °C and then the plates were centrifuged at 4000 rpm for 25 minutes. After centrifugation, approximately 400 µL of supernatant was transferred to a new 2.2 mL deep well plate containing 600 µL of DNA binding solution in each well (6M Guanidine-HCl and 63% ethanol). The samples were mixed by pipetting and transferred to a glass filter plate (Acroprep Advance, Pall Corporation) placed on top of a 2.2 mL deep well plate, then incubated at room temperature for 10 minutes. Plates were centrifuged at 3000 rpm for five minutes and flow-through liquid was discarded. A total of 800 µL of wash solution (10 mM Tris pH 8.0, 1 mM EDTA pH 8.0, 50 mM NaCl, and 67% ethanol) was added to each well of the glass filter plate and incubated at room temperature for 10 minutes. Plates were then centrifuged for five minutes at 3000 rpm and the flow-through liquid was discarded. The DNA wash step was repeated once and following the second wash, the glass filter plates were transferred to a new 1.2 mL deep well plate and 200 µL of elution buffer (10 mM Tris pH 8.0, RNAse (20 µg.mL)) was added to each well and incubated at room temperature for five minutes. The plates were centrifuged at 3000 rpm for five minutes and an additional 200 µL of elution buffer was added to each well followed by an additional centrifugation at 3000 rpm for 10 minutes. The glass filter plate was discarded and the eluted DNA was covered and stored at -20° C.

Candidate Gene Identification

Sequence of genetic markers flanking the previously mapped *Spt1* region, rpt-M8 and SCRI_RS_165041, (Fig 3.1; Chapter 3) were used in BLAST searches of the *B. distachyon* genome to identify orthologous positions for regional gene content analysis. Orthologous genes within the region were extracted from the barley chromosome 6H genome zipper (Mayer et al.

2011) and were subjected to BLASTX searches to identify putative gene function with an emphasis on the identification of genes with predicted domains implicated in host immunity responses. Barley orthologs of predicted *B. distachyon* genes were identified via BLASTN searches of barley expressed sequence tags (ESTs) on NCBI, the barley EST assembly 35 on HarvEST (Muñoz-Amatriaín et al. 2015), and annotated genes of the cultivar Morex reference genome v1.0. Primers were designed to amplify full-length and domain specific gene products. PCR reactions consisted of 2 µL genomic DNA template (~50 ng/µL), 5 µL 10x GoTaq buffer (1x), 3 µL forward primer (1.20 µM), 3 µL reverse primer (1.20 µM), 0.50 µL dNTPs (200 µM), 0.25 µL GoTaq (1.25 units), and 11.25 µL H_2O. PCR parameters are as follows: initial denaturation at 95 °C for five minutes, 35 cycles of 94 °C for 30 seconds, 62 °C for 30 seconds, and 72 °C for 60 seconds/kb of target amplicon length, followed by a final extension at 72 °C for seven minutes. PCR products were visualized on 1% agarose gels containing GelRed (Biotum). The amplicons were purified using E.Z.N.A. PCR Purification Kit (Omega-Biotek) and Sanger sequenced (Genscript). Gene sequences from Rika and Kombar were aligned in VectorNTI (Invitrogen) for the identification of polymorphism. If polymorphisms were detected, the 14 immortal critical recombinants, derived from a cross of Rika x Kombar, harboring recombination within the previously mapped *Spt1* region, were genotyped with the corresponding marker using the aforementioned parameters (Chapter 3).

Genome Walking and Candidate Gene Sequence Analysis

Due to the inability to amplify full-length candidate *Spt1* from Rika or Kombar, utilizing the Morex *Spt1.cg* sequence mined from the genome sequence, an adaptor-ligation genome walking method was employed to obtain full-length gene sequence using a modified Universal Genome Walker 2.0 kit (Clontech). Approximately 2.5 µg of genomic DNA was digested with

six base-pair blunt end restriction enzymes *Dra*I, *Eco*RV, *Nae*I, and *Pvu*II, to develop four genome walking libraries per barley line. Digestion reactions consisted of 25 µL genomic DNA (~2.5 µg), 8 µL restriction enzyme (80 units), 10 µL of respective buffer (1x), and 57 µL H_2O. Reactions were incubated at 37 °C for two hours, slowly vortexed, and further incubated at 37 °C overnight, approximately 16 hours. Digestion reactions were purified using the E.Z.N.A. PCR Purification Kit (Omega-Biotek) according to manufacturer's instructions and eluted in 30 µL of H_2O. Genome walking adaptors were blunt-end ligated in a reaction consisting of 4.8 µL digested and purified genomic DNA, 1.9 µL GenomeWalker Adaptor (2.5 µM), 0.80 µL 10x ligation buffer (1x), and 0.50 µL T4 DNA ligase (3 units). Ligation reactions were incubated overnight, approximately 16 hours, at 16 °C. Reactions were inactivated by incubation at 70 °C for five minutes and each library was diluted to 40 µL with H_2O.

A nested PCR strategy was utilized to target gene specific fragments of the digested libraries. Gene specific primers rpt-M12 F1/R1 (M12 F1: 5'-CACTACCTGCAAACTTGGGCTTCTC-3'; M12 R1: 5'-CGTCTTCGGCTGGCTCAGGAACGAG-3'), capable of amplifying the more conserved LRR region of the candidate *Spt1* gene from Rika and Kombar, were used as the primary primer pair. Sequence of the rpt-M12 amplicons from each cultivar were used to design a nested set of primers specific to Rika and Kombar for use in the second genome walking PCR reaction. The first round of genome walking was initiated using primers specific to the ligated adaptor sequence and the gene-specific primers rpt-M12 F1 and rpt-M12 R1 for 3' and 5' walks, respectively. PCR reactions were as follows: 2 µL adaptor ligated genome walking library, 5 µL 10x GoTaq buffer (1x) (Promega), 1 µL gene-specific primer (0.20 µM), 1 µL AP1 primer (0.20 µM), 1 µL dNTPs (200 µM), 1 µL GoTaq (5 units) (Promega), and 39 µL H_2O. Cycling

parameters were as follows: seven cycles of 94 °C for 25 seconds and 72 °C for three minutes, followed by 32 cycles of 94 °C for 25 seconds and followed by 67 °C for three minutes, with a final extension of 67 °C for seven minutes. PCR reactions from the first round of amplification were diluted in a 1:50 ratio and used as template for the second round of PCR. The second round of PCR reactions consisted of 1 µL template (1:50 dilution of first round of PCR), 5 µL 10x GoTaq buffer (1x) (1 µL nested gene-specific primer (0.20 µM), 1 µL AP2 primer (0.20 µM), 1 µL dNTPs (200 µM), 1 µL GoTaq (5 units), and 40 µL H_2O. Cycling parameters were as follows: five cycles of 94 °C for 25 seconds and 72 °C for three minutes, followed by 20 cycles of 94 °C for 25 seconds followed by 67 °C for three minutes, with a final extension of 67 °C for seven minutes. PCR products were visualized on a 1% agarose gel containing GelRed (Biotum). Positive bands were excised from the gel and amplicon DNA was purified using the E.Z.N.A. Gel Extraction Kit (Omega-Biotek) per manufacturer's instructions. Amplicons were sequenced via Sanger sequencing (Genscript) and aligned to the previously identified gene sequence to extend it in the 5' and 3' direction. From the newly synthesized sequence, nested primer pairs were developed for use in continued 5' and 3' genome walking using the previous protocol to obtain predicted full length genomic DNA sequence from the candidate *Spt1* gene.

The predicted amino acid sequence of the full-length alleles identified for each of the candidate *Spt1* genes were aligned in pairwise combinations using BLASTP (NCBI) and Vector NTI software (Invitrogen). The prediction of transmembrane domains was conducted using TMpred (Hofmann and Stoffel 1993). Interpro (Mitchell et al. 2015) was used to predict the presence of functional protein domains. The alignments of the predicted amino acid sequences of the three candidate *Spt1* alleles (Morex, Rika and Kombar) were visualized using VectorNTI software (Invitrogen).

Phenotyping of Steptoe x Morex DH Population

Two *P. teres* f. *teres* isolates, Tra-A5 (Koladia et al. 2016) and TD10, were collected from Montana and used for the phenotyping of a double haploid (DH) population derived from a cross of barley cultivars Steptoe and Morex consisting of 146 individuals, hereafter referred to as the SM population (Steffenson et al. 1996). Inoculum preparation and inoculations were conducted as described by Friesen et al. (2006). Briefly, fungal isolates were plated on V8-PDA (150 mL V8 juice, 10 g PDA, 3 g $CaCO_3$, 10 g agar, and 850 mL sterile distilled H_2O) and incubated in the dark at room temperature for five days. Plates were then moved to the light at room temperature for 24 hours, followed by 24 hours in the dark at 15 °C. Conidia were harvested from each plate by adding sterile distilled H_2O and scraping the cultures with a sterile inoculation loop. The spores from each plate were collected and diluted to a concentration of 2000 spores/mL. One drop of Tween 20 was added per 50 mL of prepared inoculum. Three seeds of each DH individual, Steptoe, and Morex were planted in cone-tainers (Stuwe and Sons, Inc., Corvallis, OR) in a 98 cone rack. Susceptible barley cultivar Robust was planted as a border consisting of 38 cones. Plants were grown under greenhouse conditions for approximately 14 days, until the second leaf was fully expanded. Inoculum was applied using an air sprayer until full coverage of the leaves were achieved, but before runoff occurred. Inoculated plants were placed in a mist chamber at 100% humidity in the light at 21 °C for 24 hours. Plants were then transferred to a growth chamber on a 12 hour photoperiod at a temperature of 21 °C. Disease ratings were conducted seven days post-inoculation using a 1-10 scale (Tekauz 1985). Three and two replications were conducted for isolates Tra-D10 and Tra-A5, respectively. The arithmetic means of the replications were used for QTL analysis.

Linkage Mapping and QTL Analysis

The SM DH population was genotyped with the GoldenGate assay, resulting in a total of 833 polymorphic single nucleotide polymorphism (SNP) markers with less than 10% missing data across the entire population. Data was obtained from the T3 Barley database (https://triticeaetoolbox.org/barley/) and imported into MapDisto 1.7.5.1 for linkage mapping (Lorieux 2012). Markers were placed into linkage groups using the 'find groups' command with a logarithm of the odds (LOD) value of 3.0 and rmax of 0.3. The 'AutoOrder', 'AutoCheck Inversions', and 'AutoRipple' commands were used to develop a linkage map at a LOD of 3.0 and genetic distances calculated using the Kosambi mapping function. A representative marker containing the least amount of missing data was selected from each locus and the remaining co-segregating markers were removed, producing a final linkage map for QTL analysis.

Homogeneity of variances between the replications of each isolate inoculation was calculated using Bartlett's Chi-squared test in the R statistical environment (R Core Team 2016). QTL analysis was conducted in QGene 4.3.1 (Johannes et al. 2008) using the average disease scores with the single-trait multiple interval mapping (MIM) algorithm. A LOD threshold at the significance level of alpha = 0.01 level was calculated by 1000 permutations for each analysis. Phenotypic variation attributed to the identified QTL was determined by fitting significant markers into a multiple regression model. Sequence of the SNP markers flanking the identified QTL were used in BLAST searches of the barley cultivar Morex reference genome v1.0 for physical comparison of the identified region to the position of candidate *Spt1*.

Allele and Association Analysis

Allele analysis of a diverse set of barley lines was conducted to determine a correlation between the presence of a candidate *Spt1* allele and isolate specific susceptibility. Initially, a set

of 15 previously phenotyped barley lines from the NFNB differential set and 16 barley lines selected on the basis differential reactions to *P. teres* f. *teres* isolates 15A and 6A from previous phenotyping (Chapter 2) were genotyped with primer pairs specific to the Rika, Kombar, and Morex alleles of candidate *Spt1* gene. PCR reactions consisted of 2 µL of genomic DNA (~50 ng), 3 µL forward primer (0.40 µM), 3 µL reverse primer (0.40 µM), 5 µL 5x GoTaq buffer, 0.50 µL dNTPs (200 mM), 0.25 µL GoTaq (1.25 units), and 13.25 µL H_2O. Cycling parameters are as follows: initial denaturation at 95 °C for five minutes, 35 cycles of 94 °C for 30 seconds, 62 °C for 30 seconds, and 72 °C for 60 seconds, followed by a final extension at 72 °C for seven minutes. PCR amplicons were visualized on a 1% agarose gel containing GelRed (Biotum) and scored as positive or negative for the presence of a specific candidate *Spt1* allele.

An additional 79 barley lines previously phenotyped with *P. teres* f. *teres* isolates 15A and 6A (Chapter 2) were selected for further allele analysis. The newly selected lines were additionally phenotyped with *P. teres* f. *teres* isolates Tra-A5 and Tra-D10. Fungal inoculum preparation, inoculation, and disease scoring were conducted as previously described. Three replications were completed for each isolate and the average of the three replications were used for further analysis. This second subset of barley lines was genotyped with Rika, Kombar, and Morex candidate *Spt1* allele specific primers as described above.

Physical positions of markers used in a GWAS using *P. teres* f. *teres* isolates 15A and 6A (Chapter 2) were obtained by using the corresponding marker sequences in BLAST searches of the barley cultivar Morex reference genome v1.0. $-\log_{10}(p)$ values of each marker calculated in the GWAS were plotted by position in the R statistical environment for further analysis.

Phylogenetic Analysis

Exome capture data for 267 barley lines including barley cultivars, landraces, and wild barley accessions was synthesized and utilized by Russell et al. (2016) for SNP identification. The obtained SNP data was filtered for SNPs present in the candidate *Spt1* gene and combined with genotypic data previously obtained from barley cultivars Rika, Kombar and Morex. Heterozygous genotype calls were converted to missing data to conform to software requirements and any lines missing data were removed from the dataset. SNPs were collapsed to form single haplotypes for each accession and utilized for phylogenetic analysis. Data was imported into the software MEGA v7.0.2. Haplotype sequences were aligned via ClustalW and a phylogenetic tree was calculated using maximum-likelihood method with the Tamura 3-parameter nucleotide substitution model. Confidence of the phylogenetic tree was tested with 1000 bootstraps.

BSMV-VIGS

The barley stripe mosaic virus (BSMV) virus induced gene silencing (VIGS) system was utilized to suppress the expression of *Spt1* in barley cultivar Kombar. The tri-partite genome of BSMV was exploited by cloning of a 260 base-pair fragment from the 5' region of *Spt1* into the BSMV γRNA vector (Hein et al. 2005). As the 5' region of *Spt1* is the most diverse among the known alleles, it was targeted to prevent the possibility of cross-suppression of homologous genes. Two primer pairs specific to the target *Spt1* region were designed with *Not*I and *Pac*I adaptor sequences attached to the 5' ends, with one set having a *Not*I forward adaptor and *Pac*I reverse adaptor and the other pair having a *Pac*I forward adaptor and *Not*I reverse adaptor. This primer design facilitated the directional cloning of the target *Spt1* sequence into the BSMV γ infectious cDNA vector clone PSL38.1 in the sense and anti-sense orientations. The infectious

clone pSL38.1 contains an *E. coli* replication high copy origin of replication and ampicillin selection marker. PCR reactions consisted of 2 µL cDNA template, 5 µL 10x GoTaq buffer (1x), 3 µL forward primer (1.20 µM), 3 µL reverse primer (1.20 µM), 0.50 µL dNTPs (200 µM), 0.25 µL GoTaq (1.25 units), and 11.25 µL H_2O. PCR parameters are as follows: initial denaturation at 95 °C for five minutes, 35 cycles of 94 °C for 30 seconds, 62 °C for 30 seconds, and 72 °C for 30 seconds, followed by a final extension at 72 °C for seven minutes. PCR products were visualized on 1% agarose gels containing GelRed (Biotum). PCR amplicons were purified using E.Z.N.A. PCR Purification Kit (Omega-Biotek) according to manufacturer's instructions. Purified PCR reactions and the BSMV γ RNA infectious clone PSL38.1 were used in double digestions reactions consisting of 2 µL PSL38.1 pDNA (55 ng), 1.5 µL of directional Kombar *Spt1* fragment (15 ng), 1 µL NEB Buffer 2.1, 1 µL *Pac*I (NEB), 1 µL *Not*I (NEB), and 3.5 µL H_2O. Digestion reactions were incubated at 37 °C for one hour and heat inactivated at 65 °C for 20 minutes. A ligation master mix consisting of 1 µL of T4 ligase (Promega), 1.5 µL 10x ligation buffer, and 2.5 µL H_2O were added to the digests, mixed thoroughly by pipetting, and incubated at room temperature for two hours. OneShot TOP10 chemically competent *E. coli* cells were transformed with the *Spt1* VIGS fragment-pSL38.1 ligation according to manufacturer's instructions (Invitrogen). A total of 100 µL of each transformation was plated onto Luria broth (LB) agar plates (5 g NaCl, 5 g tryptone, 2.5 g yeast extract, 7.5 g agar, H_2O up to 500 mL) amended with ampicillin (100 µg/mL) and incubated overnight, for approximately 16 hours, at 37 °C. Twelve colonies were selected from each plate and cultured in LB broth (5 g NaCl, 5 g tryptone, 2.5 g yeast extract, H_2O up to 500 mL) amended with ampicillin (100 µg/mL) and incubated overnight at 37 °C and shaking at 230 rpm. Cell cultures were transferred to a 2 mL Eppendorf tube and centrifuged at maximum speed for two minutes. The supernatant was

removed and 400 µL of GTE buffer (50mM glucuose, 25 mM Tris-HCl pH 8.0, 10 mM EDTA pH 8.0, RNase A 100 µg/mL) was added to each sample and mixed thoroughly by pipetting. Following resuspension, 400 µL of NaOH-SDS (0.2 N NaOH, 1% SDS) was added and mixed by inversion, followed by the addition of 400 µL of KOAc (29.5 g KAc, 11.5 mL glacial acetic acid, H_2O up to 100 mL). Samples were mixed by inversion and centrifuged on maximum speed for eight minutes. The supernatant was transferred to a new 1.5 mL tube and 0.6 volumes of isopropanol was added, mixing by inversion. Samples were centrifuged at maximum speed for 10 minutes and the supernatant discarded. The DNA pellet was washed with 1.5 mL of 70% ethanol, briefly centrifuged, and the ethanol discarded. Pellets were dried at room temperature for ~ 15 minutes and resuspended in 50 µL H_2O.

The BSMV tripartite viral RNAs corresponding to the α and ß genomes, and the γ genome containing 260 base pair fragment of the Kombar allele of the candidate *Spt1* cloned in the anti-sense and sense orientation, were synthesized using a modified protocol of the mMESSAGE mMACHINE T7 Transcription Kit (ThermoFisher Scientific). Single in vitro transcription reactions consisted of 80 ng plasmid DNA (α genome, ß genome, or γ genome), 0.25 µL reaction buffer, 1.25 µL nucleotide mix, and 0.25 µL enzyme mix. GP buffer was prepared as follows: 18.77 g glycine, 26.13 g K_2HPO_4 dibasic, and 500 mL H_2O). A total of 20 µL of each the α genome, ß genome, and γ genome were combined with 390 µL FES buffer (100 mL GP buffer, 5 g sodium pyrophosphate decahydrate, 5 g bentonite, 5 g celite, up to 500 mL H_2O) for the viral control inoculum. A total of 20 µL of each the α genome, ß genome, γKD sense, and γKD antisense genome were combined with 370 µL FES buffer for use as the viral knockdown inoculum. Single seeds of barley cultivar Kombar were planted in cone-tainers along with barley cultivar Rika as a susceptible check and grown in a growth chamber at 21 °C with a

12 hour photoperiod for 10 days, until the second leaf was approximately 4 cm long. Plants were heavily misted with H_2O and 5 µL of control, knockdown, and FES buffer was used to inoculate emerging secondary leaves of 40, 40, and 10 Kombar plants, respectively. Individual plants were misted and inoculum applied by gently rubbing leaves with FES buffer containing viral RNA. Inoculated plants were then placed in a mist chamber at 100% humidity for 24 hours and moved to a growth chamber at 21 °C and a 12 hour photoperiod. Viral symptom development was observed approximately 7 days post inoculation. *P. teres* f. *teres* isolates 15A x 6A #20 and 15A x 6A #63, derived from a cross of isolates 6A and 15A and contained the single virulence loci VK1 and VK2, respectively, were used for evaluation lines infected with BSMV in the VIGS assay. Fungal cultures and inoculations were conducted as previously described. Secondary and tertiary leaves were scored on a 1-10 scale (Tekauz 1985) five days post-inoculation.

RNA Extraction, cDNA synthesis, and qPCR

Tissue from Kombar lines inoculated with BSMV knockdown and control viral constructs were collected following inoculation and NFNB disease rating for RNA extractions. Leaf tissue samples were collected from individual plants by excising approximate 4 cm of leaf tissue from the center of the youngest leaf. Six samples were collected from each group of BSMV knockdown and BSMV control, as well as three samples from mock-inoculated plants. Kombar mock-inoculated tissue samples were bulked for RNA extraction while RNA from BSMV inoculated plant samples were isolated separately. Tissue was placed in liquid nitrogen and stored at -80 °C. RNA was extracted using the RNeasy Plant Mini Kit (Qiagen) according to the manufacturer's protocol. Approximately 2 µg of total RNA was used in a 20 µL reaction containing oligo$(dT)_{15}$ primer (0.50 µg), Reaction Buffer (1x), $MgCl_2$ (1.5 mM), PCR nucleotide mix (0.50 mM each dNTP), Recombinant RNasin (20 units), and Reverse Transcriptase using the

GoScript Reverse Transcription System with recommended parameters to synthesize cDNA (Promega). Newly synthesized cDNA samples were diluted by adding 30 µL H_2O.

qPCR was conducted to quantify the amount of candidate *Spt1* silencing in individually scored plants compared to viral and mock inoculated controls. A candidate *Spt1* primer pair specific a 3' portion of the gene not used to develop the BSMV knockdown constructs was used to avoid amplifying the modified viral cDNA from infected samples. The barley *Gapdh* gene (KC661221.1) was used as an internal control to calculate relative gene expression values. qPCR reactions consisted of 2 µL cDNA, forward primer (500 nM), reverse primer (500 nM), and 5 µL SsoAdvanced Universal SYBR Green Supermix (Bio-Rad). At least four biological replications were conducted for BSMV knockdown and BMSV control samples. The bulked Kombar mock inoculated tissue was used as a control. Three technical replicates were conducted for each biological sample. Standards of the *Gapdh* and *Spt1* target sequence were used in the following concentrations: 2 ng, 200 pg, 20 pg, 2 pg, 200 fg, 20 fg, 2 fg, and 200 ag. qPCR was conducted using a CFX96 Real_time System thermalcycler (Bio-Rad) and cycling conditions were as follows: 95 °C for 3 minutes, followed by 40 cycles of 95 °C for 15 seconds, 62 °C for 20 seconds, and 72 °C for 30 seconds. Differential expression was examined by calculating relative expression of each sample compared to the internal control, as described by Wang et al. (2013).

Results

Candidate Gene Identification

Analysis of the syntenous *Spt1* region delimited by high resolution genetic mapping (Richards et al., 2016; Chapter 3) in the annotated *Brachypodium distachyon* genome identified six barley genes with predicted known plant immunity function (Table 4.1). These genes included a leucine-rich repeat (LRR) receptor like kinase (RLK), two LRR-receptor like proteins

(RLPs), a transmembrane receptor, and two wall associated kinases (WAKs). Of the six candidate genes, polymorphism was only identified in the RLP MLOC_59726. Primers designed from barley cultivar Morex sequence did not amplify across the full-length MLOC_59726 gene from Rika or Kombar. However, primers specific to the LRR domain of MLOC_59726, hereafter referred to as the *Spt1* candidate gene (*Spt1.cg*) successfully amplified from Rika and Kombar and were subsequently used for genome walking to obtain the full-length *Spt1.cg* allele sequences.

Table 4.1. Candidate *Spt1* Genes Identified from *Brachypodium distachyon* Synteny.

Brachypodium Gene	Barley Gene	Predicted Function	Polymorphism
Bradi3g48760	MLOC_12033.1	LRR-RLK	None
Bradi3g48770	MLOC_65042.1	LRR-RLP	Exon
Bradi3g48780	MLOC_59726.1	LRR-RLP	None
Bradi3g48890	MLOC_79211.1	Transmembrane Receptor	Intron
Bradi3g49160	MLOC_12685.2	WAK	None
Bradi3g49170	MLOC_52001.2	WAK	None

Genome Walking and Candidate Gene Sequence Comparison

Utilizing a pair of primers specific to the 3' LRR of the *Spt1.cg*, genome walking was initiated to elucidate the full-length genomic DNA sequences from the Rika and Kombar alleles. The Morex allele was predicted to produce a mRNA transcript with a single exon of 1287 nucleotides encoding a predicted protein of 429 amino acids (aa) with a molecular weight of ~47.2 kDa (Fig. 4.1).

The Rika allele consists of a single open reading frame corresponding to 1320 nucleotides predicted to encode a 440 aa protein (~48.4 kDa). Additionally, two independent genome walks in the 3' direction from cultivar Rika yielded two distinct fragments, one containing a 15 base pair insertion in the 3' UTR suggesting two recently duplicated *Spt1.cg* copies, nearly identical except for the small insertion in the 3'UTR. The predicted candidate *Spt1* allele from Kombar consists of a predicted 1314 nucleotide mRNA transcript encode a 435 aa protein (~48.2 kDa). Comparison of the predicted aa sequences of all three known alleles illustrated a high level of N-terminal divergence (Fig. 4.2). However, the C-terminal region, including the LRR domain, remained relatively conserved (Fig 4.2). The aa alignment of the Rika and Kombar alleles revealed 75% aa identity and 82% functional similarity. While alignment of the Rika allele to Morex, revealed 68% aa identity and 78% aa functional similarity. The comparison of the Kombar and Morex candidate *Spt1* alleles showed 66% aa identity and 76% functional similarity.

Fig 4.1. Gene model of candidate *Spt1*. (Top) Genomic DNA. (Middle) Predicted mRNA structure. (Bottom) Protein domain structure, including a predicted N-terminal transmembrane domain (TM) and C-terminal LRR.

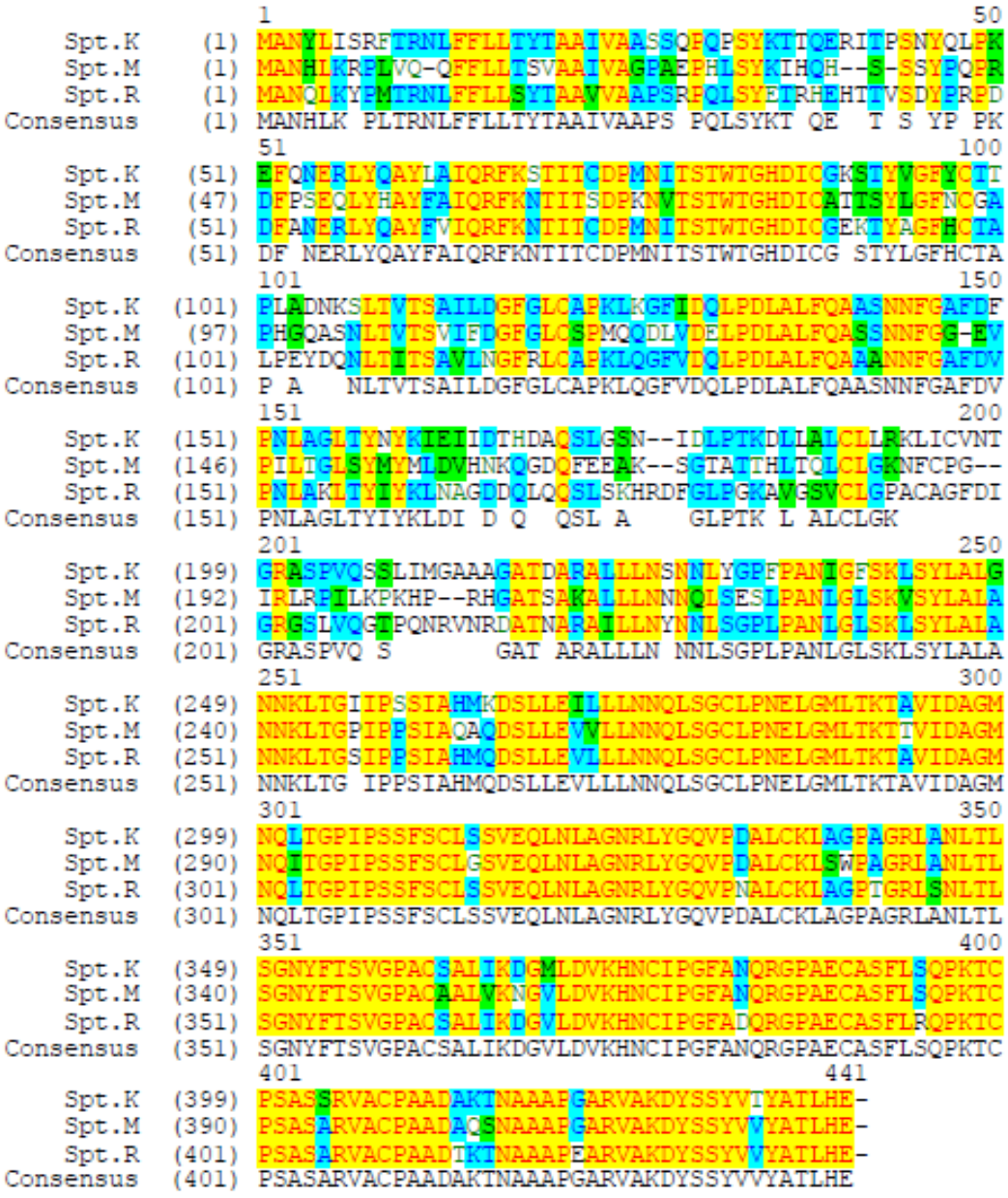

Fig. 4.2. Predicted amino acid alignment of candidate *Spt1* alleles from Rika (*Spt.R*), Kombar (*Spt.K*), and Morex (*Spt.M*).

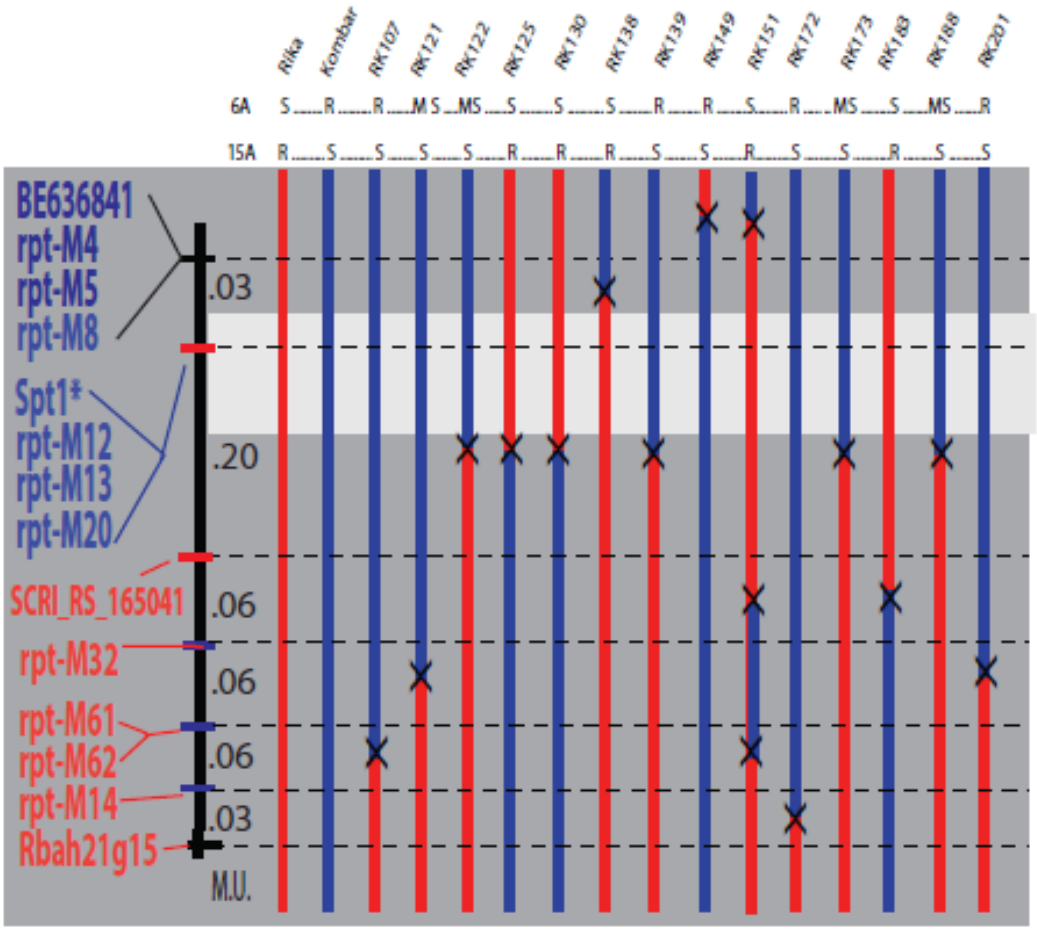

Fig. 4.3. High-resolution map of the *Spt1* locus (light grey shaded area). Individual recombinant lines, including parents Rika and Kombar, are listed at the top of the figure. Below each individual name are the corresponding phenotypes to *P. teres* f. *teres* isolates 6A and 15A: Resistant (R), Moderately Susceptible (MS), and Susceptible (S). Red corresponds to Rika genotype, blue corresponds to Kombar genotype. "X" designates recombination events. Genetic distances are listed as map units to the right of the thick black line. Genetic markers are listed to the left of the thick black line. The "*" designates the marker corresponding to the primary candidate gene.

The fourteen critical Rika x Kombar recombinant lines were genotyped utilizing primer pairs specific to both the Rika and Kombar *Spt1.cg* and the genotyping data was utilized to map the susceptible/resistant phenotypes to isolates 6A and 15A. The high-resolution mapping showed that the respective Rika and Kombar *Spt1.cg* alleles co-segregate with the susceptible phenotype to 6A and 15A, respectively (Fig. 4.3)

Phenotyping

Barley cultivar Steptoe exhibited resistant reactions to both *P. teres* f. *teres* isolates Tra-A5 and Tra-D10 with average scores of 2.25 and 3, respectively (Fig 4.4a). Cultivar Morex was highly susceptible to both isolates, exhibiting scores averages of 8.5 and 9 to isolates Tra-A5 and Tra-D10, respectively (Fig. 4.4b). Average disease ratings of the SM DH individuals inoculated with *P. teres* f. *teres* isolate Tra-A5 ranged from 1.25-9.25 and from 1.33-9 with isolate Tra-D10 (Fig. 4.5).

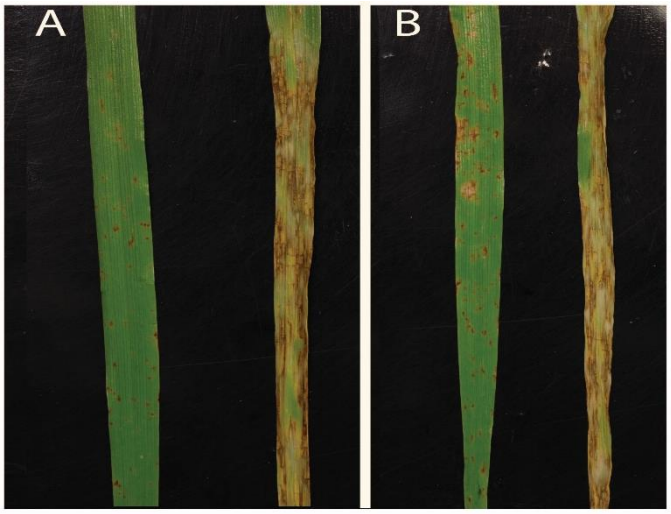

Fig. 4.4. (A) Phenotypic reaction of Steptoe (left) and Morex (right) inoculated with *P. teres* f. *teres* isolate Tra-A5. (B) Phenotypic reaction of Steptoe (left) and Morex (right) inoculated with *P. teres* f. *teres* isolate Tra-D10.

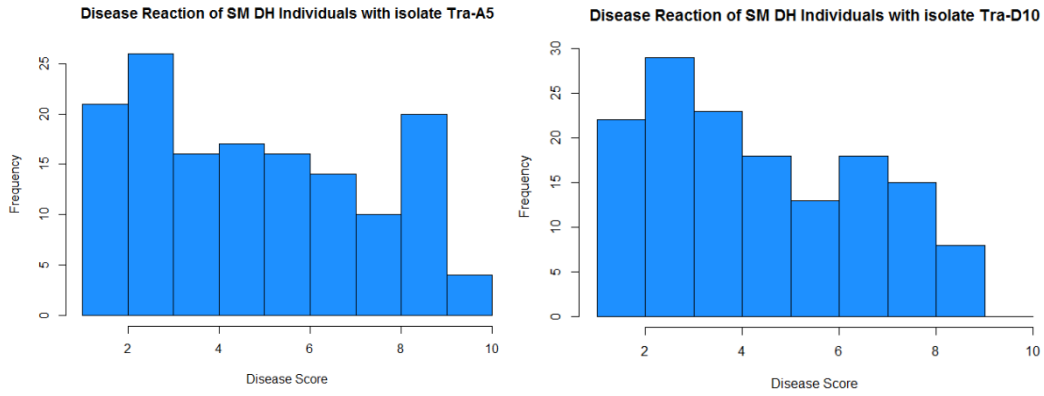

Fig. 4.5. Distribution of Disease Reaction Scores of the SM DH individuals to *P. teres* f. *teres* isolates Tra-A5 (left) and Tra-D10 (right). Disease score is illustrated on the x-axis and frequency is seen on the y-axis.

Linkage Mapping and QTL Analysis

A total of 833 polymorphic SNP markers segregating in a double haploid population derived from a cross of Steptoe x Morex were used to construct a genetic linkage map. The resulting genetic map consisted of seven linkage groups corresponding to each barley chromosome totaling 947.46 cM in size. The size of each linkage group ranged from 93.00 cM (chromosome 6H) to 178.48 cM (chromosome 5H) averaging approximately 119 markers per linkage group. The number of markers mapped to each linkage group ranged from 73 (chromosome 6H) to 158 (chromosome 3H). Following removal of co-segregating markers, 396 markers represented unique loci and are spaced at average intervals of 2.39 cM/marker.

As evidenced by Bartlett's Chi-squared test, the variances between reps of each isolate inoculation were not significantly different (Tra-A5: $\chi^2_{df=1}$=0.472, P=0.49; Tra-D10: $\chi^2_{df=2}$=1.77, P=0.41) and were subsequently combined for QTL analysis. A genome-wide LOD threshold at a significance level of 0.01, calculated by 1000 permutations, was determined to be 4.71 and 4.34 for isolates Tra-A5 and Tra-D10, respectively. For comparison of both isolates, the larger threshold value of 4.71 was used to determine significant QTL common to both isolates. Two

QTL located on chromosome 4H and 6H were identified for susceptibility to both *P. teres* f. *teres* isolates. The major QTL on chromosome 6H is located between SNP markers 12_11140 and 11_10513 with LOD values of 33.60 and 49.8 for isolates Tra-A5 and Tra-D10, respectively (Fig. 4.6).. The QTL interval corresponds to the physical region of 352,363,201-374,876,188 on barley chromosome 6H which spans the physical location of candidate *Spt1* at position 373,417,238. An additional QTL was identified on chromosome 4H between SNP markers 11_20180 and 11_21303 common to both isolates (Fig. 4.6). The 4H QTL had a LOD value of 12.02 and was also identified with isolate Tra-D10, exhibiting a LOD value of 16.96. The two QTL accounted for approximately 65.1% and 77.3% of the overall phenotypic variation for isolates Tra-A5 and Tra-D10, respectively.

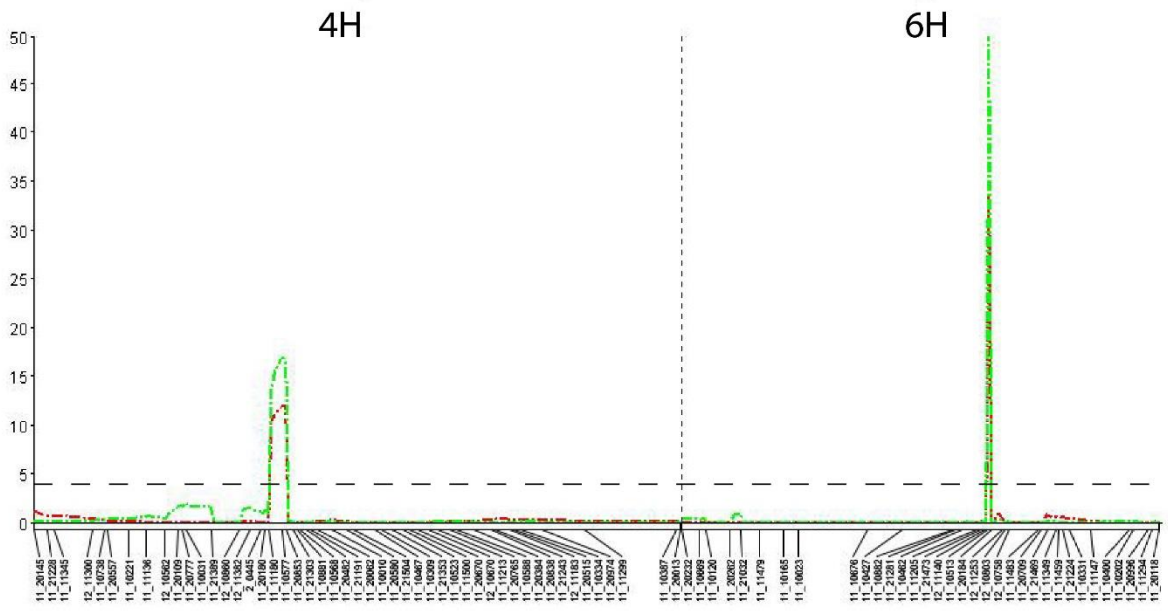

Fig. 4.6. QTL analysis of resistance/susceptibility towards *P. teres* f. *teres* isolates Tra-A5 (red) and Tra-D10 (green) in the SM DH population. Markers are illustrated on the x-axis and LOD values on the y-axis. The dashed line represents the LOD threshold of 4.71 as determined by 1000 permutations.

Allele and Association Analysis

Genotyping of 110 barley lines resulted in the identification of 54 accessions, which harbor a known candidate *Spt1* allele (Rika, Kombar, or Morex) and have been phenotyped with *P. teres* f. *teres* isolates 15A, 6A, Tra-A5, or Tra-D10. Approximately 50.9% of the lines genotyped did not possess a Rika, Kombar, or Morex *Spt1.cg* allele indicating a high level of diversity among this subset of barley lines. Of the 54 lines with a known allele, 13 harbored a Kombar allele, 14 contained a Rika allele, and 27 possessed a Morex allele. Barley lines were scored for disease on a 1-10 scale and an individual score above 5 was considered susceptible and below 5 resistant. In 83.3% of the genotyped lines, the presence of a Rika, Kombar, or Morex allele correlated with susceptibility to *P. teres* f. *teres* isolates 6A, 15A, or Tra-A5/Tra-D10, respectively (Table 4.2).

Significant markers from a previous GWAS (Chapter 2) spanning the *Spt1* region, approximately 370-385 Mb on the barley cultivar reference genome v1.0, were examined at high resolution for determination of proximity to candidate *Spt1*. SNP markers SCRI_RS_176650, the most significantly associated marker to the disease reaction to *P. teres* f. *teres* isolate 15A, and SNP marker SCRI_RS_188243, the second most associated marker to disease reaction to isolate 6A, are both localized to approximately 6 kb downstream of *Spt1.cg* (Fig. 4.6). Due to the significance of these markers near *Spt1.cg* and the rapid decline in significance of flanking markers, high-resolution association analysis conservatively delimits the *Spt1* region to approximately 3.1 Mb of physical sequence, which contains 12 genes, but only the candidate *Spt1.cg* is an immunity related gene with polymorphism between the differential lines.

Table 4.2. Allele analysis of barley lines with candidate *Spt1* allele specific markers.

Line	Allele	15A	6A	TA5	TD10
Hazera	Kombar	5.30	1.50	1.25	1.50
CIho497	Kombar	7.83	1.00	NA	NA
CIho2483	Kombar	6.33	1.33	NA	NA
CIho4159	Kombar	7.33	1.17	NA	NA
CIho10521	Kombar	8.17	1.50	NA	NA
CIho13824	Kombar	7.67	1.67	NA	NA
PI182684	Kombar	8.50	1.50	1.00	3.00
CIho11792	Kombar	1.67	1.33	1.83	1.83
PI157651	Kombar	7.17	2.17	3.50	4.50
PI178594	Kombar	2.67	5.25	3.33	2.67
PI268186	Kombar	3.17	5.83	6.50	6.17
PI327998	Kombar	7.00	3.00	5.50	5.50
PI382275	Kombar	6.83	1.17	1.00	1.00
Morex	Morex	NA	NA	8.00	7.75
Manchuria	Morex	NA	NA	8.00	7.75
Manchurian	Morex	NA	NA	8.00	8.50
CI4922	Morex	NA	NA	7.50	7.25
Robust	Morex	NA	NA	8.25	8.25
Can. Lk. Sh.	Morex	NA	NA	8.00	7.50
Lacey	Morex	NA	NA	7.50	NA
Harbin	Morex	NA	NA	8.25	8.00
Tifang	Morex	NA	NA	7.00	6.25
Ming	Morex	NA	NA	8.00	7.00
Prato	Morex	NA	NA	4.00	3.75
Hector	Morex	7.50	7.75	8.75	8.75
NDB112	Morex	1.25	1.00	4.50	6.75
CIho6510	Morex	1.67	7.17	3.50	6.00
CIho14291	Morex	6.33	2.00	3.50	4.00
PI60663	Morex	7.33	1.33	3.50	2.75
CIho15313	Morex	7.83	6.83	7.67	7.17
PI328327	Morex	5.33	3.50	9.00	7.67
PI349907	Morex	3.33	2.67	8.50	7.83
PI411030	Morex	2.17	6.17	4.50	4.17
PI415348	Morex	3.17	5.67	6.83	6.83
PI415365	Morex	5.50	7.00	7.67	6.83
PI422571	Morex	3.83	2.67	5.17	3.33
PI434760	Morex	2.25	4.00	8.33	7.67

Table 4.2. Allele analysis of barley lines with candidate *Spt1* allele specific markers (continued).

Line	Allele	15A	6A	TA5	TD10
PI467364	Morex	7.17	6.83	8.33	7.50
PI467382	Morex	7.50	6.50	9.33	7.67
PI467737	Morex	2.17	1.67	5.25	2.67
PI197617	Rika	1.83	8.67	NA	NA
PI197622	Rika	3.17	8.83	NA	NA
PI202873	Rika	1.50	8.50	NA	NA
PI262220	Rika	1.33	8.17	NA	NA
PI328950	Rika	1.50	8.33	NA	NA
PI327704	Rika	2.17	7.83	NA	NA
PI330400	Rika	1.67	7.67	NA	NA
PI337142	Rika	1.33	8.50	NA	NA
PI392423	Rika	1.67	7.50	NA	NA
PI40387	Rika	2.00	5.33	7.67	8.17
PI205638	Rika	1.50	2.33	4.83	4.00
PI328855	Rika	1.67	2.00	3.33	2.17
PI467851	Rika	2.67	5.33	7.00	5.67
PI473574	Rika	2.33	7.83	8.17	7.67

*Bold text signifies a lack of correlation between presence of a candidate *Spt1* allele and susceptibility to the corresponding isolate

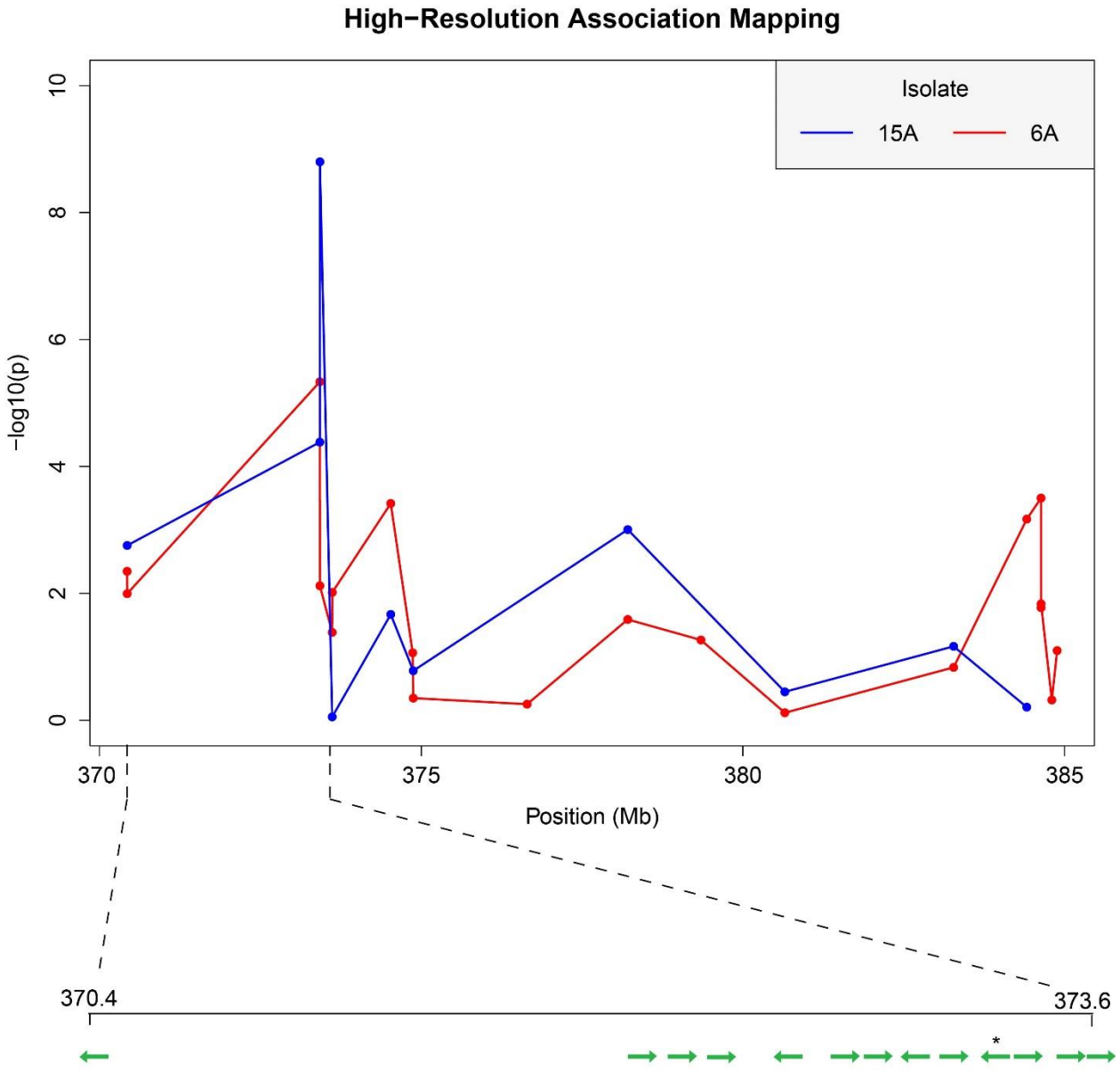

Fig. 4.7. High-resolution association analysis. Physical positions (Mb) are illustrated on the x-axis. Marker significance reported as $-\log_{10}(p)$ is shown on the y-axis. Blue corresponds to isolate 15A, red corresponds to isolate 6A. Green arrows indicate orientation of genes within the region. "*" indicates the position of candidate *Spt1*.

Phylogenetic Analysis

Analysis of SNP data derived from barley exome capture of wild barley accessions, landraces, and cultivars, revealed a total 56 SNPs within a 540 base-pair region of the 3' LRR of *Spt1.cg*. Haplotype analysis of 63 barley accessions containing no missing data at the 56 polymorphic sites within *Spt1.cg* revealed 17 unique haplotypes. Of the 56 variable sites, 42 are polymorphic among the lines with no missing data, indicating a greater haplotype diversity present in the entire collection of 278 lines which may be resolved through further allele sequencing especially if the diversity could be captured at the highly diverse N-terminal region. Phylogenetic analysis resulted in the clustering of barley accessions into 14 clades (Fig. 4.7). Individual clades contained a mixture of wild barley accessions, landraces, and barley cultivars, indicating that the diversification of the *Spt1.cg* had occurred in *Hordeum vulgare* ssp. *spontaneum* natural populations prior to domestication.

BSMV-VIGS

Functional analysis of candidate *Spt1* was attempted through post-transcriptional gene silencing using the BSMV system. Barley cultivar Kombar plants inoculated with BSMV knockdown and control constructs were subsequently phenotyped with two *P. teres* f. *teres* progeny isolates, each possessing a single virulence QTL (VK1 and VK2) derived from isolate 15A. Results indicate no significant difference in phenotypic reaction when comparing the plants inoculated with the knockdown construct to the control (Table 4.3). However, following qPCR analysis, it appears that there was insufficient suppression of candidate *Spt1* expression when compared to the controls and no conclusive conclusions could be made (Table 4.4).

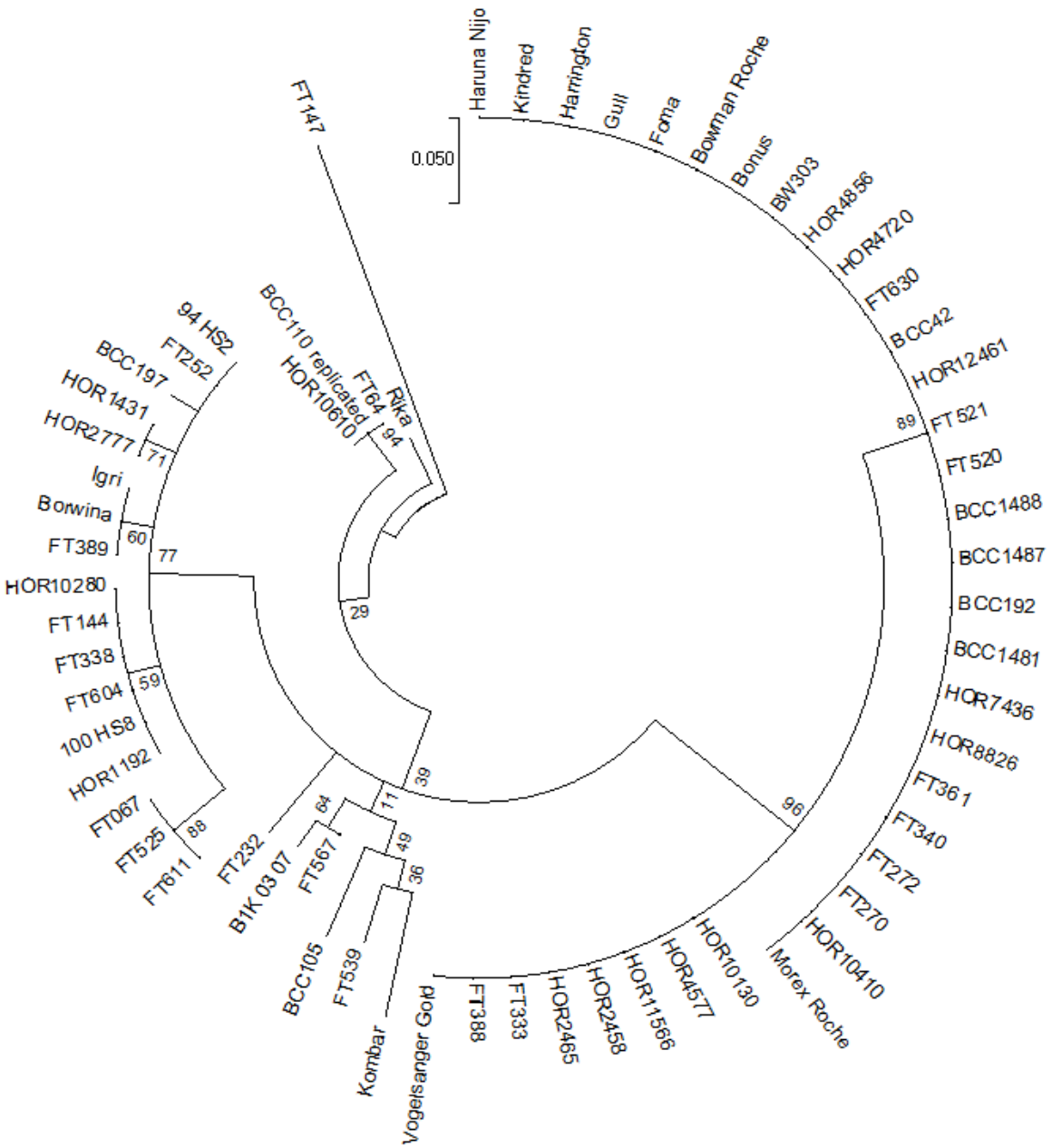

Fig. 4.8. Phylogenetic analysis using 56 SNPs within the 3'-LRR of candidate *Spt1*.

Table 4.3. Phenotypic analysis of BSMV-VIGS plants inoculated with *P. teres* f. *teres* 15A x 6A progeny isolates harboring virulence QTL VK1 and VK2.

Treatment	2nd Leaf (VK1)	3rd Leaf (VK1)	2nd Leaf (VK2)	3rd Leaf (VK2)
Knockdown	5.08 ± 1.67	4.83 ± 1.53	5.21 ± 1.5	4.47 ± 1.23
Control	4 ± 1.08	4.39 ± 1.9	4.33 ± 1.18	3.43 ± 1.35
Kombar WT	4.71 ± 0.95	3.57 ± 0.53	5 ± 0.95	4 ± 0.96
Rika WT	2.43 ± 0.76	2.71 ± 0.83	2.46 ± 0.63	2.68 ± 0.61

Table 4.4. Relative expression levels candidate *Spt1* of BSMV-VIGS plants.

Sample	*Gapdh*[1]	*Spt1*[1]	RE[2]
Knockdown (VK1)	16.65	24.29	0.69
Control (VK1)	16.13	24.25	0.67
Wildtype (VK1)	16.75	23.49	0.71
Knockdown (VK2)	16.71	24.44	0.68
Control (VK2)	17.28	24.71	0.70
Wildtype (VK2)	20.20	25.34	0.80

[1]Average Cq value across all biological and technical replications
[2]Relative expression (RE)

Discussion

This research presents the identification of the predicted membrane-bound receptor-like protein, *Spt1,* that appears to function as a multi-allelic target of *P. teres* f. *teres* NEs for the induction of programmed cell death, resulting in a compatible disease reaction. Analysis of this region in *Brachypodium distachyon* revealed six genes containing predicted functional domains associated with plant disease immunity (Table 4.1). Additionally, utilizing the newly annotated barley reference genome, an additional RLK, HORVU6Hr1G057370.1, was identified in the physical region. On the basis of high-resolution association mapping, the *Spt1* region was conservatively delimited to approximately 3.1 Mb, excluding MLOC_79211.1, MLOC_12685.2, and MLOC_52001.2 from further consideration. Additionally, both MLOC_12685.2 and MLOC_52001.2, both WAKs, did not exhibit observable polymorphism between Rika and Kombar. MLOC_79211.1, however, did contain a SNP, but it was located in an intron, therefore

not affecting structural or functional properties of the protein. Barley gene MLOC_12033.1, an RLK, could not be amplified from Rika or Kombar using primers targeting the full-length gene, as well as small, overlapping gene fragments. This indicates that this gene may be absent from Rika and Kombar or highly diverged. Further characterization of the newly identified RLK, HORVU6Hr1G057370.1, via allele sequencing of Rika and Kombar, will still be necessary to accept or exclude it as a candidate gene.

A homolog of *Spt1*.cg, MLOC_65042.1, is predicted to be within the region based on synteny with *Brachypodium distachyon*. However, sequence of this gene is not anchored to the barley genome. This close relative of candidate *Spt1* likely arose from a tandem duplication event and may be embedded within repetitive elements, hindering its ability to be anchored to the reference genome. This agrees with results from genome walking of candidate *Spt1* in cultivar Rika, where two identical fragments were obtained extending into the 3' UTR, however, one fragment contained a 15 bp insertion, indicating Rika possesses two copies of the gene. These copies at the translated region appear to be identical and were only detected via a small insertion in the 3' UTR. These data suggest that this small gene family represents a very recent duplication event with very little evolutionary time to accumulate mutations in either copy suggesting that both may maintain their original function.

Previously, a Morex x Steptoe DH population was used to map disease reaction to North Dakota isolate *P. teres* f. *teres* isolate ND89-19. Three QTL, one residing near the centromere of chromosome 4H and two near the centromere of chromosome 6H, were identified and designated as resistance QTL (Steffenson et al. 1996). However, the prevalence of inverse gene-for-gene interactions within this pathosystem are becoming more evident (Liu et al. 2015; Richards et al. 2016) and these QTL may in fact correspond to dominant susceptibility genes stemming from

cultivar Morex, rather than resistance from cultivar Steptoe. Due to the lack of high-throughput molecular resources, the QTL identified by Steffenson et al. (1996) are defined by broad intervals, making comparison to more recent findings less conclusive. Results from a QTL analysis conducted with the same population, but with much greater marker density, and two *P. teres* f. *teres* isolates collected from Montana resolved two of the previously identified QTL to higher resolution intervals, one at the centromeric region of 4H and one near the centromere of chromosome 6H (Fig. 4.5). Interestingly, the 6H QTL spans the previously fine-mapped *Spt1* locus, indicating that an allele of the same gene conferring susceptibility to isolates 6A and 15A may be responsible for susceptibility to these isolates as well. Evidence for this hypothesis can be seen via allele analysis of diverse barley lines harboring candidate *Spt1.cg* Rika, Kombar and Morex having high correlation with susceptibility to the corresponding 6A, 15A and TA5/TD10 isolates. These data provide strong evidence towards *Spt1.cg* functioning as a multi-allelic dominant susceptibility factor that is keyed in on or targeted by multiple diverse NEs. Shjerve et al., (2014) showed that in a QTL analysis using a 6A x 15A cross that at least four virulence QTL, two from 6A and two from 15A, targeted the *Spt1.cg* region, suggesting that at least four distinct NEs could be keying in on this susceptibility target that is under a very high level of diversifying selection at its apoplastic N-terminal receptor region. The *Spt1.cg* co-segregated with the susceptible phenotypes to isolates 6A and 15A in a high-resolution Rika x Kombar mapping population which showed two recessive resistance specificities, more appropriately functional dominant susceptibility targets, segregating in near perfect repulsion. Thus, the *Spt1.cg* alleles co-segregate with the previously localized ~0.24 cM susceptibility locus (Richards et al. 2016; Chapter 3). A total of 27 barley lines were identified to harbor a Rika or Kombar allele, which correlated to susceptibility to *P. tere* f. *teres* isolates 6A and 15A in all but

five lines. Additionally, 27 barley lines were identified to possess the Morex candidate *Spt1* allele, of which, 23 lines were susceptible to both or either *P. teres* f. *teres* isolate Tra-A5 or Tra-D10 isolates. The Morex allele was the most prevalent allele observed in lines used for allele analysis, which was also observed when examining the phylogenetic relatedness of the *Spt1* allele of lines used for exome capture (Fig. 4.7). Overall, this high level of correlation indicates the presence of a specific candidate *Spt1* allele facilitating inappropriate perception of the pathogen, resulted in NETS. The few lines that did not fit this correlation can be explained by confounding genetic factors, such as the presence of a resistance, which may override the susceptibility. Previously, a dominant resistance present in barley line CI 5791 was characterized to be highly resistant to nearly all isolates tested and subsequently mapped near the centromere of barley chromosome 6H (Koladia et al. 2016). Additionally, barley cultivar Hector was observed to contain a dominant susceptibility factor, which recognizes the proteinaceous effector PttNE1, leading to susceptibility (Liu et al. 2015). Genetic analysis of F_1 individuals derived from a cross of CI 5791 (broad spectrum resistance) x Hector (dominant susceptibility) resulted in all individuals being resistant. However, F_1 individuals derived from an NDB112 (lacks broad spectrum resistance) x Hector (dominant susceptibility) resulted in all individuals being susceptible (Timothy Friesen, personal communication). This indicates that dominant resistance within this pathosystem may take precedence over dominant susceptibility, possibly due to temporal differences in the initiation of defense related molecular pathways. Additionally, these lines that do not fit the observed correlation require further allele analysis, as the presence of currently unidentified SNPs or small insertions/deletions within the gene coding sequence may result in significant protein function alteration. Functional validation of *Spt1* was attempted through BSMV-VIGS, however, results of the assay were inconclusive. Sufficient levels of gene

knockdown were not observed, indicating a low efficiency of the viral construct. The possibility also exists that this method of gene validation may not be suitable for this particular system. Future directions of further gene validation will be accomplished through CRISPR/CAS9 gene editing and mutant analysis.

The *Spt1* protein appears to have undergone antagonistic forces of selection on two regions of the predicted apoplastic receptor region of the protein. The LRR domain appears to be relatively conserved, undergoing purifying selection, possibly to retain its function as a receptor and recognizing a conserved pathogen associated molecular pattern. However, the N-terminal region, between the predicted transmembrane domain and the LRR, with the exception of several small conserved stretches of amino acids, is highly diverged among the fully sequenced alleles from Rika, Kombar, and Morex (Fig. 4.2). Additionally, results of exome capture sequencing revealed variants detected only within the more conserved LRR domain, indicating a lack of capture due to low homology between the Morex-specific capture target and the highly diversifies N-terminal region in the sampled lines. As observed in the phylogenetic analysis, wild barley accessions did not appear to cluster together, but were interspersed with barley landraces and cultivars indicating that all the identified allelic diversity identified in this study is present in wild barley. This suggests that the allelic diversity captured in domesticated barley was pulled from the wild barley gene pool and that the high level of diversifying selection at the N-terminus of the *Spt1.cg* was due to pathogen imposed selection pressure to avoid detection of diverse NE in the natural ecosystem. Additionally, the subset of wild barley lines used in the exome capture and phylogenetic analysis showed 56 allelic variants in the most conserved LRR region, suggesting if we could analyze the diversity in the N-terminus through further allele sequencing or genome walking, unprecedented levels of divergence within a NE susceptibility target or R-

gene may exist. This would suggest that the molecular arms race between barley and *P. teres* f. *teres* has been ongoing for millenia, yet this gene must have a very important primary function served by the conserved LRR region because it was not lost, but continued to undergo extreme diversification in the N-terminus. However, it must be an important weak link or susceptibility hub as *P. teres* f. *teres* evolved multiple independent NEs to key in on *Spt1* to facilitate disease via NETS.

RLPs have generally been associated with the extracellular perception of non-self by the plant. The proteins LeEIX1 and LeEIX2 in tomato have the ability to recognize xylanase and the CEBiP RLP in rice recognizes chitin, resulting in the initiation of plant defense responses (Ron and Avni 2004; Kaku et al. 2006). This mode of extracellular perception is beneficial to the plant and maintenance of its function would be of its upmost importance. Thus, we hypothesize that the *Spt1.cg* functions as a PAMP-like receptor, conferring broad range resistance to fungal, or possibly other classes of pathogens. Upon *Spt1* recognition of this conserved elicitor molecule, it may transduce signals across the plasma membrane to the cytoplasm via constitutive association to a RLK, as seen in the Cf4/SOBIR1 interaction in tomato (Liebrand 2013). *P. teres* f. *teres* may have evolved NEs which functioned in the manipulation of the N-terminal region of *Spt1*, intentionally inducing a later timed NETS response (Fig. 4.8). This would then place a strong negative selection pressure on this region of the protein, to avoid manipulation by the pathogen. Alternatively, *Spt1* may have had biological functions unrelated to *P. teres* f. *teres*. *Spt1* may have originally developed as a resistance gene towards biotrophic pathogens, effectively initiating ETI. A positive selection may have been placed on the receptor portion of the Spt1 protein to maintain the resistance capability. As previous speculation, *P. teres* f. *teres* has

probably continually evolved new NEs to intentionally trigger the cell death response through *Spt1*, as *Spt1* continually evolves to diversify and break these interactions.

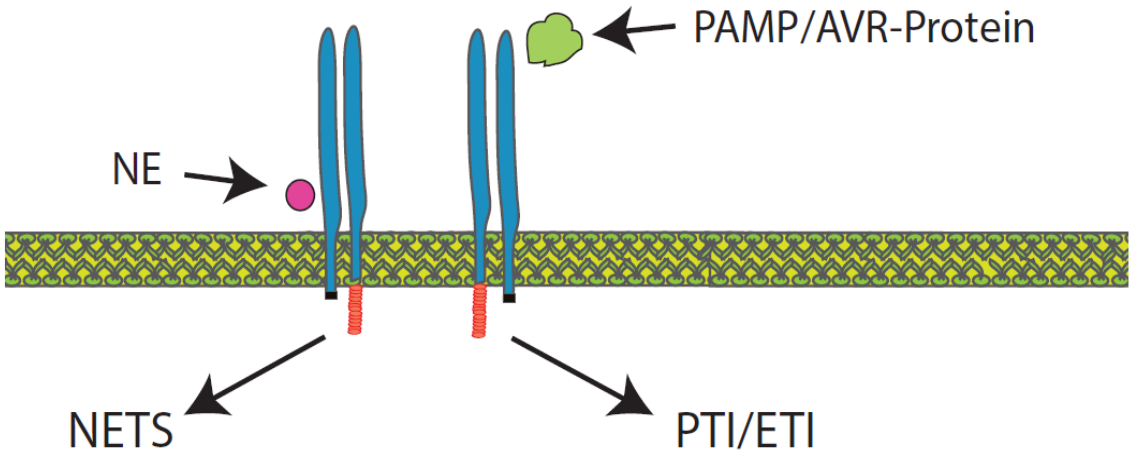

Fig. 4.9. Proposed model illustrating function of *Spt1*. The conserved extracellular C-terminal LRR region of the recognizes a PAMP and signals into the cytoplasm to trigger PTI via association with a RLK (right). Alternatively, the receptor may be under purifying selection to recognize an avirulence protein secreted from a biotrophic pathogen, triggering ETI. *P. teres* f. *teres* evolved NEs to target the diverged extracellular portion of the N-terminal region, intentionally triggering NETs (left). The negative outcome of this interaction places a diversifying selection on the region of the protein, leading to high levels of diversity.

Literature Cited

Abu Qamar, M., Liu, Z. H., Faris, J. D., Chao, S., Edwards, M. C., Lai, Z., Franckowiak, J. D., and Friesen, T. L. 2008. A region of barley chromosome 6H harbors multiple major genes associated with net type net blotch resistance. Theor. Appl. Genet. 117:1261

Cakir, M., Gupta, S., Platz, G. J., Ablett, G. A., Loughman, R., Emebiri, L. C., Poulsen, D., Li, C. D., Lance, R. C. M., Galwey, N. W., Jones, M. G. K., and Appels, R. 2003. Mapping and validation of the genes for resistance to Pyrenophora teres f. teres in barley (Hordeum vulgare L.). Aust. J. Agric. Res. 54:1369-1377

Dodds, P. N., and Rathjen, J. P. 2010. Plant immunity: towards an integrated view of plant-pathogen interactions. Nature Genet. 11:539-548

Dodds, P. N., Lawrence, G. J., Catanzariti, A., The, T., Wang, C. A., Ayliffe, M. A., Kobe, B., and Ellis, J. G. 2006. Direct protein interaction underlies gene-for-gene specificity and coevolution of the flax resistance genes and flax rust avirulence genes. Proc. Natl. Acad. Sci. 103:8888-8893

Emebiri, L. C., Platz, G., and Moody, D. B. 2005. Disease resistance genes in a doubled haploid population of two-rowed barley segregating for malting quality attributes. Aust. J. Agric. Res. 56:49-56

Faris, J. D., Zhang, Z., Lu, H., Lu, S., Reddy, L., Cloutier, S., Fellers, J. P., Meinhardt, S. W., Rasmussen, J. B., Xu, S. S., Oliver, R. P., Simons, K. J., and Friesen, T. L. 2010. A unique wheat disease resistance-like gene governs effector-triggered susceptibility to necrotrophic pathogens. Proc. Natl. Acad. Sci. 107:13544-13549

Flor, H. H. 1956. The Complementary Genic Systems in Flax and Flax Rust. Adv. Genet. 8:29-54

Friesen, T. L., Faris, J. D., Lai, Z., and Steffenson, B. J. 2006. Identification and chromosomal location of major genes for resistance to *Pyrenophora teres* in a doubled-haploid barley population. Genome. 49:855-859

Friesen, T. L., Meinhardt, S. W., and Faris, J. D. 2007. The *Stagonospora nodorum*-wheat pathosystem involves multiple proteinaceous host-selective toxins and corresponding host sensitivity genes that interact in an inverse gene-for-gene manner. Plant J. 51:681-692

Gomez-Gomez, L., and Boller, T. 2002. Flagellin perception: a paradigm for innate immunity. Trends Plant Sci. 7:251-256

Graner, A., Foroughi-wehr, B., and Tekauz, A. 1996. RFLP mapping of a gene in barley conferring resistance to net blotch (*Pyrenophora teres*). Euphytica. 91:229-234

Grewal T. S., Rossnagel B. G., Pozniak C. J., and Scoles G. J. 2008 Mapping quantitative trait loci associated with barley net blotch resistance. Theor Appl Genet 116:529-539

Hein, I., Barciszewska-Pacak, M., Hrubikova, K., Williamson, S., Dinesen, M., Soenderby, I. E., Sundar, S., Jarmolowski, A., Shirasu, K., and Lacomme, C. 2005. Virus-Induced Gene Silencing-Based Functional Characterization of Genes Associated with Powdery Mildew Resistance in Barley. Plant Physiol. 138:2155-2164

Hematy, K., Cherk, C., and Somerville, S. 2009. Host-pathogen warfare at the plant cell wall.

Biotic Inter. 12:406-413

Hoffman, K. and Stoffel, W. 1993. TMbase- A database of membrane spanning proteins segments. Biol. Chem. 374:166

International Barley Genome Sequencing Consortium. 2012. A physical, genetic and functional sequence assembly of the barley genome. Nature. 491:711-716

Joehanes, R. and Nelson, J. C. 2008. Qgene 4.0, an extensible Java QTL-analysis platform. Bioinformatics. 24:2788-2789

Jones, J. D. G., and Dangl, J. L. 2006. The plant immune system. Nature 444:323-329

Kaku, H., Nishizawa, Y., Ishii-Minami, N., Akimoto-Tomiyama, C., Dohmae, N., Takio, K., Minami, E., and Shibuya, N. 2006. Plant cells recognize chitin fragments for defense signaling through a plasma membrane receptor. Proc. Natl. Acad. Sci. 103:11086-11091

Koladia, V. M., Faris, J. D., Richards, J. K., Brueggeman, R. S., Chao, S., and Friesen, T. L. 2016. Genetic analysis of net form net blotch resistance in barley lines CIho 5791 and Tifang against a global collection of *P. teres* f. *teres* isolates. Theor. Appl. Genet. doi:10.1007/s00122-016-2801-4

Liebrand, T. W. H., van den Berg, G. C. M., Zhang, Z,. Smit, P., Cordewener, J. H. G., America, A. H. P., Sklenar, J., Jones, A. M. E., Tameling, W. I. L., Robatek, S., Thomma, B. P. H. J., and Joosten, M. H. A. J. 2013. Proc. Natl. Acad. Sci. 100:10010-10015

Liu, Z., Ellwood, S. R., Oliver, R. P., and Friesen, T. L. 2011. *Pyrenophora teres*: profile of an increasingly damaging barley pathogen. Mol. Plant Pathol. 12:1-19

Liu, Z., Faris, J. D., Edwards, M. C., and Friesen, T. L. 2010. Development of Expressed Sequence Tag (EST)-based Markers for Genomic Analysis of a Barley 6H Region Harboring Multiple Net Form Net Blotch Resistance Genes. Plant Genome. 3:41-52

Liu, Z., Holmes, D. J., Faris, J. D., Chao, S., Brueggeman, R. S., Edwards, M. C., and Friesen, T. L. 2015. Necrotrophic effector-triggered susceptibility (NETS) underlies the barley-*Pyrenophora teres* f. *teres* interaction specific to chromosome 6H. Mol. Plant Pathol. 16:188-200

Lorieux, M. 2012. MapDisto: fast and efficient computation of genetic linkage maps. Mol. Breeding. 30:1231-1235

Ma, Z., Lapitan, N. L. V., and Steffenson, B. 2004. QTL mapping of net blotch resistance genes in a doubled-haploid population of six-rowed barley. Euphytica. 137:291-296

Manninen, O. M., Jalli, M., Kalendar, R., Schulman, A., Afanasenko, O., and Robinson, J. 2006. Mapping of major spot-type and net-type net-blotch resistance genes in the Ethiopian barley line CI 9819. Genome. 49:1564-1571

Manninen, O., Kalendar, R., Robinson, J., and Schulman, A. H. 2000. Application of *BARE*-1 retrotransposon markers to the mapping of a major resistance gene for net blotch in barley. Mol. Gen. Genet. 264:325-334

Martin, R. A. 1985. Disease progression and yield loss in barley associated

Mathre, D. E. 1997. Compendium of Barley Diseases. The American Phytopathological Society. St. Paul

Mayer, K. F. X., Martis, M., Hedley, P. E., Simkova, H., Liu, H., Morris, J. A., Steuernagel, B., Taudien, S., Roessner, S., Gundlach, H., Kubalakova, M., Suchankova, P., Murat, F., Felder, M., Nussbaumer, T., Graner, A., Salse, J., Endo, T., Sakai, H., Tanaka, T., Itoh, T., Sato, K., Platzer, M., Matsumota, T., Scholz, U., Dolezel, J., Waugh, R., and Stein, N. 2011. Unlocking the Barley Genome by Chromosomal and Comparative Genomics. Plant Cell. 23:1249-1263

Mitchell, A., Chang, H., Daugherty, L., Fraser, M., Hunter, S., Lopez, R., McAnulla, C., McMenamin, C., Nuka, G., Pesseat, S., Sangrador-Vegas, A., Scheremetjew, M., Rato, C., Yong, S., Bateman, A., Punta, M., Attwood, T. K., Sigrist, C. J. A., Redaschi, N., Rivoire, C., Xenarios, I., Kahn, D., Guyot, D., Bork, P., Letunic, I., Gough, J., Oates, M., Haft, D., Huang, H., Natale, D. A., Wu, C. H., Orengo, c., Sillitoe, I., Mi, H., Thomas, P. D., and Finn, R. D. 2014. Nucleic Acids Res. Doi: 10.1093/narlgkul1243

Mode, C. J., and Schaller, C. W. 1958. Two Additional Factors for Host Resistance to Net Blotch in Barley. Agron. J. 50:15-18

Muñoz-Amatriaìn, M., Lonardi, S., Luo, M., Madishetty, K., Svensson, J. T., Moscou, M. J., Wanamaker, S., Jiang, T., Kleinhofs, A., Muehlbauer, G. J., Wise, R. P., Stein, N., Ma, Y., Rodriguez, E., Kudrna, D., Bhat, P. R., Chao, S., Condamine, P., Heinen, S., Resnik, J., Wing, R., Witt, H. N., Alpert, M., Beccuti, M., Bozdag, S., Cordero, F., Mirebrahim, H., Ounit, R., Wu, Y., You, F., Zheng, J., Simkova, H., Dolezel, J., Grimwood, J., Schmutz, J., Duma, D., Altschmied, L., Blake, T., Bregitzer, P., Cooper, L., Dilbirligi, M., Falk, A., Feiz, L., Graner, A., Gustafson, P., Hayes, P. M., Lemaux, P., Mammadov, J., and Close, T. J. 2015. Sequencing of 15,6222 gene-bearing BACs clarifies the gene-dense regions of the barley genome. Plant J. 84:216-227

R Core Team. 2016. R: A language and environment for statistical computing. R Foundation for Statistical Computing, Vienna, Austria. https://www.R-project.org/

Raman, H., Platz, G. J., Chalmers, K. J., Raman, R., Read, B. J., Barr, A. R., and Moody, D. B. 2003. Mapping of genomic regions associated with net form of net blotch resistance in barley. Aust. J. Agric. Res. 54:1359-1367

Richards, J., Chao, S., Friesen, T., and Brueggeman, R. 2016. Fine Mapping of the Barley Chromosome 6H Net Form Net Blotch Susceptibility Locus. G3 G3-116

Richter, K., Schondelmaier, J., and Jung, C. 1998. Mapping of quantitative trait loci affecting *Drechslera teres* resistance in barley with molecular markers. Theor. Appl. Genet. 97:1225-1234

Ron, M. and Avndi, A. 2004. The Receptor for the Fungal Elicitor Ethylene-Inducing Xylanse is a Member of a Resistance-Like Gene Family in Tomato. Plant Cell. 16:1604-1615

Russell, J., Mascher, M., Dawson, I. K., Kyriakidis, S., Calixto, C., Freund, F., Bayer, M., Milne, I., Marshall-Griffiths, T., Heinen, S., Hofstad, A., Sharma, R., Himmelbach, A., Knauft, M., van Zonneveld, M., Brown, J. W. S., Schmid, K., Kilian, B., Muehlbauer, G. J., Stein, N., and Waugh, R. 2016. Exome sequencing of geographically diverse barley landraces and wild relatives gives insights into environmental adaptation. Nature Genet. 48:1024-1030

Shjerve, R. A., Faris, J. D., Brueggeman, R. S., Yan, C., Zhu, Y., Koladia, V., and Friesen, T. L. 2014. Evaluation of a *Pyrenophora teres* f. *teres* mapping population reveals multiple independent interactions with a region of barley chromosome 6H. Fungal Genet. Biol. 70:104-112

St. Pierre, S., Gustus, C., Steffenson, B., Dill-Macky, R., and Smith, K. P. 2010. Mapping Net Form Net Blotch and Septoria Speckled Leaf Blotch Resistance Loci in Barley. Phytopathol. 100:80-84

Steffenson, B. J., Hayes, P. M., and Kleinhofs, A. 1996. Genetics of seedling and adult plant resistance to net blotch (*Pyrenophora teres* f. *teres*) and spot blotch (*Cochliobolus sativus*) in barley. Theor. Appl. Genet. 92:552-558

Tans-Kersten, J., Huang, H., and Allen, C. 2001. *Ralstonia solanacearum* Needs Motility for Invasive Virulence on Tomato. J. Bacteriol. 183:3597-3605

Tekauz, A. 1985 A numerical scale to classify reactions of barley to Pyrenophora teres. Can. J. Plant Pathol. 7: 181-183

Thomma, B. P. H. J., Nurnberger, T., and Joosten, M. H. A. J. 2011. Of PAMPs and Effectors: The Blurred PTI-ETI Dichotomy. Plant Cell 23:4-15

Wang, X., Richards, J., Gross, T., Druka, A., Kleinhofs, A., Steffenson, B., Acevedo, M., and Brueggeman, R. 2013. The *rpg4*-Mediated Resistance to Wheat Stem Rust (*Puccinia graminis*) in Barley (*Hordeum vulgare*) Requires *Rpg5*, a Second NBS-LRR Gene, and an Actin Depolymerization Factor. Mol. Plant Microbe In. 26:407-418

Wu, H. L., Steffenson, B. J., Li, Y., Oleson, A. E., and Zhong, S. 2003. Genetic variation for virulence and RFLP markers in *Pyrenophora teres*. Can. J. Plant Pathol. 25:82-90

Yun, S. J., Gyenis, L., Hayes, P. M., Matus, I., Smith, K. P., Steffenson, B. J., and Muehlbauer, G. J. 2005. Quantitative Trait Loci for Multiple Disease Resistance in Wild Barley. Crop Sci. 45:2563-2572

Zipfel, C. 2008. Pattern-recognition receptors in plant innate immunity. Curr. Opin. Immunol. 20:10-16

Zipfel, C. 2009. Early molecular events in PAMP-triggered immunity. Curr. Opin. Plant Biol. 12:414-420

CHAPTER 5. IDENTIFICATION AND VALIDATION OF *RPR2* ACTING AS A KEY COMPONENT OF BASAL RESISTANCE IN *HORDEUM VULGARE*

Abstract

The plant immune system consists of two separate, yet overlapping, pathways. Pathogen associated molecular patterns (PAMPs) are conserved molecules from a pathogen which serve to increase pathogen fitness. Recognition of PAMPs by host receptors results in the activation of a basal defense response and is often effective against a broad range of microbes. The barley *rpr2* mutant was previously characterized to have lost *Rpg1*-mediated stem rust resistance and the mutation was mapped near the centromere of barley chromosome 6H. Additionally, this mutant appears to have a compromised resistance response to the necrotrophic pathogen *P. teres* f. *teres*, indicating a potential role in the basal plant immune response. Here we report on the identification of *Rpr2* via exome capture of barley cultivar Morex and the Morex *rpr2* mutant. Analysis of the exome capture data revealed a predicted protein containing a plant homeodomain finger and fibronectin domains to harbor a 12 base pair deletion, resulting in the loss of four amino acids in a putative phosphorylation block. Based on analysis of barley genome physical sequence and synteny based gene order, this candidate gene is localized to the previously mapped region. We hypothesize that *Rpr2* functions to recognize a spore coat effector protein complex produced by the pathogens *P. teres* f. *teres* and *P. graminis* f. sp. *tritici* to prevent the pathogen effectors from manipulation of *Rpg1*. The spore coat effector complex may have originally functioned to disrupt the plasma-membrane-extracellular matrix interface, allowing the pathogen to create an adhesion pad to facilitate further growth and infection.

Introduction

Plants have evolved an effective immune system consisting of two temporally and spatially distinct yet overlapping layers. The first layer is a basal resistance mechanism that recognizes pathogen associated molecular patterns (PAMPs) via PAMP recognition receptors (PRRs) at the plant cell periphery triggering an early resistance response elicited by a wide taxa of pathogens (Boller and He 2009). PAMPs are conserved motifs in the pathogen that are required for the maintenance of a suitable level of fitness (Zipfel 2008). Common examples of PAMPs include chitin in fungal pathogens, as well as flagella in bacterial pathogens (Gomez-Gomez and Boller 2002; Chinchilla et al. 2006; Zipfel 2014). Often times, these PAMPS are recognized directly by a PRR, which is most commonly a membrane bound receptor-like kinase consisting of an extracellular leucine-rich repeat (LRR) and an intracellular protein kinase signaling domain. Upon recognition by the PRRs, downstream processes such as signaling via mitogen-activated protein kinases (MAPKs), expression of pathogenesis related proteins, occurrence of calcium ion influxes, and the production of reactive oxygen species are triggered, leading to PAMP triggered immunity (PTI) and the successful defense from the pathogen (Jones and Dangl 2006; Zipfel 2008; Zipfel 2009;Boller and He 2009; Dodds and Rathjen 2010; Thomma et al. 2011; Bigeard et al. 2015). Adaptive pathogens counter evolved effectors which act to suppress components of the PTI response typically targeting kinase domains underlying these signaling mechanisms (Jones and Dangl 2006; Boller and He 2009; Dodds and Rathjen 2010). However, in this host-parasite molecular arms race, plant lineages counter-evolved cytoplasmically localized resistance proteins with the capability to recognize the pathogen effectors, eliciting a later higher amplitude programmed cell death response, also known as the hypersensitive response (HR) (Dangl and Jones 2001; Jones and Dangl 2006; Dodds and Rathjen

2010). In respects to a biotrophic pathogen, which requires living host tissue to survive, the cell death caused by the recognition of effectors is often referred to as effector triggered immunity (ETI), due to the successful sequestration of the biotroph by the elimination of its source of nutrients (Jones and Dangl 2006). This resistance response often operates in the classic gene-for-gene paradigm, with a dominant avirulence effector from the biotrophic pathogen being recognized by a dominant resistance gene (*R*-gene) in the host, resulting in an incompatible reaction (Flor 1956). In the flax-flax rust pathosystem, alleles of the dominant R-gene at the L6 locus directly recognize unique avirulence effectors from the flax rust pathogen, resulting in ETI (Dodds et al. 2006). However, necrotrophic pathogens, which complete their life cycle on dead host tissue, evolved effectors to intentionally trigger this defense response. By hijacking this intricate immune system, they successfully provide themselves with a source of nutrients, and is termed necrotrophic effector triggered susceptibility (NETS) (Friesen et al. 2007; Liu et al. 2015). NETS functions within the inverse-gene-for-gene model, where the recognition of a dominant, or functional, necrotrophic effector (NE) protein by a dominant host susceptibility receptor protein typically encoded by a gene with typical R-gene like protein domains results in a compatible reaction or disease phenotype (Friesen et al. 207). In wheat, the host dominant susceptibility factor Tsn1, which contains the typical NBS-LRR and protein kinase R-protein domains, indirectly recognizes the homologous NEs PtrToxA and SnToxA from the necrotrophic pathogens *Pyrenophora tritici-repentis* and *Paratagonospora nodorum*, respectively, activating a high-amplitude hypersensitive response (HR) (Faris et al. 2010; Friesen et al. 2006).

Net form net blotch (NFNB) is an economically important foliar disease of barley present in all major barley production regions of the world and is caused by the necrotrophic specialist fungal pathogen *Pyrenophora teres* f. *teres*. As evidenced by numerous studies on pathogen

virulence patterns (Tekauz and Buchannon 1977; Tekauz 1978; Tekauz 1990; Steffenson and Webster 1992; Wu et al. 2003; Liu et al. 2012; Akhavan et al. 2016) and the genetic mapping of host resistance or susceptibility (reviewed by Liu et al. 2011), the genetic basis of this molecular pathosystem appears exceedingly complex. Several genetic studies have been conducted on both the host and pathogen side to investigate the NETS response that occurs in the *P. teres* f. *teres*-barley dominant susceptibility interactions. Four distinct virulence QTL spread throughout different regions of the *P. teres* f. *teres* genome were identified using a bi-parental pathogen population of *P. teres* f. *teres* isolates 15A x 6A. The distinct, putative NEs underlying these QTL all appear to target the same *Spt1* dominant susceptibility locus that was fine mapped to ~0.24 cM (Richards et al., 2016; chapter 2) and elicit a NETS response (Shjerve et al. 2014; Richards et al. 2016). Additionally, a proteinaceous effector was identified from *P. teres* f. *teres* isolate 0-1 that was found to trigger necrosis, accumulation of reactive oxygen species, and electrolyte leakage, all hallmarks of the HR associated with dominant susceptibility to a necrotrophic pathogen (Liu et al. 2015). Although dominant resistances to *P. teres* f. *teres* have been identified (Koladia et al. 2016), little is known about the molecular mechanisms where a presumed resistance response occurs early in the infection or colonization process.

Puccinia graminis f. sp *tritici* is a biotrophic plant pathogen and the causal agent of wheat stem rust in both wheat and barley. Barley is a host to *P. graminis* f. sp. *tritici* and wheat stem rust caused major epidemics to barley production in the upper Midwestern US prior to the deployment of genetic resistance in both wheat and barley. In wheat, the disease was managed by pyramiding several R-genes, whereas in barley, the single dominant R-gene, *Rpg1*, was deployed in 1942 and has provided durable resistance to a wide range of pathogen races for

greater than 70 years until the emergence of races QCCJ in North Dakota during the 1989 growing season and TTKSK (A.K.A. ug99) in Uganda in 1999 (Steffenson et al. 2009).

The *Rpg1* gene was identified via a mapped-based cloning approach and predicted to encode a novel plant R-protein containing tandem protein kinase domains (Brueggeman et al. 2002). Upon infection by avirulent races of *P. graminis* f. sp. *tritici*, the intracellularly localized RPG1 protein is phosphorylated within five minutes and subsequently degraded after 20 hours, leading to HR (Nirmala et al. 2007; Nirmala et al. 2010). Additionally, two spore coat effector proteins, an arginine-glycine-aspartatic acid (RGD)-binding protein and vacuolar sorting protein (VPS) 9, were identified from *P. graminis* f. sp. *tritici* race MCCF and determined to interact with each other as well as RPG1 (Nirmala et al. 2011). Simultaneous infiltration of both proteins induced RPG1 phosphorylation, degradation, and subsequent HR, as observed with inoculation of MCCF urediniospores. However, treatment of MCCF urediniospores with RGD peptides suppressed spore germination and formation of adhesion pads when in contacts with the barley host, as well as the phosphorylation of RPG1 (Nirmala et al. 2011), but interestingly spores treated with RGD were still able to germinate on water agar.

The barley cultivar Morex gamma irradiated mutant *rpr2* was characterized to have lost *Rpg1*-mediated stem rust resistance but harbored a functional copy of *Rpg1*. Upon inoculation of the Morex *rpr2* mutant with wheat stem rust race HKHJ, normal phosphorylation of RPG1 occurs, however, degradation of the protein occurs at an earlier time point when compared to wild-type Morex (Gill et al. 2016). Recently, the recessive *rpr2* mutation was genetically mapped near the centromere of barley chromosome 6H in a region predicted to contain approximately 157 genes (Gill et al. 2016).

Exome capture allows for the resequencing of the mRNA coding regions of the genome and been used to successfully identify genes underlying genetic disorders in human research (reviewed by Bamshad et al. 2011). Recently, a custom barley exome capture was developed which represents approximately 60 Mb of the barley genome gene space and allows for the rapid and efficient capture of gene sequence from *Hordeum vulgare* as well as other species within the *Hordeum* genus (Mascher et al. 2013). Recently, the utility of the barley exome capture array was seen by the successful identification of the gene underlying the *mnd* mutation conferring a phenotype of rapid leaf emergence (Mascher et al. 2014). In addition to gene identification, it was observed to be a useful tool for the identification of single nucleotide polymorphisms (SNPs) within the coding region of the genome. Variants detected from exome sequence of barley cultivars, landraces, and wild barley accessions have shed light on the evolutionary and domestication history of this crop by the examination of functional intragenic polymorphisms (Mascher et al. 2016; Russell et al. 2016). The utilization of capture technologies has also extended specifically into the realm of plant disease with the development of resistance gene enrichment sequencing (Ren-Seq). As many of the genes implicated in host resistance to phytopathogenic organisms are of the NBS-LRR class, Ren-Seq allows for the specific capture and sequencing of NBS-LRRs for candidate gene identification (Jupe et al. 2013). This methodology has recently been used in conjunction with PacBio SMRT sequencing to rapidly clone the potato late blight resistance gene *Rpi-amr3i* (Witek et al. 2016).

In this study, we have determined that the Morex *rpr2* stem rust mutant has also lost moderate resistance to the necrotrophic specialist *Pyrenophora teres* f. *teres* and through the utilization of a barley exome capture array, have identified a gene containing fibronectin and plant homeodomain (PHD)-finger domains as a strong candidate for the *Rpr2* gene. The results

of this study illustrates the overlap of a basal resistance response to two phylogenetically diverged fungal pathogens, each with a distinct lifestyle.

Materials and Methods

Biological Materials and Phenotyping

Three Morex *rpr2* seeds were sown in a single conetaner. A total of three cones per isolate were placed into a rack surrounded by a border row of barley cultivar Robust. Plants were grown under greenhouse conditions until the second leaf was fully expanded, approximately 14 day old seedlings. *P. teres* f. *teres* isolates 15A (Wu et al. 2003), 6A (Steffenson and Webster 1992), and 0-1 (Weiland et al. 1999) were used to phenotype the *rpr2* mutant. Inoculum was prepared and inoculated as previously described (Friesen et al. 2006). Briefly, dried agar plugs were plated on V8 potato dextrose agar (PDA) plates (150 mL V8 Juice, 10 g Potato Dextrose Agar, 10 g agarose, 3 g $CaCO_3$, and 850 mL H_2O) and incubated in the dark at room temperature for 5 days. The plates were then pl aced under light conditions for 24 hours at room temperature and then moved to the dark at 15 ^oC for an additional 24 hours. Following incubation, the plates were flooded with sterile water and scraped with a sterile inoculation loop. Spore concentrations were adjusted to approximately 2000 spores per mL and one drop of Tween20 was added per 50 mL of inoculum. Plants were spray inoculated and placed into a mist chamber at 100% humidity for approximately 22 hours and subsequently placed into a climate controlled growth chamber at 21 ^oC with a 12 hour photoperiod. Plants were rated 7 days post-inoculation using the 1-10 rating scale developed by Tekauz (1985).

DNA Extraction

Seeds of a Morex *rpr2*/Morex WT $BC_1F_{2:4}$ family were germinated on wet filter paper in glass petri dishes overnight. The embryos were excised and DNA extracted from 4 mature

embryos using PowerPlant Pro DNA isolation kit (MoBio Laboratories, Inc.) according the manufacturer's protocol. DNA was quantified with the Qubit fluorometer (Life Technologies) and visualized on a 1% agarose gel containing GelREd (Biotum) to check the DNA integrity and to get a visual assessment confirming the absence of RNA.

Exome Capture and Sequencing

The Roche Nimblegen SeqCap EZ Developer probe pool design 120426_Barley_BEC_DO4.EZ was used to prepare exome capture libraries of Morex wild-type and a Morex/Morex *rpr2* $BC_1F_{2:4}$ pooled sample. Genomic DNA was randomly sheared in a 20 µL reaction consisting of DNA (~1.2 µg), Fragmentase Reaction Buffer v2 (1x), $MgCl_2$ (10 mM), and dsDNA Fragmentase (New England Biolabs). Digestion reactions were incubated at 37 °C for 15 minutes and subsequently inactivated by adding 5 µL of 0.50 M ethylenediaminetetraacetic acid (EDTA). Fragmented genomic DNA samples were then purified using the AMPure XP purification kit according to manufacturer's instructions (Agencourt). Size distribution of purified fragmented DNA samples were analyzed on an Agilent 2100 Bioanalyzer using an Agilent DNA 1000 kit to confirm the target size range of 180-220 base pairs. End repair, A-Tailing, and ligation of sequencing indexes to the fragmented libraries was completed using the KAPA DNA Library Preparation Kit for Illumina according to the manufacturer's specifications, with minor adjustments. Briefly, an end repair reaction consisting of 50 µL of fragmented DNA, 7 µL 10x end repair buffer, and 5 µL of end repair enzyme mix was incubated at 20 °C for 30 minutes to create 5'-phosphorylated blunt ends of DNA fragments. End repair reactions were purified by adding 120 µL of AMPure XP beads to each reaction and mixing thoroughly, followed by incubation at room temperature for 15 minutes. The bead-bound DNA samples were then placed on a DynaMag-2 magnet (ThermoFisher Scientific) and the clear

supernatant was discarded. Beads were washed with 200 µL of 80% ethanol for 30 seconds while remaining on the magnetic block. The ethanol was discarded and was repeated for a total of two washes. The beads were then dried at room temperature for 5 minutes to remove any residual ethanol. A-tailing reactions were prepared by adding 42 µL H_2O, 5 µL 10x A-Tailing buffer, and 3 µL A-Tailing enzyme to the dried DNA-bound beads and incubated at 30 °C for 30 minutes. Reactions were purified by adding 90 µL of PEG/NaCl solution to each reaction, mixing thoroughly, and incubated at room temperature for 15 minutes. Reactions were then placed on a DynaMag-2 magnet and the clear supernatant was removed. As in the end-repair bead cleanup, two 30 second 80% ethanol washes were conducted and the DNA-bound beads were dried at room temperature for approximately 5 minutes. Ligation reactions were prepared by adding 30 µL H_2O, 10 µL 10x ligation buffer, 5µL DNA ligase, and 5 µL unique adaptor (10 µM) to each bead-bound DNA sample, mixed well, and incubated at 20 °C for 15 minutes. Bead-bound DNA was purified by adding 50 µL of PEG/NaCl solution, incubated at room temperature for 15 minutes, and placed on the magnetic block. Ethanol washes were conducted as in the aforementioned A-Tailing reaction clean-up. DNA was eluted off of the beads by adding 50 µL of elution buffer (10 mM Tris-HCl, pH 8.0). DNA libraries were then size selected for fragments ranging from 250-450 base pairs using a Pippin Prep (Sage Science). Size selected libraries were amplified in 50 µL reactions consisting of 20 µL sample library, 25 µL KAPA HiFi HotStart ReadyMix, and 5 µL Pre LM-PCR Oligos 1 and 2 (5 µM). Cycling parameters are as follows: initial denaturing at 98° C for 45 seconds, followed by seven cycles of 98 °C for 15 seconds, 60 °C for 30 seconds, and 72 °C for 30 seconds, with a final extension at 72 °C for 60 seconds. For purification of PCR reactions, 90 µL of room temperature DNA Purification Beads (SeqCap EZ Pure Capture Kit, Roche Nimblegen) was added to each reaction, vortexed, and incubated at

room temperature for 15 minutes. Following placement on a magnetic block, the supernatant was removed, and washed with ethanol as previously described. The beads were dried at room temperature for approximately 10 minutes and 52 µL of H_2O was added to resuspend the samples. Following a two-minute incubation at room temperature, 50 µL of the supernatant was removed, representing the hybridization ready library. An aliquot of one µL of each library was analyzed on the bioanalyzer as previously described to verify proper library size distribution and to check for the presence of any contaminants. DNA libraries were pooled in equal proportions by mass and was combined with 5 µL COT Human DNA and Multiplex Hybridization Enhancing Oligo Pool (2000 pmol), followed by drying in a DNA vacuum concentrator for approximately 45 minutes on high heat. The dried samples were resuspended in 7.5 µL 2x Hybridization buffer and 3 µL Hybridization Component A (Roche Nimblegen). The resuspended sample was then vortexed, incubated at 95 °C for 10 minutes for DNA denaturation, and combined with 4.5 µL of the 120426_Barley_BEC_DO4.EZ library. The reaction was briefly vortexed, centrifuged, and incubated at 47 °C for 72 hours. Hybridized libraries were washed and captured DNA was bound using the SeqCap EZ Hybridization and Wash Kit according to manufacturer's instructions (Roche Nimblegen). Exome capture libraries were amplified using 20 µL bead-bound capture DNA as template, 50 µL KAPA HiFI HotStart ReadyMix, and 10 µL Post-LM-PCR Oligos 1 and 2 (5 µM). Cycling parameters are as follows: initial denaturing at 98 °C for 45 seconds, followed by 14 cycles of 98 °C for 15 seconds, 60 °C for 30 seconds, and 72 °C for 30 seconds, with a final extension at 72 °C for 60 seconds. PCR reactions were purified using 180 µL of DNA Purification Beads (SeqCap EZ Pure Capture Bead Kit, Roche Nimblegen) as previously described. Concentration, size distribution, and quality were examined using the bioanalyzer, as previously described. Libraries were sequenced on a

single Illumina NextSeq flowcell producing 150 base pair single end reads at the USDA-ARS Cereal Genotyping Laboratory (Fargo, North Dakota).

Bioinformatics

Sequencing reads were aligned to the Morex draft reference genome (IBGSC 2012) using the Burrows-Wheeler aligner 'mem' algorithm with default settings (Li and Durbin 2010). Read depth at each nucleotide position of the exome capture target regions was calculated using SAMtools 'depth' and coverage analysis was conducted in the R Statistical Environment (R Core Team 2016). Variants were detected in SAMtools (Li et al. 2009) using the 'mpileup' command and the output was filtered with VCFtools (Danecek et al. 2011). Parameters used to filter include a genotype quality of >10, read depth of >2, and to only include insertions or deletions. In Microsoft Excel, putative insertions were deleted from the dataset. Variant calls containing missing data or lack polymorphism between the Morex wild-type and Morex *rpr2* mutant pool were excluded from further analysis. Additionally, only variants in which the Morex wild-type sample had a homozygous allele lacking a putative deletion and had an overall variant quality > 100 were retained in the dataset. POPSEQ positions of Morex WGS contigs were obtained from the barley genome database (ftp://ftpmips.helmholtz-muenchen.de/plants/barley/public_data/popseq_IPK/) and used to annotate the variant call data (Mascher et al. 2013). Deletions that mapped to the *rpr2* region between 48-52 cM using the POPSEQ derived genetic positions were considered top priority candidates for further analysis. BAM files from the analysis were imported into CLC Genomics Workbench version 8.0.3 (Qiagen) for the visualization of sequence alignments.

Mutation Validation

To validate the mutation detected in the exome capture analysis, a primer set was developed to genotype Morex wild-type, Morex *rpr2* mutant, and Morex *rpr2*/Morex $BC_1F_{2:4}$ individuals. Primers Rpr2.cg1 F1 (5'-TCCAGCATTCTCTGCTTAGATAGTC-3') and Rpr2.cg1 Del R1 (5'-CTCCTGACAAACTACAGTCATGGAG-3') act as a dominant marker by amplifying a 109 base pair fragment from wild-type Morex, but fail to amplify from mutant lines due to the 3' end of the Rpr2.cg1 Del R1 oligo being specific to the 12 base pair deletion discovered via exome capture. Cycling parameters used are as follows: 95 °C for 5 minutes, followed by 35 cycles of 94 °C for 30 seconds, 62 °C for 30 seconds, and 72 °C for 30 seconds, followed by a final extension of 72 °C for 7 minutes. PCR amplicons were visualized on a 1% agarose gel with GelRed (Biotum).

Candidate Gene and Putative Effector Analysis

Primer sequence of the flanking markers of the previously mapped *rpr2* region (Contig2884_at and GMS006) and the candidate *Rpr2* gene were used in BLAST searches of the pre-publication barley reference genome sequence to obtain physical coordinates. Additionally, a synteny derived position was obtained via the barley genome zipper (Mayer et al. 2011) for comparison to the previously mapped *rpr2* region. The predicted amino acid structure of the candidate *Rpr2* was input into TMHMM (Moller et al. 2001) and Interpro (Mitchell et al. 2015) to predict the presence of transmembrane and functional domains, respectively. Additionally, the predicted amino acid sequence was analyzed with cNLS Mapper (Kosugi et al. 2009) and NetPhos 3.1 (Blom et al. 1999) to determine the presence of a nuclear localization signal or putative phosphorylation sites, respectively.

Amino acid sequence of candidate effectors from *P. graminis* f. sp. *tritici*, RGD-binding protein (AEN84768.1) and VPS9 (AEN84769.1) were used in BLAST searches of the *P. teres* f. *teres* protein database to identify putative homologs (Nirmala et al. 2011). Protein sequence of *Arabidopsis thaliana* protein NDR1 (OAP02983.1) was used in a BLAST search of the annotated barley protein database (http://webblast.ipk-gatersleben.de/barley/viroblast.php) to identify potential homologs and corresponding genomic coordinates.

Results

Phenotyping

Phenotyping of the Morex *rpr2* mutant with *P. teres* f. *teres* isolates 6A, 15A, and 0-1, indicate a loss of moderate NFNB resistance (Fig. 5.1).

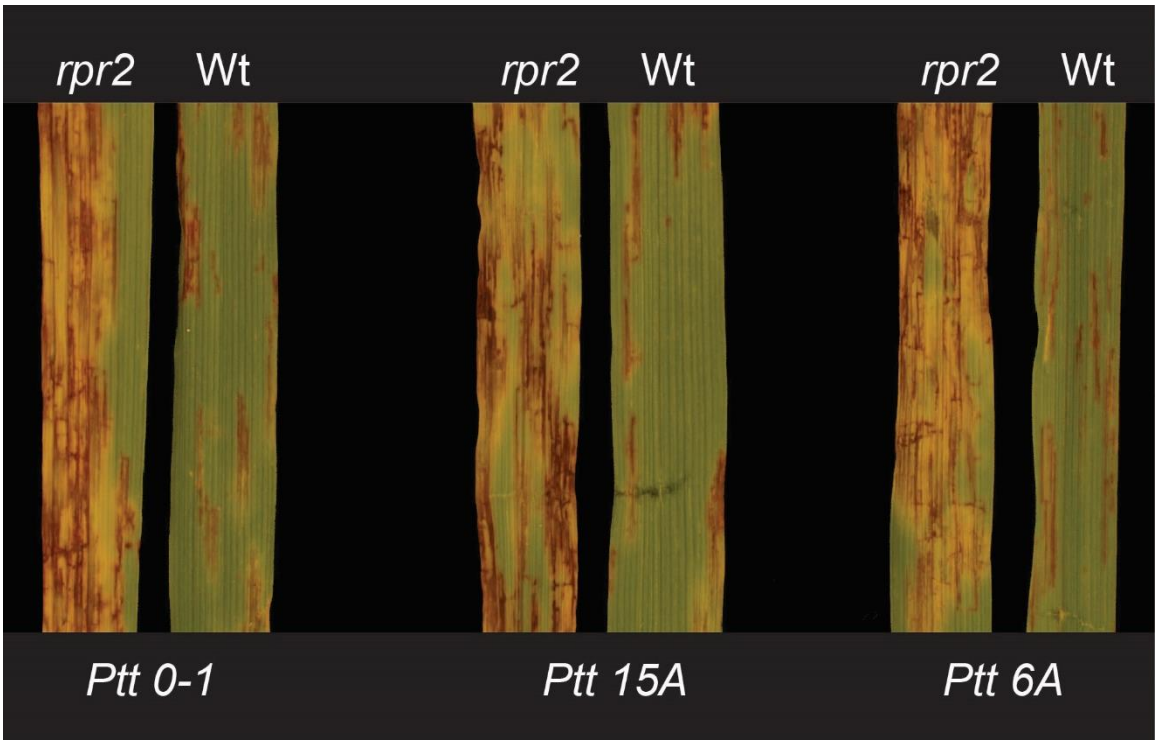

Fig. 5.1. Phenotypic reaction of Morex wild-type and Morex *rpr2* mutant inoculated with *P. teres* f. *teres* isolates 0-1, 15A, and 6A.

Sequencing and Bioinformatics

Sequencing of the Morex wild-type and Morex/Morex *rpr2* $BC_1F_{2:4}$ pool resulted in a total of 151,480,838 and 127,843,546 reads, respectively. Approximately 98.52% and 98.77% of the Morex wild-type and Morex/Morex *rpr2* $BC_1F_{2:4}$ pooled reads, respectively, successfully mapped to the Morex draft genome sequence. Coverage of the Morex wild-type sample ranged from 53.40 Mb at 1x coverage to 40.82 Mb at 50x coverage of the Morex draft genome anchored exome capture targets, representing 95.9% and 73.3%, of the targeted regions, respectively (Fig. 5.2). The Morex *rpr2*/Morex $BC_1F_{2:4}$ sample had coverage levels ranging from 53.38 Mb at 1x coverage to 37.30 Mb at 50x coverage, representing 95.8% and 67.00% of the targeted capture space, respectively (Fig. 4.2).

Upon filtering the identified exome capture variants by the aforementioned parameters, a total of 38 deletions were detected in either a homozygous or heterozygous state. Only a single gene, MLOC_66063.2, fell between POPSEQ positions 48 cM and 52 cM on barley chromosome 6H. As the use of POPSEQ positions were a conservative estimate for the *rpr2* interval, physical coordinates of the region were obtained for comparison of physical position of the candidate gene and the previously mapped region. The previously mapped *rpr2* physical genomic coordinates delimit the region to ~43 Mb between positions 70.35-113.63 Mb on chromosome 6H and between loci 331 and 488 of the putative barley gene order based on synteny analyses (Mayer et al. 2011). BLAST searches of MLOC_66063.2 reveal a genomic location on chromosome 6H at ~72.97 Mb and locus 337 of the genome zipper, indicating that it is localized in the previously mapped region.

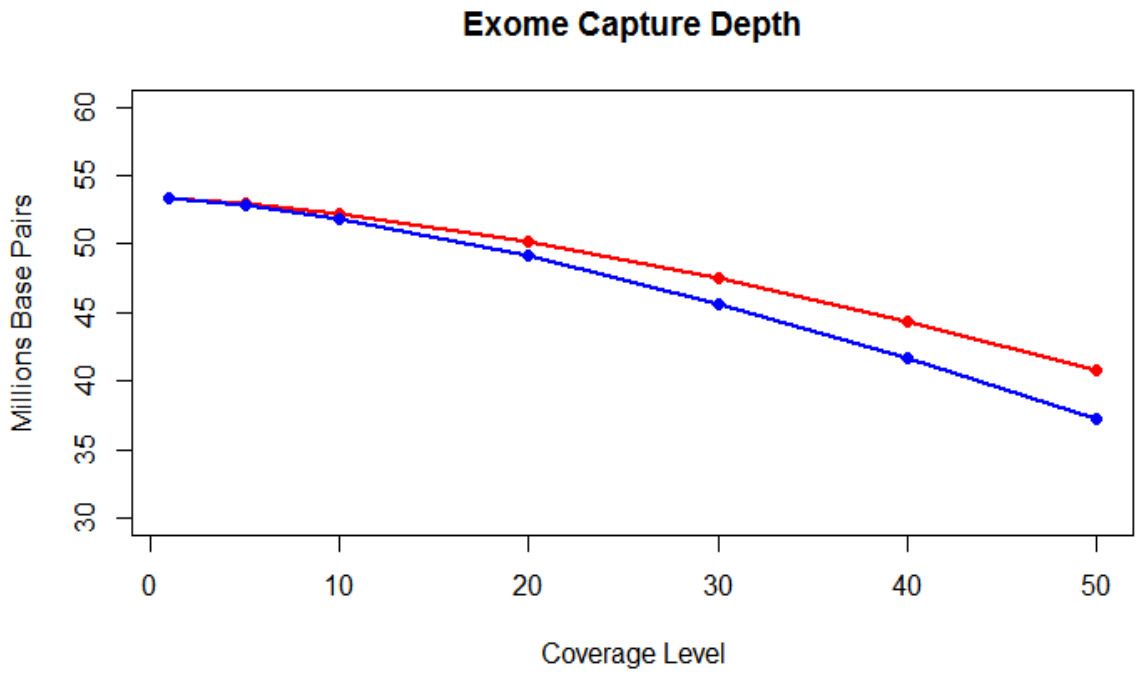

Fig. 5.2. Coverage level of exome capture target regions which were anchored to the draft genome sequence of barley cultivar Morex. Level of coverage in reads per base pair is shown on the x-axis and amount of sequence covered at specified level is shown on the y-axis. Coverage of the Morex wild-type sample is illustrated by the red line and the Morex *rpr2* $BC_1F_{2:4}$ pooled sample is shown by the blue line.

Candidate Gene Analysis

Variant analysis of the exome capture libraries discovered a 12 base pair deletion in barley gene MLOC_66063.2 of the Morex *rpr2* $BC_1F_{2:4}$ pooled sample (Fig. 4.3). The deletion was present in a heterozygous state due to erroneous phenotyping while selecting a susceptible BC_1F_2 line. PCR conducted with a primer pair specific to the deleted gene sequence on Morex wild-type, Morex *rpr2*, and 12 Morex *rpr2*/Morex $BC_1F_{2:4}$ DNA samples revealed the mutation to be present in the original Morex *rpr2* mutant and in two $BC_1F_{2:4}$ lines, indicating a real mutation which is segregating in an expected 3 wild-type : 1 mutant ratio (Fig. 5.4).

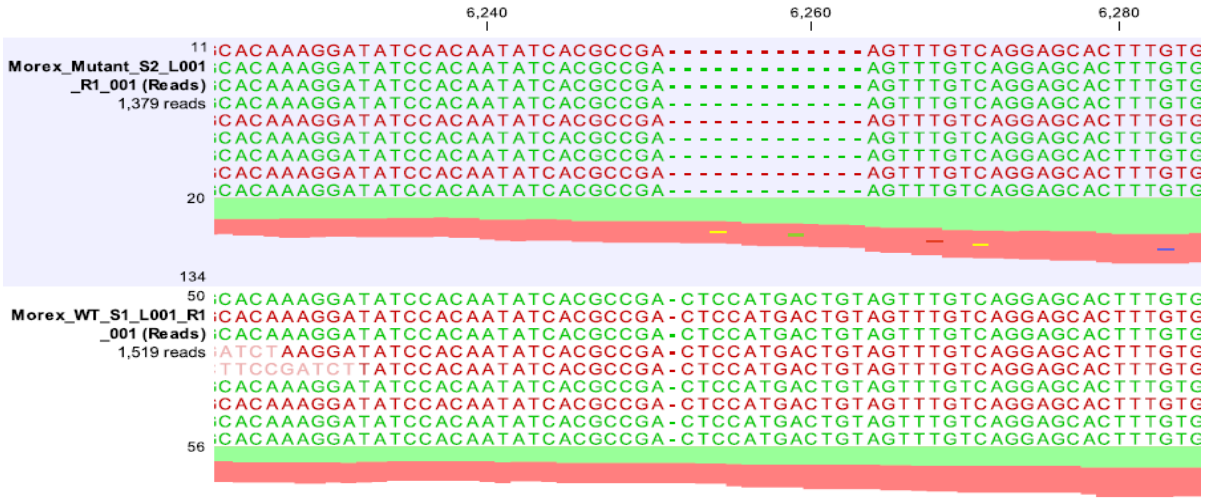

Fig. 5.3. Sequencing alignment of reads mapping to MLOC_66063.2 of the Morex *rpr2*/Morex $BC_1F_{2:4}$ sample (top frame) and Morex wild-type sample (bottom frame).

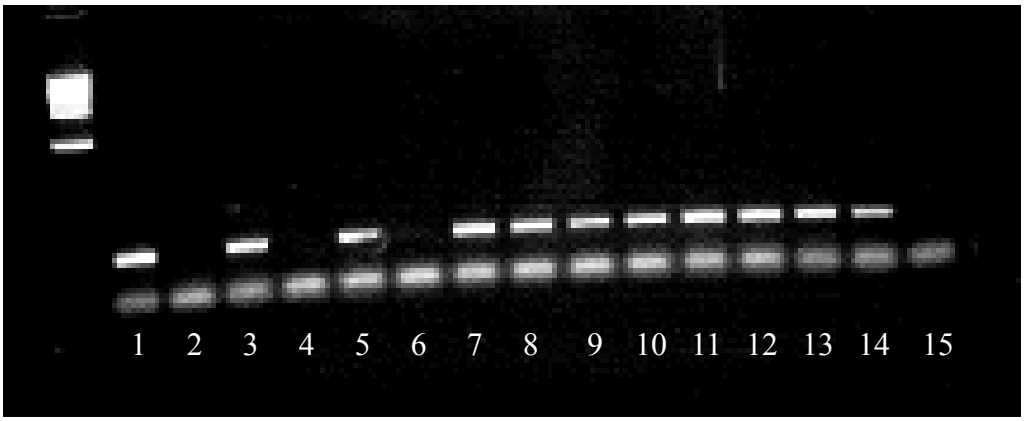

Fig. 5.4. Genotyping of Morex wild-type (1), Morex *rpr2* mutant (2), Morex *rpr2*/Morex $BC_1F_{2:4}$ individuals (3-14), and a non-template control (15) with a primer pair specific to the 12 base pair deletion within MLOC_66063.2.

MLOC_66063.2 is a 4380 base pair gene encoding an mRNA transcript consisting of 4 exons, 2253 nucleotides of coding sequence, and predicted to encode a protein of 750 amino acids containing a PHD-finger and a fibronectin type III (FN3) domain (Fig. 5.5). This gene appears to be a homolog of Arabidopsis protein VERNIALIZATION INSENSITIVE 3 (VIN3).

It is not predicted to contain a transmembrane domain but is predicted to possess a monopartite nuclear localization signal corresponding to amino acid sequence YPAKRQRKS, beginning at amino acid position 106. The 12 base pair deletion in Morex *rpr2* causes a four amino acid deletion (QSWS) at positions 42-45, which is situated in a putative phosphorylation block.

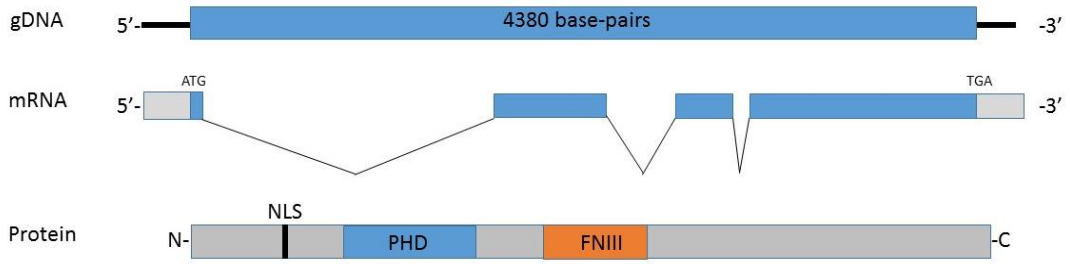

Fig. 5.5. Gene model illustrating the genomic DNA sequence (top), mRNA structure (middle), and protein structure including a predicted nuclear localization signal (NLS), plant homeodomain finger (PHD), and fibronectin III (FNIII) domain. (bottom).

BLASTP searches of the non-redundant protein sequence database of *P. teres* f. *teres* isolate 0-1 with the amino acid sequence of RGD-binding protein and VPS9 from *P. graminis* f. sp. *tritici* confirmed the existence of *P. teres* f. *teres* proteins with homologous domains to those of RGD-binding protein and VPS9. Similar to the RGD-binding protein of *P. graminis* f. sp. *tritici*, protein PTT_14255 of *P. teres* f. *teres* contains an N-terminal dimerization domain, a BRCA1 C Terminal (BRCT) domain, and a fibronectin type III domain. Additionally, *P. teres* f. *teres* protein PTT_00152 harbors coupling of ubiquitin to endoplasmic reticulum degradation (CUE) and VPS9 domains, indicating that functional homologs of the aforementioned *P. graminis* f. sp. *tritici* proteins are present in the *P. teres* f. *teres* proteome. BLASTP searches of the barley protein database using Arabidopsis NDR1 amino acid sequence as a query identified an NDR1 homolog (MLOC_54013.1), designated HvNDR1, located in the centromeric region of barley chromosome 2H at ~57.4 cM.

Discussion

Eukaryotic organisms rely on integral communication processes to perceive their environment and relay messages into the cell. In mammalian systems, integrin proteins are a key component in the interface between the extracellular matrix components (ECM), such as fibronectin, and the cytoskeleton. These proteins aid in the formation of protein complexes known as focal adhesions and act as connective features of the actin cytoskeleton and the ECM. Additionally, signaling molecules are recruited to focal adhesions and serve as important constituents of signal transduction pathways (van der Flier and Sonnenberg 2001). A specific RGD motif constitutes the basis of integrin-mediated recognition of ECM proteins, the disruption of which comprises the integrity of plasma membrane-ECM adherence (Canut et al. 1998). This disruption can be observed by inhibition of integrin-fibronectin binding in eukaryotic cells following treatment of a synthetic RGD peptide (Haas and Plow 1994).

Although integrins do not exist in plant species, an Arabidopsis protein, NDR1, was identified by homology modeling to possess structural similarities to mammalian integrins. NDR1 harbors an NGD motif required to localize between the plant cell wall and the plasma membrane and is also predicted to be critical for the binding of extracellular matrix components, including fibronectin (Knepper et al. 2011b). Both NDR1 mutants and Arabidopsis plants treated with a synthetic NGD peptide exhibited severely decreased plasma membrane-cell wall adherence. Previous research has indicated that a compromised plasma membrane-cell wall interface facilitates pathogen penetration and the maintenance of this adherence correlates with an increase of defense responses (Mellersh and Heath 2001; Underwood 2012). Interestingly, NDR1 has been implicated in both ETI and PTI host immune responses. NDR1 was observed to interact with Arabidopsis protein RIN4, which also interacts with *P. syringae* resistance protein

RPS2. Under wild-type conditions in the presence of resistance gene RPS2, RIN4 is cleaved by AvrRpt2, resulting in the induction of a programmed cell death pathway. However, when the NDR1-RIN4 interaction is disrupted, susceptibility is enhanced indicating the requirement of NDR1 in RPS2 mediated *P. syingae* ETI (Day et al. 2006). In addition to its contribution to ETI, loss of function NDR1 mutants were seen to be deficient in the induction of mitogen activated protein kinase (MAPK) cascades following treatment of well-characterized PAMP flg22, indicating a role in the early defense response associated with PTI (Knepper et al. 2011a). These results demonstrate a significant role of NDR1 in both the structure of the plasma membrane-cell wall interface, as well as its function in plant immunity as it relates to plant cell structural integrity.

Utilizing a forward genetics approach, the *Rpr2* gene required for basal resistance to two phylogenetically distinct plant pathogens was identified via exome sequencing of barley cultivar Morex and the respective *rpr2* mutant. Bioinformatic analysis revealed barley gene MLOC_66063.2, harboring a fibronectin III and PHD-finger domains, to contain a 12 base pair deletion resulting in the loss of amino acid residues QSWS comprising a putative phosphorylation block. Under our current hypothesis, *Rpr2* acts as a cytoplasmic receptor of conserved spore coat proteins from *P. teres* f. *teres* and *P. graminis* f. sp. *tritici* following recognition of a spore coat protein by HvNDR1 and endocytosis to the interior of the cell (Fig. 5.6).

P. graminis f. sp. *tritici* race MCCF is avirulent on barley lines harboring dominant resistance gene *Rpg1*. Previous research demonstrated that urediniospores of race MCCF treated with an RGD-peptide were unable to form an adhesion pad, germinate on the leaf surface and induce HR (Nirmala et al. 2011). Affinity chromatography utilizing a sepharose RGD peptide

column resulted in the retention of two spore proteins, that were identified as an RGD-binding protein and VPS9 protein via mass spectrometry. The proteins were expressed in Pichia and purified, determined to interact via yeast two hybrid, and shown to induce RPG1 phosphorylation and degradation followed by the HR response when simultaneously infiltrated. Infiltration of RGD-binding protein alone elicited RPG1 phosphorylation but no HR occurred, and VPS9 did not induce any observable responses (Nirmala et al. 2011). These results indicate that RGD-binding protein alone possesses the ability to trigger RPG1 phosphorylation, but the addition of VPS9 is required for induction of HR. Additionally, the results also suggest an RGD peptide binding affinity of one or both spore coat proteins. RGD-binding protein harbors a fibronectin domain, which is involved in binding proteins with an RGD or RGD derivative motif, such as an NGD or RLD sequence (Knepper et al. 2011b; Ruoslahti 1996). As proteins with homologous domains are present in the *P. teres* f. *teres* proteome, we speculate that a molecular progenitor of RGD-binding protein existed in an ancestral organism, which served to alter the connection between the plant cell plasma membrane and the ECM, allowing for adhesion to the host tissue. However, the host counter-evolved a signaling mechanism to combat the cellular manipulation by the pathogen by triggering HR. Previous research has shown that RIN4 acts as a hub for cellular processes such as stomatal opening (Liu et al. 2009) and pathogen-induced defense responses (Mackey et al. 2002), as well as association with NDR1 in Arabidopsis (Knepper et al. 2011). Additionally, it was demonstrated that RPG1 directly interacts with the barley homolog of RIN4 (Gill et al. 2012). We propose that upon pathogen induced disruption of the plasma membrane-ECM adherence via RGD-binding protein, NDR1 rapidly signals to the cytoplasmically localized HvRIN4 via direct association to phosphorylate RPG1, triggering HR and pathogen sequestration. However, now being unable to proliferate, a selection pressure

placed upon the pathogen to suppress this newly formed defense response. Previous research has indicated that VPS9 homolog from yeast, also containing a CUE domain, functions in the endocytic and intramolecular monoubiquitination pathway (Hicke and Dunn 2003; Shih et al. 2003). Monoubiquitination is involved in various protein regulatory processes, including membrane transport and degradation (Hicke 2001; Boutet et al. 2007). The fibronectin domain of RGD-binding protein may be responsible for the binding of VPS9 via the recognition of the VPS9 RLD motif and the complex subsequently endocytosed via functional activity of the CUE/VPS9 domains of VPS9 (Shih et al. 2003). As both RGD-binding protein and VPS9 have been seen to directly interact with RPG1, following endocytosis, the RGD-binding protein/VPS9 complex may target RPG1 for post-translational modification or subcellular trafficking for early degradation in the absence of RPR2, essentially suppressing HR. Timing of degradation appears to be essential for proper induction of *Rpg1*-mediated resistance. RPG1 was observed to not fully degrade in a barley line Golden Promise transformant containing multiple copies of *Rpg1*, resulting in a failed induction of HR (Chai et al. 2012). Additionally, RPG1 appears to be degraded at an earlier time point in the Morex *rpr2* mutant when compared to Morex wild-type and other non-allelic mutants (Gill et al. 2016). Early degradation of RPG1 may be initiated by intramolecular monoubiquitination by the RGD-binding/VPS9 complex following association with RPG1, essentially suppressing the basal programmed cell death response. Treatment of urediniospores with a synthetic RGD peptide would theoretically block the binding site of RGD-binding protein and suppress its ability to bind to HvNDR1 and VPS9 through competitive inhibition, thereby eliminating its ability to disrupt the plasma membrane-ECM adhesion and be endocytosed with VPS9.

RPR2 may have evolved to intercept the RGD-binding/VPS9 protein complex to prevent modification of RPG1. The four amino acid deletion in RPR2 may have altered its protein conformation and ability to bind the effector complex. Alternatively, a subsequent signaling event by RPR2 may be needed following perception of the effector complex which is compromised by the deletion within a putative phosphorylation block (Fig. 5.6).

This research has identified *Rpr2* as a key component of a basal resistance pathway to two diverse pathogens. Evolutionarily, the pathogen may have evolved to become pathogenic on a non-host plant via successful disruption of the ECM-plasma membrane interface by the deployment of an RGD-binding protein, essentially creating an environment suitable for infection by associating with HvNDR1. By interference with the constitution of the ECM-plasma membrane connection, the pathogen may then adhere to the plant tissue, an indispensable requirement for pathogenicity. Current research is being conducted on testing the putative interactions between the spore coat effector proteins and RPR2. Additionally, subcellular localization and effects of post-transcriptional gene silencing of RPR2 will be studied to further elucidate its role in an early and integral plant disease resistance molecular pathway.

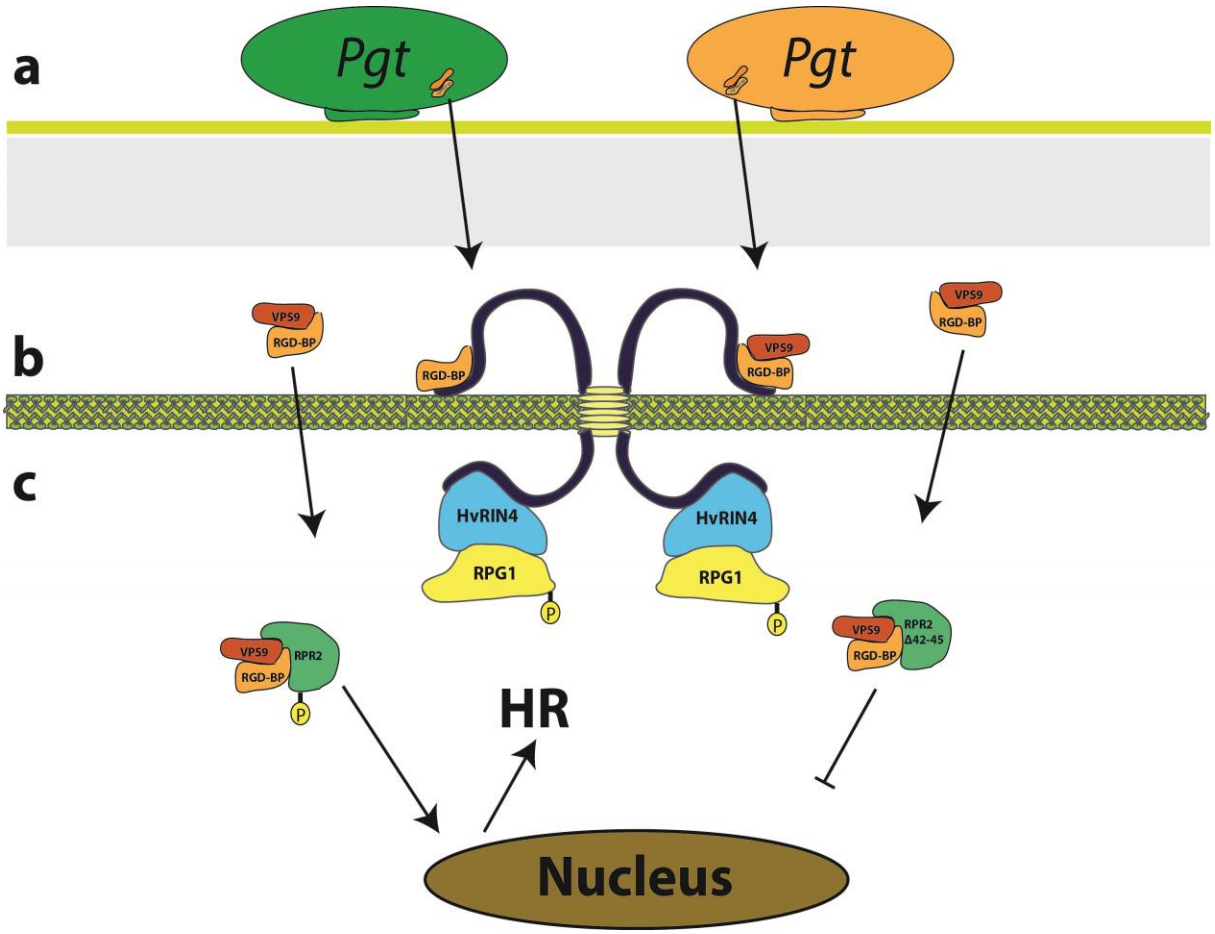

Fig. 5.6. Proposed model of the function of RPR2. (a) Spores of *P. teres* f. *teres* and *P. graminis* f. sp. *tritici* land on the plant cell surface and produce spore coat effector proteins RGD-binding protein and VPS9. (b) RGD-binding protein interacts with HvNDR1, either alone or along with VPS9. The pathogen may have evolved this interaction to disrupt the plasma membrane-ECM interface, allowing for the development of an adherence pad. NDR1 signals interior to the cell via RIN4 to phosphorylate RPG1 in response to pathogen adherence. (c) In the wild-type plant (left) RPR2 intercepts the complex of RGD-binding protein/VPS9, preventing manipulation of RPG1 and ensuring continuance of the defense response. Alternatively, RPR2 may localize to the nucleus, triggering components required for the defense response. In the mutant plant (right), the mutation in RPR2 may lose the ability to bind the spore coat effectors. Alternatively, the mutation may compromise the ability to localize to the nucleus or transmit signals via phosphorylation.

Literature Cited

Akhavan, A., Turkington, T. K., Askarian, H., Tekauz, A., Xi, K., Tucker, J. R., Kutcher, H. R., and Strelkov, S. E. 2016. Can. J. Plant Pathol. 38:183-196

Bamshad, M. J., Ng, S. B., Bigham, A. W., Tabor, H. K., Emond, M. J., Nickerson, D. A., and Shendure, J. 2011. Exome sequencing as a tool for Mendelian disease gene discovery. Nat. Rev. Genet. 12:745-755

Blom, N., Gammeltoft, S., and Brunak, S. 1999. Sequence- and structure-based prediction of eukaryotic protein phosphorylation sites. J. Mol. Biol. 294:1351-1362

Boller, T., and He, S. Y. 2009. Innate Immunity in Plants: An Arms Race Between Pattern Recognition Receptors in Plants and Effectors in Microbial Pathogens. Science. 324:742-744

Boutet, S. C., Disatnik, M., Chan, L. S., Iori, K., and Rando, T. A. 2007. Regulation of Pax3 by Proteasomal Degradation of Monoubiquitinated Protein in Skeletal Muscle Progenitors. Cell. 130:349-362

Brueggeman, R., Rostoks, N., Kudrna, D., Kilian, A., Han, F., Chen, J., Druka, A., Steffenson, B., and Kleinhofs, A. 2002. The barley stem rust-resistance gene *Rpg1* is a novel disease-resistance gene with homology to receptor kinases. Proc. Natl. Acad. Sci. 99:9328-9333

Canut, H., Carrasco, A., Galaud, J., Cassan, C., Bouyssou, H., Vita, N., Ferrara, P., and Pont-Lezica, R. 1998. High affinity RGD-binding sites at the plasma membrane of *Arabidopsis thaliana* links the cell wall. Plant J. 16:63-71

Century, K. S., Shapiro, A. D., Repetti, P. P., Dahlbeck, D., Holub, E., and Staskawicz, B. J. 1997. NDR1, a Pathogen-Induced Component Required for Arabidopsis Disease Resistance. Science. 278:1963-1965

Chai, Y., Nirmala, J., Kleinhofs, A., and Steffenson, B. J. 2012. Failure of RPG1 protein to degrade in high-copy *Rpg1* transgenic barley lines results in susceptibility to stem rust. Physiol. Mol. Plant Pathol. 80:10-18

Chinchilla, D., Bauer, Z., Regenass, M., Boller, T., and Felix, G. 2006. The *Arabidopsis* Receptor Kinase FLS2 Binds flg22 and Determines the Specificity of Flagellin Perception. Plant Cell. 18:465-476

Dangl, J. L., and Jones, J. D. G. 2001. Plant pathogens and integrated defence responses to infection. Nature 411:826-833

Day, B., Dahlbeck, D., and Staskawicz, B. J. 2006. NDR1 Interaction with RIN4 Mediates the Differential Activation of Multiple Disease Resistance Pathways in Arabidopsis. Plant Cell. 18:2782-2791

Dodds, P. N., and Rathjen, J. P. 2010. Plant immunity: towards an integrated view of plant-pathogen interactions. Nature Genet. 11:539-548

Dodds, P. N., Lawrence, G. J., Catanzariti, A., The, T., Wang, C. A., Ayliffe, M. A., Kobe, B., and Ellis, J. G. 2006. Direct protein interaction underlies gene-for-gene specificity and coevolution of the flax resistance genes and flax rust avirulence genes. Proc. Natl. Acad. Sci. 103:8888-8893

Faris, J. D., Zhang, Z., Lu, H., Lu, S., Reddy, L., Cloutier, S., Fellers, J. P., Meinhardt, S. W., Rasmussen, J. B., Xu, S. S., Oliver, R. P., Simons, K. J., and Friesen, T. L. 2010. A unique wheat disease resistance-like gene governs effector-triggered susceptibility to necrotrophic pathogens. Proc. Natl. Acad. Sci. 107:13544-13549

Flor, H. H. 1956. The Complementary Genic Systems in Flax and Flax Rust. Adv. Genet. 8:29-54

Friesen, T. L., Faris, J. D., Lai, Z., and Steffenson, B. J. 2006. Identification and chromosomal location of major genes for resistance to *Pyrenophora teres* in a doubled-haploid barley population. Genome. 49:855-859

Friesen, T. L., Meinhardt, S. W., and Faris, J. D. 2007. The *Stagonospora nodorum*-wheat pathosystem involves multiple proteinaceous host-selective toxins and corresponding host sensitivity genes that interact in an inverse gene-for-gene manner. Plant J. 51:681-692

Friesen, T. L., Stukenbrock, E. H., Liu, Z., Meinhardt, S., Ling, H., Faris, J. D., Rasmussen, J. B., Solomon, P. S., McDonald, B. A., and Oliver, R. P. 2006. Emergence of a new disease as a result of interspecific virulence gene transfer. Nature Genet. 38:953-956

Gill, U., Brueggeman, R., Nirmala, J., Chai, Y., Steffenson, B., and Kleinhofs, A. 2016. Molecular and genetic characterization of barley mutants and genetic mapping of mutant *rpr2* required for *Rpg1*-mediated resistance against stem rust. Theor. Appl. Genet. 129:1519-1529

Gill, U., Nirmala, J., Brueggeman, R., and Kleinhofs, A. 2012. Identification, characterization and putative function of *HvRin4*, a barley homolog of *Arabidopsis Rin4*. Physiol. Mol. Plant Pathol. 80:41-49

Gomez-Gomez, L., and Boller, T. 2002. Flagellin perception: a paradigm for innate immunity. Trends Plant Sci. 7:251-256

Haas, T. A. and Plow, E. F. 1994. Integrin-ligand interactions: a year in review. Curr. Opin. Cell Biol. 6:656-662

Hicke, L. 2001. Protein regulation by monoubiquitin. Nature Rev. Mol. Cell Biol. 2: 195-201

Hicke, L. and Dunn, R. 2003. Regulation of Membrane Protein Transport by Ubiquitin and Ubiquitin-Binding Proteins. Ann. Rev. Cell Devel. Biol. 19:141-172

International Barley Genome Sequencing Consortium. 2012. A physical, genetic and functional sequence assembly of the barley genome. Nature. 491:711-716

Jones, J. D. G., and Dangl, J. L. 2006. The plant immune system. Nature 444:323-329

Knepper, C., Savory, E. A., and Day. B. 2011b. The role of NDR1 in pathogen perception and plant defense signaling. Plant Signal. Behav. 6:1114-1116

Knepper, C., Savory, E., and Day, B. 2011a. Arabidopsis NDR1 is an Integrin-Like Protein with a Role in Fluid Loss and Plasma Membrane-Cell Wall Adhesion. Plant Cell. 156:286-300

Kosugi, S., Hasebe, M., Tomita, M., and Yanagawa, H. 2009. Systematic identification of yeast cell cycle-dependent nucleocytoplasmic shuttling proteins by prediction of composite motifs. Proc. Natl. Acad. Sci. 106:10171-10176

Li, H. and R. Durbin, 2009 Fast and accurate short read alignment with Burrows-Wheeler Transform. Bioinformatics. 25: 1754-60

Li, H., B. Handsaker, A. Wysoker, T. Fennell, J. Ruan *et al.*, 2009. The sequence alignment/map format and SAMtools. Bioinformatics. 25: 2078-2079.

Liu, Z. H., Zhong, S., Stasko, A. K., Edwards, M. C., and Friesen, T. L. 2012. Virulence Profile and Genetic Structure of a North Dakota Population of *Pyrenophora teres* f. *teres*, the Causal Agent of Net Form Net Blotch of Barley. Phytopathol. 102:539-546

Liu, Z., Ellwood, S. R., Oliver, R. P., and Friesen, T. L. 2011. *Pyrenophora teres*: profile of an increasingly damaging barley pathogen. Mol. Plant Pathol. 12:1-19

Liu, Z., Holmes, D. J., Faris, J. D., Chao, S., Brueggeman, R. S., Edwards, M. C., and Friesen, T. L. 2015. Necrotrophic effector-triggered susceptibility (NETS) underlies the barley-*Pyrenophora teres* f. *teres* interaction specific to chromosome 6H. Mol. Plant Pathol. 16:188-200

Mascher, M., G. J. Muehlbauer, D. S. Rokhsar, J. Chapman, J. Schmutz *et al.*, 2013 Anchoring and ordering NGS contig assemblies by population sequencing (POPSEQ). Plant J. 76: 718-727.

Mascher, M., Jost, M., Kuon, J., Himmelbach, A., Abfalg, Z., Beier, S., Scholz, U., Graner, A., and Stein, N. 2014. Mapping-by-sequencing accelerates forward genetics in barley. Genome Biol. 15:R78

Mascher, M., Richmond, T. A., Gerhardt, D. J., Himmelbach, A., Clissold, L., Sampath, D., Ayling, S., Steuernagel, B., Pfeifer, Mm., D'Ascenzo, M., Akhunov, E. D., Hedley, P. E., Gonzalez, A. M., Morrell, P. L., Kilian, B., Blattner, F. R., Scholz, U., Mayer, K. F. X., Flavell, A. J., Muehlbauer, G. J., Waugh, R., Jeddeloh, J. A., and Stein, N. 2013. Barley whole exome capture: a tool for genomic research in the genus *Hordeum* and beyond. Plant J. 76:494-505

Mascher, M., Schuenemann, V. J., Davidovich, U., Marom, N., Himmelbach, A., Hubner, S., Korol, A., David, M., Reiter, E., Riehl, S., Schreiber, M., Vohr, S. H., Green, R. E., Dawson, I. K., Russell, J., Kilian, B., Muehlbauer, G. J., Waugh, R., Fahima, T., Krause, J., Weiss, E., and Stein, N. 2016. Genomic analysis of 6,000-year-old cultivated grain illuminates the domestication history of barley. Nature Genet. 45:1089-1093

Mayer, K. F. X., Martis, M., Hedley, P. E., Simkova, H., Liu, H., Morris, J. A., Steuernagel, B., Taudien, S., Roessner, S., Gundlach, H., Kubalakova, M., Suchankova, P., Murat, F., Felder, M., Nussbaumer, T., Graner, A., Salse, J., Endo, T., Sakai, H., Tanaka, T., Itoh, T., Sato, K., Platzer, M., Matsumota, T., Scholz, U., Dolezel, J., Waugh, R., and Stein, N. 2011. Unlocking the Barley Genome by Chromosomal and Comparative Genomics. Plant Cell. 23:1249-1263

Mitchell, A., Chang, H., Daugherty, L., Fraser, M., Hunter, S., Lopez, R., McAnulla, C., McMenamin, C., Nuka, G., Pesseat, S., Sangrador-Vegas, A., Scheremetjew, M., Rato, C., Yong, S., Bateman, A., Punta, M., Attwood, T. K., Sigrist, C. J. A., Redaschi, N., Rivoire, C., Xenarios, I., Kahn, D., Guyot, D., Bork, P., Letunic, I., Gough, J., Oates, M., Haft, D., Huang, H., Natale, D. A., Wu, C. H., Orengo, c., Sillitoe, I., Mi, H., Thomas, P. D., and Finn, R. D. 2014. Nucleic Acids Res. Doi: 10.1093/narlgkul1243

Moller, S., Croning, M. D. R., and Apweiler, R. 2001. Evaluation of methods for the prediction of membrane spanning regions. Bioinformatics. 17:646-653

Nirmala, J., Dahl, S., Steffenson, B. J., Kannangara, C. G., von Wettstein, D., Chen, X., and Kleinhofs, A. 2007. Proteolysis of the barley receptor-like protein nkinase RPG1 by a proteasome pathway is correlated with *Rpg1*-mediated stem rust resistance. Proc. Natl. Acad. Sci. 104:10276-10281

Nirmala, J., Drader, T., Chen, X., Steffenson, B., and Kleinhofs, A. 2010. Stem Rust Spores Elicit Rapid RPG1 Phosphorylation. Mol. Plant Microbe In. 23:1635-1642

Nirmala, J., Drader, T., Lawrence, P. K., Yin, C., Hulbert, S., Steber, C. M., Steffenson, B. J., Szabo, L. J., von Wettstein, D., and Kleinhofs, A. 2011. Concerted action of two avirulent spore effectors activates *Reaction to Puccinia graminis 1* (*Rpg1*)-mediated cereal stem rust resistance. Proc. Natl. Acad. Sci. 108:14676-14681

R Core Team. 2016. R: A language and environment for statistical computing. R Foundation for Statistical Computing, Vienna, Austria. https://www.R-project.org/.

Ruoslahti, E. 1996. RGD and Other Recognition Sequences for Integrins. Ann. Rev. Cell Devel. Biol. 12:697-715

Russell, J., Mascher, M., Dawson, I. K., Kyriakidis, S., Calixto, C., Freund, F., Bayer, M., Milne, I., Marshall-Griffiths, T., Heinen, S., Hofstad, A., Sharma, R., Himmelbach, A., Knauft, M., van Zonneveld, M., Brown, J. W. S., Schmid, K., Kilian, B., Muehlbauer, G. J., Stein, N., and Waugh, R. 2016. Exome sequencing of geographically diverse barley landraces and wild relatives gives insights into environmental adaptation. Nature Genet. 48:1024-1030

Shih, S. C., Prag, G., Francis, S. A., Sutanto, M. A., Hurley, J. H., and Hicke, L. 2003. A ubiquitin-binding motif required for intramolecular monoubiquitylation, the CUE domain. EMBO J. 22:1273-1281

Shjerve, R. A., Faris, J. D., Brueggeman, R. S., Yan, C., Zhu, Y., Koladia, V., and Friesen, T. L. 2014. Evaluation of a *Pyrenophora teres* f. *teres* mapping population reveals multiple independent interactions with a region of barley chromosome 6H. Fungal Genet. Biol. 70:104-112

Steffenson, B. J. and Webster, R. K. 1992. Pathotype Diversity of *Pyrenophora teres* f. *teres* on Barley. Phytopathol. 82:170-177

Steffenson, B. J., Jin, Y., Brueggeman, R. W., Kleinhofs, A., and Sun, Y. 2009. Resistance to Stem Rust Race TTKSK Maps to the *rpg4/Rpg5* Complex of Chromosome 5H of Barley. Phytopathol. 99:1135-1141

Tekauz, A. 1978. Incidence and severity of net blotch of barley and distribution of *Pyrenophora teres* biotypes in the Canadian prairies in 1976. Can. Plant Dis. Surv. 58:9-11

Tekauz, A. 1990. Characterization and distribution of pathogenic variation in *Pyrenophora teres* f. *teres* and *P. teres* f. *maculata* from western Canada. Can. J. Plant Pathol. 12:141-148

Tekauz, A., 1985 A numerical scale to classify reactions of barley to Pyrenophora teres. Can. J. Plant Pathol. 7: 181-183

Tekauz, A., and Buchannon, K. W. 1977. Distribution of and Sources of Resistance to Biotypes of *Pyrenophora teres* in Western Canada. Can. J. Plant Sci. 57:389-395

Thomma, B. P. H. J., Nurnberger, T., and Joosten, M. H. A. J. 2011. Of PAMPs and Effectors: The Blurred PTI-ETI Dichotomy. Plant Cell 23:4-15

Underwood, W. 2012. The plant cell wall: a dynamic barrier against pathogen invasion. Front. Plant Sci. 3(85):67

Van der Flier, A. and Sonnenberg, A. 2001. Function and itneractions of integrins. Cell Tissue Res. 305:285-298

Weiland, J. J., Steffenson, B. J., Cartwright, R. D., and Webster, R. K. 1999. Identification of molecular genetic markers in *Pyrenophora teres* f. *teres* associated with low virulence on 'Harbin' barley. Phytopathol. 89:176-181

Wu, H. L., Steffenson, B. J., Li, Y., Oleson, A. E., and Zhong, S. 2003. Genetic variation for virulence and RFLP markers in *Pyrenophora teres*. Can. J. Plant Pathol. 25:82-90

Zipfel, C. 2008. Pattern-recognition receptors in plant innate immunity. Curr. Opin. Immunol. 20:10-16

Zipfel, C. 2009. Early molecular events in PAMP-triggered immunity. Curr. Opin. Plant Biol. 12:414-420

Zipfel, C. 2014. Plant pattern-recognition receptors. Trends Immunol. 35:345-351

CONCLUSION

Net form net blotch (NFNB), caused by the necrotrophic fungal pathogen *Pyrenophora teres* f. *teres*, is an economically important foliar pathogen of barley and is present in most barley production regions of the world. With potential to cause yield losses typically ranging from 10%-40%, successful management of this disease is of upmost importance for the barley industry. Although control of this disease can be achieved through chemical application and cultural practices, the deployment of effective and durable host genetic resistance is often deemed the most desirable method of disease management. However, the genetic and molecular nature of host resistance and susceptibility has been observed to be highly complex, warranting further investigation. The research presented in this dissertation dissects these aspects of host resistance/susceptibility, advancing our knowledge within the field of molecular plant pathology.

Using a globally diverse set of 957 barley accessions, a genome wide association study approach was utilized to identify regions of the barley genome significantly associated with resistance or susceptibility to three North American *P. teres* f. *teres* isolates. Results of this research identified 16 genomic loci associated with disease reaction to these isolates. Five loci had not been previously described, providing barley breeders with potential novel sources of resistance to incorporate into elite barley lines.

The NFNB dominant susceptibility locus *Spt1* was previously mapped at low-resolution in a double haploid population derived from a cross of barley cultivars Rika and Kombar. Using 2976 recombinant gametes from a Rika x Kombar cross and molecular markers developed within the *Spt1* region via the exploitation of the syntenous relationship between barley chromosome 6H and *Brachypodium distachyon* chromosome 3, the *Spt1* dominant susceptibility locus was delimited to ~0.24 cM near the centromere of barley chromosome 6H. The results of this

research greatly facilitate the map-based cloning of *Spt1* and demonstrate the utility of marker development using synteny between barley and *B. distachyon*.

Following the further fine-mapping of *Spt1*, candidate gene analysis was conducted by the examination of polymorphic genes within the newly delimited region typically associated with plant immune responses. Synteny analysis discovered a polymorphic gene predicted to encode a receptor-like protein within the region. A molecular marker designed from this gene revealed it to co-segregate with *Spt1*. Additionally, barley cultivar Morex was characterized to be susceptible to two Montana *P. teres* f. *teres* isolates, Tra-A5 and Tra-D10, whereas cultivar Steptoe was characterized as resistant. Phenotyping and subsequent QTL analysis of a Steptoe x Morex double hapoloid population revealed a major QTL spanning the previously identified *Spt1* locus. The full-length candidate gene sequence was obtained from barley cultivar Morex and identified from barley cultivars Rika and Kombar via an adaptor-ligation genome walking method. Comparison of predicted amino acid sequences revealed a high level of divergence in the N-terminal portion of the gene, with the C-terminal leucine-rich repeat remaining relatively conserved. Allele analysis of a diverse set of barley lines illustrated a strong correlation with the presence of a Rika, Kombar, or Morex allele and susceptibility to *P. teres* f. *teres* isolates 6A, 15A, and Tra-A5/Tra-D10, respectively. The diversity of candidate *Spt1* appeared to stem from wild barley populations, as evidenced in a phylogentic analysis using exome capture data of *Hordeum vulgare* ssp. *spontaneum* accessions, as well as cultivated barley and barley landraces. These diverse candidate *Spt1* alleles may be targeted by unique necrotrophic effectors produced by the pathogen, initiating necrotrophic effector triggered susceptibility. These results further our knowledge of the intricate host molecular mechanisms which this pathogen may be hijacking.

The barley cultivar Morex *rpr2* mutant was previously characterized to have lost *Rpg1*-mediated resistance to wheat stem rust and mapped to the centromeric region of chromosome 6H. However, the underlying gene remained to be identified. In addition to the loss of stem rust resistance, we observed this mutant to have lost basal resistance to the distantly related pathogen *P. teres* f. *teres*. Using exome capture to sequence the majority of annotated barley genes, a 12 base-pair deletion was identified in a gene containing a plant homeodomain and fibronectin domain and is localized to the mapped *rpr2* region. We hypothesize that this gene functions in the molecular perception of the disruption of the extracellular matrix-plasma membrane interface caused by two spore-coat effector proteins and loss of *Rpr2* function results in enhanced susceptibility to wheat stem rust and NFNB.

In summary, this research identified regions of the barley genome significant associated with resistance/susceptibility to NFNB, allowing barley breeders to efficiently incorporate resistance or remove susceptibility from their elite barley lines. Addtionally, the NFNB dominant susceptibility locus *Spt1* was mapped at high-resolution and a receptor-like protein was identified as a stong candidate gene. The *Rpr2* gene conditioning basal resistance to wheat stem rust and NFNB in barley was identified via exome capture and represents a potential novel gene class implicated in host resistance to two phylogenetically diverged plant pathogens. This dissertation broadens our knowledge of the genetic and molecular intricacies of this pathosystem and advances our understanding of how the host protects itself from infection and how the pathogen circumvents defense responses.